

## Durham E-Theses

---

### *Chemical and ESCA investigations of some halogenated heterocyclic systems*

R. King

#### How to cite:

---

King, R. (1973) Chemical and ESCA investigations of some halogenated heterocyclic systems. Doctoral thesis, Durham University.

#### Use policy

---

The full-text may be used and/or reproduced, and given to third parties in any format or medium, without prior permission or charge, for personal research or study, educational, or not-for-profit purposes provided that:

- a full bibliographic reference is made to the original source
- a <https://etheses.durham.ac.uk/id/eprint/8561/> is made to the metadata record in Durham E-Theses
- the full-text is not changed in any way

The full-text must not be sold in any format or medium without the formal permission of the copyright holders.

Please consult the [full Durham E-Theses policy](#) for further details.

UNIVERSITY OF DURHAM

A Thesis

entitled

CHEMICAL AND ESCA INVESTIGATIONS OF  
SOME HALOGENATED HETEROCYCLIC SYSTEMS

submitted by

R. King B.Sc.

(Van Milaert College)

A candidate for the degree of Doctor of Philosophy

1973.



To My Mother and to the

Memory of My late, Dear Father.

MEMORANDUM

The work described in this thesis was carried out in the University of Durham between October 1970 and May 1973. This work has not been submitted for any other degree and is the original work of the author except where acknowledged by reference.

## ACKNOWLEDGEMENTS

I am indebted to my supervisors, Dr G.M. Brooke, under whose excellent guidance this work was carried out, and Professor W.K.R. Musgrave, whose personal advice and encouragement over the years has been greatly appreciated. Thanks also go to Dr D.T. Clark who sacrificed a great deal of time in numerous discussions and whose assistance and advice on all aspects of ESCA have been invaluable. I would also like to thank Mr I. Scanlan and Mr D.B. Adams for advice on computational problems, and all the technical staff and members of the chemistry department, too numerous to mention, who have made their own contributions.

I am grateful to the Science Research Council and A.E.I. (Manchester) Ltd for the provision of equipment and a studentship.

Finally, I would especially like to thank my wife, Lynne, whose devotion and understanding throughout made this thesis possible.

## ABSTRACT

2,3,4,5,6,7-Hexachlorobenzo-[b]-thiophen reacted with n-butyllithium to give either the 2-lithio derivative or the 2,6-dilithio derivative depending on the reaction conditions; a mixture of mono (2-) and di(2,6-) Grignard reagents were formed from hexachlorobenzo-[b]-thiophen and magnesium. Nucleophilic replacement of the 2-chlorine atom has been established for the reaction of hexachlorobenzo-[b]-thiophen with lithium aluminium hydride; sodium benzenethiolate replaced a chlorine in the five membered ring; sodium isopropoxide gave a mono substituted product, while sodium thiomethoxide caused multiple substitution to give a dichlorotetrathiomethoxybenzo-[b]-thiophen.

Catalytic hydrogenation of hexachlorobenzo-[b]-thiophen [Pd/C] gave 4,5,6,7-tetrachlorobenzo-[b]-thiophen which was also synthesised unambiguously by a reaction sequence which involved the initial treatment of sodium pentachlorobenzenethiolate with diethyl acetylenedicarboxylate to give diethyl 4,5,6,7-tetrachlorobenzo-[b]-thiophen (A), followed by de-esterification and decarboxylation. 4,5,6,7-Tetrachlorobenzo-[b]-thiophen served as a model for  $^1\text{H}$  n.m.r. spectroscopy studies. Under certain conditions both the cyclised material (A) and the uncyclised product, trans-diethyl-1-pentachlorothiophenoxybutenedioic acid were formed. With ethyl propiolate, sodium pentachlorobenzenethiolate gave only the uncyclised product, cis-ethyl  $\beta$ -pentachlorophenylthioacrylate. Hexachlorobenzo-[b]-thiophen readily formed the 1,1-dioxide on treatment with peroxytrifluoroacetic acid, the vacuum pyrolysis of which gave hexachlorophenylacetylene.

4,5,6,7-Tetrachlorobenzo-[b]-thiophen undergoes multiple substitution with thiolates. With sodium benzenethiolate the major product was a dichloro-dithiophenoxybenzo-[b]-thiophen, the minor, mono substituted product was only identified by Mass Spectroscopy. With sodium thiomethoxide mixtures of mon- and di-thiomethoxy or di- and tri-thiomethoxy substituted products were formed, depending on the reaction conditions.

ESCA spectra have been recorded and molecular core binding energies determined for indene, indole, benzo-[b]-thiophen, benzo-[b]-thiophen-1,1-dioxide, benzo-[b]-furan and some of their chloro and fluoro derivatives. Binding energies were assigned and data interpreted with the aid of CNDO/2 SCF MO calculations and the charge potential model.

## CONTENTS

<u>CHAPTER 1</u>	<u>Page</u>
<u>SYNTHESIS OF BENZO-[b]-THIOPHEN DERIVATIVES</u>	
Introduction	1
A. <u>Formation of the 3,9-bond on Ring Closure</u>	2
(i) Electrophilic attack on the benzene nucleus	2
(ii) Nucleophilic attack on the benzene nucleus	5
B. <u>Formation of the 2,3-bond on Ring Closure</u>	5
Nucleophilic Reactions	5
C. <u>Formation of the 1,2-bond on Ring Closure</u>	10
Nucleophilic Reactions	10
D. <u>Formation of the 1,8-bond on Ring Closure</u>	13
(i) Electrophilic Reactions	13
(ii) Nucleophilic Reactions	19
E. <u>Simultaneous Formation of the 1,8- and 3,9-bonds</u>	21
 <u>CHAPTER 2</u>	
<u>SYNTHESIS AND REACTIONS OF SOME HIGHLY CHLORINATED</u>	
<u>BENZO-[b]-THIOPHENS</u>	
Introduction	23
<u>Synthesis of 2,3,4,5,6,7-Hexachlorobenzo-[b]-thiophen</u>	24
<u>Attempted Preparation of 6-methoxy-2,3,4,5,7-pentachloro-</u>	
<u>benzo-[b]-thiophen</u>	29
<u>Synthesis of 4,5,6,7-Tetrachlorobenzo-[b]-thiophen</u>	30
<u>Some Reactions of 2,3,4,5,6,7-Hexachlorobenzo-[b]-thiophen</u>	39
(i) Metallation reactions	39
(ii) Reduction reactions	42

## CHAPTER 2 continued

(iii) Oxidation	49
<u>Nucleophilic Reactions of Polyhalo aromatic Compounds</u>	52
a. Polyhalobenzenoid Compounds	53
b. Rationalisation of Orientation	54
c. Nucleophilic substitution in Polyhalohetero aromatic Systems	57
(i) Nitrogen Heterocycles	57
(ii) Heterocycles containing oxygen and sulphur	59
<u>Some Nucleophilic Reactions of Hexachloro and 4,5,6,7-Tetrachlorobenzo-[b]-thiophen</u>	60

## CHAPTER 3

### ELECTRON SPECTROSCOPY FOR CHEMICAL ANALYSIS

(i) <u>Introduction</u>	64
(ii) <u>History and Development of ESCA</u>	66
(iii) <u>Theory of Electron Spectroscopy</u>	69
a. Photoionisation Processes	71
b. Electronic Relaxation Processes	72
c. Properties of Core Orbitals	74
d. Calculation of Binding Energies from ESCA Spectra	81
e. Relationships between Calculated and Experimental Binding Energies for Gaseous and Solid Samples	84
f. Linewidths and their significance in Studying Core Levels	88
(iv) <u>The Electron Spectrometer</u>	89

a.	The Source Region	91
b.	Electron Energy Analysers	93
c.	Detection Systems	96
d.	Data Acquisition	97
e.	Recent Developments in Instrumental Design	99
(v)	<u>Review of ESCA applications in Organic Chemistry</u>	101

#### CHAPTER 4

##### ESCA INVESTIGATIONS OF SOME HALOGENATED AROMATIC AND HETEROCYCLIC SYSTEMS

	Introduction	116
	Experimental	117
	<u>Results</u>	
A.	<u>Molecular Core Binding Energies for benzo-[b]-thiophen, indole benzo-[b]-furan and their 4,5,6,7-tetrachloro and tetrafluoro derivatives</u>	123
a.	Qualitative Discussion	123
	(i) The effect of annelation on the $C_{1s}$ levels	123
	(ii) Hetero atom core levels	128
b.	Substituent effects of chlorine and fluorine in the 4,5,6,7-tetrahalogeno derivatives	128
	(i) $C_{1s}$ levels for atoms directly bonded to halogen	128
	(ii) The bridging carbon atoms (8,9)	131
	(iii) Five membered ring carbons (2,3)	133
	(iv) The hetero atom	134
c.	Quantitative Discussion	134

B.	<u>Molecular Core Binding Energies for Indene and some Highly Fluorinated Derivatives</u>	140
	Introduction	140
a.	Qualitative Discussion	142
	(i) Carbon $1_s$ levels	142
	(ii) Fluorine $1_s$ levels	149
b.	Quantitative Discussion	152
C.	<u>The Effect of chlorine substitution on the Molecular Core Binding Energies of Benzo-[b]-thiophens</u>	154
a.	Qualitative Discussion	154
b.	Distinction between two isomeric Tetrachlorobenzo-[b]-thiophens using ESCA	161
c.	Quantitative Discussion	166
D.	<u>A Comparison of the Molecular Core Binding Energies in Some Benzo-[b]-thiophens and their corresponding S-dioxides</u>	168
	Introduction	
a.	Qualitative Discussion	171
b.	The Hetero Atom	173
c.	Quantitative Discussion	175
E.	<u>The Effect of Chlorine Substitution on the Molecular Core Binding Energies of Indoles.</u>	
a.	Qualitative Discussion	179
b.	Quantitative Discussion	187
F.	<u>A Comparison of Hetero atom Effects on Molecular Core Binding Energies</u>	190

Introduction	190
Discussion	193

#### APPENDIX I

Apparatus and Instrumentation	198
<u>Experimental</u>	
2,3,4,5,6,7-Hexachlorobenzo-[b]-thiophen(I)	198
Attempted preparation of 6-methoxy, 2,3,4,5,7-Pentachlorobenzo-[b]-thiophen	199
3,4,5,6,7-Pentachlorobenzo-[b]-thiophen	
(a) From the 2-lithio derivative	199
(b) From (I) and lithium aluminium hydride	200
3,4,5,7-Tetrachlorobenzo-[b]-thiophen	
(a) From a dilithio derivative	201
(b) From a Grignard reagent	202
A mono-isopropoxy pentachlorobenzo-[b]-thiophen	203
A mono chloro-monothiophenoxy-4,5,6,7-tetrachlorobenzo-[b]-thiophen	203
A dichloro tetrathiomethoxybenzo-[b]-thiophen	204
2,3,4,5,6,7-Hexachlorobenzo-[b]-thiophen-1,1-dioxide	204
Pyrolysis of Hexachlorobenzo-[b]-thiophen-1,1-dioxide	205
Diethyl 4,5,6,7-tetrachlorobenzo-[b]-thiophen-2,3-dicarboxylate	205
<u>Trans</u> -diethyl-1-pentachlorothiophenoxybutenedioin acid	206
<u>Cis</u> -ethyl- $\beta$ -pentachlorophenylthioacrylate	206
Ethyl 4,5,6,7-tetrachlorobenzo-[b]-thiophen-2-carboxylate	207
4,5,6,7-Tetrachlorobenzo-[b]-thiophen-2,3-dicarboxylic acid dihydrate	208

4,5,6,7-Tetrachlorobenzo-[b]-thiophen	
(a) From 4,5,6,7-tetrachlorobenzo-[b]-thiophen-2,3-dicarboxylic acid dihydrate	208
(b) From 2,3,4,5,6,7-hexachlorobenzo-[b]-thiophen	209
(c) From 3,4,5,6,7-pentachlorobenzo-[b]-thiophen	209
(d) From the monochloro monothiophenoxy-4,5,6,7-tetrachlorobenzo-[b]-thiophen	209
Reactions of 4,5,6,7-tetrachlorobenzo-[b]-thiophen	
(a) Sodium thiophenoxide	210
(b) Sodium thiomethoxide	
i. Room Temperature	210
ii. Reflux Temperature	211
Infrared Spectra	213

## APPENDIX II

<u>Theoretical Calculations</u>	217
Introduction	
A. Elementary Quantum Mechanics	217
a. The Hartree-Fock Self Consistent Field Method	225
The Basis Functions	231
b. Semi-empirical All Valence Electron Neglect of Diatomic Overlap Method (NDDO)	233
c. All Valence Electron Complete Neglect of Differential Overlap Method (CNDO)	234
Evaluation of Integrals in CNDO/2	237
(i) One electron integrals $U_{ii}$	237
(ii) One-centre, two electron integrals $\Gamma_{AA}$	238
(iii) Two-centre, two electron integrals $\Gamma_{AB}$	238

(iv) Two-centre, one electron integrals $H_{ij}$	238
(v) Coulomb Penetration Integrals $V_{AB}$	239
Electron Distribution in Molecules	
Charge Density	239
$\pi$ Charge	241
$\sigma$ Charge	241
<u>APPENDIX III</u>	
A None-Rigorous Derivation of the Charge Potential Model	242
REFERENCES	

CHAPTER I

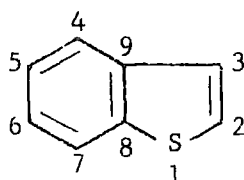
SYNTHESIS OF BENZO-[b]-THIOPHEN DERIVATIVES

## Introduction

Methods for synthesising the benzo-[b]-thiophen system have been widely reviewed,<sup>4</sup> most recently as part of an extensive review of benzothiophen chemistry by Iddon and Scrowston.<sup>4</sup> However, in this chapter the various synthetic methods will be examined, particularly from a mechanistic point of view, especially in relation to their use in the formation of polyhalobenzothiophens.

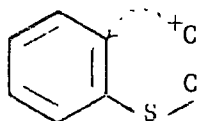
The most widely used methods involve the formation of a thiophen ring on an already existing benzene nucleus. Although a number of benzothiophen syntheses involving the formation of a thiophen ring on a cyclohexane ring<sup>5-7</sup> and the formation of a benzene ring on a thiophen nucleus<sup>8</sup> have been reported, these are less common methods and are not generally applicable to polyhalobenzothiophen synthesis. Only those methods involving the fusion of a thiophen ring onto an existing benzene nucleus will be considered here.

These syntheses can be conveniently categorised according to the bond formed on closure of the thiophen ring and further subdivided according to mechanism. The currently accepted numbering system (Chemical Abstracts) for benzo-[b]-thiophen (I) is given below.



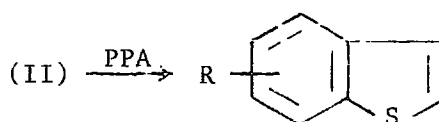
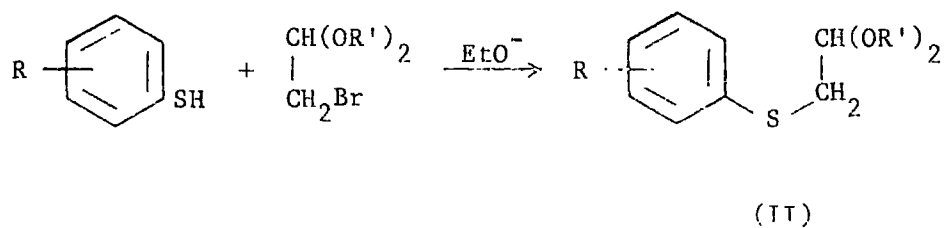
(I)



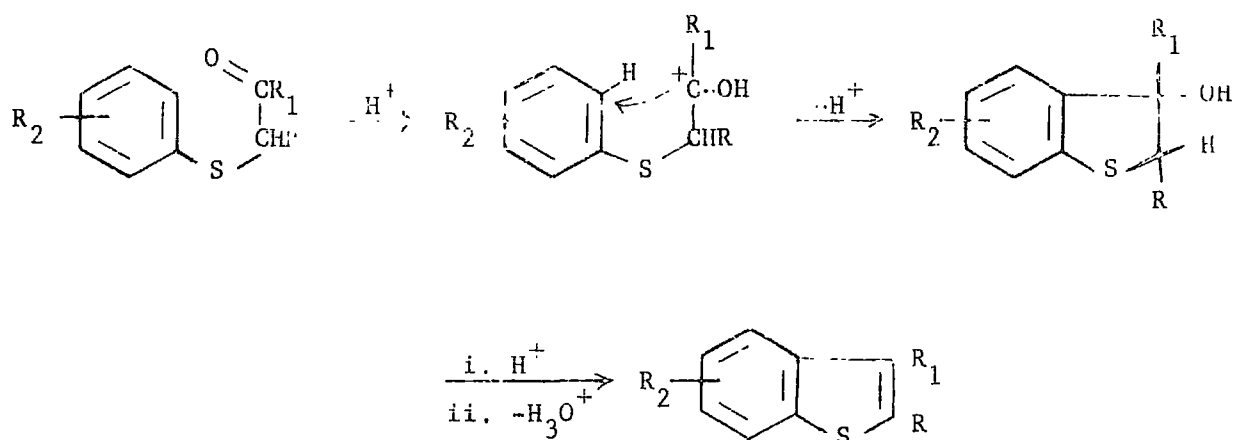
A. Formation of the 3,9-bond on ring closurei. Electrophilic attack on the benzene nucleus

One of the most widely used methods for benzothiophen synthesis involves the acid promoted cyclisation of arylthioacetals, arylthioketones and arylthioglycolic acids.

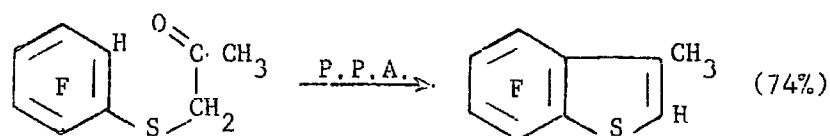
The arylthioacetals are readily prepared from arylmercaptans and bromoacetaldehyde dialkylacetal and cyclised with polyphosphoric acid (P.P.A.).



Cyclodehydration of arylthioketones also proceeds readily in the presence of  $\text{P}_2\text{O}_5$  or  $\text{ZnCl}_2$ .

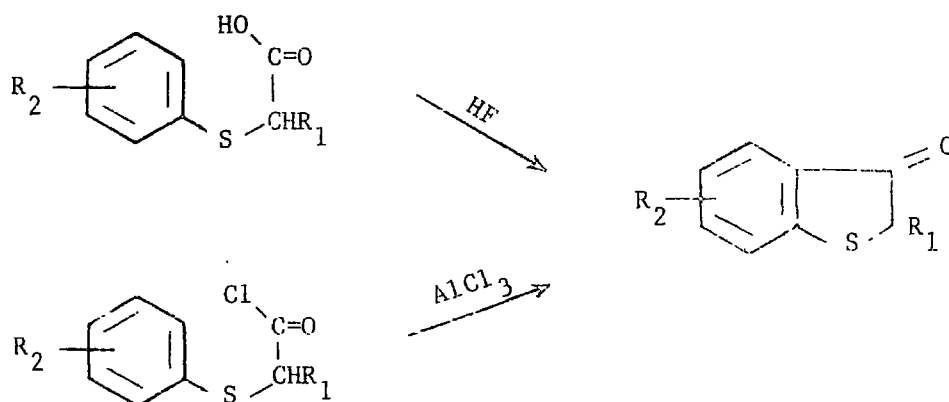


4,5,6,7-Tetrafluorobenzothiophen(III) has been prepared by this route from tetrafluorophenylthiopropionone.<sup>9</sup>



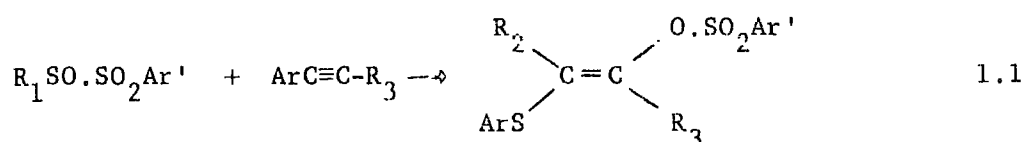
(III) Unmarked bonds to fluorine

Substituted thioindoxyls result from the cyclisation of arylthioglycolic acids with  $P_2O_5$ ,  $HF$ , etc., or more conveniently from the Friedel-Crafts cyclisation of the corresponding acid chloride.



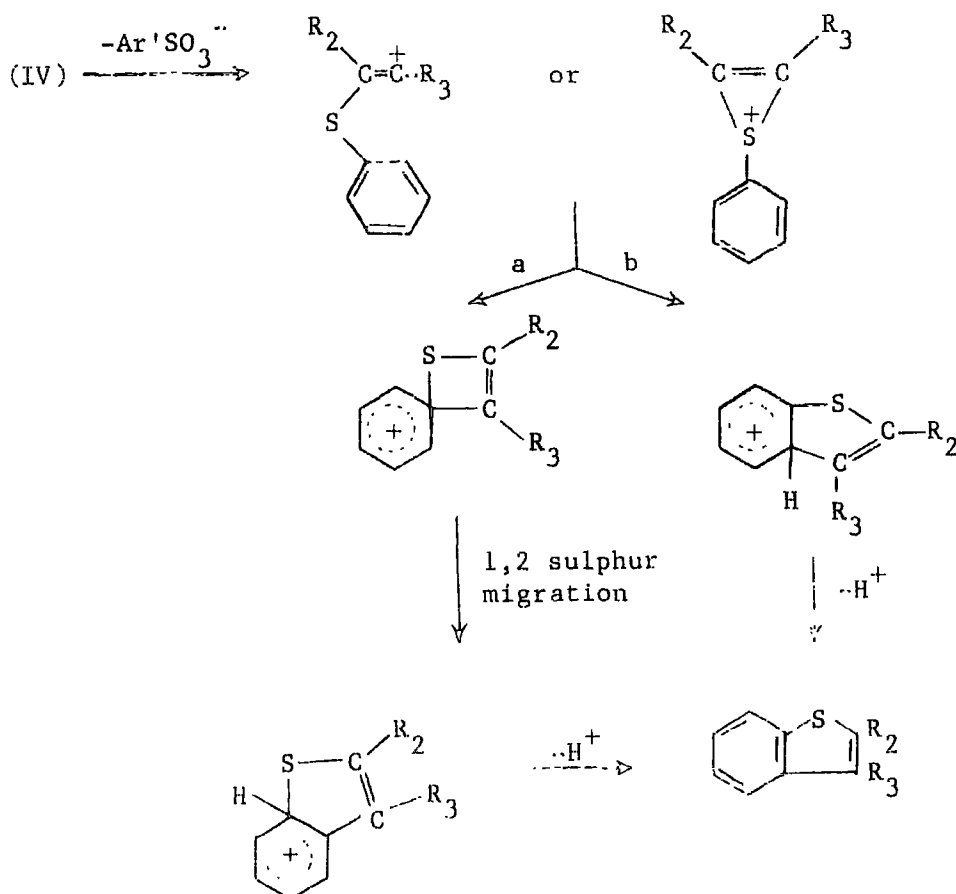
5,6,7-Trichlorothioindoxyl has also been successfully prepared,<sup>10</sup> although these methods are not generally applicable to polyhalobenzothiophen synthesis.<sup>11</sup> More recently a novel synthesis of benzothiophens has been reported which proceeds via an electrophilic reaction.

The addition of *o*-sulphenylarenesulphonates to arylacetylenes gives vinylsulphonic esters<sup>13</sup> (1.1), which in the presence of  $\text{BF}_3$  cyclise to



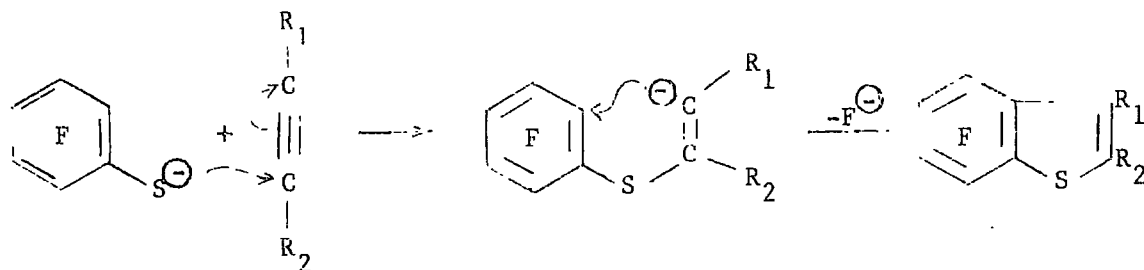
(IV)

give benzothiophens via a vinyl cation or thiirenium cation. The two mechanisms (a and b) proposed to account for the observed substituent effects are given below.



ii. Nucleophilic attack on the benzene nucleus

The ability of polyhalo benzene derivatives to undergo halide replacement in a nucleophilic attack makes this mechanism ideally suited to the synthesis of polyhalo benzothiophens. Brooks and Quasem<sup>14</sup> showed that the addition of pentafluorobenzenethiolate to diethylacetylenedicarboxylate (D.E.A.D.) proceeded by overall cis addition to give a carbanion which immediately cyclised to a benzothiophen in excellent yield. More recently the reaction has been extended to other acetylenes.<sup>15</sup>

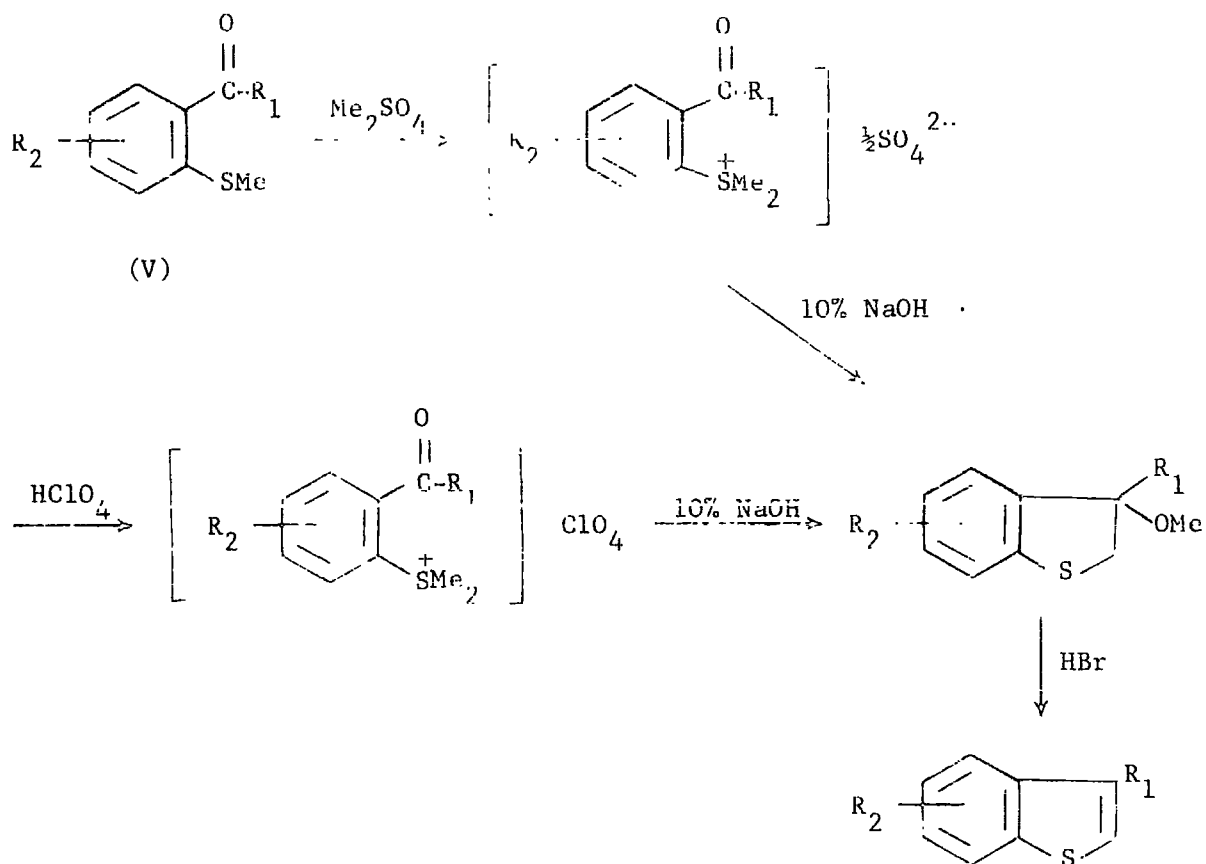


This reaction has now been successfully applied to the synthesis of tetrachlorobenzothiophen. (See later).

B. Formation of the 2,3-bond on Ring Closure

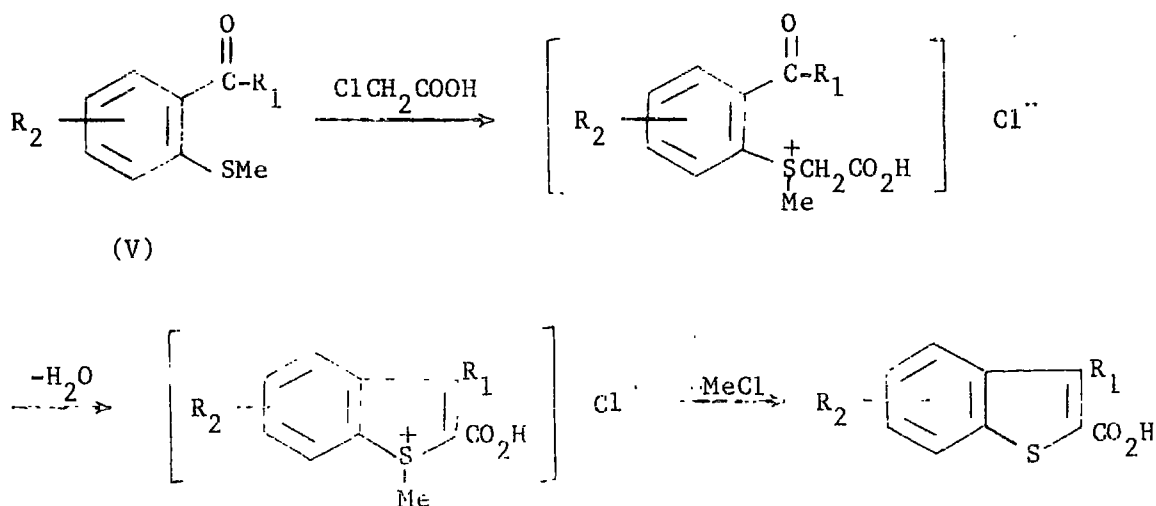
Nucleophilic reactions

The treatment of (ortho-acylphenyl)alkylsulphides(V) with dimethyl sulphate followed by base gives an excellent general method for the preparation of benzothiophens (Krollpfeiffer synthesis)



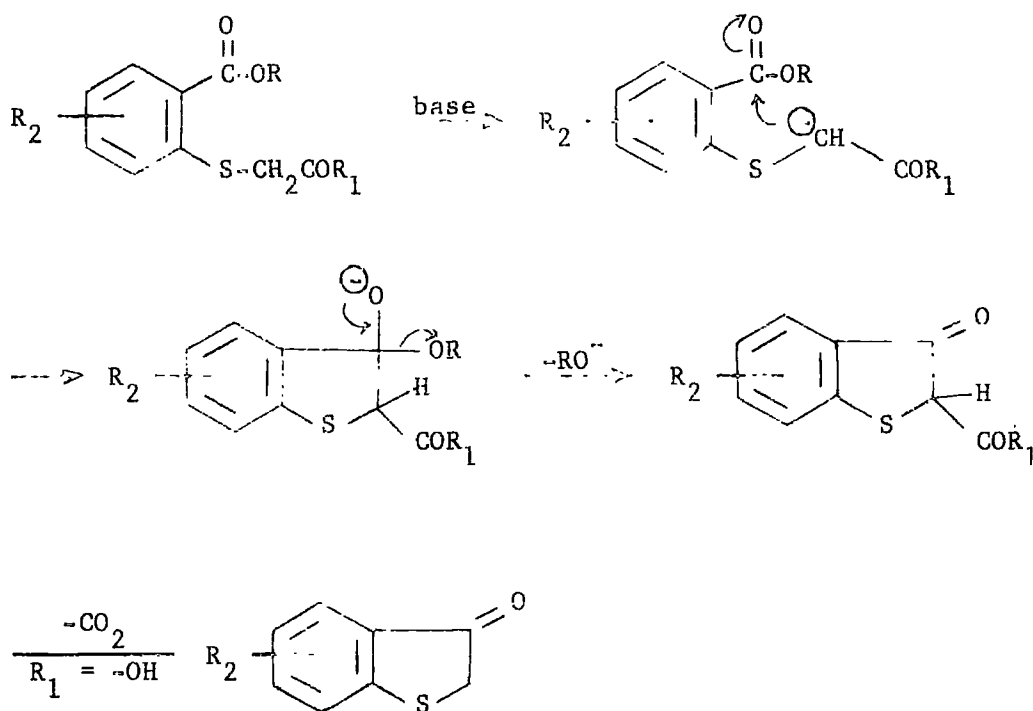
Isolation of the crystalline salt as either the sulphate or perchlorate and use of hydrogen bromide in the final stage gives improved yields.

Substituted 2-carboxybenzothiophenes can be prepared by treatment of (V) with chloroacetic acid.

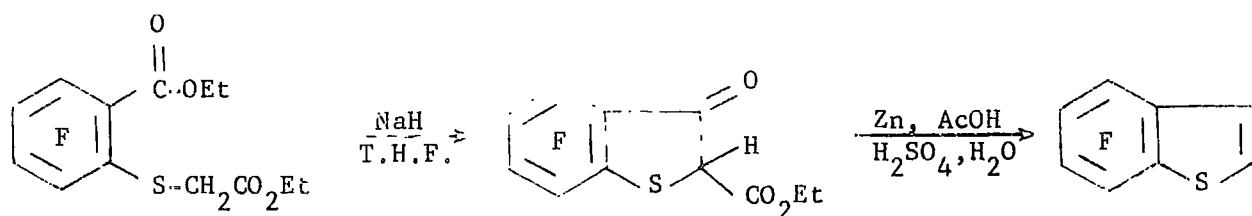


Both these methods involve reactions on side chains rather than on the benzene nucleus and this makes them potentially useful for the synthesis of benzothiophens with several halogens in the benzo ring. So far, neither method seems to have been successfully applied to polyhalo-benzothiophen formation.

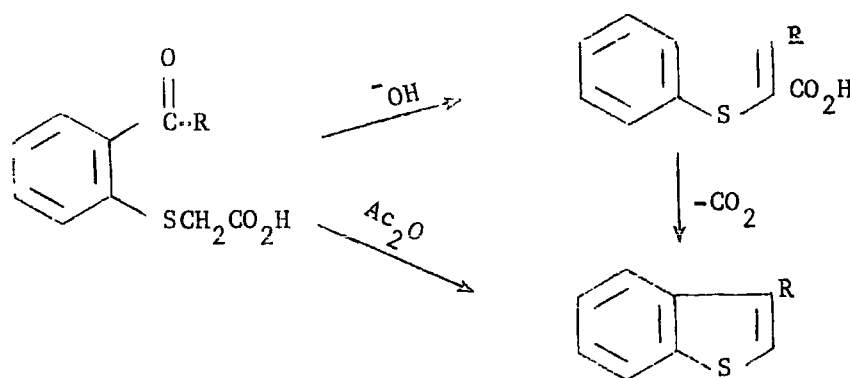
Base induced cyclisation of orthocarboxy-5-arylthioglycolic acids yields the corresponding thioindoxyl-2-carboxylic acids or, by decarboxylating the thioindoxyls.



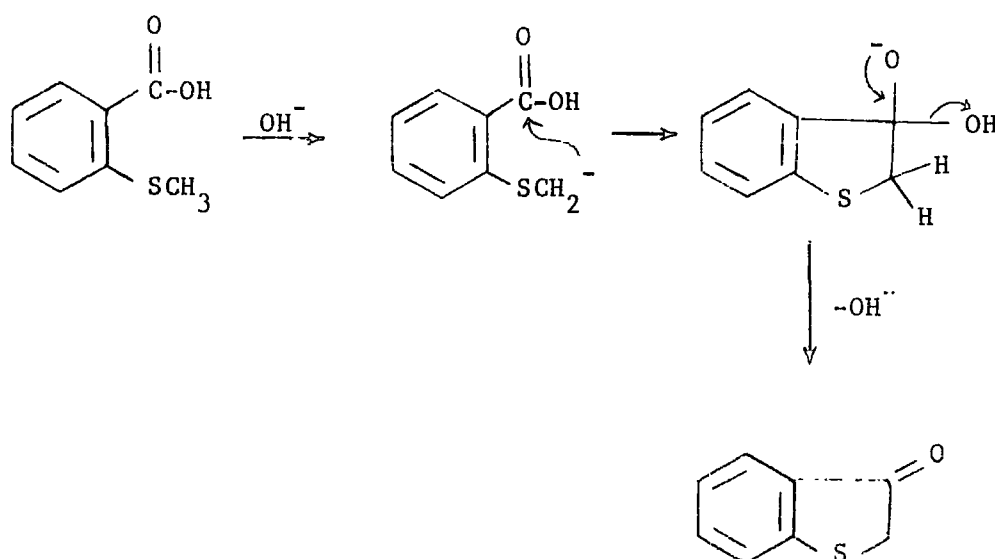
A variety of reagents have been used to cyclise thioglycolic esters ( $R_1, R_2 = \text{alkyl}$ ) including sodium in toluene, ethoxide ion and sodium hydride. This method has been applied to the synthesis of tetrafluoro-benzothiophen.<sup>14</sup>



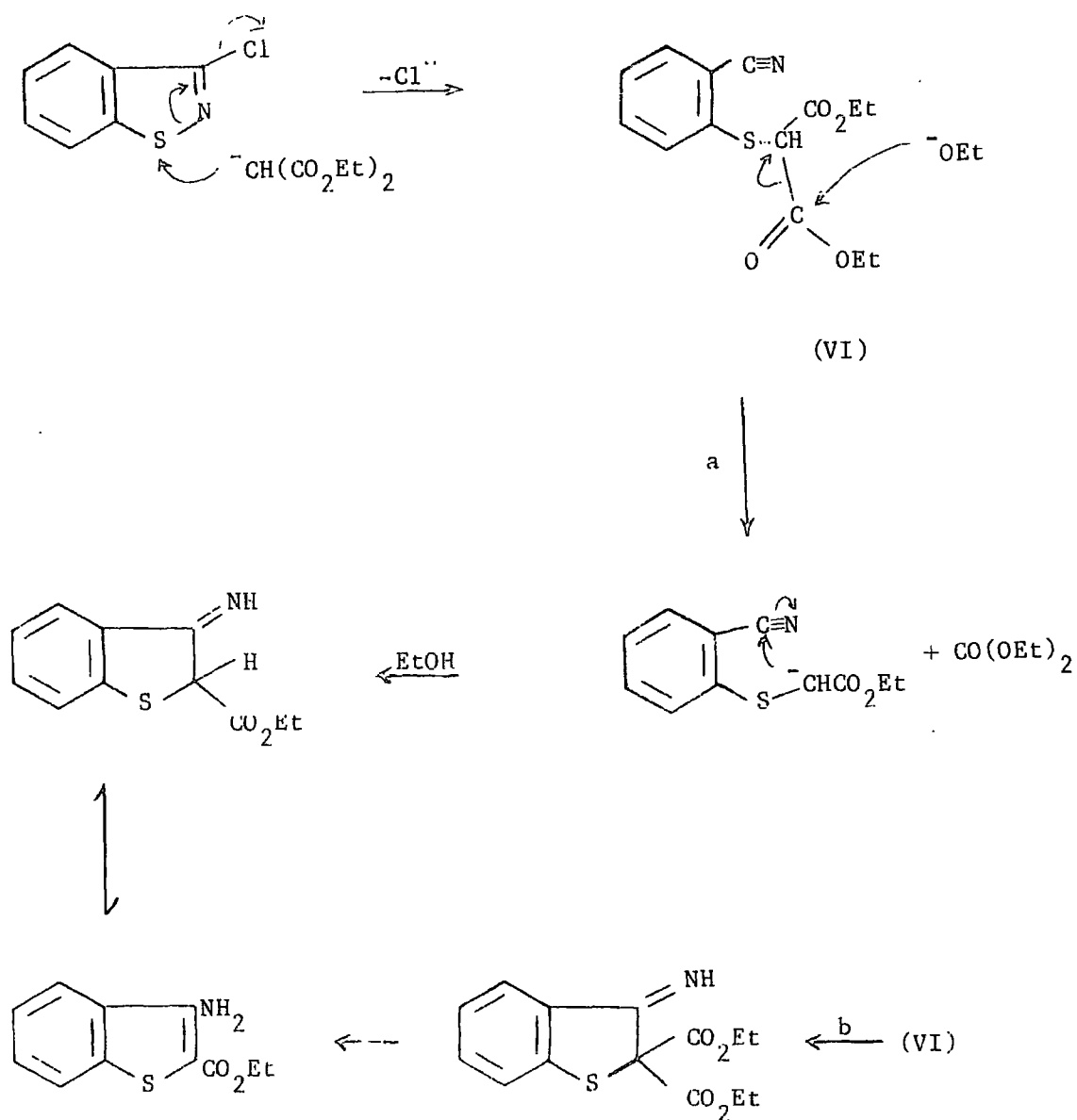
An extension of the above method to the cyclisation of ortho-acyl-S-phenylthioglycolic acids with acetic anhydride or dilute alkali gives the corresponding 3-alkyl or arylbenzothiophen.



Ortho-carboxyphenylmethylsulphide can also be cyclised to thioindoxyl.



Recently a novel ring opening of a 1,2-benzisothiazole has been reported<sup>16</sup> in which nucleophilic attack at the sulphur atom leads to opening of the thiazole ring followed by ring closure to give a 2-substituted 3-aminobenzothiophen (previously inaccessible compounds). The proposed reaction mechanisms are outlined below (a or b).



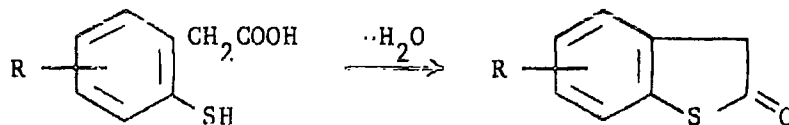
Isobenzothiazolones have also been rearranged to benzothiophens.<sup>17</sup>

As observed previously, methods involving side chain cyclisations are potentially useful for the synthesis of polyhalobenzothiophens.

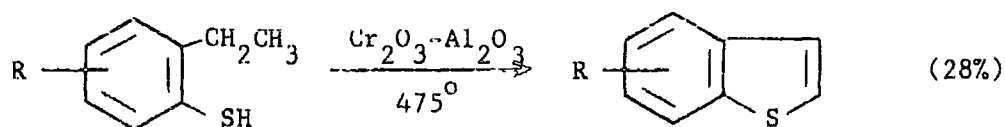
### C. Formation of the 1,2-bond on Ring Closure

#### Nucleophilic reactions

Cyclodehydration of ortho-mercaptophenylacetic acid with phosphorus pentoxide, acetic anhydride or steam and hydrochloric acid gives a convenient route to 2-hydroxybenzothiophens (thiooxindoles).

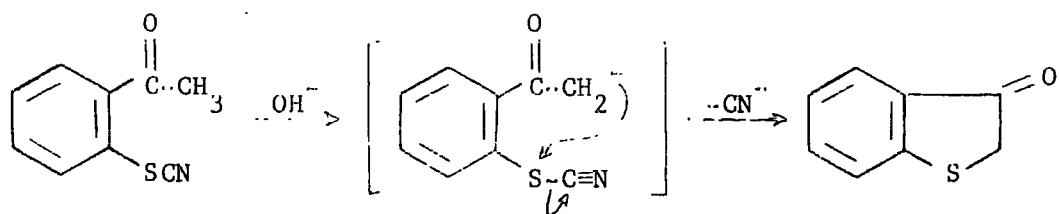


Benzothiophens are formed by passing substituted o-ethylthiophenols over a heated catalyst.<sup>18</sup>

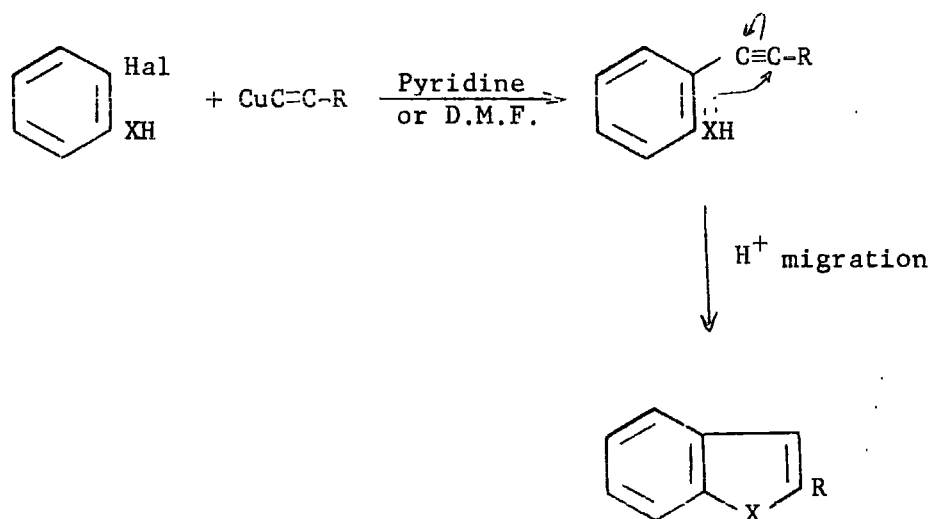


The stability to pyrolysis of polyhalobenzene derivatives could make this method useful where R = F or Cl although inaccessibility of starting materials might prove a serious limitation.

Thioindoxyl is formed from the base catalysed cyclisation of ortho-thiocyanatoacetophenone.<sup>19</sup>

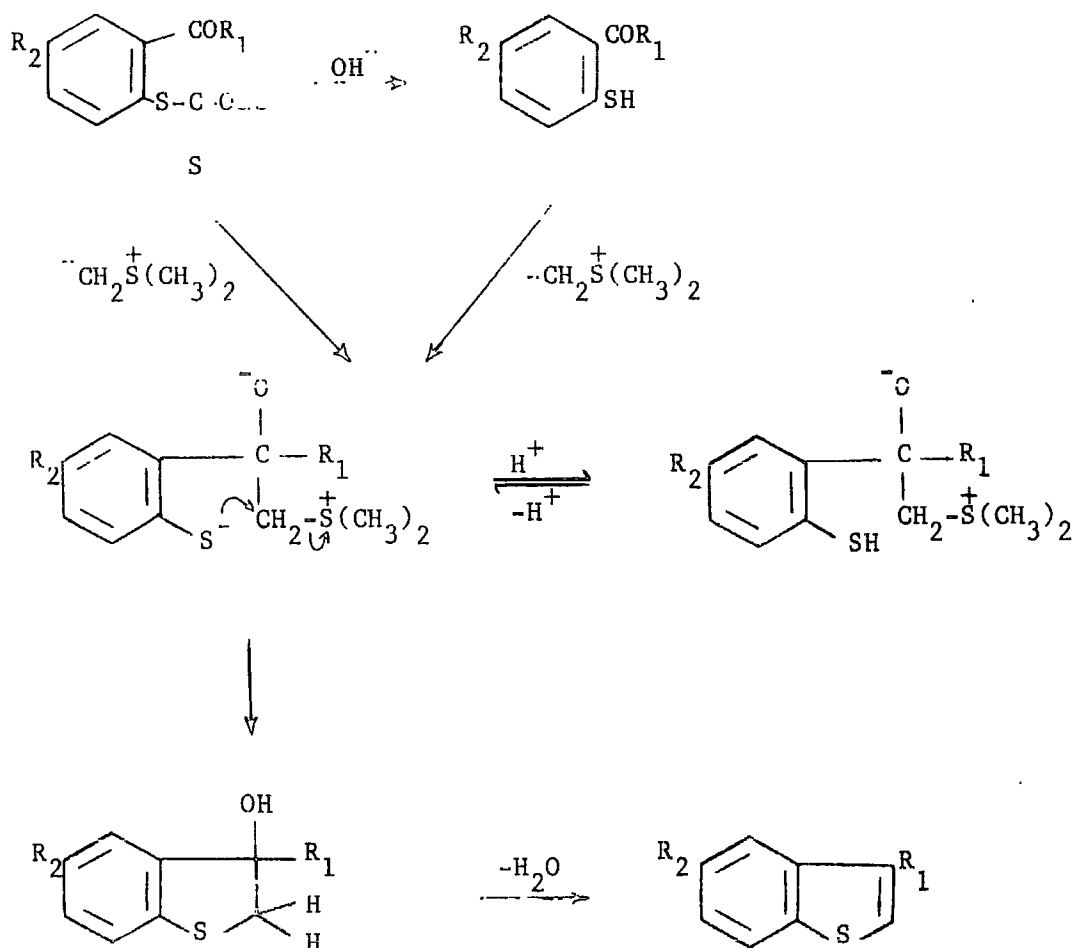


The reaction of ortho-substituted aryl halides with cuprous acetylides to give benzofurans and indoles<sup>20</sup> has been extended to the synthesis of 2-substituted benzothiophens,<sup>21</sup>



where Hal = I, Br; X = O, NH, S; R = alkyl, aryl.

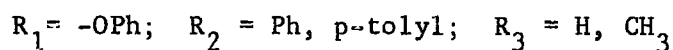
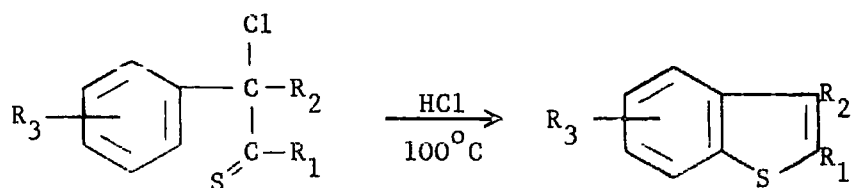
A new synthesis of substituted benzothiophens has been reported,<sup>22</sup> which utilises the reaction of ortho-mercaptoketones or the corresponding xanthates with dimethylsulphoniummethylid. The reaction scheme is outlined below. (Compare the Krollpfeiffer synthesis p.5).



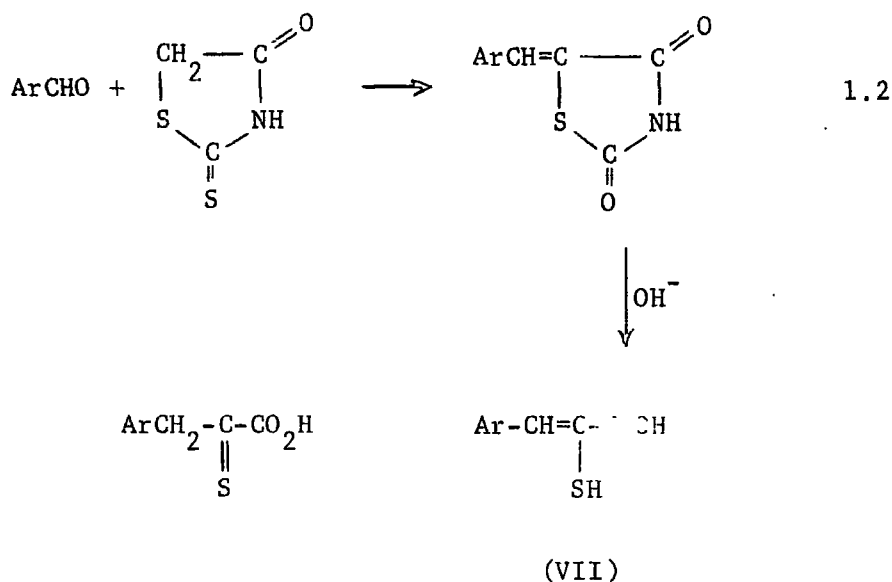
$\text{R}_1 = \text{CH}_3, \text{Ph}; \text{R}_2 = \text{Cl}, \text{H}.$

D. Formation of the 1,8-bond on Ring Closurei. Electrophilic reactions

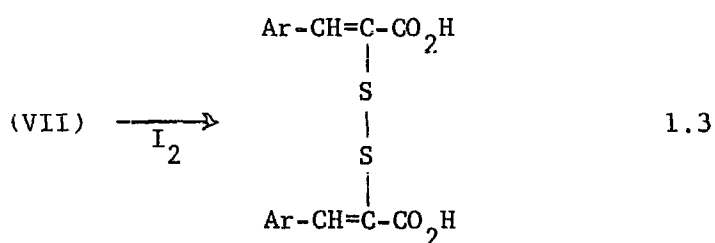
Ring closure of some substituted acetothionates to give 2,3-substituted benzothiophens has been reported<sup>23</sup> although little attention has been given to this reaction.



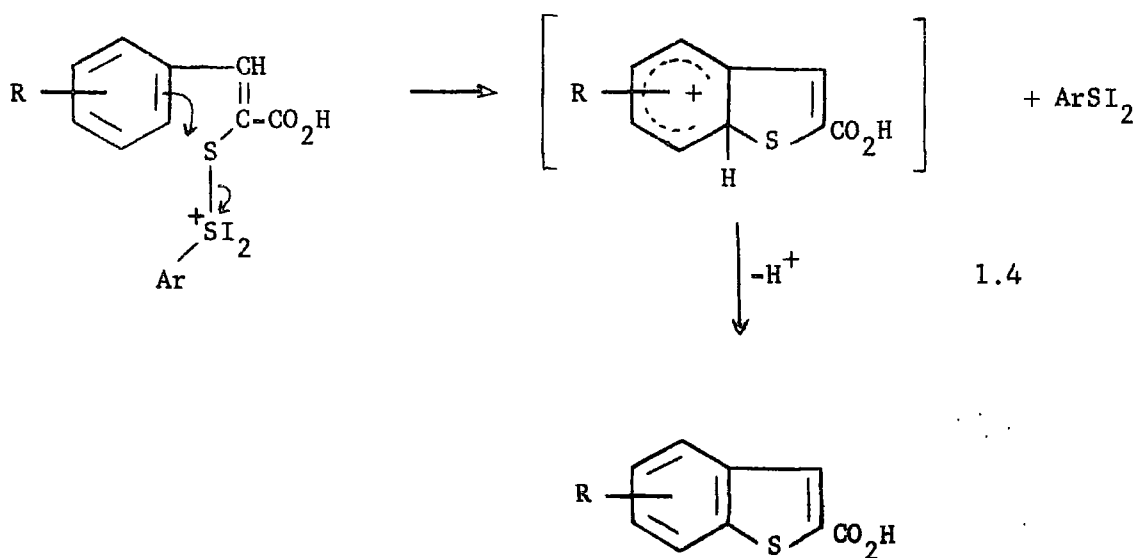
However, a related reaction of  $\beta$ -aryl- $\alpha$ -mercaptoacrylic acids has received considerable attention and has shown great utility for the preparation of substituted benzothiophen-2-carboxylic acids.<sup>24</sup> The  $\beta$ -aryl- $\alpha$ -mercaptoacrylic acids (VII) are prepared by base hydrolysis of the condensation product of an aromatic aldehyde and rhodanine (1.2).



Oxidation of (VII) with iodine or chlorine in dry dioxan gives the corresponding benzothiophen-2-carboxylic acid. An acid catalysed electrophilic mechanism has been proposed.<sup>25</sup> Oxidation by  $I_2$  or  $Cl_2$  converts (VII) into a disulphide (1.3) in a fast reaction.



Further oxidation and cyclisation of the disulphide gives the desired benzothiophen (1.4).

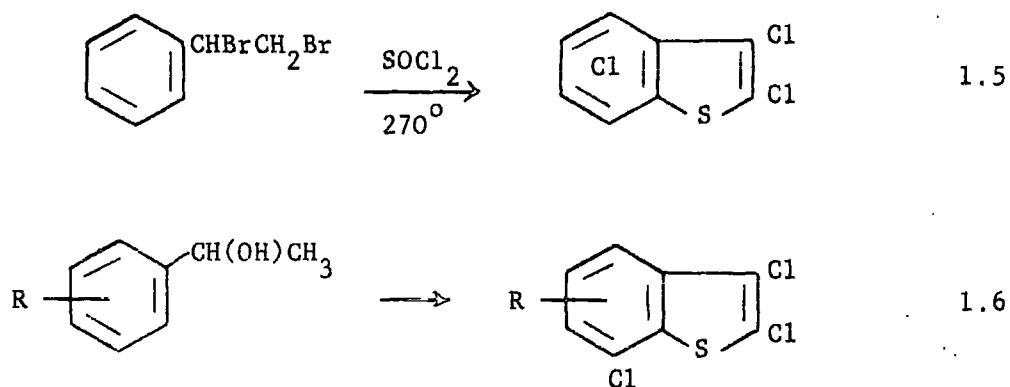


where  $\text{Ar} = \text{Ar-CH=C-CO}_2\text{H}$

The reaction is facilitated by electron releasing groups ( $\text{R} = \text{OH}, \text{OR}$ ) in accordance with this mechanism.

Improved yields have been reported from the use of chlorine in the reaction<sup>26</sup> and this method has now been extended to the synthesis of polyfluorobenzothiophens (see next section - Nucleophilic reactions). Recently interest has been revived in the reactions of sulphur chlorides ( $\text{SCl}_2$ ,  $\text{S}_2\text{Cl}_2$  and  $\text{SOCl}_2$ ) with phenylacetylene and styrene derivatives to produce chlorinated benzothiophens.<sup>27-33</sup>

As far back as 1908 Barger and Ewins<sup>34</sup> described the synthesis of highly chlorinated benzothiophens from the reactions of thionyl chloride with  $\alpha$ - $\beta$ -dibromostyrenes and substituted 1-aryl ethanols (1.5 and 1.6).



Several groups of workers<sup>28,29,31</sup> have now reported the preparation of 3-chlorobenzothiophens from the reaction of styrene and cinnamic acid derivatives with thionylchloride. Some examples are given in Fig.1.1. Nakagawa et al. have also prepared 3-chlorobenzothiophens and substituted isothiazoles from the action of sulphur monochloride on styrene derivatives.<sup>28</sup> The reactions have been shown to proceed via an intermediate sulphenyl chloride, which in some cases has been isolated.<sup>27,30,32</sup> For example, the addition of sulphur dichloride to

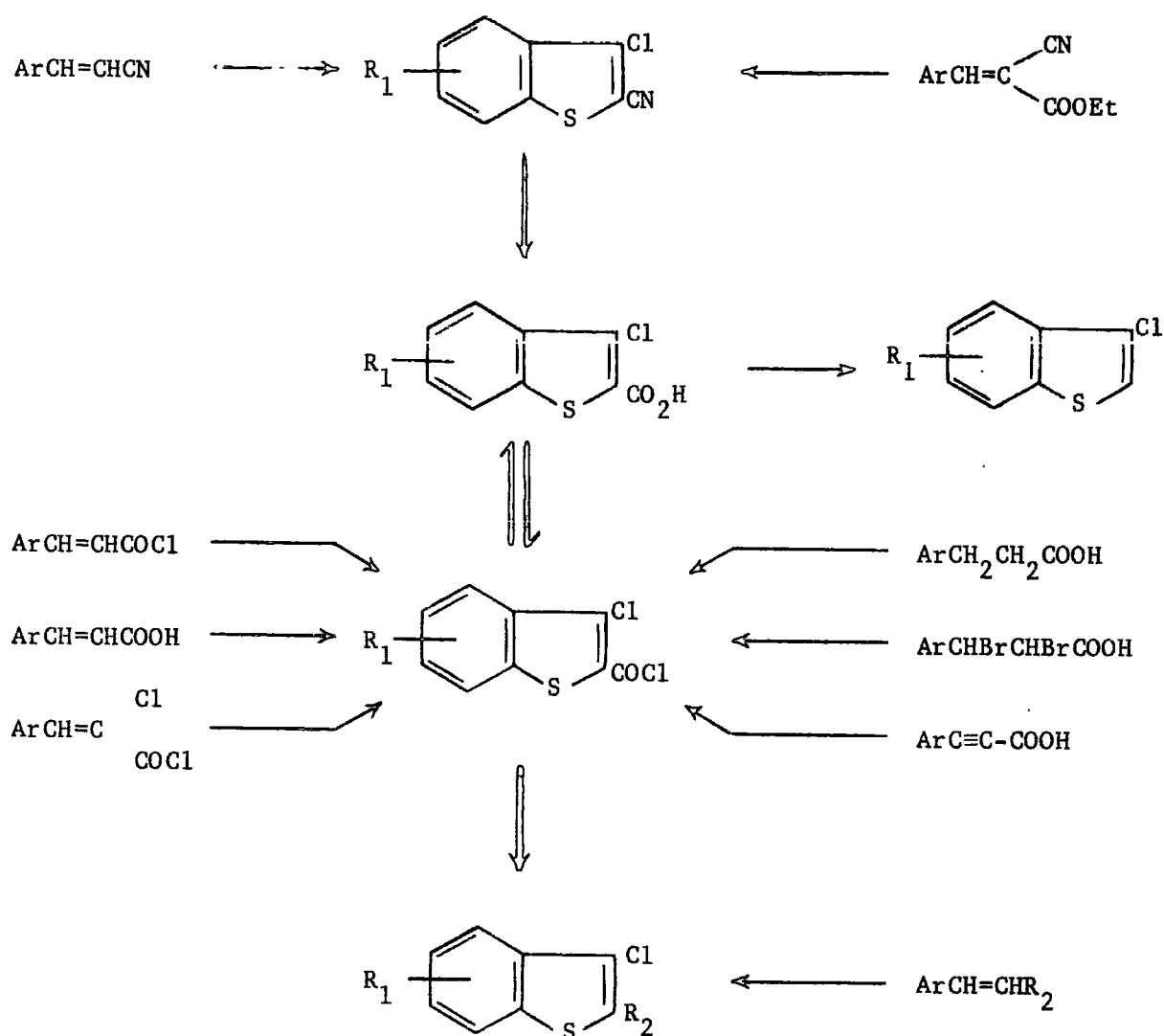


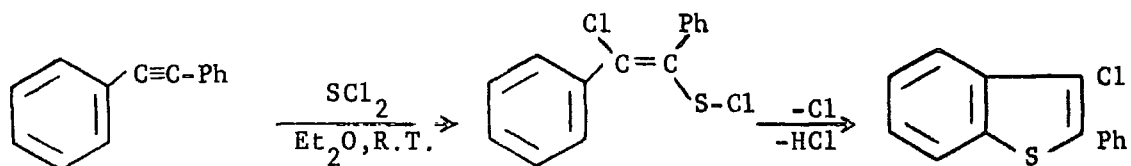
Fig.1.1<sup>a</sup>

a. adapted from Ref.28.

$\text{R}_1 = \text{H, 6-CH}_3, 4\text{-Cl, 6-Cl, 5-F, 6-F, 4,6-diCl, 6NO}_2, 6\text{CH}_3\text{O-7-Cl}$

$\text{R}_2 = \text{H, CO}_2\text{Me, CO}_2\text{Et, CHO, C}_6\text{H}_5, \text{Cl.}$

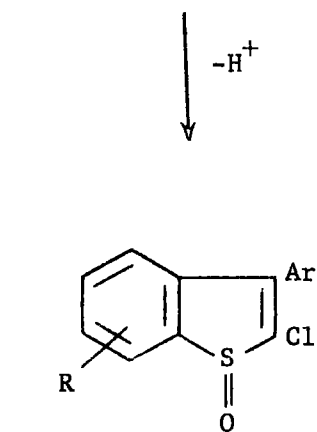
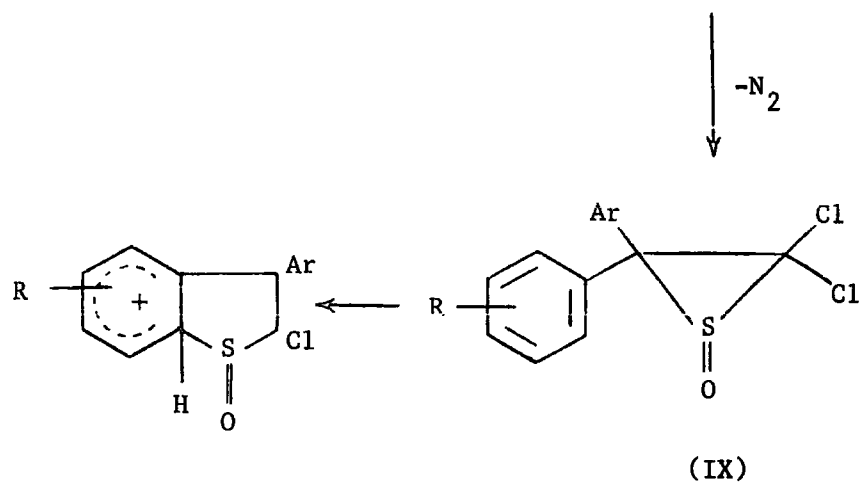
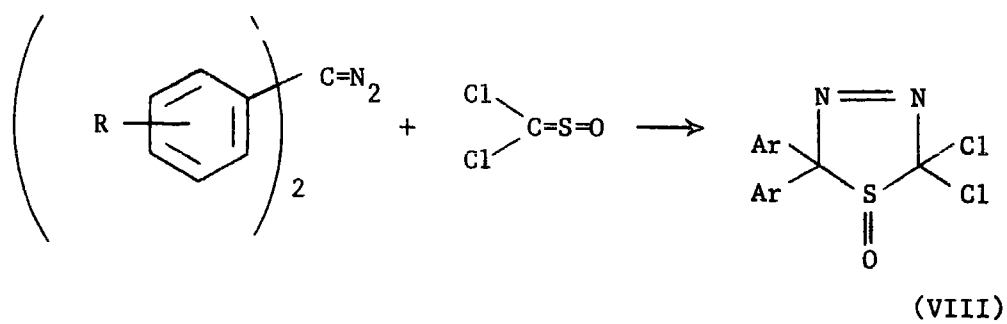
diphenyl acetylene (1.7)



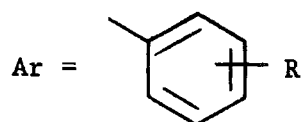
1.7

The reactions of styrene and phenylacetylene derivatives with sulphur chlorides all appear to take place by similar mechanisms. In the case of thionyl chloride reactions the detailed mechanism will be discussed in relation to the authors work on perchlorobenzothiophen (see later).

A novel reaction between dichlorosulphine and diaryldiazomethanes has recently been reported to give benzothiophen-S-oxides.<sup>33</sup> The reaction appears to proceed by a 1,3-dipolar cyclo-addition to give an intermediate thiadiazoline-S-oxide (VIII) which loses nitrogen to give an episulphoxide (IX). Spontaneous cyclisation of IX gives the corresponding benzothiophen-S-oxide (X). The proposed mechanism is outlined below.



R = H, 4-CH<sub>3</sub>, 4-Cl  
4-OCH<sub>3</sub>, 3-OCH<sub>3</sub>

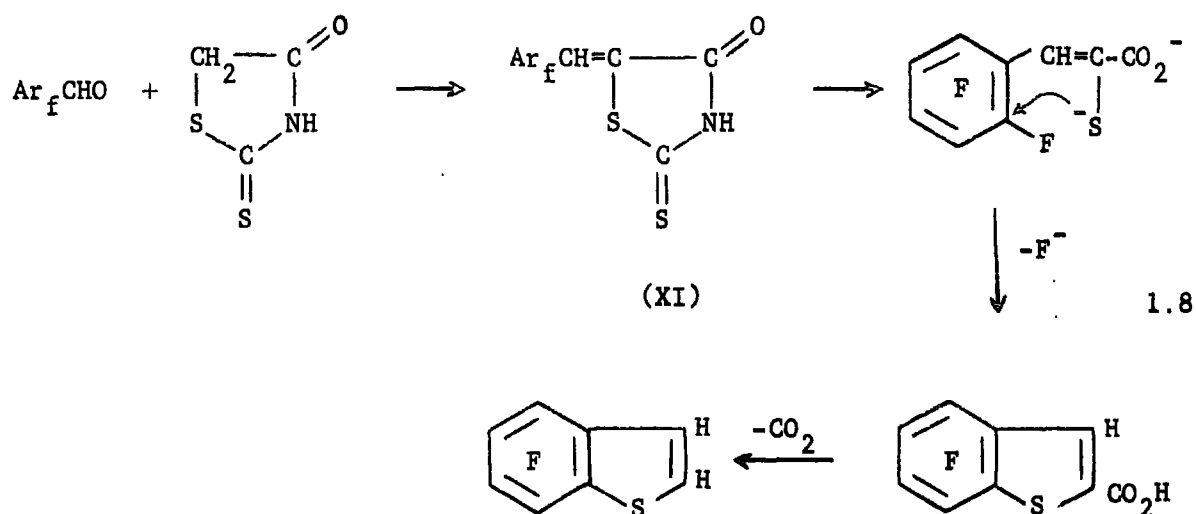


Benzothiophen 1-oxides are relatively little known compounds although a few examples have been reported;<sup>35</sup> they are normally prepared by partial oxidation of the parent benzothiophen with hydrogen peroxide and acetic acid.

ii. Nucleophilic reactions

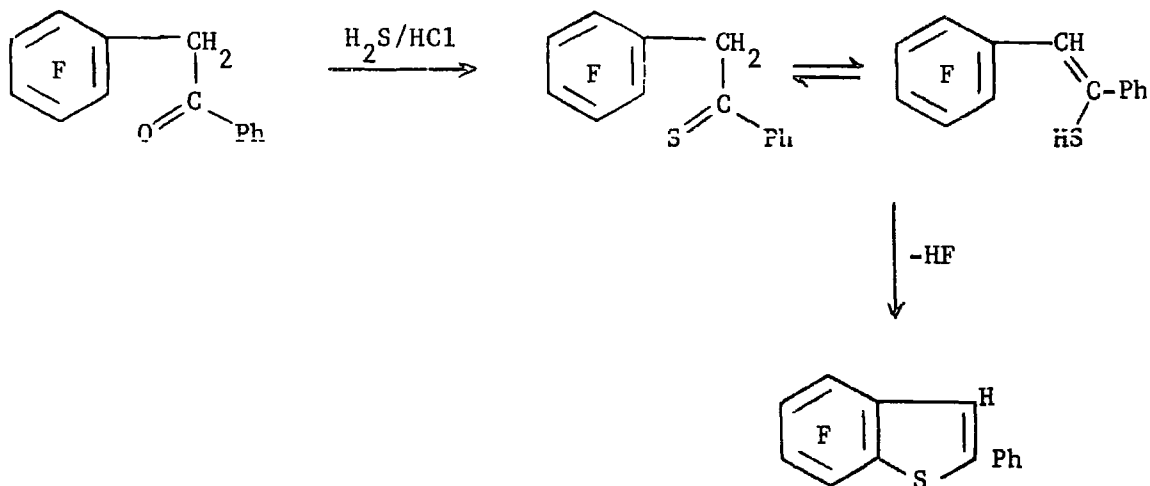
To date this has been the most widely used mechanism for the synthesis of polyhalo-benzothiophens, -benzofurans and -indoles.<sup>15,36-38</sup>

Highly fluorinated benzaldehydes readily form benzylidene derivatives (XI) with rhodanine, but on alkaline hydrolysis the  $\beta$ -polyfluoroaryl- $\alpha$ -mercapto acrylic acid formed undergoes spontaneous cyclisation to the corresponding benzothiophen-2-carboxylic acid. The latter can be readily decarboxylated to the parent polyfluorobenzothiophen (1.8).



4,5,6,7-tetrafluoro-, 4,5,7-, 4,6,7- and 5,6,7-trifluorobenzothiophens have been prepared by this method.<sup>36</sup>

Brooke<sup>37,15</sup> has shown that pentafluorophenylpropan-2-one- and pentafluorophenylacetophenone (XII) both give 2-substituted tetrafluorobenzothiophens on treatment with hydrogen sulphide and base.

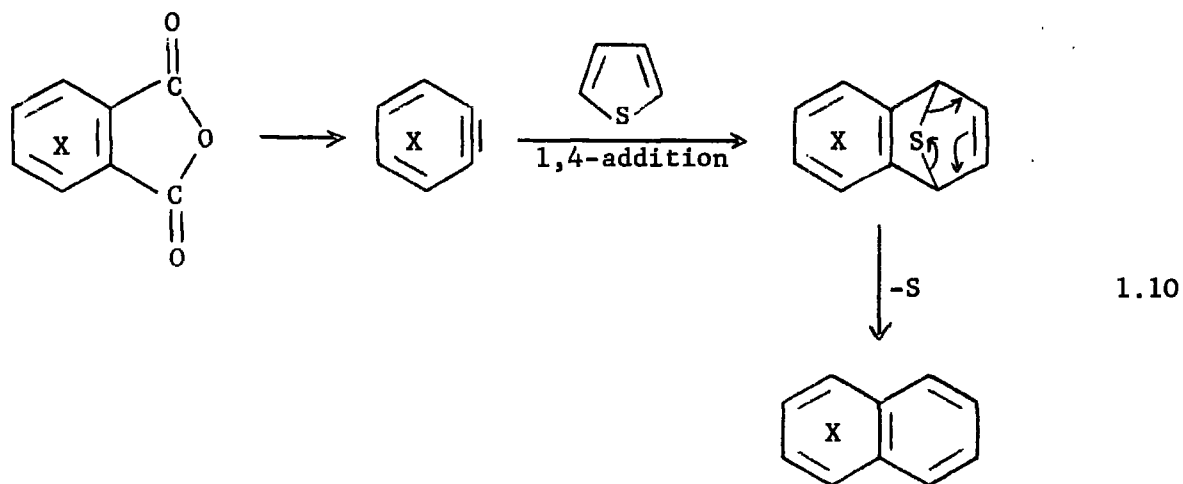
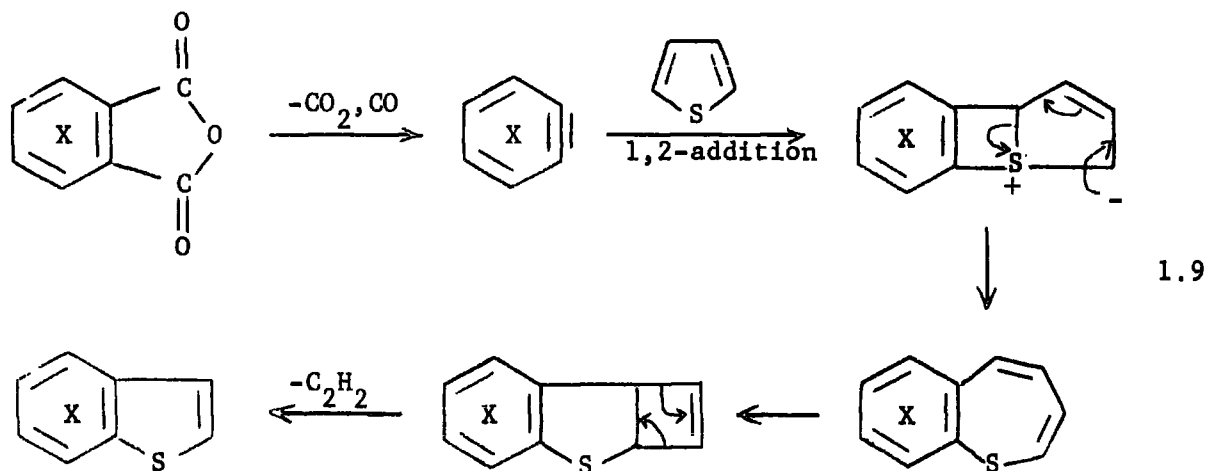


In the case of pentafluorophenylpropan-2-one a gem dithiol intermediate could be isolated. This was converted to the benzothiophen on treatment with base.

This is an ideal method of producing benzothiophens (and also benzofurans and indoles) halogenated in the benzo ring. The hetero atom acts as a good nucleophile and the polyhalobenzene nucleus is readily susceptible to nucleophilic displacement of halide ion. Thus far there have been no reports of this method being extended to the synthesis of polychlorobenzothiophens.

E. Simultaneous Formation of the 1,8 and 3,9-Bonds

Substituted benzenes, from the pyrolysis of corresponding phthalic anhydrides, react with thiophen at high temperatures to give small yields of benzothiophens by 1,2-cycloaddition and subsequent rearrangement,<sup>39</sup> (1.9). The main product, tetrachloronaphthalene is formed by 1,4-cycloaddition of benzyne and subsequent loss of sulphur (1.10). This is the main mode of addition when thiophen is reacted with benzyne generated by more 'conventional' methods at lower temperatures.<sup>40</sup>



The products from the above reactions were not isolated but the mixtures were analysed and the major constituents identified by gas chromatography-mass spectrometry. Although the reactions are not synthetically useful as such, they have led to the formation of many new thiophen derivatives, including the first report of 4,5,6,7-tetrachlorobenzothiophen.

CHAPTER 2

SYNTHESIS AND REACTIONS OF SOME HIGHLY CHLORINATED

BENZO-[b]-THIOPHENS

## Introduction

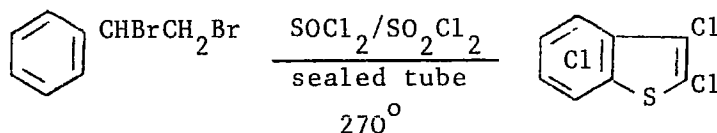
Current interest in the chemistry of highly chlorinated heteroaromatic compounds is centred mainly around nitrogen-containing six-membered ring systems related to benzene (pentachloropyridine,<sup>41</sup> tetrachloro-pyridazine,<sup>42</sup> -pyrimidine,<sup>43,44</sup> and pyrazine<sup>44</sup>) and ten-membered ring systems related to naphthalene (heptachloro-quinoline<sup>45</sup> and isoquinoline,<sup>45</sup> hexachloro-cinnoline,<sup>46</sup> phthalazine,<sup>47</sup> -quinazoline<sup>48</sup> and -quinexaline<sup>49</sup>), especially with regard to their conversion to the corresponding fluoro-analogues. Some of the wider aspects of chloroheteroaromatic chemistry are now being examined.<sup>50</sup>

Apart from the recently reported fluorination of tetrachlorothiophen,<sup>51</sup> the chemistry of highly chlorinated heteroaromatic compounds containing heteroatoms other than nitrogen has been pursued less vigorously. In this section, some studies into the chemistry of highly chlorinated benzo-[b]-thiophens are discussed.

Because of the problems often associated with structural determination in chlorocarbon chemistry, the necessity to relate products directly, or indirectly, to compounds containing hydrogen atoms directly attached to the aromatic ring system which would be amenable to examination by <sup>1</sup>H n.m.r. spectroscopy, has been borne in mind. 4,5,6,7-Tetrachlorobenzo-[b]-thiophen has been unambiguously synthesised as a model for spectroscopic examination. Some compounds have also been examined by X-ray photoelectron spectroscopy (ESCA) as part of a systematic investigation of applications of ESCA to halocarbon chemistry.

Synthesis of 2,3,4,5,6,7-Hexachlorobenzo-[b]-thiophen(I)

In 1908 Barger and Ewins<sup>52</sup> reported the synthesis of a number chlorinated benzo-[b]-thiophen derivatives from the reaction of substituted 1-phenyl ethanols and styrene derivatives with thionyl chloride. Hexachlorobenzo-[b]-thiophen(I) was prepared by the reaction of thionyl and sulphuryl chlorides with dibromostyrene, in a sealed tube at 270°.



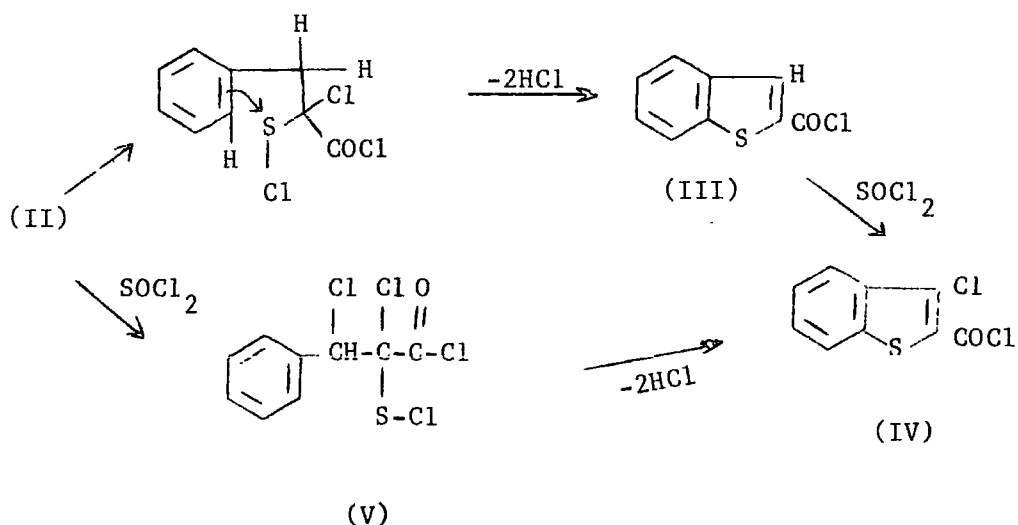
(I)

The authors could not obtain a benzo-[b]-thiophen derivative from either  $\alpha$ ,  $\beta$ -dichloroethylbenzene or 1-phenylethanol although, in a similar reaction it was claimed that 1-(4-methoxyphenyl)ethanol gave a mixture of trichloro- and tetrachloro-6-methoxybenzo-[b]thiophens. No mechanism was proposed for the reaction and until recently little interest was shown in the preparation of benzo-[b]-thiophen derivatives from sulphur chlorides.

Several groups of workers have now reported the synthesis of benzo-[b]-thiophen derivatives from the reaction of sulphur chlorides ( $\text{SOCl}_2$ ,  $\text{SCl}_2$ ,  $\text{S}_2\text{Cl}_2$ ) with acetylenes,<sup>27,28</sup> cinnamic acids,<sup>28-32</sup> styrenes<sup>28</sup> and 3-phenylpropionic acids.<sup>28,30</sup> Experimental details were given in only two cases.<sup>27,29</sup> In a series of papers Krubsack and Higa<sup>30-32</sup> have elucidated the mechanism for the reactions, and Nahagawa et al. have shown<sup>28</sup> that substituted benzo-[b]-thiophens can be synthesised from the reaction of a wide variety of precursors with thionyl chloride in the presence of pyridine. A comparison between these recent reactions and the earlier

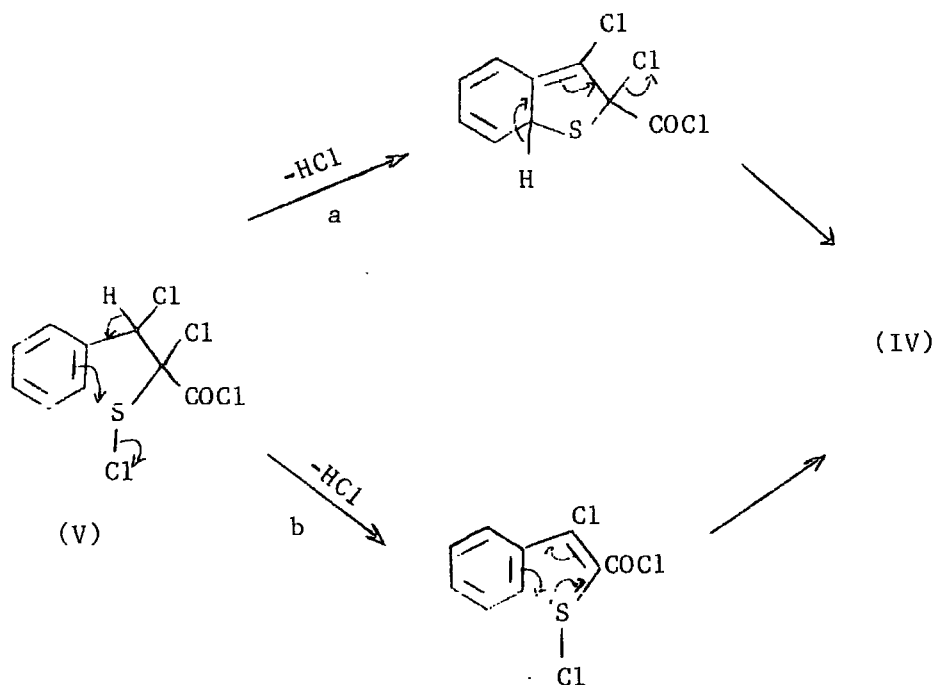


identical conditions, (IV) was formed only slowly and in poor yield. This suggested that further chlorination took place before cyclisation and that the sulphenyl chloride (V) might be an intermediate.



(V) could be prepared independently from the reaction of cinnamic acid with thionyl chloride in the presence of pyridine and readily cyclised to (IV) under conditions identical to the ones used previously.

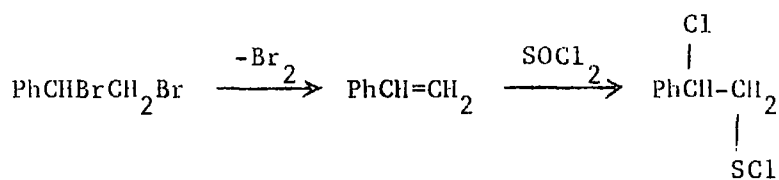
Cyclisation of (V) by electrophilic or nucleophilic reactions ~~were~~ discounted on the basis of the relative ease of reaction of meta-nitro- and meta-methoxy-cinnamic acids with thionyl chloride. Krubsack and Higa proposed a concerted cyclisation of (V) to account for their observations.



The two mechanisms (a and b) differ by whether the benzylic hydrogen is lost simultaneous with, or prior to, cyclisation.

If this mechanism is correct and the sulphenyl chloride (V) is an intermediate in the reaction, then it will also account for the formation of 2-substituted-3-chloro-benzo-[b]-thiophens from precursors of the form  $\text{Ph-CH=CHR}$ , with either  $\text{SCl}_2$  or  $\text{SOCl}_2$  and pyridine ( $\text{R} = \text{H}, \text{CO}_2\text{H}, \text{CN}, \text{CHO}, \text{CO}_2\text{Et}, \text{C}_6\text{H}_5$ ).<sup>28</sup> The mechanism may also apply to the synthesis of perchlorobenzo-[b]-thiophen(I) from dibromostyrene and thionyl chloride.<sup>52</sup>

Nahagawa et al. have reported that styrene gives 2,3-dichloro-benzo-[b]-thiophen and dibromocinnamic acid gives 3-chloro-2-chlorocarbonyl benzo-[b]-thiophen with thionyl chloride and pyridine.<sup>28</sup> These two facts indicate that the first step in the synthesis of (I) might be loss of elemental bromine from dibromostyrene to give styrene which can then react with thionyl chloride to give the sulphenyl chloride (VI)



(VI)

Cyclisation of (VI) to 2,3-dichlorobenzo-[b]-thiophen and further free radical chlorination (in the presence of  $\text{SO}_2\text{Cl}_2$ ) would give (I).

Although this may seem an excellent route to highly chlorinated benzo-[b]-thiophens, using relatively cheap and readily available starting materials, the reaction suffers from several severe drawbacks.

In a typical reaction, 1.5 gms of dibromostyrene, 5 ml. of thionyl chloride and 2 ml. of sulphuryl chloride were heated to  $270^\circ$  in a Carius tube for 13 hr. On cooling, crystals of perchlorobenzo-[b]-thiophen could be filtered off from the red liquid in the tube.

(i) The reaction only proceeds in sealed glass tubes. Attempts to carry out the reaction in nickel or stainless steel autoclaves produced only decomposition products.

(ii) The yield of perchlorobenzo-[b]-thiophen is extremely variable ranging from 0% to a maximum of 55% even when attempts were made to keep conditions in each Carius tube as identical as possible.

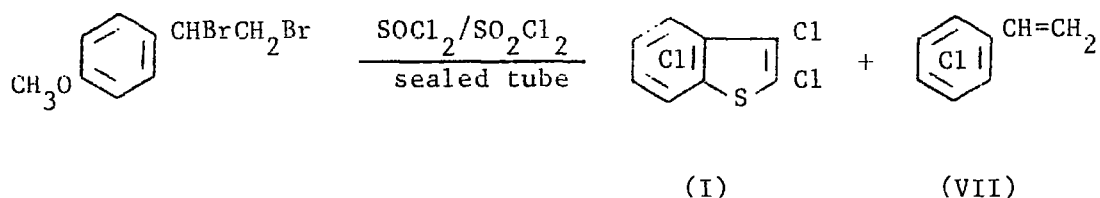
(iii) High pressures produced in the Carius tubes (especially at  $270^\circ$ ) limit the maximum scale of the reaction because of the relatively low pressures that glass tubing can contain.

Factors (i) and (iii) are technological problems that may be overcome by using high pressure glass-lined autoclaves, but (ii) would still appear to limit the usefulness of the reaction.

Attempted Preparation of 6-methoxy-2,3,4,5,7-pentachlorobenzo-[b]-thiophen

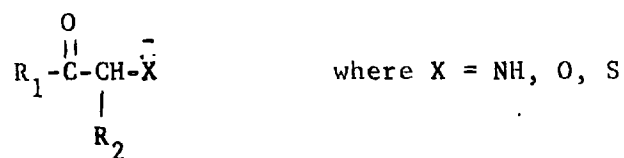
In an attempt to synthesise highly chlorinated benzothiophens with substituents in well defined positions, the reaction between para-methoxy-dibromostyrene, thionyl chloride and sulphuryl chloride in a sealed tube, at  $\sim 200^{\circ}$  was examined. Barger and Ewins<sup>52</sup> reported the preparation of trichloro- and tetrachloro-6-methoxybenzo-[b]-thiophens from the reaction of 1 (4 methoxyphenyl)ethanol with thionyl chloride and Krubsack and Higa<sup>32</sup> have reported the preparation of methoxy substituted-3-chlorobenzo-[b]-thiophens from cinnamic acid derivatives and thionyl chloride.

However, the reaction of para-methoxydibromostyrene with thionyl and sulphuryl chloride, under a variety of conditions, produced only two products - perchlorobenzo-[b]-thiophen (I) and pentachlorostyrene<sup>53</sup> (VII)

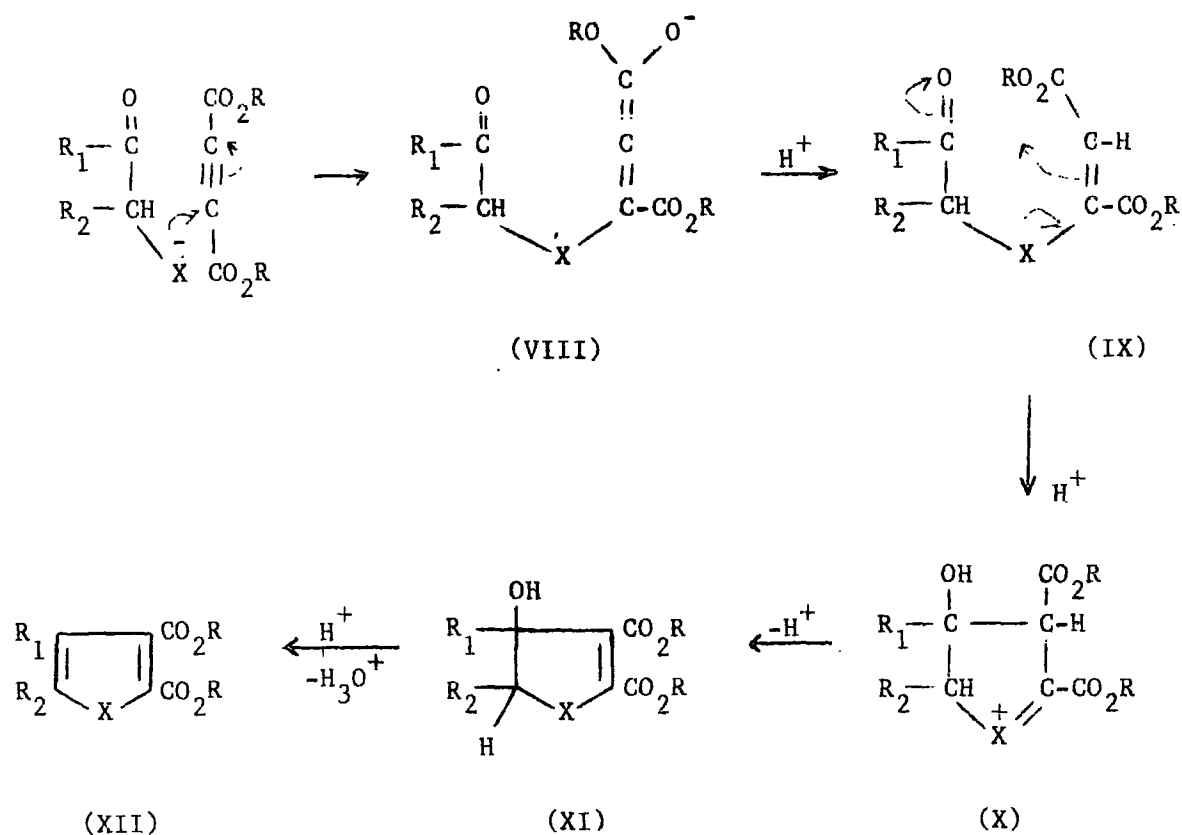


Under the conditions of the reaction ( $\sim 200^{\circ}$ , excess  $\text{SOCl}_2/\text{SO}_2\text{Cl}_2$ ) the methoxy group is completely lost, probably by a free radical displacement reaction. The production of (VII) can be rationalised if some chlorination of the phenyl ring takes place before cyclisation and if addition of thionyl chloride to the double bond is reversible under the conditions employed. No evidence could be obtained for the presence of methoxy containing compounds in the reaction product. Some pentachloro styrene is also formed in low yield in the preparation of (I) from dibromo styrene.



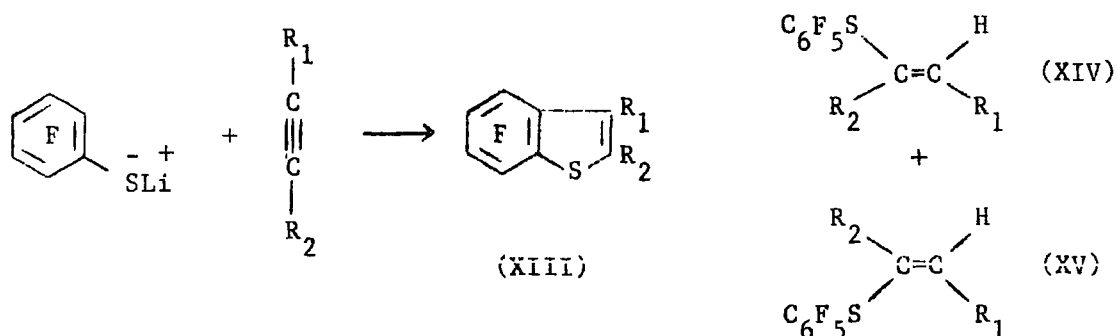


The proposed mechanism for the reactions (normally run in methanol) is outlined below.



A simple trans-addition product (IX) is first formed through protonation of the enolatic anion (VIII) and this can cyclise via (X) to (XII). In some cases the alcohol (XI) could be isolated in good yield and converted to (XII) with acid. In the case of sulphur heterocycles ( $\text{X}=\text{S}$ ) a Dieckmann-type cyclisation was proposed because the intermediate (X) would not be favourable for sulphur.

Brooke and Quasem<sup>14,15</sup> have studied the addition of lithium pentafluorobenzenethiolate to acetylenes in tetrahydrofuran.



- $\text{R}_1 = \text{R}_2 = \text{CO}_2\text{Et}$
- $\text{R}_1 = \text{CO}_2\text{Et}, \text{R}_2 = \text{H}$
- $\text{R}_1 = \text{CO}_2\text{Et}, \text{R}_2 = \text{Ph}$
- $\text{R}_1 = \text{R}_2 = \text{Ph}$
- $\text{R}_1 = \text{R}_2 = \text{CF}_3$

The reaction of lithium pentafluorobenzenethiolate with diethyl acetylenedicarboxylate (a) gave only the corresponding benzo-[b]-thiophen (XIIIa) and none of the olefinic products, even at very low temperatures. In the case of acetylenes (c) and (e) both cyclised products and olefins were formed although the latter were in less than 5% overall yield. In marked contrast, acetylenes (b) and (d) gave no cyclised material with the lithium thiolate but both isomeric olefins were formed, corresponding to overall cis- and trans-addition of  $\text{C}_6\text{F}_5\text{SH}$  to the acetylenes. Problems presented by the different products formed from the various acetylenes could not be resolved but the apparent violations of the "trans-addition rule" were explained by isomerisation of the intermediate vinyl-lithium derivatives.



no cyclised material was formed and the sole product was the olefin (XVIIb) [52.5%].

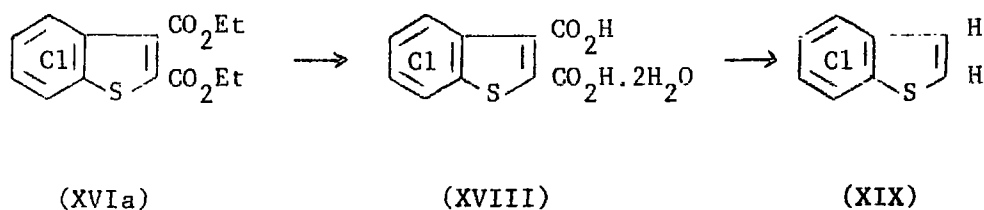
The stereochemistry of the two olefins (XVIIa and b) could be assigned on the basis of their  $^1\text{H}$  n.m.r. spectra. Delfini,<sup>57</sup> and Winterfeldt and Preuss<sup>58</sup> have assigned the stereochemistry of olefins, obtained from the addition of a variety of nucleophiles to ethyl propiolate and diethyl acetylenedicarboxylate, from  $^1\text{H}$  n.m.r. data. Brooke et al. have given  $^1\text{H}$  n.m.r. data for the products obtained from the addition of pentafluoroaniline to diethyl acetylenedicarboxylate<sup>62</sup> and pentafluorothiophenol to ethyl propiolate.<sup>15</sup> The data is summarised in Table 2.1.

The  $^1\text{H}$  n.m.r. spectrum of olefin (XVIIb) showed a triplet for the methyl protons at 8.87 $\tau$  a quartet for the methylene protons at 5.78 $\tau$  ( $J = 7.0\text{Hz}$ ) and two doublets at 4.1 $\tau$  and 3.23 $\tau$ . The stereochemistry of the olefin was assigned as cis on the basis of both the coupling constant ( $J = 9.9\text{ Hz}$ )<sup>63</sup> and chemical shifts of the olefinic protons. The  $^1\text{H}$  n.m.r. spectrum of olefin (XVIIa) showed two overlapping triplets due to the methyl protons at 8.96 $\tau$  and 8.70 $\tau$ , two overlapping quartets due to methylene protons at 6.03 $\tau$  and 5.79 $\tau$  [ $J = 7.2\text{ Hz}$ ] and a singlet due to the olefinic proton at 3.38 $\tau$ . The chemical shift of the olefinic proton is characteristic of the trans-olefin (see Table 2.1) Both olefins are the products of overall trans-addition to the acetylenes. In neither case was any evidence found for olefins arising from overall cis-addition.

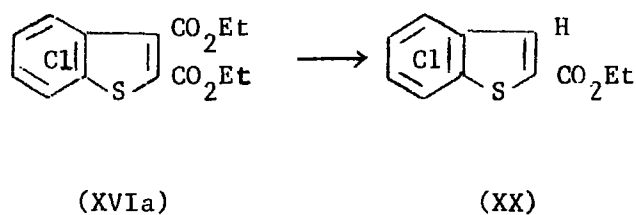
Hydrolysis of the diester (XVIa) with either 50% sulphuric acid or aqueous alkali gave the hydrated dicarboxylic acid (XVIII) [86%] which in turn was decarboxylated by copper in quinoline to give 4,5,6,7-tetrachloro-benzo-[b]thiophen (XIX) [52%]. The  $^1\text{H}$  n.m.r. spectrum of (XIX) gave the

TABLE 2.1

R	trans		cis		trans			cis		
	EtO <sub>2</sub> C	H <sub>A</sub>	EtO <sub>2</sub> C	CO <sub>2</sub> Et	H <sub>A</sub>	H <sub>B</sub>	J <sub>AB</sub>	H <sub>A</sub>	H <sub>B</sub>	J <sub>AB</sub>
	H <sub>A</sub> (τ)		H <sub>A</sub> (τ)		H <sub>A</sub> (τ)	H <sub>B</sub> (τ)	J <sub>AB</sub> (Hz)	H <sub>A</sub> (τ)	H <sub>B</sub> (τ)	J <sub>AB</sub> (Hz)
	3.85		4.69		2.49	4.69	(13.5)	3.36	4.87	(9.0)
CH <sub>3</sub> O- <sup>58</sup>	3.90		4.85		2.45	4.85	(12.5)	3.60	5.30	(7.0)
(CH <sub>3</sub> ) <sub>2</sub> CHO- <sup>58</sup>	3.90		4.90		2.55	4.85	(12.5)	3.55	5.35	(7.0)
C <sub>6</sub> H <sub>5</sub> O- <sup>58</sup>	3.55		4.95		2.25	4.45	(12.5)	3.15	4.90	(7.0)
C <sub>6</sub> F <sub>5</sub> S- <sup>15</sup>					2.56	4.37	(15.0)	3.15	4.02	(10.0)
C <sub>6</sub> F <sub>5</sub> NAC- <sup>62</sup>	3.1		4.5							



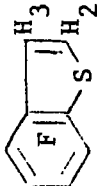
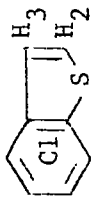
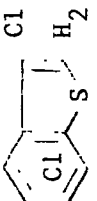
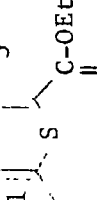
coupling constant  $J_{2,3} = 5.5$  Hz which is typical for this substitution pattern,<sup>64</sup> while the actual identity of the protons was determined from the relative shifts in the absorptions on changing solvents. It has recently been shown for benzo-[b]-thiophen, that while overall deshielding of protons occurs in acetone relative to carbon tetrachloride, the effect is particularly marked at position 2. [Solvent shift = 0.27 ppm. cf. 0.15 ppm for position 3].<sup>65a</sup> On this basis, the absorption centred at  $2.46\tau$  ( $\text{CCl}_4$ ) and  $1.96\tau$  (acetone) [solvent shift = 0.50 ppm] was assigned to H<sub>2</sub>, and that centred at  $2.56\tau$  ( $\text{CCl}_4$ ) and  $2.38\tau$  (acetone) [solvent shift = 0.18 ppm] to H<sub>3</sub>. The much larger solvent shift of H<sub>2</sub>, relative to all other positions, can be particularly useful for structure determinations in these highly chlorinated systems. Recently, Yuste and Walls<sup>65b</sup> have reported the use of  $^1\text{H}$  n.m.r. pyridine-induced solvent shifts in structure determinations of substituted benzo-[b]-furans.



Reaction of the diester (XVIa) with 1 mole equivalent of base in refluxing pyridine gave a monoethyl ester (XX, 81%) as the sole product. Hydrolysis and subsequent decarboxylation of only one ester group had taken place under the reaction conditions. It was possible to identify the product as ethyl 4,5,6,7-tetrachlorobenzo-[b]-thiophen-2-carboxylate (XX) from measurements of its  $^1\text{H}$  n.m.r. spectra in carbon tetrachloride and acetone. Table 2.2 gives solvent shift measurements for a series of benzo-[b]-thiophens. Both 4,5,6,7-tetrafluoro and tetrachlorobenzo-[b]-thiophens show a solvent shift (from  $\text{CCl}_4$  to acetone) of 0.5 ppm (30 Hz) for the 2-proton and much smaller shifts of 0.1 ppm (6 Hz) and 0.18 ppm (10 Hz) respectively for the 3-proton. Introduction of an acetyl group at position 3 in the tetrafluorobenzo-[b]-thiophen causes an increase of 0.71 ppm (43 Hz) in the solvent shift of the 2-proton to 1.21 ppm (73 Hz). Introduction of a chlorine at position 3 in the chloro-derivatives causes an increase of approximately 0.08 ppm (5 Hz) in the solvent shift of the 2-proton.

The carbonyl group in the tetrachloromono ester benzo-[b]-thiophen could be at either position 2 or 3. If it was at position 3 an increase in the solvent shift of the 2-proton would be expected. However, the measured shift of 0.37 ppm (22 Hz) is actually less than that of the 2-proton in 4,5,6,7-tetrachlorobenzo-[b]-thiophen but slightly greater than that for the 3-proton. Therefore the most likely position of the carbonyl group is position 2 and the structure can be assigned as (XX). Brooke<sup>62</sup> has reported that the alkaline hydrolysis of diethyl 4,5,6,7-tetrafluoroindole-2,3-dicarboxylate is accompanied by partial decarboxylation to give the 2-carboxylic acid.<sup>65b</sup>

TABLE 2.2

												
	H <sub>2</sub>	H <sub>3</sub>	H <sub>2</sub>	H <sub>3</sub>	H <sub>2</sub>	H <sub>3</sub>	H <sub>2</sub>	H <sub>6</sub>	H <sub>2</sub>	H <sub>6</sub>	H <sub>2</sub>	H <sub>3</sub>
$\tau(\text{CCl}_4)$	2.6	2.6	2.63	2.56	2.6	2.56	2.6	2.54	2.6	2.54	2.6	2.14
$\tau(\text{Acetone})$	2.1	2.5	1.42	2.38	2.02	2.38	2.02	2.29	2.04	2.29	2.04	1.77
$\Delta$ ppm	0.5	0.1	1.21	0.18	0.58	0.18	0.58	0.25	0.56	0.25	0.56	0.37
$\Delta$ Hz	30.0	6.0	73.0	10.0	35.0	10.0	35.0	15.0	34.5	15.0	34.5	22.0

Some Reactions of 2,3,4,5,6,7-Hexachlorobenzo-[b]-thiophen

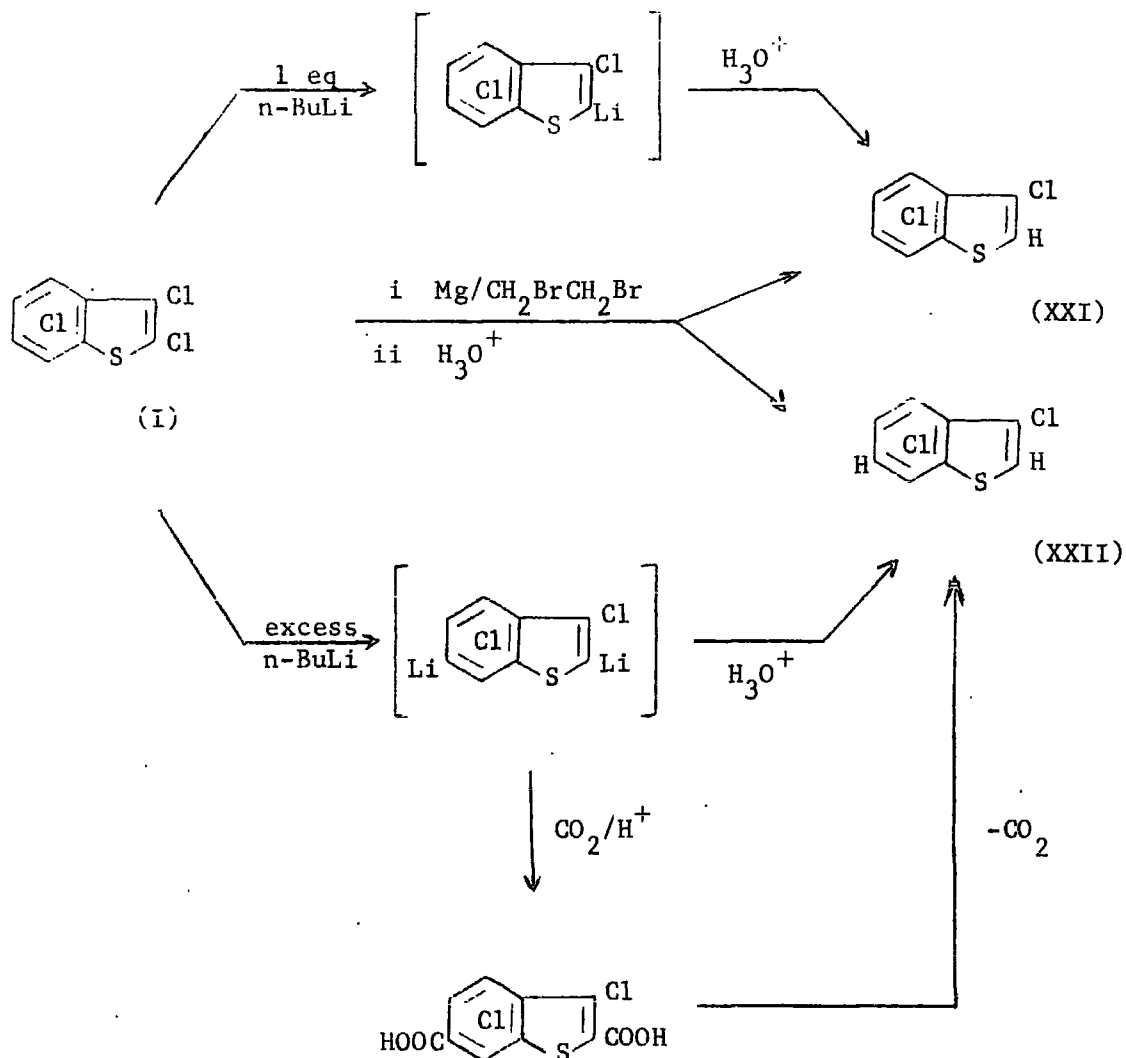
(i) Metallation reactions

Metallation of benzo-[b]-thiophen has been shown to occur at position 2.<sup>66</sup> Benzo-[b]-thiophens can be metallated in other positions by use of the appropriate bromo derivative. Metallation of 5-bromobenzo-[b]-thiophen with one molar equivalent of n-butyllithium gives the 5-bromo-2-benzo-[b]-thionyllithium but, with 2 molar equivalents of n-butyllithium a dilithium compound is obtained which on carbonation affords the 2,5-dicarboxylic acid.<sup>67</sup> 2,3-dibromobenzo-[b]-thiophen with excess n-butyllithium gives only the 2-lithio derivative.<sup>68</sup> The 2,3-dilithio compound can be prepared by treating the 3-bromo-2-benzo-[b]-thionyllithium with powdered lithium.<sup>69</sup> The 2,3-dilithio derivative may also be prepared by treating 3-bromobenzo-[b]-thiophen with 2 molar equivalents of n-butyllithium. 3-benzo-[b]-thionyllithium has been prepared from the 3-bromobenzo-[b]-thiophen using one equivalent of n-butyllithium in ether at  $-70^{\circ}$  and has been shown to be a useful intermediate for the preparation of 3-substituted benzo-[b]-thiophens.<sup>70</sup> Some of these have been prepared from the 3-benzo-[b]-thionylmagnesium halides but because the Grignard compounds have to be synthesised by the entrainment procedure, yields are often variable. Metal halogen exchange does not take place with 3-chlorobenzo-[b]-thiophen since with n-butyllithium only 3-chloro-2-benzo-[b]-thionyllithium<sup>71</sup> is formed.

Treatment of hexachlorobenzo-[b]-thiophen in tetrahydrofuran with one molar equivalent of n-butyllithium followed by hydrolysis gave 3,4,5,6,7-pentachlorobenzo-[b]-thiophen (XXI, 56%) accompanied by unchanged starting material (I, 39%) showing that metal-halogen exchange

was incomplete. The structure of (XXI) was determined by  $^1\text{H}$  n.m.r. spectroscopy from the large downfield shift (0.58 ppm) of the absorption in changing from carbon tetrachloride to acetone as solvent (Table 2.2). In an attempt to drive the metal halogen exchange to completion, (I) was treated with excess n-butyllithium (6 equivalents) in tetrahydrofuran and hydrolysed. Thin layer chromatography showed the absence of both (I) and (XXI) and the presence of two new components. The major component (XXII, 89%) was 3,4,5,7-tetrachlorobenzo-[b]-thiophen while the minor component, an oil was not examined. The two protons were identified at positions 2(2.6 $\tau$ ,  $\text{CCl}_4$ ) and 6(2.54 $\tau$ ,  $\text{CCl}_4$ ) by  $^1\text{H}$  n.m.r. spectroscopy. Both protons showed a downfield shift in acetone (relative to  $\text{CCl}_4$ ), but one proton was readily assigned to position 2 from its larger solvent shift (0.56 ppm compared to 0.25 ppm for the other proton). The protons were coupled ( $J = 0.6$  Hz) which is characteristic of the long range coupling associated with H2 and H6 ( $J_{2,6} = 0.5-0.6$  Hz).<sup>64</sup> H2 has been shown to couple only with H3 and H6 although peak broadening has been attributed to coupling of H7 and H5 with H2 ( $J_{2,7}$  and  $J_{2,5} < 0.03$  Hz)<sup>65,72</sup>

When (I) was treated with excess n-butyllithium in tetrahydrofuran followed by carbonation a dicarboxylic acid was formed ( $M = 358$ ) which was not characterised but was decarboxylated by copper in quinoline to (XXII).



The preparation of Grignard reagents from aryl halides has been extensively studied and the 'entrainment' method using ethylene dibromide has been widely used to obtain Grignards from unreactive aromatic and heterocyclic halides.<sup>73-75</sup>

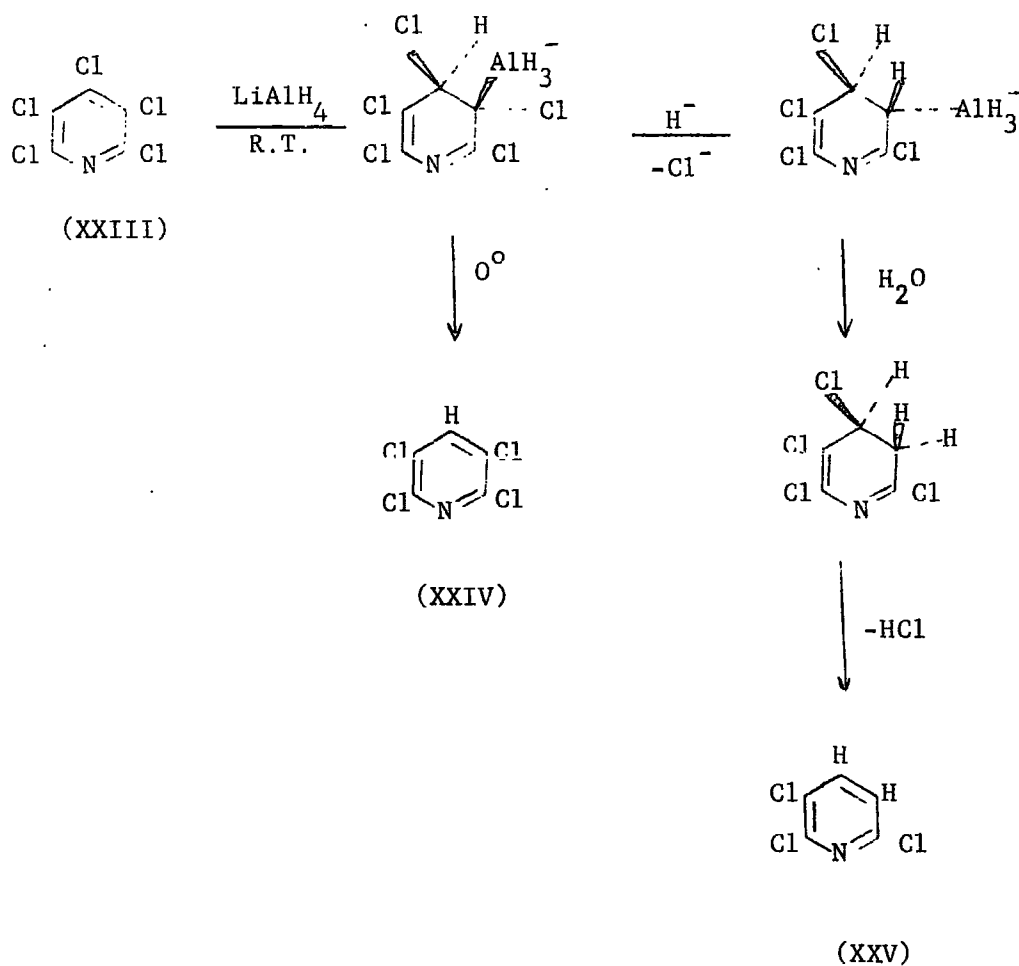
Reaction of (I) in tetrahydrofuran with excess magnesium at room temperature (using ethylene dibromide to start the reaction), followed by hydrolysis, gave an equimolar mixture of (XXI, 29%) and (XXII, 29%) together with unchanged starting material (I, 29%). The reaction

products were separated by column chromatography from starting material (I) but no separation of (XXI) and (XXII) was achieved.

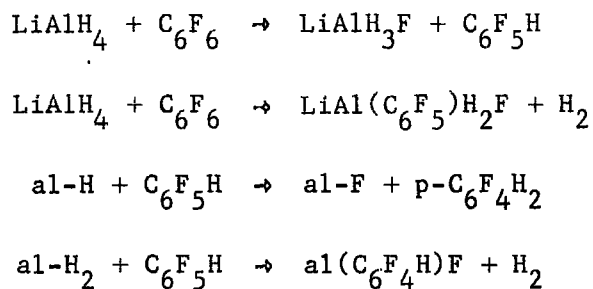
The  $^1\text{H}$  n.m.r. spectrum of the mixture in carbon tetrachloride showed two absorptions at  $2.54\tau$  (one proton) and  $2.6\tau$  (two protons). In acetone the spectrum could be resolved into three absorptions at  $2.29\tau$ ,  $2.04\tau$  and  $2.02\tau$  (one proton each). When the reaction was repeated under more forcing conditions (3 hr. reflux) the only product isolated after hydrolysis was compound (XXII, 9%). Although (XXI) could be separated from a mixture of (XXI) and (XXII) by fractional recrystallisation from light petroleum (b.p.  $40-60^\circ$ ) it was found impossible to produce either compound alone in good yield, a mixture was always obtained, usually containing unreacted starting material (I).

(ii) Reduction reactions

Suschitzky et al.<sup>76</sup> have investigated the reduction of pentachloropyridine with complex metal hydrides and have shown that an addition-elimination reaction takes place in the case of lithium aluminium hydride reduction. The products obtained depended critically on the reaction temperature, at  $0^\circ\text{C}$  the major product from the reaction of pentachloropyridine (XXIII) with lithium aluminium hydride in ether at  $0^\circ\text{C}$  was 2,3,5,6-tetrachloropyridine (XXIV, 80%). At room temperature the main product was 2,3,6-trichloropyridine (XXV, 75%). The proposed mechanism is outlined below.



However, Dickson and Sutcliffe<sup>77</sup> found that in the reaction of lithium aluminium hydride with hexafluoro-, pentafluoro-, and tetrafluorobenzenes in tetrahydrofuran, molecular hydrogen was evolved and that this could be explained by postulating the formation of fluorocarbon-aluminium compounds. The reaction of hexafluorobenzene with lithium aluminium hydride in tetrahydrofuran give pentafluorobenzene and 1,2,4,5-tetrafluorobenzene as well as unchanged starting material and molecular hydrogen. The following sequence of reactions was proposed.



The reactions were also found to proceed faster in tetrahydrofuran than in diethyl ether. Tatlow et al.<sup>78</sup> investigated the reactions of pentafluorobenzene and 1,2,3,4-tetrafluoronaphthalene with lithium aluminium hydride. They obtained a mixture of 1,2,3,4-, 1,2,3,5- and 1,2,4,5-tetrafluorobenzenes from the reaction of pentafluorobenzene with  $\text{LiAlH}_4$  in refluxing ether. 1,2,3,4-tetrafluoronaphthalene reacted only slowly with  $\text{LiAlH}_4$  in ether at reflux temperature (40% after 5 days) but readily gave 1,2,4-trifluoronaphthalene as the only product, in tetrahydrofuran.

From these reports the mechanism of the reaction of  $\text{LiAlH}_4$  with aromatic halides would appear to depend on both the solvent system and the reacting substrate. No explanation of this behaviour has yet been proposed.

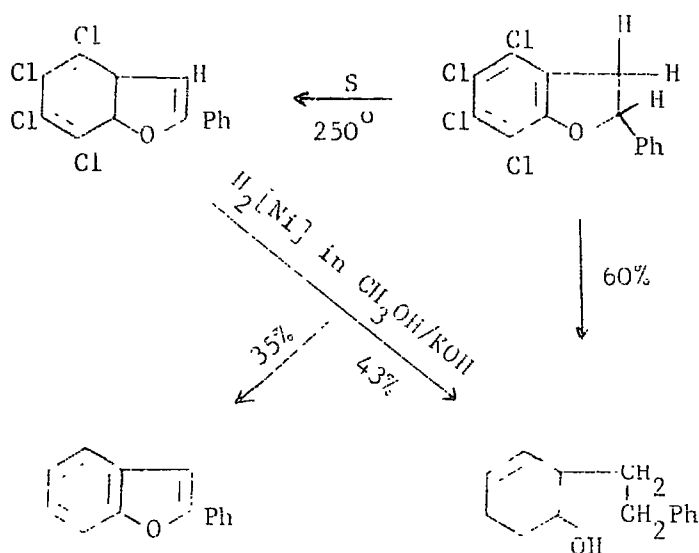
Treatment of hexachlorobenzo-[b]-thiophen(I) with an equimolar amount of lithium aluminium hydride in tetrahydrofuran at room temperature for 48 hrs., gave 3,4,5,6,7-pentachlorobenzo-[b]-thiophen (XXI, 42%) and unreacted starting material (I, 42%). Under more vigorous conditions, (excess in  $\text{LiAlH}_4$ , reflux for 16 hr.) both the amounts of (XXI, 32%) and (I, 16%) were reduced but no other products could be detected by chromatography or  $^1\text{H}$  n.m.r. spectroscopy. It is possible that a similar addition-elimination reaction to that with pentachloropyridine may be taking place but the much lower reactivity of hexachlorobenzo-[b]-thiophen

is amply demonstrated by the incompleteness of the reaction with lithium aluminium hydride even under extreme conditions.

The lower reactivity of the benzo-[b]-thiophen ring system in nucleophilic reactions compared to the pyridine ring system might be expected on this basis of their electronic structures. Whereas the pyridine ring is electron deficient because of the electronegative nitrogen atom, the benzothiophen system, in common with other five membered heterocycles, is electron rich. In the five membered ring systems  $6\pi$ -electrons are shared by only five atoms and in the case of benzo-[b]-thiophen, where the hetero atom is least electronegative, the effect is at a maximum.

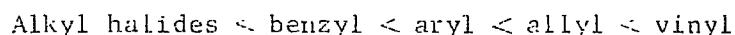
The replacement of the 2-chlorine in (I) by hydrogen (using  $\text{LiAlH}_4$ ) has been shown by  $^1\text{H}$  n.m.r., but it has also been possible to show by a chemical method that a chlorine in the five membered ring had been replaced.

Raney nickel hydrodesulphurisation in the determination of structures of unknown benzo-[b]-thiophens is being increasingly used. Unfortunately, even under mild conditions, non-aromatic double bonds are saturated, halogens (except fluorine) are removed, and nitro groups are reduced.<sup>79</sup> Brooke and Quasem have successfully used Raney nickel hydrodesulphurisation to determine the structures of products obtained in the reactions of 4,5,6,7-tetrafluorobenzo-[b]-thiophen with methoxide ion and acetic anhydride/aluminium trichloride.<sup>80</sup> Huisgen et al.<sup>81</sup> reported that the nickel catalysed reduction of 2-phenyl-4,5,6,7-tetrachlorobenzo-[b]-furan caused complete dechlorination as well as opening the furan ring.

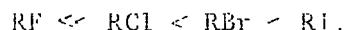


All attempts at dehydrosulphurisation of highly chlorinated benzo-[b]-thiophen compounds using Raney nickel in ethanol failed. Only complex mixtures of unidentifiable products were obtained. G.l.c. analysis of the product obtained from treatment of hexachlorobenzothiophen with Raney nickel in refluxing ethanol showed that none of the expected ethyl benzene was present in the complex mixture.

Catalytic hydrogenolysis of alkyl and aryl halides with palladium or platinum catalysts has been widely studied.<sup>82</sup> The order of reactivities are



and for all types of halogen compounds

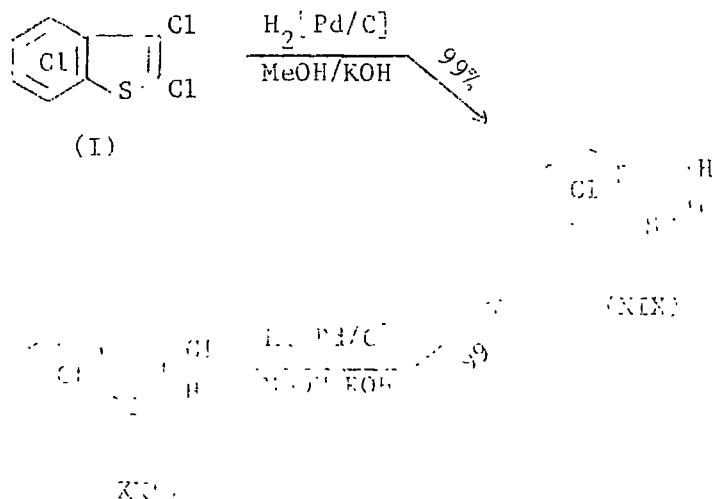


Palladium is superior to other catalysts for dehalogenations being least affected by the catalytic poisoning properties of the halide. The presence of base and polyhydroxylic solvents increases the rate of catalytic hydrodehalogenations.

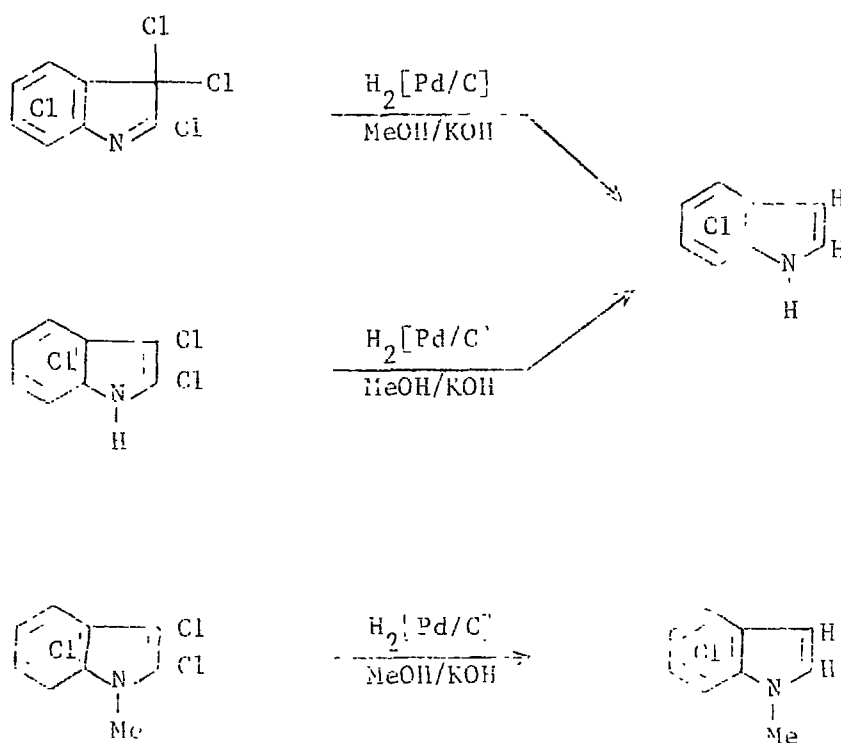
2-Halobenzo-[b]-thiophens are readily dehalogenated by hydrogen in the presence of palladium.<sup>83</sup> 3-Halobenzo-[b]-thiophens have been reported to be unaffected by hydrogen and palladium so that a 2-halo atom can be removed selectively in the presence of 3-halo atom.<sup>84</sup>

When hexachlorobenzo-[b]-thiophen (I) was reacted with hydrogen at atmospheric pressure in methanolic potassium hydroxide using palladium-charcoal catalyst, the sole product was 4,5,6,7-tetrachlorobenzo-[b]-thiophen (XIX) in 99% yield. In an attempt to selectively remove only one chlorine, the reaction was repeated and stopped after the uptake of only mole equivalent of hydrogen. Examination of the product by t.l.c. and <sup>1</sup>H n.m.r. showed only unreacted starting material (I) and (XIX) were present, no evidence was obtained for an intermediate pentachlorobenzo-[b]-thiophen.

Treatment of the pentachlorobenzo-[b]-thiophen (XXI) (obtained from the reaction of (I) with either LiAlH<sub>4</sub> or n-butyllithium) with hydrogen and palladium under the same conditions, also gave exclusively (XIV) in 99% yield showing by a chemical method that the original hydrogen atom was in the five membered ring of (XXI). Extending the reaction time produced no further products and it seems that the reaction is specific



for halogens in the 2 and 3 positions, probably because the 2,3 bond is more 'localised' than those in the benzenoid ring and addition of hydrogen across it is more favourable than for aromatic double bonds. It seemed likely that the reaction would be general for the series, benzo-thiophen, indole, benzofuran and it has recently been shown in this laboratory that highly chlorinated indoles are selectively dechlorinated in the 2 and 3 positions using this method<sup>85</sup>



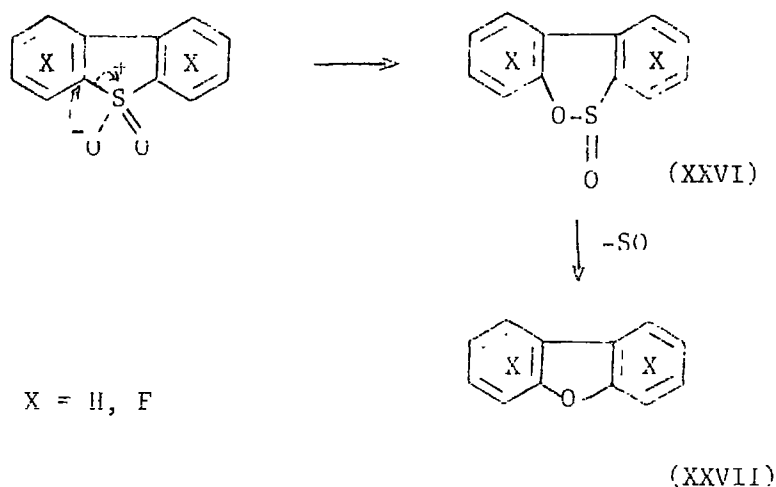
The catalytic replacement of chlorine by hydrogen at position 3 in benzo-thiophen derivatives has not been previously reported.<sup>84</sup> In an attempt to exploit this reaction, products from the reaction of (1) with various nucleophiles were subjected to catalytic hydrogenolysis (see later).

(iii) Oxidation

Benzo-*b*-thiophens are readily converted to the corresponding 1,1-dioxides by peracid oxidation using peracetic, perbenzoid, permalic or trifluoroperacetic acids. It has been reported that benzo-*b*-thiophens with halogens in the 2,3<sup>positions</sup> are difficult to oxidise and in some cases do not give 1,1-dioxides with peracids. Schlesinger and Mowry<sup>86</sup> failed to oxidise a tetrachloro- and a pentachlorobenzo-*b*-thiophen with peracid. Each compound was known to contain chlorines in the 2- and 3-positions and it was suggested that oxidation may be sterically hindered by the presence of a 7-chlorine substituent. However, no difficulty was experienced in oxidising hexachlorobenzo-*b*-thiophen (I) to 2,3,4,5,6,7-hexachlorobenzo-*b*-thiophen-1,1-dioxide (XXVIII, 85%) using trifluoroperacetic acid. The difficulties experienced in oxidising halogenated benzo-*b*-thiophens can be attributed to electronic, rather than steric factors. Chambers et al.<sup>88</sup> found that octafluorodibenzo-thiophen was not oxidised by 85% hydrogen peroxide in acetic acid or by chlorination followed by hydrolysis, or by potassium metaperiodate in methanol. However, both octafluorodibenzothiophen<sup>88</sup> and 4,5,6,7-tetrafluorobenzo-*b*-thiophen<sup>89</sup> have been readily oxidised using 85-90% hydrogen peroxide in trifluoroacetic anhydride.

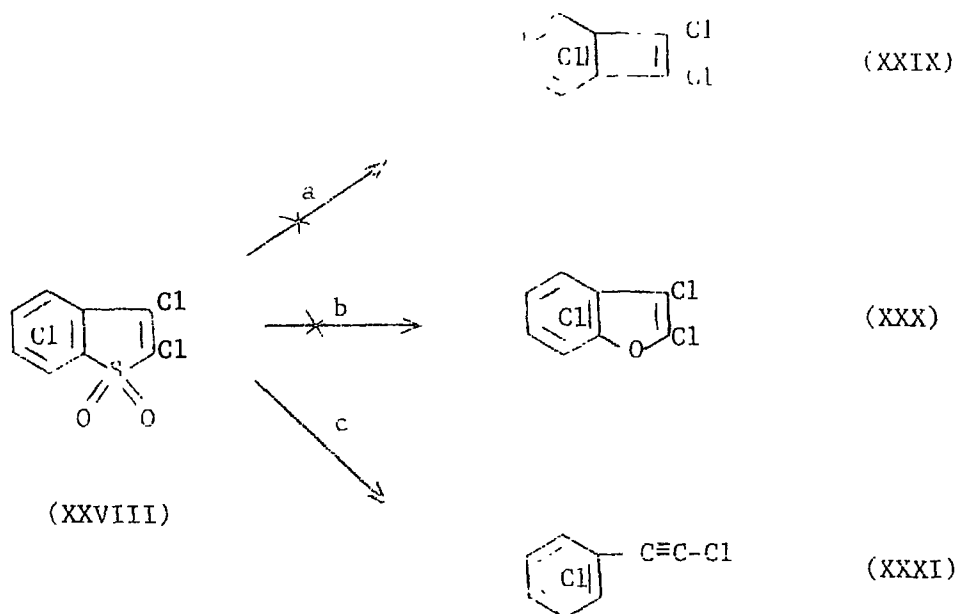
Pyrolytic eliminations of SO<sub>2</sub>, forming carbon-carbon bonds are well known<sup>90</sup> but a number of investigations have shown that, in some circumstances, elimination of SO, rather than SO<sub>2</sub>, can occur during pyrolysis.<sup>88,91-93</sup> The latter process has also been observed in the mass spectra of S-dioxides.<sup>88,94</sup>

Vacuum pyrolysis of both dibenzothiophen 1,1-dioxide<sup>91</sup> and octa-<sup>88</sup>fluorodibenzothiophen 1,1-dioxide results in the formation of the corresponding dibenzofuran (XXVII) by extrusion of SO. It has been suggested<sup>88,91,94</sup> that the mechanism of SO elimination most probably involves intramolecular rearrangement to an unstable sulphinic ester (XXVI), followed by SO loss.



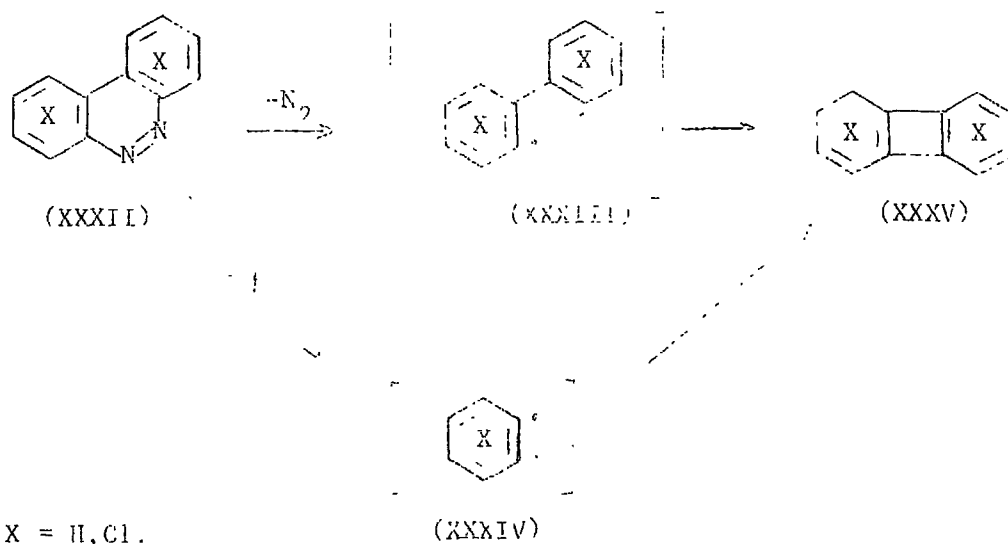
The mass spectrum of hexachlorobenzo-[b]-thiophen 1,1-dioxide (XXVIII) showed a base peak at  $m/e$  306 corresponding to loss of  $SO_2$  from the parent ion. This indicated that loss of  $SO_2$  rather than loss of SO might be the main rearrangement on pyrolysis. Three possible reactions could be envisaged for the pyrolysis of (XXVIII)

- (a) Loss of  $SO_2$  and carbon-carbon bond formation to give the benzocyclobutadiene (XXIX)
- (b) Rearrangement and loss of SO to give the corresponding benzo-[b]-furan (XXX)
- (c) Loss of  $SO_2$  and chlorine migration to give perchlorophenylacetylene (XXXI)

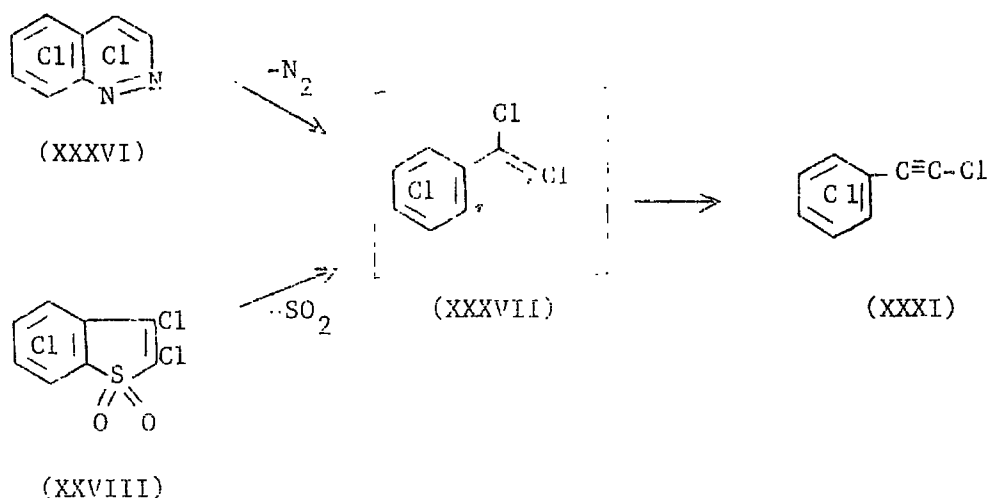


The dioxide (XXVIII) was pyrolysed by slowly subliming ( $10^{-2}$  mm.Hg) it into a quartz tube packed with silica fibre at  $840^{\circ}$  to give hexachloro-phenylacetylene<sup>95</sup> (XXXI) quantitatively.

MacBride<sup>96</sup> has noted that the high yields of biphenylenes (XXXV) produced by thermal extrusion of molecular nitrogen from benzo-[c]-cinnolines (XXXII) suggests that the reactions occur via diradicals (XXXIII) and not by fragmentation to benzyne (XXXIV) followed by recombination.



Pyrolysis of perchlorocinnoline<sup>95</sup> (XXXVI) gives perchlorophenyl acetylene (XXXI) by extrusion of nitrogen probably via a diradical intermediate (XXXVII). It is possible that the pyrolysis of (XXVII) proceeds by the same mechanism.



Presumably, if the benzocyclobutadiene (XXIX) were formed it would be thermally unstable and would itself rearrange to the phenylacetylene (XXXI) under the reaction conditions.

#### Nucleophilic Reactions of Polyhalo aromatic Compounds

In general, highly halogenated aromatic compounds undergo nucleophilic substitution by a process analogous to electrophilic substitution in aromatic hydrocarbon chemistry. The orientation of substitution in polyhalobenzenoid compounds can be predicted largely on the basis of a controlling  $I_{-1}$  effect, except in certain instances where steric or specific interactions are important. In contrast, the orientation of substitution in polyhaloheteroaromatic compounds is not as straightforward and the nature of the heterocycle must be taken into account.

a. Polyhalobenzenoid Compounds

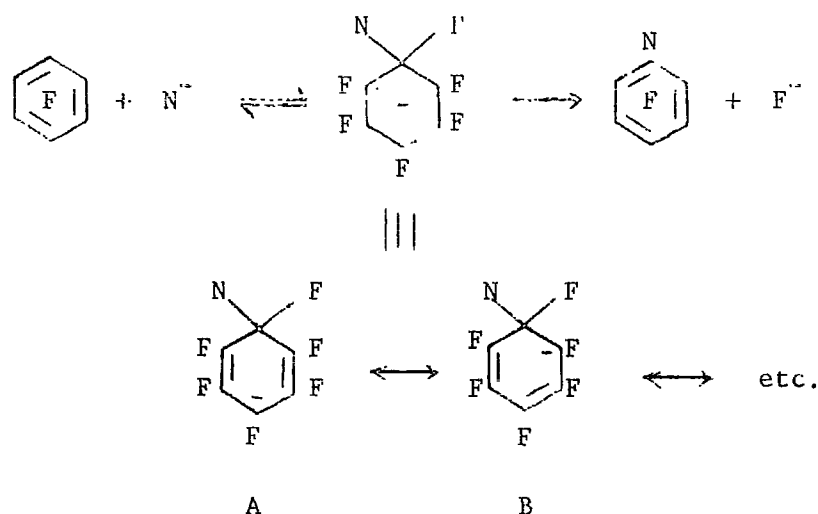
Nucleophilic substitution in fluorocarbons has received by far the widest attention although some work has been done with the corresponding chlorocarbons. Generally, patterns of substitution have been found to be the same for both the chloro and fluoro systems. There is some evidence that polybromo aromatics may behave anomalously under certain circumstances.<sup>97</sup> The general principles of nucleophilic substitution can be most easily discussed with reference to polyfluoroaromatic systems, where the most data is available, but the results apply equally well to the chlorinated series.

Hexafluorobenzene has been reacted with a great variety of nucleophiles ( $\text{OCH}_3^-$ ,  $\text{OH}^-$ ,  $\text{NH}_3$ ,  $\text{NH}_2\text{CH}_3$ ,  $\text{NH}_2\text{NH}_2$ ,  $\text{SH}^-$ ,  $\text{CH}_3^-$ ,  $\text{C}_6\text{H}_5^-$ <sup>99-103</sup>), resulting in replacement of a single fluorine atom under fairly moderate conditions to give good yields of the corresponding pentafluorophenyl compounds. Hexachloro benzene undergoes nucleophilic displacement of chlorine in the same way but under more vigorous reaction conditions, showing its much lower reactivity.<sup>61</sup>

Tatlow, Burdon and co-workers have extensively studied nucleophilic substitution in pentafluorobenzene derivatives ( $\text{C}_6\text{F}_5\text{X}$ ) with regard to the isomer distributions. When  $\text{X} = \text{H}$ ,  $\text{CH}_3$ ,  $\text{CF}_3$ ,  $\text{SCH}_3$ ,  $\text{SO}_2\text{CH}_3$ ,  $\text{N}(\text{CH}_3)_2$ ,  $\text{C}_6\text{F}_5$  and  $\text{OCF}_3$ , para substitution predominates. For  $\text{X} = \text{O}^-$ <sup>104</sup> or  $\text{NH}_2$ <sup>105</sup> meta replacement predominates, and for  $\text{X} = \text{OCH}_3$ ,<sup>104</sup>  $\text{NHCH}_3$ <sup>105</sup> then both meta and para substituted products are formed. Anomalous high ortho replacement when  $\text{X} = \text{COO}^-$ ,  $\text{NO}$ ,  $\text{NO}_2$  or when  $\text{X} = \text{NO}_2$  and  $\text{Nuc.} = \text{NH}_3$ ,  $\text{NHR}_2$ <sup>105-109</sup> were attributed to solvent effects and specific nucleophile-substituent interactions.

b. Rationalisation of Orientation

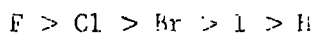
A rationalisation of orientation of nucleophilic substitution in polyhalo aromatic systems has been given by Burdon,<sup>110</sup> in which the relative stabilities of the transition states (approximated by a Wheland-type intermediate) are considered.



The resonance hybrid A is assumed to be the main contributor to the Wheland intermediate;

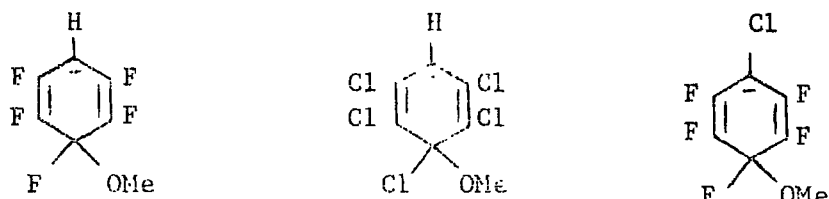
In substitution reactions of  $C_6F_5X$  compounds the problem is essentially a consideration of the effect of the substituent attached to the carbon bearing the negative charge in the transition state. If the substituent X stabilises a negative charge more than fluorine substitution will take place para to X, if less than fluorine then meta attack will occur. For a substituent with the same effect as fluorine a statistical ratio (O:M:P = 2:2:1) should result. These generalisations were put forward with the proviso that solvent, steric and specific interactions could be neglected.

The effect of the substituent on a carbanion in an aromatic system will be in the order of the  $I_{\text{tr}}$  repulsions.<sup>111</sup>



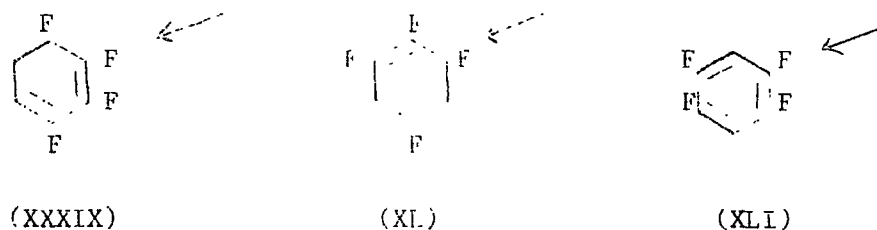
Unlike the halogens,  $I_{\text{tr}}$  effects for oxygen and nitrogen can not be estimated from spectroscopic measurements, but are taken to be in the order  $N > O > F$ .<sup>110</sup>

The observation that chloropentafluorobenzene reacts with methoxide ion faster than pentafluorobenzene, although pentachlorobenzene substitutes para to the hydrogen, is explained by consideration of the intermediates:



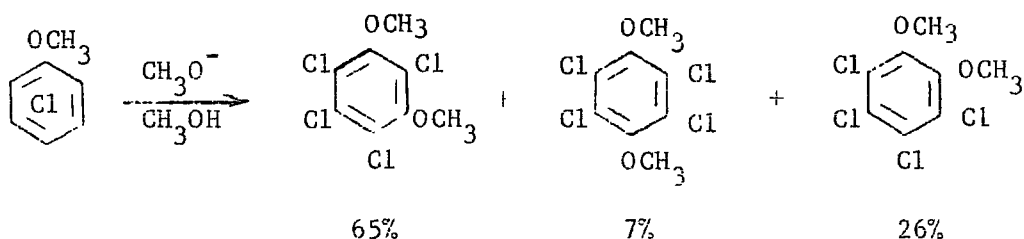
The relative stabilities of a negative charge on carbon bearing hydrogen, chlorine or fluorine is in the order  $\bar{C}-H > \bar{C}-Cl > \bar{C}-F$ .

Of the three tetrafluorobenzenes, (XLI) reacts  $\sim 10^3$  times slower with methoxide ion than either (XXXIX) or (XL). The positions of substitution in each compound is indicated.

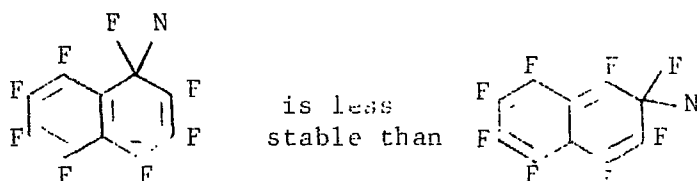


Nucleophilic substitution in the 1,2,3,4-tetrafluoro-5-halobenzenes (Hal = B, Cl, I) occurs mainly in the 3-position.<sup>112</sup> Substitution in this position involves localising the negative charge in the para hybrid intermediate on a carbon atom bearing a hydrogen rather than a halogen. The increase in the proportion of replacement para to the halogen increases along the series Cl < Br < I following the decreasing  $I_{\text{H}}$  effect.

Yakobsen and co-workers have studied the orientation of nucleophilic substitution in pentachlorobenzene derivatives.<sup>113,114</sup> Pentachloroaniline reacts with methylamine and methoxide ion to give solely the meta-substituted product, while pentachloroanisole with methoxide ion gives products arising from attack at positions ortho, meta and para to the  $\text{CH}_3\text{O}$  group.



Nucleophilic substitution in polyhalo polycyclic aromatic compounds has also been rationalised on the basis of Burdon's theory.<sup>110</sup> For example, substitution in polyfluoronaphthalene occurs in the 2-position where the negative charge in the intermediate can be localised on a bridging carbon atom rather than a carbon bearing a fluorine atom.

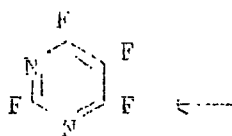


c. Nucleophilic substitution in Polyhaloheteroaromatic Systems

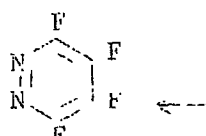
By far the most widely studied polyhaloheterocyclic systems are those containing nitrogen although some data is now available for some oxygen and sulphur heterocycles. Again it is the fluorinated systems that have received the most attention.

(i) Nitrogen Heterocycles

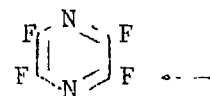
Studies of the nitrogen heterocycles have shown that the hetero atom plays a predominant part in determining the orientation of substitution. Pentafluoropyridine undergoes nucleophilic attack at the four position and is much more reactive than hexafluorobenzene. If the four position is blocked then substitution occurs in the 2-position. Of the three tetrafluorodiazines, (XLIV) is the least reactive although all three are more reactive than pentafluoropyridine.<sup>115</sup> The position of nucleophilic substitution is indicated for all three diazines below:



(XLII)

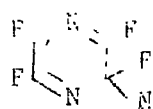


(XLIII)



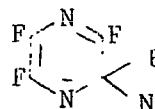
(XLIV)

The lower reactivity of (XLIV) can be explained in terms of the stability of Wheland-type intermediate. Only in the ortho-quinoid (XLVI) form is the negative charge localised on a nitrogen atom.



(XLV)

.....

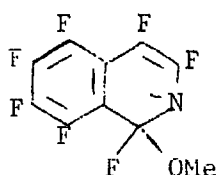


(XLVI)

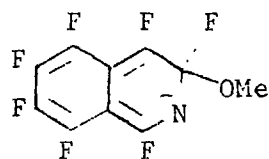
In contrast to pentafluoropyridine, pentachloropyridine gives both 4- and 2-substitution with nucleophiles.<sup>116</sup> The larger the nucleophile the more 2-substitution is observed; the 2-position being less sterically crowded. Multiple substitution appears to take place almost as readily as monosubstitution, mixtures of mono, di- and tri-substituted products are often formed. Disubstitution gives 2,4 and 2,6 isomers while tri-substitution give only the 2,4,6-trisubstituted product. The ratio of 2,4 and 2,6 isomers also appears to depend on the size of the nucleophile.

Little information is available for the chlorodiazines but tetrachloropyridazine reacts with aqueous ammonia in ethanol and sodium hydroxide in water to give 4-amino and 4-hydroxytrichloropyrimidine respectively.<sup>117</sup> Tetrachloropyrimidine reacts with amines to give the 4-substituted product and further reaction gives the 4,6-disubstituted product.<sup>118</sup> Tetrachloropyrazine has only one position for monosubstitution. All other chlorodiazines appear to give the same substitution patterns as the corresponding fluorocarbons. No steric effects have yet been reported for this group.

Hexafluoroquinoline<sup>119</sup> undergoes 2- and 4-substitution with nucleophiles (i.e. *ortho* and *para* to the nitrogen), although heptafluoroquinoline appears to behave anomalously giving 1-substitution rather than 2-substitution as expected on the basis of Burdon's theory.



(XLVII)



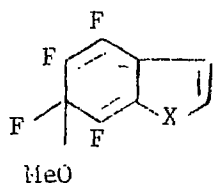
(XLVIII)

Only in the ortho-quinoid forms can the negative charge be localised on the nitrogen atom and (XLVII) is believed to be more stable than (XLVIII) as the aromaticity of the benzenoid ring is not broken.

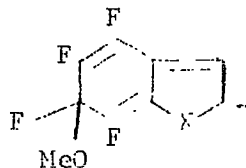
(ii) Heterocycles containing oxygen and sulphur

4,5,6,7-Tetrafluorobenzo-[b]furan<sup>120</sup> undergoes nucleophilic substitution with methoxide ion to give a mixture of 4-, 6-, and 7-methoxy trifluorobenzo-[b]-furans in the ratio 27:57:16. 4,5,6,7-Tetrafluorobenzo-[b]-thiophen<sup>121</sup> also reacts with methoxide ion to give the 6-isomer as the major product.

Octafluoro-dibenzothiophen and octafluorodibenzofuran have recently been shown to react with methoxide ion in the 2-position.<sup>122,123</sup>

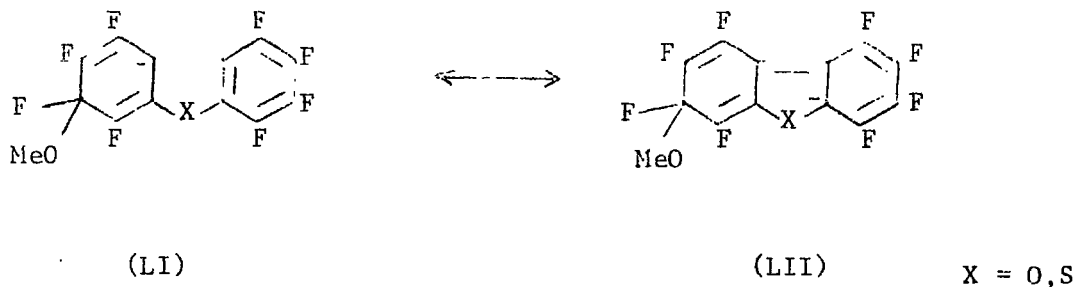


(XLIX)



(L)

X = O, S



From a consideration of the Wheland-type intermediates it can be seen that in (XLIX) and (LI) the negative charge is localised on a bridging carbon atom and that further delocalisation is possible in the second ring. Attack para to the heteroatom would mean that for X = O the charge would be localised on a carbon attached to oxygen and destabilised by the  $I_{\pi}$  effect. Further delocalisation would also not be possible.

Tetrafluorothiophen has recently been synthesised and shown to give nucleophilic replacement in the 2-position.<sup>124</sup> (cf. hexachlorobenzo-[b]-thiophen).

#### Some Nucleophilic Reactions of Hexachloro- and 4,5,6,7-Tetrachlorobenzo-[b]-thiophen

The reaction of hexachlorobenzo-[b]-thiophen (I) with lithium aluminium hydride (which can essentially be considered as nucleophilic replacement of chlorine by hydride ion) to give 3,4,5,6,7-pentachlorobenzo-[b]-thiophen, has already been discussed.

The reaction of (I) with methoxide ion under a variety of conditions in various solvents (methanol, pyridine, dimethylsulphoxide, tetrahydrofuran, N,N-dimethylformamide) was investigated but no tractable

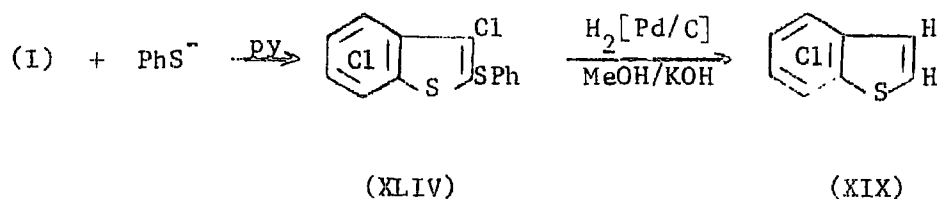
products could be isolated. Reactions carried out in aprotic solvents (e.g. pyridine) gave complex mixtures of highly coloured materials, presumably formed from demethylation and further reaction of the initially formed methoxy derivatives. Demethylation of chlorinated anisoles by methoxide ion has been reported to take place readily.<sup>125</sup>

Sodium isopropoxide in isopropanol reacted only slowly with (I) even at reflux temperature. When the solvent was changed to pyridine a monoisopropoxypentachlorobenzo-[b]-thiophen (LIII, 64%) was obtained. The role of dipolar aprotic solvents in nucleophilic reactions is well known<sup>126</sup> and Rocklin<sup>61</sup> has observed that pyridine (as solvent) seems to have a catalytic effect on the reactions of hexachlorobenzene with nucleophiles. A similar effect is apparent in the reactions of hexachlorobenzo-[b]-thiophen. In all cases reaction with nucleophiles proceeded faster and with fewer side products in pyridine than in any other solvent. The structure of the monoisopropoxy compound (LIII) can tentatively be assigned as the 2-isopropoxy derivative only by analogy with the course of the reaction of (I) with  $\text{LiAlH}_4$ .

An attempted catalytic hydrogenolysis of (LIII) was completely unsuccessful; starting material being recovered unchanged. Steric effects of the isopropoxy group may be responsible for the failure of the hydrogenolysis reaction.

Sodium benzenethiolate (1.1 eq.) reacted with (I) in pyridine to give a monothiophenoxypentachlorobenzo-[b]-thiophen (XLIV, 41%) and unchanged starting material (5%). Catalytic hydrogenolysis of the thioether gave 4,5,6,7-tetrachlorobenzo-[b]-thiophen (LIX, 78%), and unreacted starting material (XLIV). Both the chlorine and the thiophenoxy

group in the five membered ring had been removed.



Again the orientation can only be inferred as the 2-thiophenoxy derivative by analogy, although substitution in the five membered ring is proved.

In contrast, the main product of the reaction between 4,5,6,7-tetrachlorobenzo-[b]-thiophen (XIX) and sodium benzenethiolate in refluxing pyridine for 4 hrs. was a dithiophenoxydichlorobenzo-[b]-thiophen (XLV, 30%). A small amount of a monothiophenoxytrichlorobenzo-[b]-thiophen (XLVI, 3%) was also obtained and identified by mass spectroscopy. Unreacted starting material (XIX, 56%) was recovered. Orientation for the thiophenoxy groups in (XLV) has not been established. Multiple substitution with sulphur nucleophiles is to be expected. Thioether groups are activating towards nucleophilic attack<sup>127,128</sup> so that the mono substituted product once formed is more reactive than the parent compound. This is amply demonstrated by the reaction of (I) and (XIX) with sodium thiomethoxide.

(I) reacts with excess sodium thiomethoxide in pyridine to give exclusively a tetrathiomethoxy-dichlorobenzo-[b]-thiophen (XLVI 53%). The <sup>1</sup>H n.m.r. of (XLVI) showed four absorptions at  $\tau$  0.755,  $\tau$  0.749,  $\tau$  0.742 and  $\tau$  0.733 due to four distinct methyl groups. An attempted catalytic desulphurisation of (XLVI) using hydrogen with palladium

catalyst failed, giving unchanged starting material. Presumably the large number of sulphur atoms in the molecule effectively poisoned the catalyst.<sup>82</sup>

The reaction of 4,5,6,7-tetrachlorobenzo-[b]-thiophen (XIX) with sodium thiomethoxide could be controlled to give either a dithiomethoxy or a trithiomethoxy derivative as the major product. At room temperature, (XIX) with sodium thiomethoxide in pyridine gave a dithiomethoxy-dichlorobenzo-[b]-thiophen, unreacted starting material (XIX) and a trace of a monothiomethoxy derivative identified by mass spectroscopy. At reflux temperature, the same dithiomethoxy derivative was formed but the major product was a trithiomethoxy-monochlorobenzo-[b]-thiophen. The orientations of substituents have not been determined.

CHAPTER 3

ELECTRON SPECTROSCOPY FOR CHEMICAL ANALYSIS

(i) Introduction

Electron spectroscopy is the name given to that branch of spectroscopy in which binding energies of electrons in a molecule are determined by measurement of the energies of electrons ejected by interactions of the molecule with an essentially monoenergetic beam of exciting radiation. Generally, three methods of exciting electron spectra are employed; X-rays, ultra-violet light or electron beams. There are advantages and limitations associated with each method.

The advantage of u.v. excitation is that much higher resolution can be obtained due to the lower inherent widths of the u.v. lines. The exciting radiation commonly employed ( $\text{He}^{\text{I}} = 21.2 \text{ eV}$ ;  $\text{He}^{\text{II}} = 40.8 \text{ eV}$ ) limits the technique to observation of low binding energy valence and molecular orbitals. Although physicists have for many years studied solids under ultra-high vacuum (photoemission spectroscopy),<sup>129</sup> the chemical applications of u.v. photoelectron spectroscopy (PES) have, until recently, been limited to gaseous samples.<sup>130</sup>

Electron excitation can not directly produce photoelectron spectra because of the elastic collisions involved, but it has been extensively used to generate Auger electron spectra (see later) of both gases and solids.<sup>131</sup> The electron beam has the advantage that being easily focussed and its energy continuously variable, a high sensitivity can be achieved, but at the expense of a lower signal to noise ratio. The penetration depths for electrons are of the order of a few atomic layers, making electron excited Auger spectroscopy ideal for studying surfaces. The possibility of using pulse techniques for exciting molecules, in situ, allows the photoelectron spectra of excited states to be recorded.

The main problems associated with this form of spectroscopy are the lack of resolution and the difficulties in interpretation of spectra.

Finally, X-ray excitation of photoelectron spectra has several advantages over other methods. The greater energy of exciting radiation available (e.g.  $\text{MgK}\alpha_{1,2} = 1253.6 \text{ eV}$  and  $\text{AlK}\alpha_{1,2} = 1486.6 \text{ eV}$ ) means both core and valence electrons for all atoms (except hydrogen) can be studied in solids or gases. The resolution of the valence energy levels is less than that for u.v. excitation due to the greater inherent line widths of X-rays (1.0 eV for  $\text{AlK}\alpha_{1,2}$ ). Auger electron spectra are obtained simultaneously with the ordinary photoelectron spectra when X-ray excitation is used, making two valuable sources of data available in one experiment.

It is only recently with the advent of commercial spectrometers that the technique of X-ray photoelectron spectroscopy (ESCA) has become widely available to chemists. Already the literature on the subject is extensive.

The main advantages of the technique are summarised below:

- a) any element above helium in the periodic table can be studied with high sensitivity, independent of any nuclear spin properties,
- b) the sample may be a solid, liquid or gas and the technique is essentially non-destructive,
- c) the sample requirement is modest; in favourable cases 1 mgm. of solid, 0.1  $\mu\text{l}$  of liquid or 0.5 cc of gas (at STP),
- d) the information obtained is directly related to the electronic structure of a molecule and the theoretical interpretation is relatively straightforward,

e) information on both core and valence levels of a molecule can be obtained,

f) in studying solids ESCA is essentially a surface technique.

Depending on the core levels studied and using the usual photon sources (Mg,Al) the escape depth of photoelectrons is in the range 0-50Å.

Since ESCA is still a relatively new technique in chemistry a discussion of its history and development, as well as basic theory and instrumentation is given in the following sections.

(ii) History and Development of ESCA

In the early part of this century a number of research workers (Robinson,<sup>132</sup> in England and de Broglie<sup>133</sup> in France) investigated the energy distribution of electrons in various elements by X-ray irradiation. The energies of the photoelectrons were analysed in a homogeneous magnetic field and recorded on a photographic plate. Although a particular anode material in the X-ray tube emits a continuous spectrum (bremsstrahlung) there are also characteristic X-ray lines of which, for commonly used targets (Al,Mg), the  $K\alpha_{1,2}$  are the strongest. The electron distributions thus obtained were characterised by long tails with edges at the high energy end. Measurement of the edge positions allowed determination of the energy of ejected photoelectrons and hence, knowing the energy of the exciting X-ray lines, the binding energies could be calculated. However, the edge positions were not well defined because the electrons underwent energy loss in the sample (usually a foil) by collision processes.

An X-ray beam passing through a thin foil undergoes absorption and this can be studied with an X-ray spectrometer. Again edges are obtained and the absorptions correspond to the excitation of an inner shell electron to the nearest empty level (the conduction band). The data obtained is closely related to that from photoelectron spectroscopy and could, until recently, be obtained more readily and with greater accuracy.

X-ray emission gives line spectra superimposed on the continuous brehmsstrahlung spectrum instead of the edges obtained in X-ray absorption. Since X-ray emission by electron bombardment (the method used in X-ray generation leads to decomposition of chemical compounds), X-ray emission spectra are obtained by secondary X-ray emission from a sample excited with a primary X-ray beam. The line spectra obtained give only energy differences within the atom and not absolute binding energies.

Only a few further attempts were made to extend the early work of Robinson and de Broglie and these met with limited success.<sup>134-138</sup> The reason for this recession was the lack of accuracy compared with that obtained by the X-ray absorption and X-ray emission techniques.

During the early 1950's, Siegbahn and co-workers at Uppsala developed an iron-free, magnetic, double-focussing electron spectrometer in a research program aimed at very high resolution study of the energy spectrum of  $\beta$ -particles.<sup>139</sup> The precision for momentum resolution for  $\beta$ -particles emitted from a radioactive source was within  $1:10^{-5}$  (equivalent to a precision of 0.1 eV in the measurement of a peak in the  $10^4$  eV region). When, in 1954, attempts were made to record, at high resolution, photoelectron spectra produced by X-rays, a new observation changed the course of development of the technique. This was the appearance, under high resolution, of a very sharp line that could be

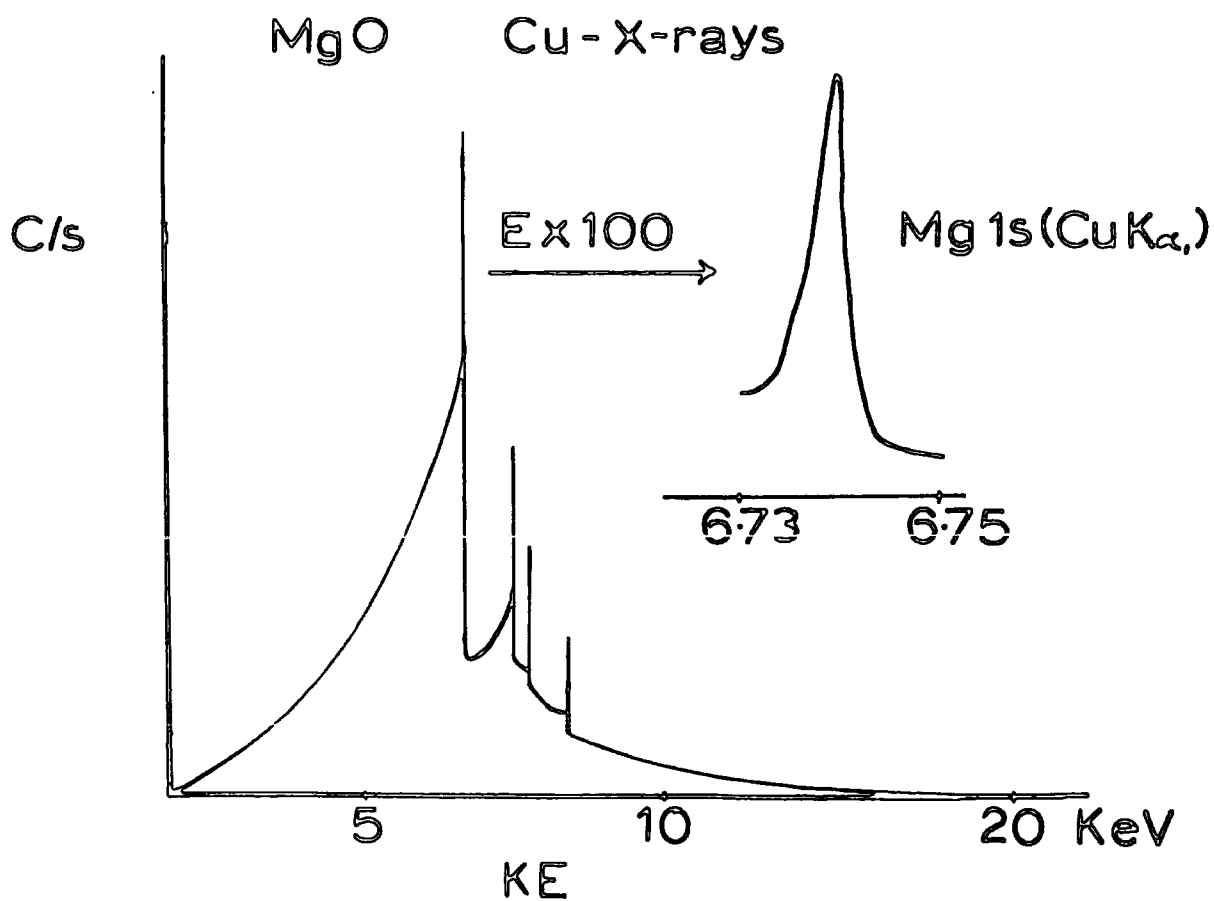


Fig.3.1.(a)

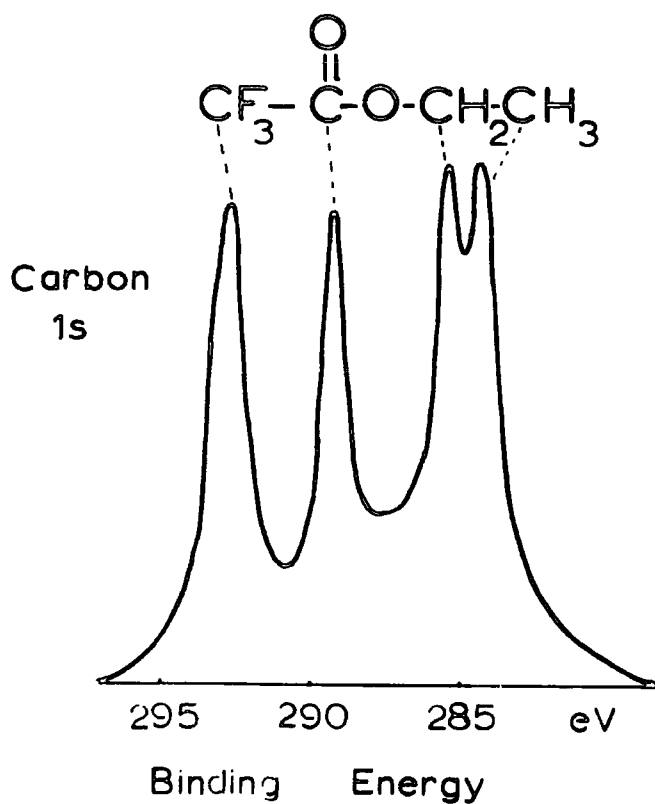


Fig.3.1(b)

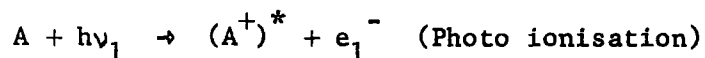
resolved from the edge of each electron veil (Fig.3.1(a)). The electrons to which the line corresponded had, it was realised, the property that they did not undergo any energy absorption and therefore possessed the binding energy of the core level from which they arose. The peak position (and hence the binding energy) could be determined with considerable accuracy, to within a few tenths of an eV.

It had previously been noted that the position of emission lines and absorption edges in X-ray spectroscopy were dependent to a small extent, on the chemical state of the atom.<sup>140,141</sup> From the first studies by Siegbahn and co-workers<sup>142</sup> on chemical effects in copper and its oxides, the value of electron spectroscopy for measuring chemical 'shifts' became apparent. Although its general utility was not appreciated until around 1964,<sup>143,144</sup> the technique has rapidly gained popularity and has come to be known as ESCA since the publication of Siegbahn's first books on the subject.<sup>145,146</sup> Fig.3.1(b) shows the now 'classic' example of ESCA chemical shifts for the carbon 1s levels of ethyltrifluoroacetate.

### (iii) Theory of Electron Spectroscopy

In this section the theory of electron spectroscopy is outlined in relation to chemical applications of ESCA. The fundamental processes involved in ESCA are:

#### Electron Ejection



where  $\nu_1$  is the frequency of the exciting radiation.

#### Electronic Relaxation

- 1)  $(A^+)^* \rightarrow A^+ + h\nu_2$  (X-ray emission)
- 2)  $(A^+)^* \rightarrow A^{++} + e_2^-$  (Auger Electron Emission)

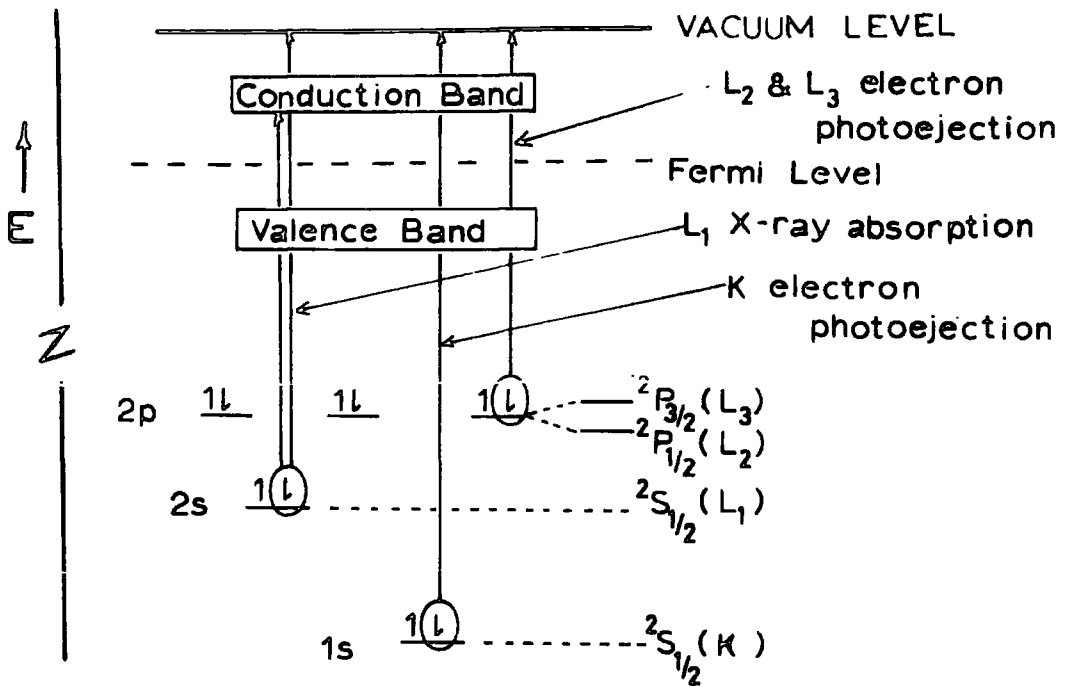


Fig.3.2

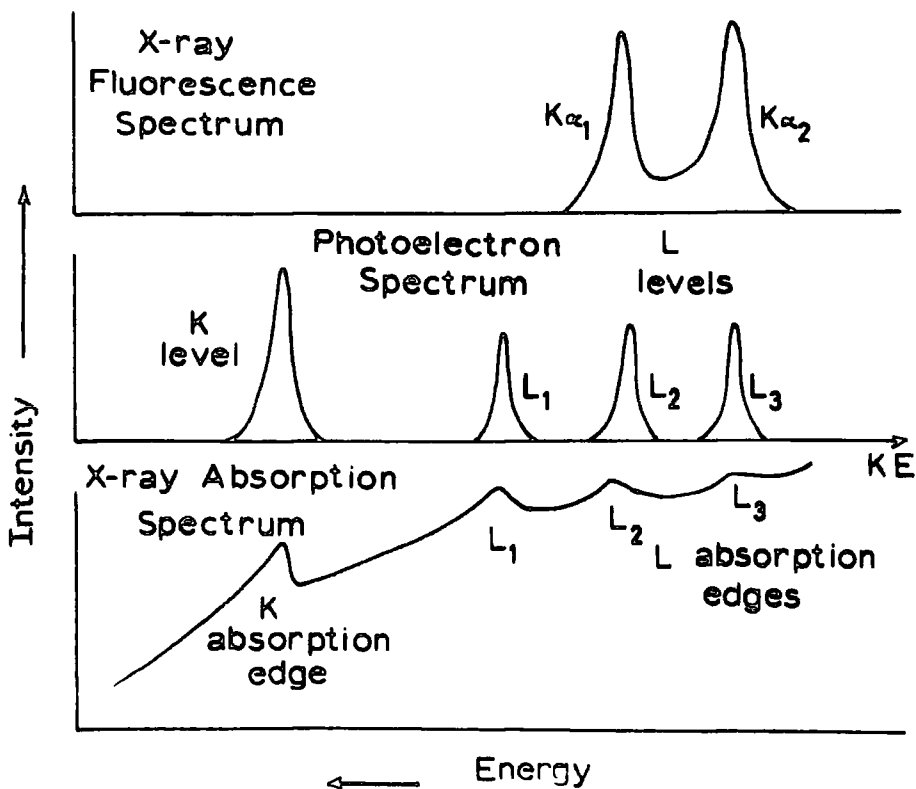


Fig.3.3

(a) Photoionisation Processes

In Fig.3.2 the energy level diagram for an insulator is given showing photoejection for the 1s and 2p electrons, and the upper and lower energy limits of X-ray absorption for the 2s electron. The upper limit for the latter transition - the vacuum level, represents the energy of an electron that has been removed to infinity (the free electron level), and this is also the same as the energy required for photoionisation of a 2s electron. Hence the two techniques are complementary, but in the case of X-ray absorption, binding energy data is much more difficult to extract. The relationship between the two types of spectra is shown in Fig.3.3. Photoelectron peaks are normally designated by the term symbols of the positive hole left after photoejection of an electron. Thus photoejection of a 1s electron leaves a K hole designated as a  $2S_{\frac{1}{2}}$  state.

The diagram in Fig.3.2 differs from that of a conductor by the position of the Fermi\* level. For a conductor, the valence and conduction bands meet and the Fermi level is defined as being at the interface of the two bands. For an insulator where there is a gap between the valence and conduction bands, the position of the Fermi level is uncertain and it is normally taken as lying midway between the top of the valence band and the bottom of the conduction band.

---

\* The Fermi level  $E_f$  may be defined by:

$$\int_0^{E_f} N(E) dE = N$$

where  $N(E) = Z(E)F(E)$  (functions of energy,  $E$ ),  $Z(E)$  is the density of states for fermi particles (in this case, electrons) i.e. the number of states (energy levels) between  $E$  and  $E + \Delta E$ .  $F(E)$  is the probability distribution; the probability that a fermi particle in a system at thermal equilibrium at temperature  $T$  will be in a state of energy  $E$  is given by

$$\frac{1}{e^{\frac{E-E_f}{kt}} + 1} \quad (kT \ll E_f)$$

$N$  is the total number of particles in the system, hence the electrons fill all the available states up to the Fermi level.

Photoionisation is not equally probable for all electrons in an atom or electrons in the same level of different atoms (i.e. the cross section for photoionisation varies from level to level and from atom to atom). Generally, the photoionisation cross section varies as  $\frac{1}{r^2}$  where  $r$  is the orbital radius. Therefore, for light atoms, photoionisation of the 2s electron is about 20 times less probable than for the 1s electron. However, orbital contraction increases with nuclear charge ( $Z$ ) and this becomes more important as the atomic number increases, thus the photoionisation cross section for a given core level is approximately proportional to  $Z^3$ . For soft X-rays, core electrons have the highest photoionisation cross sections, but ionisation of valence electrons can still occur with reasonable probability. Because the cross section for photoionisation of valence electrons varies, depending on the symmetry of the orbital involved and with the energy of the ionising radiation, comparison of valence peaks in the ESCA spectra with corresponding peaks for u.v. PES can give information about orbital symmetries, especially if such studies of cross section dependence on photon energy are coupled with angular dependence studies.

(b) Electronic Relaxation Processes

Two primary processes are available for electronic relaxation following photoionisation of a core level electron. A radiation process involving an electronic transition from a higher energy orbital to fill the primary vacancy, together with emission of the excess energy as a photon, (X-ray emission or X-ray fluorescence), or a radiationless process in which the excess energy is removed by ejection of a second electron from

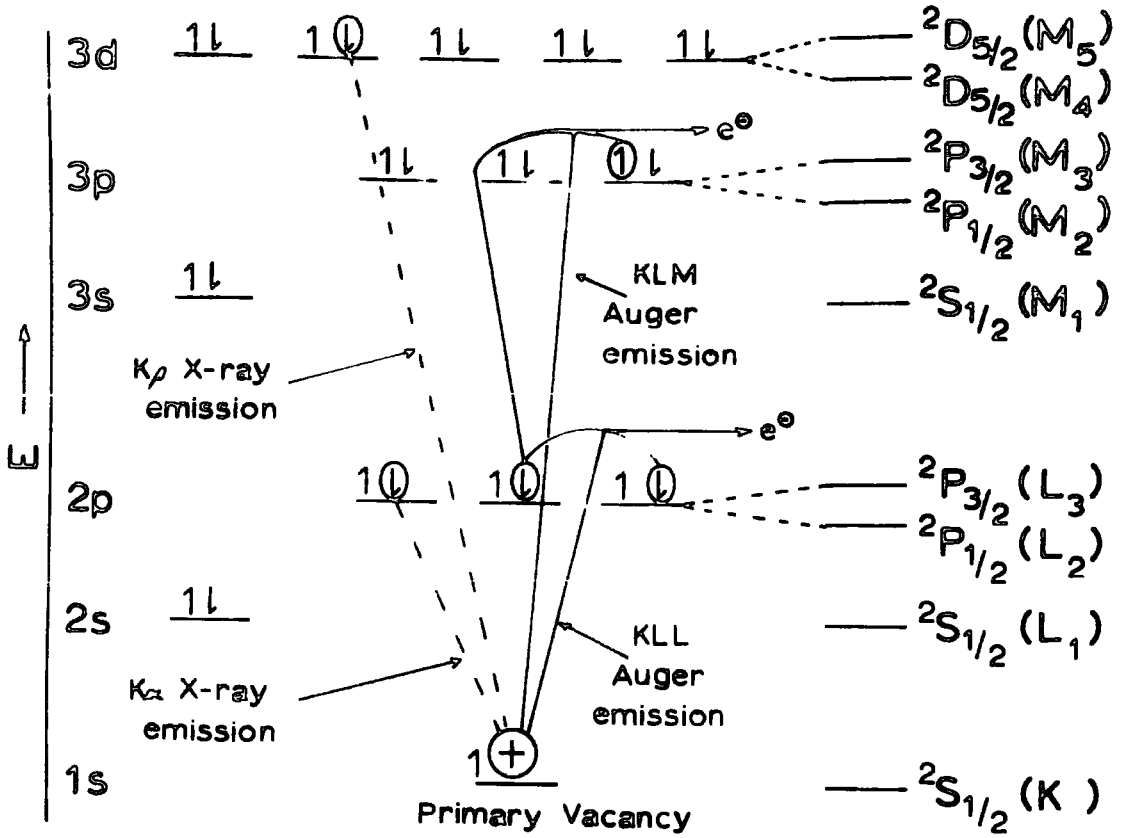


Fig.3.4.

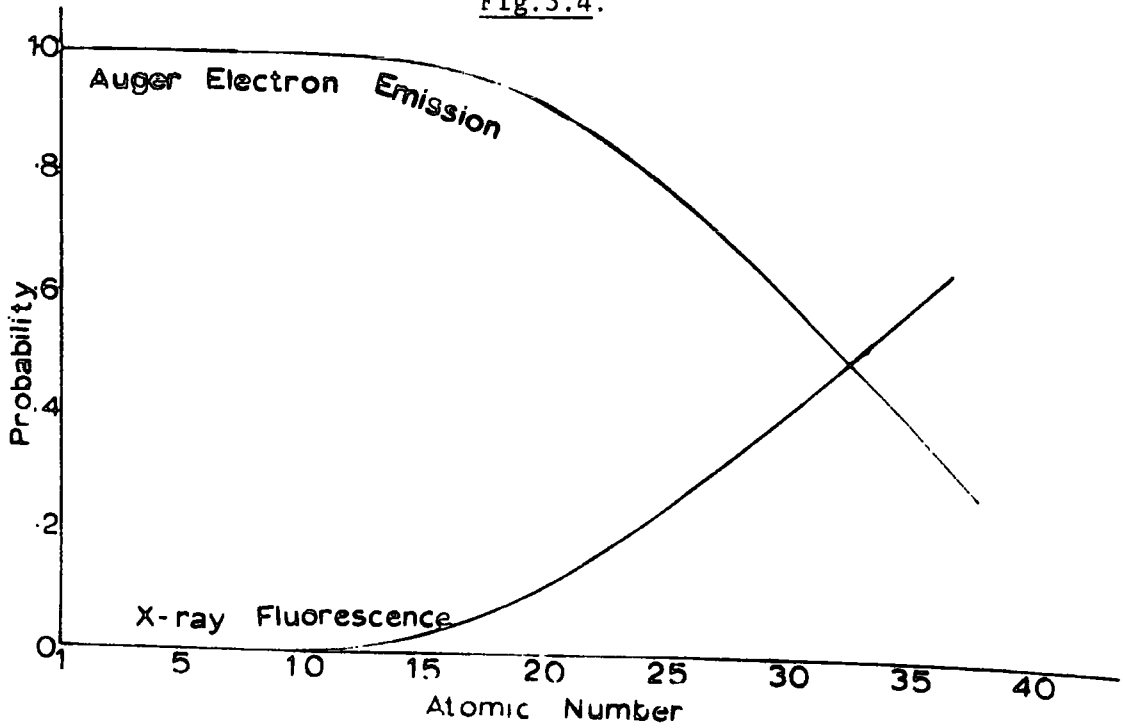


Fig.3.5

an outer shell (Auger emission). Both processes are shown diagrammatically in Fig.3.4 where a primary vacancy exists in the 1s level (i.e. a  $2S_{1/2}$  state). The X-ray emission process is shown as an electronic transition from a 3d level to the primary vacancy ( $K\beta$  emission) and an electronic transition from the 2p level ( $K\alpha$  emission). Two Auger emissions are also shown. A KLL emission, where a 2p electron (L) falls to the 1s vacancy (K) while a second 2p (L) electron is ejected, and a KLM Auger emission where a 3p (M) electron is emitted instead of the 2p electron. If the primary vacancy is created in an inner sub shell of the  $L_1M \dots$  shells the excitation energy is often sufficient to lead to one of the two final vacancies being in the outer sub shell of the primary vacancy's shell e.g.  $L_1L_3M_5$ . These are denoted as Coster-Kronig transitions and tend to give very short lifetimes for the core hole states leading to uncertainty broadening. For light elements radiationless de-excitation by electron emission is often more probable than the radiative de-excitation by X-ray emission (Fig.3.5). At low atomic numbers the Auger yield is virtually 100%, hence, the reason for X-ray fluorescence being a poor technique for studying light elements. Auger peaks are seen in ESCA spectra but are readily distinguished from photoelectron peaks because their kinetic energies are independent of the energy of the exciting radiation.

### (c) Properties of Core Orbitals

Some knowledge of the properties of core orbitals is useful in giving a clearer understanding of ESCA as a technique. In discussing the electronic structure of molecules, chemists have 'traditionally' neglected core electrons and only valence electrons have been considered; as in, for

# CARBON

<u>Orbital</u>	<u>Radial</u> <u>Maxima</u>	<u>Overlap Integrals</u>
1s -11.3255	• • •	1s - 1s    0.38 × 10 <sup>-6</sup>
2s -0.7056	• • •	2s - 2s    0.3835
2p - 0.4333	• • •	2p - 2pσ    0.2816
	• • •	2p - 2pπ    0.2962

Energies in a.u.

$$1 \text{ a.u.} = 27.2107 \text{ eV} = 627.5 \text{ Kcals/mole}$$

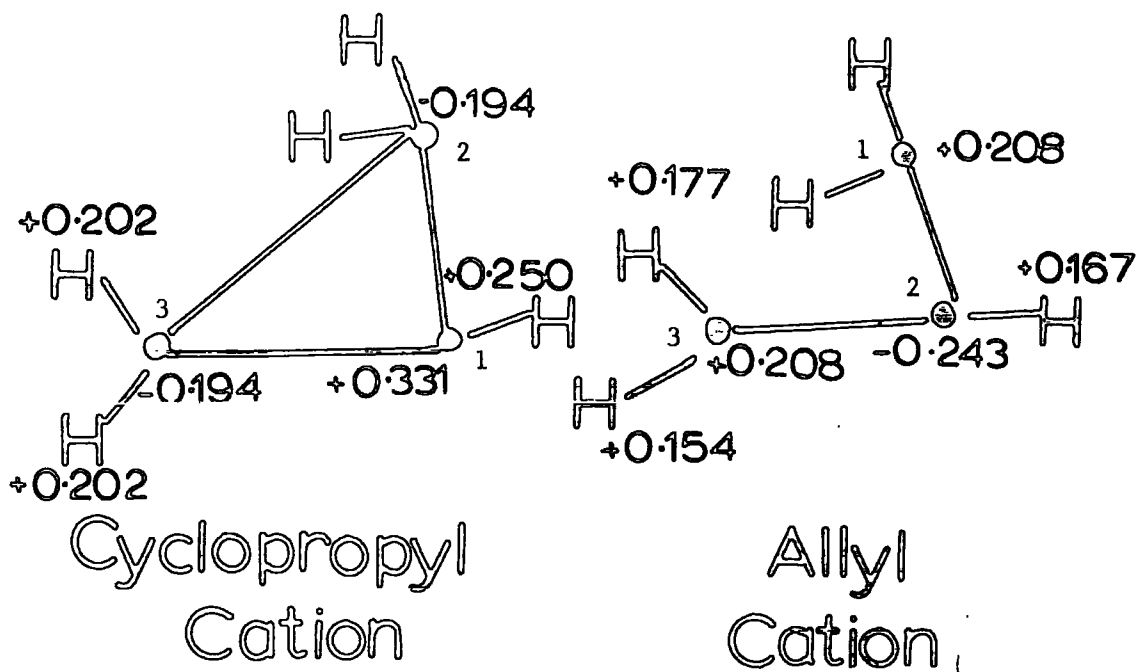
Fig. 3.6

example, simple Huckel theory. The main reasons for this are that the core electrons are not explicitly involved in bonding (though most of the total energy of a molecule resides in the core electrons) and that it is only in the last few years that sufficient computing capability has become available to allow non-empirical ('ab initio') quantum mechanical calculations on molecules in which the core electrons are explicitly considered.

However, it is now known that although the core electrons are not involved in bonding, the core levels encode a considerable amount of information concerning structure and bonding in molecules. This data is available through ESCA.

Fig.3.6 shows the orbital energies and radial maxima calculated non-empirically for the carbon atom. Also shown are the overlap integrals between orbitals on two carbon atoms with a bond length of  $1.39\text{\AA}$ . Considering first the orbital energies, it is clear that the 1s (core) level is very much lower in energy than the 2s and 2p (valence) levels. The radial maxima show that the 1s orbital is confined in a region near the nucleus while the valence orbitals are much more extended in space. Since the core orbital is essentially localised around the nucleus the overlap (and hence overlap integral) involving core orbitals on adjacent atoms is negligible. This is one reason why core orbitals are not involved in bonding.

It has been assumed by chemists in the past that in discussing molecular transformations the energies of the core electrons could be taken as constant and effectively ignored. (This is implicit in the Woodward-Hoffman approach).



Core Levels	-11.5801	-11.5613
	-11.5806	-11.6237
	-11.7122	-11.6238
Total Energies	-115.0885	-115.1447

$$\Delta E = -0.0562 \text{ a.u.} = 35.27 \text{ Kcals/mole}$$

Fig. 3.7

Clark and Armstrong<sup>147</sup> have shown that this is not the case in the transformation of cyclopropyl to allyl cation which occurs in a disrotatory fashion. Fig.3.7 shows the relevant energy levels and total charges. Large charge migrations on the carbon atoms are involved in this transformation. Thus, C<sub>1</sub> which carries a substantial positive charge in the cyclopropyl cation becomes C<sub>2</sub> with a substantial negative charge in the allyl cation. As a result the C<sub>1s</sub> orbital energy changes from -11.7122 a.u. to -11.5613 au. The almost degenerate pair of C<sub>1s</sub> orbitals for C<sub>2</sub> and C<sub>3</sub> in the cyclopropyl cation change in energy by 0.044 au. in the transformation to allyl cation.

Inspection of the charge distributions and core energy levels shows that a more negative energy (i.e. increased binding energy<sup>\*</sup>) is associated with an increased positive charge on the atom. The charge on a given atom is determined by the valence electron distribution, and the core levels reflect this. The different environments about C<sub>1</sub> and C<sub>2</sub>(C<sub>3</sub>) in the cyclopropyl cation are reflected in the 'shift' of C<sub>1s</sub> binding energies of about 4.1 eV.

Clearly, although the core levels are localised in space near the nucleus and are not involved in bonding their energies are a sensitive function of the electronic environment about an atom. The close proximity of the core levels to the nucleus is reflected in the fact that their binding energies are characteristic of a given element and this is shown by the approximate core binding energies for the first and second row elements given in Fig.3.8.

The characteristic identifying nature of the core orbitals and their

---

\* Binding energy is defined here as the energy needed to remove an electron in a given orbital to infinity (the vacuum level) and may be approximately equated to the -ve of the orbital energy (Koopman's Theorem).

Approximate core binding energies for 1<sup>st</sup> and 2<sup>nd</sup> row elements (in e.v.)

	Li	Be	B	C	N	O	F	Ne
1s	55	111	188	284	399	532	686	867
	Na	Mg	Al	Si	P	S	Cl	Ar
1s	1072	1305	1560	1839	2149	2472	2823	3203
2s	63	89	118	149	189	229	270	320
2p <sub>1/2</sub>	31	52	74	100	136	165	202	247
2p <sub>3/2</sub>			73	99	135	164	200	245

Fig. 3.8

## Energy Levels (in au.)

<chem>CH3CONH2</chem>	<chem>CH3COCH3</chem>
<p>-20.632 O<sub>1s</sub></p> <p>-15.706 N<sub>1s</sub></p> <p>-11.521</p> <p>-11.424 C<sub>1s</sub></p> <p>-1.394</p> <p>-1.220</p> <p>-1.034</p> <p>-0.792</p> <p>-0.707</p> <p>-0.642</p> <p>-0.613</p> <p>-0.564</p> <p>-0.518</p> <p>-0.505</p> <p>-0.364</p> <p>-0.350</p>	<p>-20.721 O<sub>1s</sub></p> <p>Core electrons -11.507</p> <p>-11.424</p> <p>-11.424 C<sub>1s</sub></p> <p>-1.451</p> <p>-1.069</p> <p>-1.008</p> <p>-1.758</p> <p>-0.647</p> <p>-0.622</p> <p>-0.616</p> <p>-0.570</p> <p>-0.540</p> <p>-0.530</p> <p>-0.448</p> <p>-0.389</p>

Fig.3.9

sensitivity to electronic environments is well illustrated in Fig.3.9. The  $O_{1s}$  core levels are easily distinguishable from the  $N_{1s}$  and  $C_{1s}$  levels. The differing electronic environments, in the same molecule, of the carbon atoms are reflected in slightly different binding energies of the  $C_{1s}$  levels.

(d) Calculation of Binding Energies from ESCA Spectra

The various energy considerations, and relevant energy levels for the calculation of binding energies for a core level of a sample are shown diagrammatically in Fig.3.10. The sample is taken to be an electrical insulator and to be in electrical contact with the spectrometer material so that both have a common Fermi level.

The principle of conservation of energy gives that for photoionisation of a core electron from the sample, the energy of the incident X-ray photon is distributed over four processes:

$$h\nu = E_b + E_{kin} + E_r + \phi_s \quad (3.1)$$

where,

$E_b$  = the binding energy of the photo ejected electron, relative to the Fermi level.

$E_{kin}$  = the kinetic energy of the free electron

$E_r$  = the recoil energy resulting from conservation of momentum in the photoionisation process.

$\phi_s$  = the work function of the sample, defined as the energy required to promote an electron from the Fermi level to the vacuum level.

Maximum values of the recoil energy ( $E_r$ ) have been calculated for some first group elements for three different X-radiations.

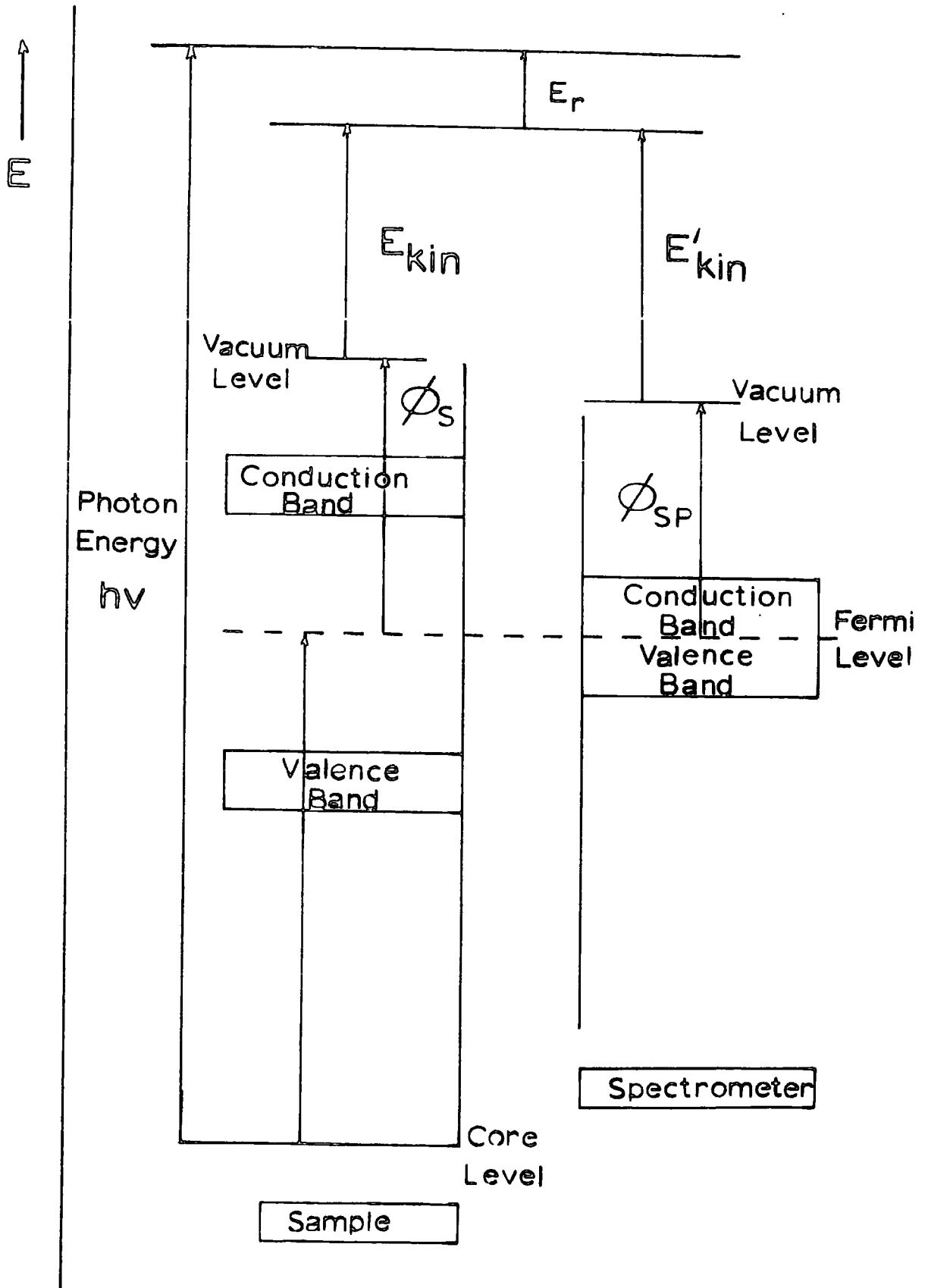


Fig.3.10

Maximum recoil energies (eV)

	AgK $\alpha$	CuK $\alpha$	AlK $\alpha$
H	16	5	0.9
Li	2	0.8	0.1
Na	0.7	0.2	0.04
K	0.4	0.1	0.02
Rb	0.2	0.06	0.01

It can be seen that for the normal exciting radiations used in ESCA (MgK $\alpha$ , AlK $\alpha$ ), the recoil energies can be effectively ignored for elements after Li in the periodic table. Therefore,  $E_r \approx 0$ .

In general there exists a small electric field in the space between the sample and the entrance slit to the spectrometer, even if both are in electrical contact. This is because their Fermi levels are the same; any difference in work function of the sample and spectrometer material gives rise to a potential, and therefore an electric field between the two. The kinetic energy of the electron when it enters the spectrometer (i.e. the analyser)  $E'_{kin}$  will be different from the energy  $E_{kin}$  it had when leaving the sample due to either retardation or acceleration in the electric field.

Therefore:

$$E_{kin} + \phi_s = E'_{kin} + \phi_{sp}$$

equation 3.1 now becomes

$$h\nu = E_b + E'_{kin} + \phi_{sp} + E_r \quad (\text{but } E_r \approx 0)$$

and

$$E_b = h\nu - E'_{kin} - \phi_{sp} \quad (3.2)$$

Since  $\phi_{sp}$  depends only on the spectrometer material and not on the sample under investigation, the same work function can be applied to all

measurements, providing it does not vary with time. A sufficient number of charge carriers must be present in the sample so that a thermodynamic equilibrium is maintained and there is no charge build up. This situation is obtained with conducting samples in contact with the spectrometer but for insulating materials this may not be so and charging effects may become important.

By calibrating the kinetic energy scale of the spectrometer to the  $\text{Au}4f_{7/2}$  level at 84.0 eV,  $\phi_{sp}$  is included in all measurements and the binding energies are then related to the spectrometer Fermi level.  $E'_{kin}$  is the energy of the electrons measured by the analyser and relative binding energies are calculated from:

$$E_b = h\nu - E'_{kin} \quad (3.3)$$

(e) Relationships between Calculated and Experimental Binding Energies for Gaseous and Solid Samples

Before discussing charge distributions in molecules as revealed by ESCA, it is important to consider the relationship between binding energies measured in solid phase, those measured in the gas phase (considered as measurements on free molecules) and binding energies obtained from quantum mechanical calculations.

Theoretical calculations inevitably refer to isolated molecules in the gas phase, and, as noted previously in relation to Koopman's Theorem, the energy reference is the vacuum level. Comparison then between gas phase measurements and theoretically determined values is relatively straightforward. On the other hand, solid phase measurements refer to the Fermi level as the energy reference. The question then

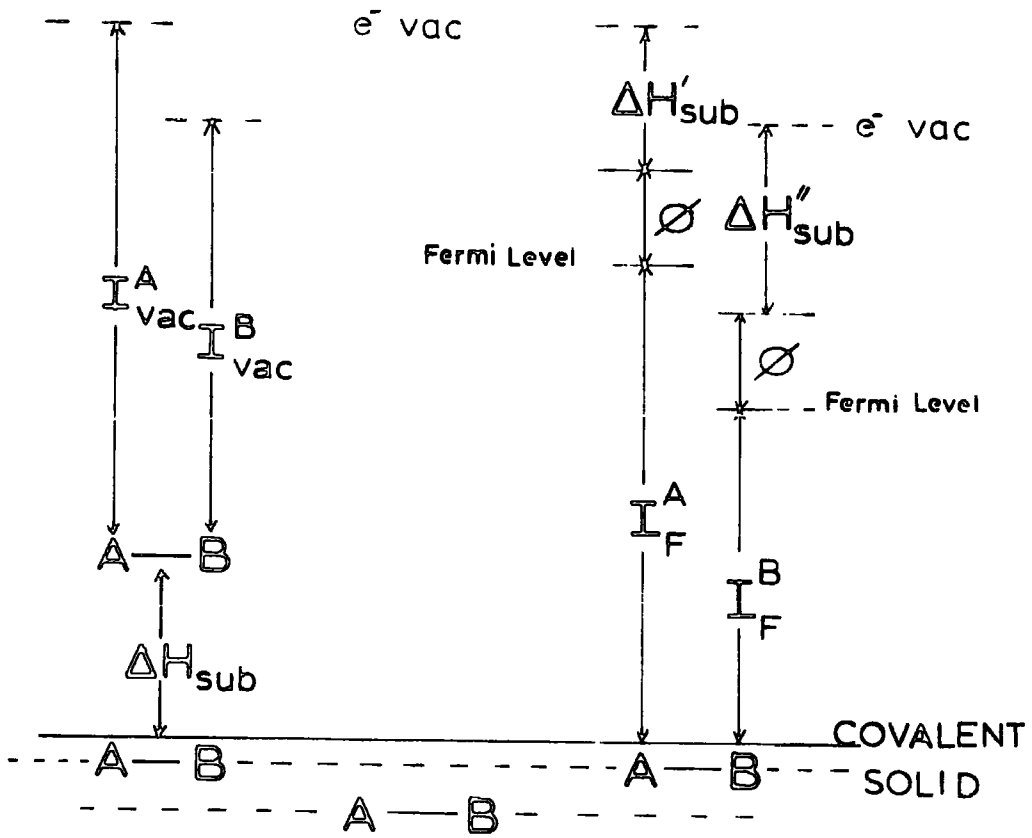


Fig.3.11.

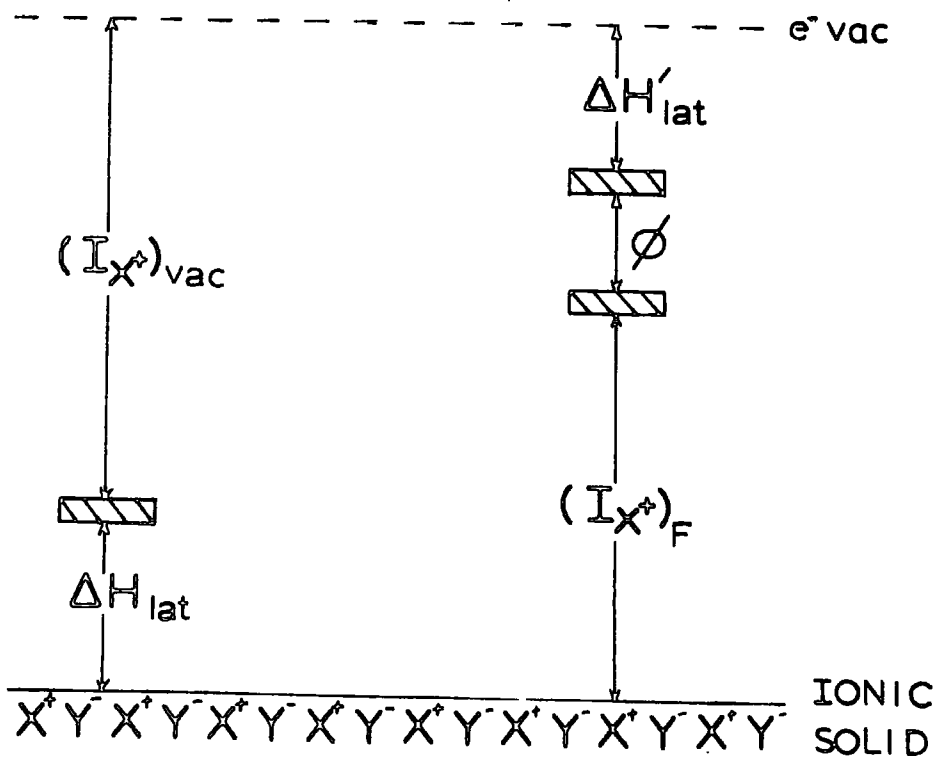


Fig.3.12

arises, when will direct comparison of the two be valid? This can readily be seen from the appropriate Born cycle. In Fig.3.11 the relationship between energy levels for a covalent solid having no appreciable long range interactions (e.g. hydrogen bonding) is illustrated. For photoionisation from A and B the binding energy separation (shift) is given by:

$$\begin{aligned}\Delta &= (I_{\text{vac}}^{\text{A}} + \Delta H_{\text{sub}}^{\text{AB}}) - (I_{\text{vac}}^{\text{B}} + \Delta H_{\text{sub}}^{\text{AB}}) \\ &= (I^{\text{A}} - I^{\text{B}})_{\text{vac}}\end{aligned}$$

also

$$\begin{aligned}\Delta &= (I_{\text{F}}^{\text{A}} + \phi_{\text{AB}} + \Delta H'_{\text{sub}}) - (I_{\text{F}}^{\text{B}} + \phi_{\text{AB}} + \Delta H''_{\text{sub}}) \\ &= (I^{\text{A}} - I^{\text{B}})_{\text{F}} + [(\Delta H'_{\text{sub}} - \Delta H''_{\text{sub}}) \approx 0]\end{aligned}$$

therefore

$$\Delta = (I^{\text{A}} - I^{\text{B}})_{\text{vac}} = (I^{\text{A}} - I^{\text{B}})_{\text{F}}$$

Now for photoionisation of atoms in different samples, charging effects must be considered and, in general, the binding energy shift ( $\Delta$ ) is:

$$\begin{aligned}\Delta &= (I^{\text{A}} - I^{\text{X}})_{\text{vac}} \\ &= (I^{\text{A}} - I^{\text{X}})_{\text{F}} + (\phi_{\text{A}} - \phi_{\text{X}}) + (\delta_{\text{A}} - \delta_{\text{X}}) + (\Delta H_{\text{X}} - \Delta H_{\text{A}})_{\text{sub}} \\ &\quad + (\Delta H'_{\text{A}} - \Delta H'_{\text{X}})_{\text{sub}}\end{aligned}$$

where

- $I^{\text{X}}$  = ionisation of energy of atom X (100-1000 eV)
- $\phi_{\text{X}}$  = work function of sample containing atom X ( $\sim 5$  eV)
- $\delta_{\text{X}}$  = charging effect on sample containing atom X ( $\sim 2$  eV)
- $\Delta H_{\text{sub}}$  = sublimation energy of molecule considered (M) ( $\sim 0.5$  eV)
- $\Delta H'_{\text{sub}}$  = sublimation energy of photoionised state (M<sup>\*</sup>)

Typical values are given in brackets.

For closely related materials in electrical contact with the spectrometer:

$$(\phi_A - \phi_X) \approx 0, (\delta_A - \delta_X) = 0, \text{ and } \Delta(\Delta H_{\text{sub}}) \text{ terms} = 0$$

Hence 
$$\underline{(I^A - I^X)_{\text{vac}}} = (I^A - I^X)_F$$
 and the comparison between

theoretical calculations on isolated molecules and measurements on thin films should be valid.

In the case of atoms in an ionic lattice the comparison does not necessarily hold. Fig.3.12 shows the energy relationships for a gaseous ion and an ionic lattice. For atoms in the same lattice the binding energy shift is:

$$\Delta = (I_{X^+} - I_{Y^-})_{\text{vac}} = (I_{X^+} - I_{Y^-})_F + \text{lattice contributions}$$

for different samples (with no charging effects)

$$\Delta = \Delta I_F + \Delta\phi + \Delta(\Delta H_{\text{lat}} - \Delta H'_{\text{lat}}) \times \text{lattice contributions.}$$

In the latter case the final three terms may not approximate to zero mainly because of the magnitude of the lattice effects so that shifts are not directly comparable to those for the free ions. Care must be taken in interpreting shifts for ionic solids. When samples are not in electrical contact with the spectrometer, as in the case of thick layers of organic solids or polymer materials, charging effects will vary from sample to sample and with time. Then terms like  $(\delta_A - \delta_X) \neq 0$  and corrections must be applied to take this into account. The problems associated with charging effects and methods of solving these will be discussed later.

(f) Linewidths and Their Significance in Studying Core Levels

The measured linewidths for core levels (after taking spin-orbit splittings into account, if they are not resolved) may be expressed as:

$$(\Delta E_m)^2 = (\Delta E_x)^2 + (\Delta E_s)^2 + (\Delta E_{cl})^2$$

where  $\Delta E_m$  = measured width at half height [the so called full width at half maximum (F.WHM)]

$\Delta E_x$  = FWHM of the exciting photon line

$\Delta E_s$  = contribution to the measured FWHM due to the spectrometer (mainly from the analyser)

$\Delta E_{cl}$  = natural line width of the core level under investigation  
For solids this includes solid state effects not directly associated with the lifetime of the hole state but rather with slightly different binding energies due to varying lattice environments.

The contribution to the total line width from  $\Delta E_x$  can be made negligible (see section iv(e)) and with well designed analysers the contribution from  $\Delta E_s$  can be ignored. Given a sufficiently narrow line width for the photon source, the major limiting factor is the inherent width of the level itself (excluding solid state effects). Some examples of natural line widths ( $\Delta E_{cl}$ ) are given below:

Approximate Natural Widths of Some Core Levels (in eV)

Level	Atom								
	S	A	Ti	Mn	Cn	Mo	Ag	Au	
1s	0.35	0.50	0.80	1.05	1.50	5.0	7.5	54.0	
2p <sub>3/2</sub>	0.10		0.25	0.35	0.50	1.7	2.2	4.4	
Radiative Widths									
1s	0.04	0.07	0.20	0.33	0.65	3.6	6.0	50.0	
Fluorescence Yields									
1s	0.10	0.14	0.22	0.31	0.43	0.72	0.80	0.93	

The uncertainty principle in the form:

$$\Delta E \cdot \Delta t \geq \frac{h}{4\pi}$$

shows that for a hole state lifetime of  $\sim 6.6 \times 10^{-16}$  sec. the linewidth (i.e. uncertainty in the energy of the state) is  $\sim 1$  eV.

It can be seen from the above values that there are large variations in natural linewidth both for different levels of the same atom and the same levels of different elements. These reflect differences in the life time of the hole state, a composite of radioactive (fluorescence) and non-radiation (Auger) contribution. This emphasises the fact that there is no virtue in studying the innermost core level of an element. The gold 1s level has a half width of  $\sim 54$  eV so that even if a monochromatic X-ray source of the requisite energy were available, any chemical shift effects would be swamped.

Typically the lifetimes of the core hole states involved in ESCA are  $\sim 10^{-14}$  -  $10^{-17}$  secs. emphasising the extremely short time scales involved compared to molecular vibrations. The process may be called sudden with respect to nuclear (but not electronic) motions.

#### (iv) The Electron Spectrometer

The discussion in this section refers mainly to the ES100 electron spectrometer manufactured by AEI Ltd. and used for the ESCA investigations described in this thesis. References are made to other instruments and designs where appropriate. Fig.3.13 shows schematically the general arrangement of components of the X-ray photoelectron spectrometer used.

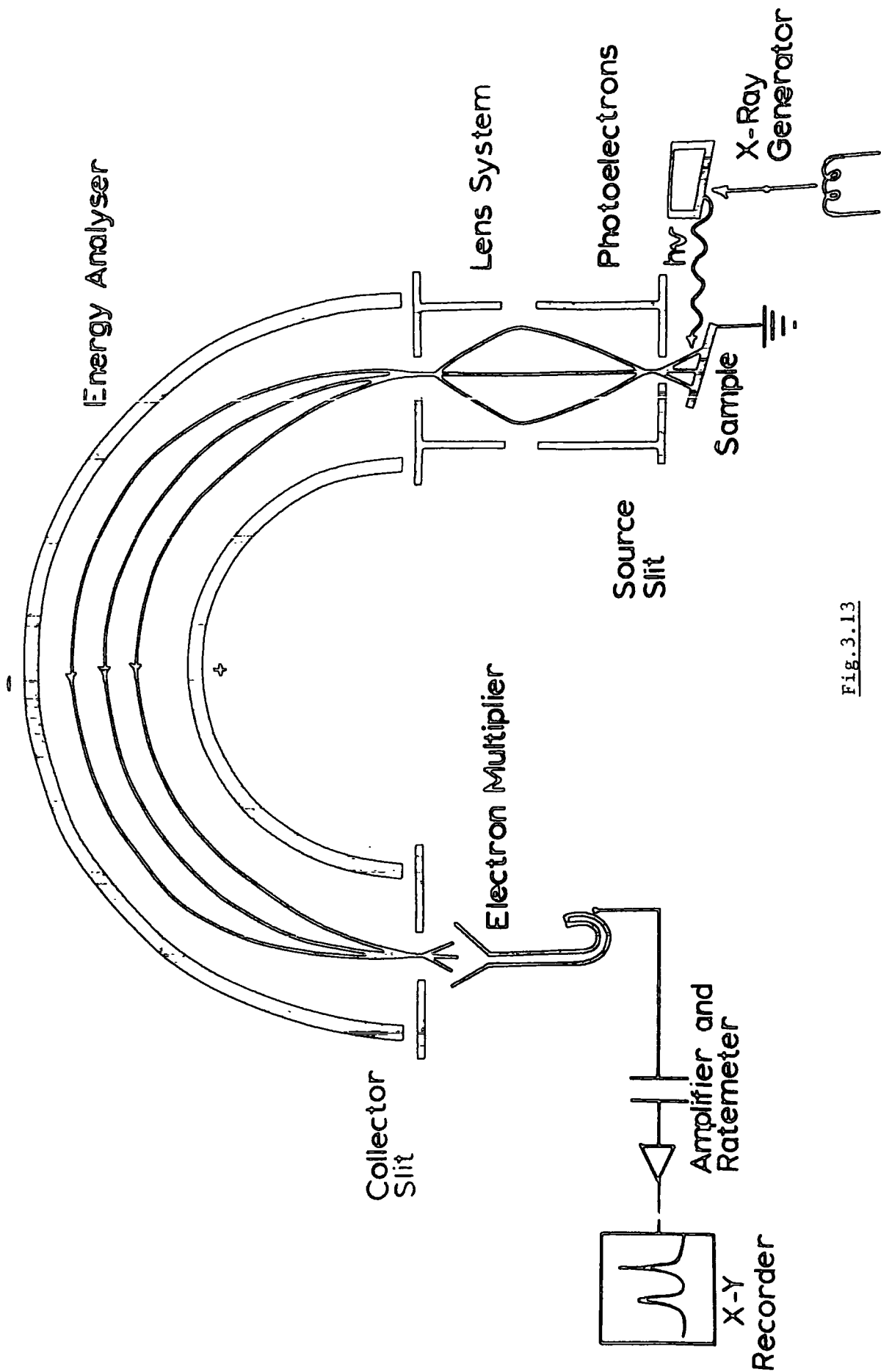


Fig. 3.13

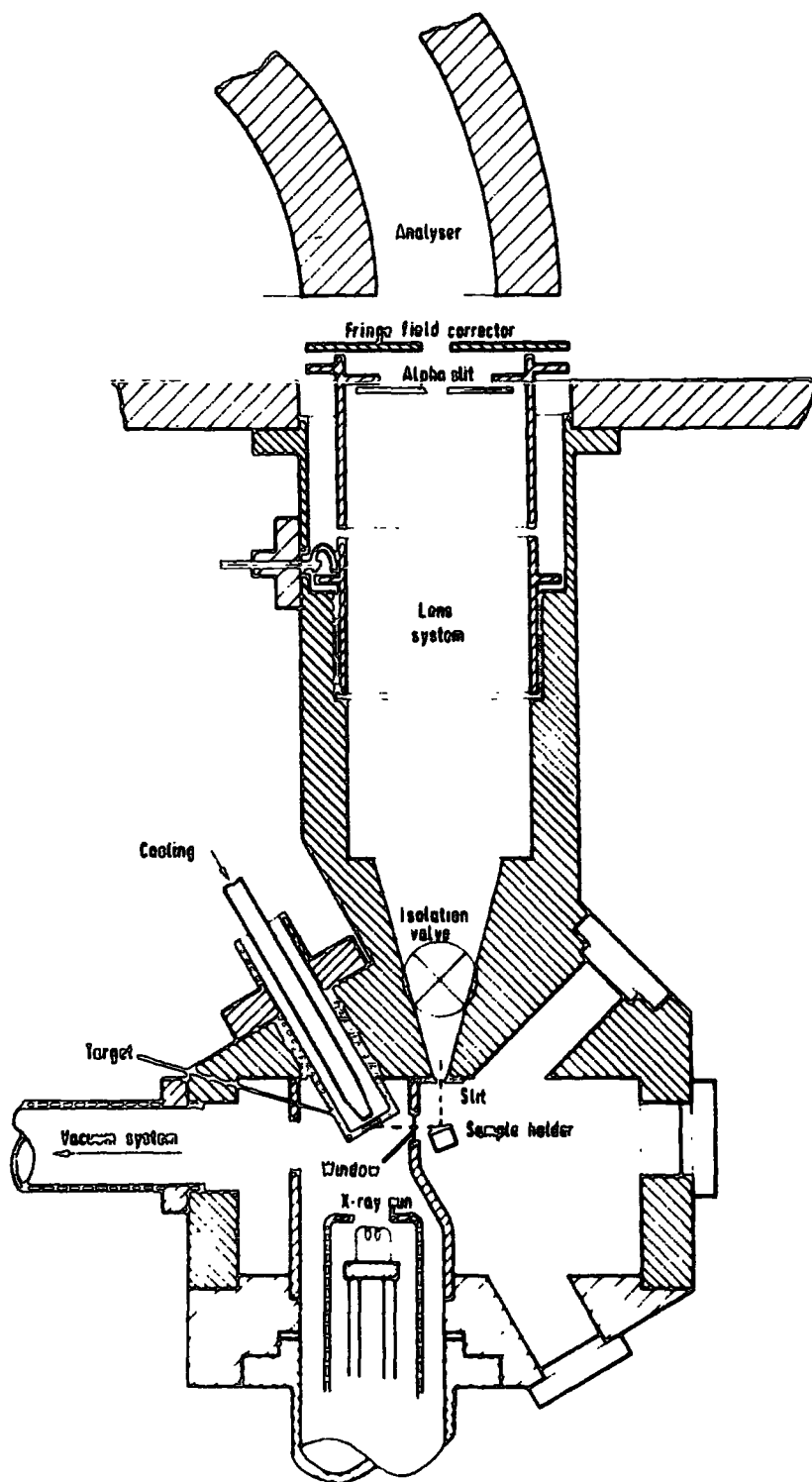
(a) The Source Region

A detailed cross-section of the ES100 source region with the main components labelled is shown in Fig.3.14. The X-ray generator consists of a heated tungsten cathode at high negative (or earth) potential and a hollow, water-cooled copper anode faced with either magnesium or aluminium at earth (or high positive) potential. Water cooling of the anode is essential because of the high power dissipated. Other anode materials can be used as X-ray sources but normally Mg and Al are the most convenient, with medium photon energies and low inherent linewidths. Harder X-ray sources (Cr, Cu) have much larger inherent linewidths and give lower resolution.

Anode	X-ray line	Energy (eV)	Linewidth (eV)
Mg	MgK $\alpha_{1,2}$	1253.6	0.7
Al	AlK $\alpha_{1,2}$	1286.6	1.0
Cr	CrK $\alpha_1$	5414.7	2.1
Cu	CuK $\alpha_1$	8047.8	2.6

Average operating conditions for the X-ray gun would be 10-15 KV at 20-50 mA and a vacuum of  $\leq 4 \times 10^{-6}$  torr.

As Fig.3.14 shows a thin window, usually of Al foil (0.0003 inch) or better Be, separates the sample region from the X-ray source. The window allows the X-ray beam to pass (with some attenuation) but prevents scattered electrons from the target entering the sample region and hence, the analyser. Tungsten deposition from the heated filament cathode onto the window and the target surface can be a problem, causing attenuation of the X-ray beam and loss of counts. In later models this has been overcome by introducing a metal plate between the filament and the target and window. The electron beam is then electrostatically focussed around



LEIS AND SOURCE ARRANGEMENT ES100

Fig. 3.14

the plate onto the target. This arrangement is known as a Henke gun.

(b) Electron Energy Analysers

The main barrier to the development of ESCA as a technique has been the design of analysers of sufficiently high resolution and luminosity. Typically a resolution of better than 1 part in  $10^4$  is needed.

The most general method of energy analysis for both high and low (X-ray and u.v.) energy electron spectroscopy is based on the deflection of electrons by magnetic (momentum analyser) or electrostatic fields (kinetic energy analyser). In early u.v. work, cylindrical retarding grid analysers were used,<sup>148</sup> but these suffered from several defects, the most serious of which was inherent lack of resolution. The relative merits of the various systems in current common use have been briefly reviewed.<sup>149</sup>

The simplest of the electrostatic analysers is shown in Fig.3.15(a). This consists of a  $127^\circ$  cylindrical sector analyser in which focussing of electrons of different energies is achieved by varying the potential applied to the plates. The angle of  $127^\circ 17'$  is chosen because there is an electron trajectory re-focussing property at that angle.<sup>150</sup> Another simple version is the parallel plate analyser shown in Fig.3.15(b). Both these devices are of the single-focussing type.

Double-focussing analysers provide a higher intensity signal for a given resolution, and it is this type of system that is used in current X-ray spectrometers. The focussing action in the plane of the analyser (as in the single-focussing types) is augmented by directional focussing along great circles of a spherical sector. This can be seen by comparing

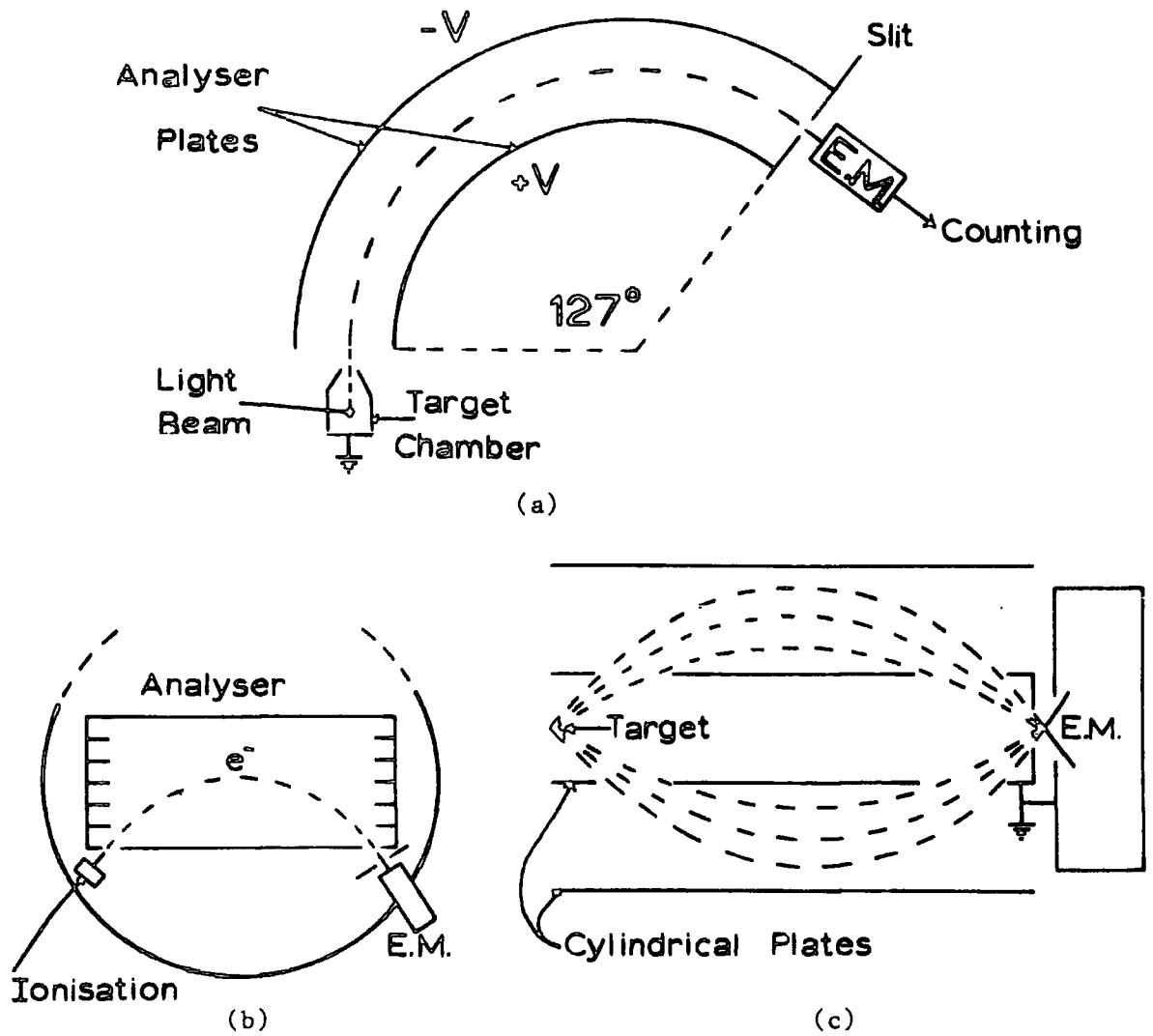


Fig. 3.15

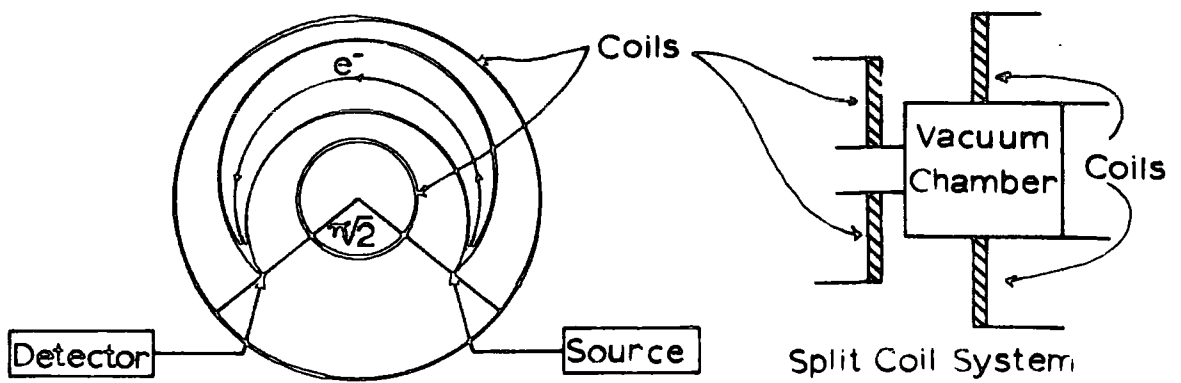


Fig. 3.16

the double-focussing cylindrical mirror analyser<sup>151</sup> (Fig.3.15(c)) with the parallel plate analyser (Fig.3.15(b)). The idea of double-focussing was originally suggested by Aston in 1919.<sup>152</sup>

The double-focussing analysers used in ESCA spectrometers can be either magnetic or electrostatic. The magnetic type was first introduced by Siegbahn<sup>153</sup> in the first ESCA instrument and new designs are still based on this system. These are iron-free instruments made from brass or aluminium with a 30 cm. radius. Double-focussing is provided by an inhomogeneous magnetic field produced by a set of four cylindrical coils placed about the electron trajectory as shown in Fig.3.16. It is necessary to eliminate stray magnetic fields, such as the earth's, from the analyser sector. This is done with vertical and horizontal Helmholtz coils, but the elaborate monitoring systems needed and bulky coils constitute a major disadvantage.<sup>154</sup> The main point in favour of these machines is their ease of construction compared to the electrostatic type.

Double-focussing electrostatic analysers are now widely used; the most popular being the hemispherical ( $180^\circ$ ) system,<sup>155</sup> shown in Fig.3.13. With this system  $\mu$ -metal shields can be used to eliminate stray magnetic fields, making the electrostatic analyser more compact. It is probably for this reason that commercial ESCA machines use this system despite the considerable problems involved in engineering spherical sector plates to high tolerances.

An instrument resolving power of  $\Delta E/E = 300$  is readily obtained with the deflection instruments described above. This corresponds to a peak half-width (full width at half maximum peak height) of 3.3 eV for a 1 KeV electron. Since the inherent width of the exciting X-ray line is

less than 1 eV for  $MgK\alpha_{1,2}$  or  $AlK\alpha_{1,2}$  at around 1.5 KeV there is room for improvement. Since the fractional resolution  $\Delta E/E = R/W$ , where  $R$  = mean radius of the sector and  $W$  is the combined width of the entrance and exit slits, the resolution can be improved by:

(i) making  $W$  smaller by decreasing the slit width.

This also reduces the signal intensity.

(ii) increasing  $R$  by using a larger radius analyser. This increases the already serious engineering difficulties.

(iii) reducing  $E$  by retarding the electrons before they reach the analyser. This can simultaneously enhance the signal intensity.<sup>156</sup>

It is solution (iii) that has been successfully used and this system is incorporated in the A.E.I. spectrometer.

#### (c) Detection Systems

The detection system needed has to be, in effect, an electron counter because of the minute electron currents involved. Three general methods have been used in ESCA instruments; Geiger-Muller counters, electron multipliers and photographic detectors.

The electron multipliers are most common and are more convenient, especially the continuous channel type ('channeltron') which have a high counting efficiency to low electron energies. The focal plane properties of double-focussing analysers can be exploited by incorporating several tiny multipliers (multichannel detectors) together over the length of the exit slit. The signal from the detector is amplified and fed to counting electronics.

(d) Data Acquisition

There are basically two ways of obtaining the required information from the detection system; continuous scanning or step scan.

In continuous scanning the field (either electrostatic or magnetic) is continuously increased with time while the detector signal is monitored by a rate meter. Synchronisation of the spectrometer current and the rate meter output allows continuous recording of a spectrum, as electron counts against kinetic energy, on an X—Y recorder. This is a convenient method of data display when the signal to noise ratio is high.

The step-scan mode increases the current through the spectrometer in a series of small steps corresponding to a 0.1 eV (0.2, 0.3 etc.) step in the measured kinetic energy of the electrons. A scalar is used to count the number of electrons over a given time interval at each step, giving a point spectrum. In this mode the system is easily automated and computerised.

A variation on both themes is the multichannel analyser. This enables a large number of increments to be continuously scanned between two set limits of the field. The number of counts at each step are collected in separate channels and the stored data can be out-putted in various ways. One main advantage of this method is in the measurement of 'weak' peaks where the signal to noise ratio is low. The spectrum can be effectively integrated over a long period and the background averaged out. Again, this mode is ideally suited to computerisation.

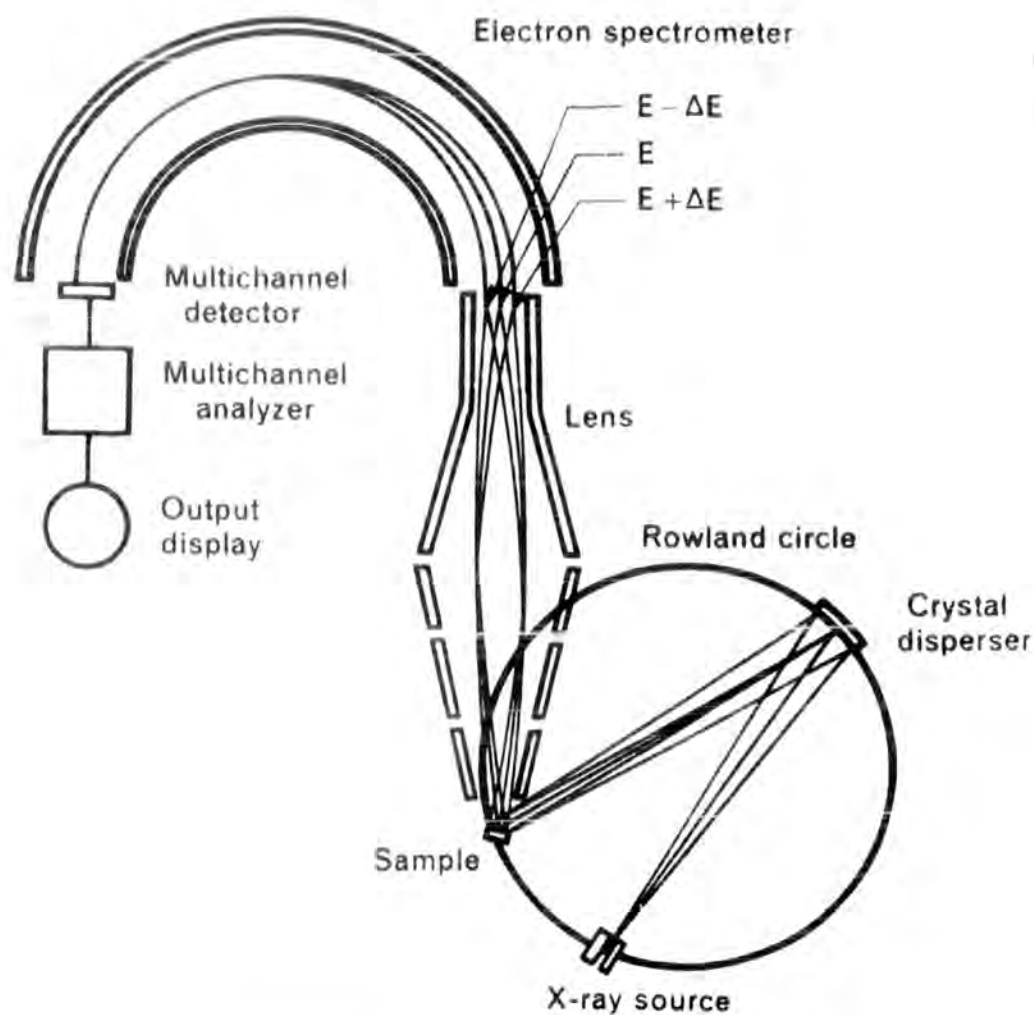


Fig. 3.17

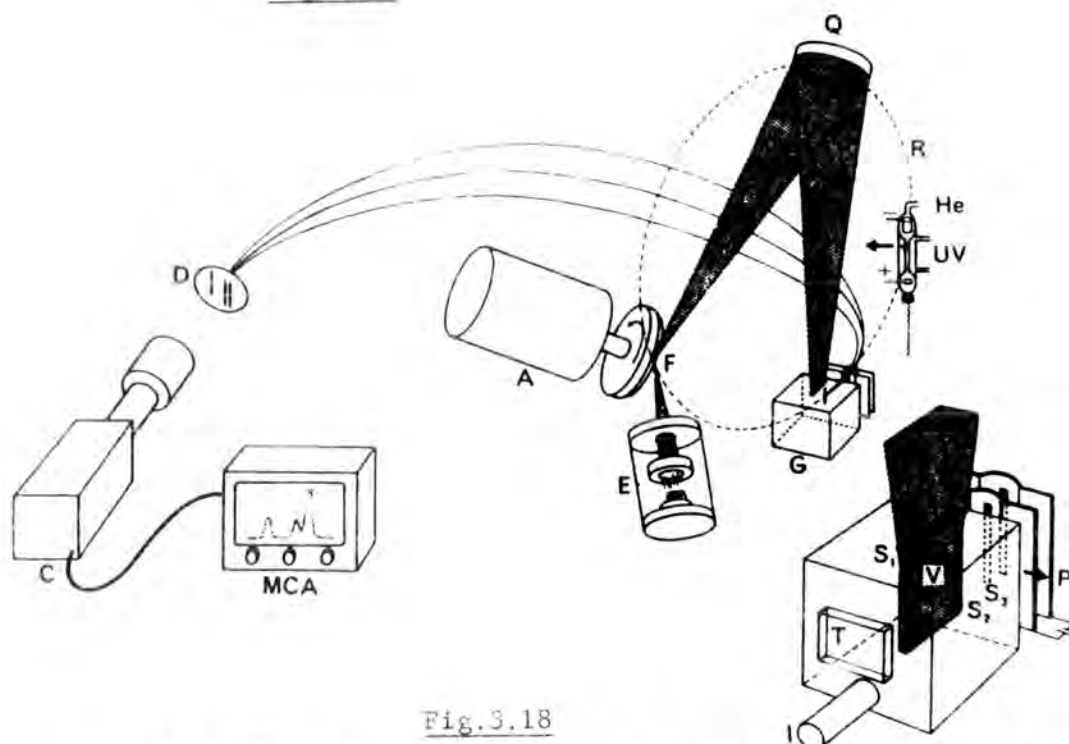


Fig. 3.18

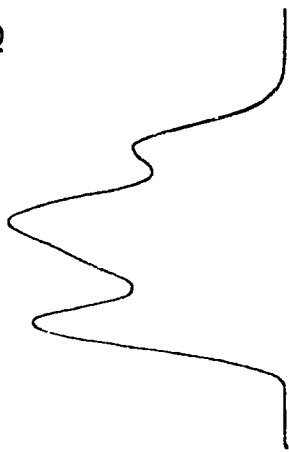
A new ESCA instrument suitable for gases with X-ray monochromatization. E=electron gun, A=rotating anode, F=focal spot, Q=spherically bent quartz crystal, R=Rowland circle, UV=helium lamp, G=gas compartment,  $S_1$ - $S_3$ =slits, V=effective irradiated gas volume, T=temperature raising device, I=gas inlet system, P=two-stage differential pumping system with an electron retardation step, D=multichannel plate detector, C=television camera, and MCA=multichannel analyser.

(e) Recent Developments in Instrumental Design

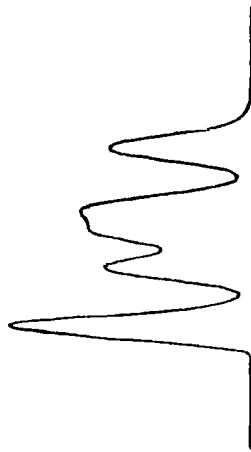
In the spectrometer designs discussed above the exciting X-ray beam was not filtered before entering the sample chamber. This results in the presence, in the exciting radiation beam, of bremsstrahlung background and other (usually less intense) X-ray emission such as the  $K\alpha_{3,4}$  lines. As already shown the attainable resolution is often limited by the inherent width of the exciting radiation, (at present around 1.0 eV) which is not negligible compared to the range of chemical shifts observed for a given element, ( $\sim 10$  eV for  $C_{1s}$ ) and is considerably greater than the natural core-level widths studied ( $\sim 0.3$  eV).

Early in the development of ESCA, monochromation of the X-ray beam was described by Siegbahn et al.<sup>145</sup> as a method of improving the line widths. This group have recently described monochromation using spherically bent quartz crystals and a 'dispersion compensation' system to increase sensitivity without losing resolution.<sup>157,158</sup> This is shown in Fig.3.17. As 'dispersion compensation' can not be used in all cases (i.e. solids with very uneven surfaces, or gases) an alternative is to use a very narrow slit between the monochromator and the target (slit filtering). Unfortunately this produces a severe loss in signal intensity and to compensate for this high power rotating anodes (5-10 KW) and improved detection systems are needed. This type of arrangement is shown in Fig 3.18. Line widths of 0.5 eV (for solid samples) have been obtained and chemical shifts can be measured to within 0.1 eV (in the gas phase). This increased resolving power can have a dramatic effect on the experimental spectrum. An example is given in Fig.3.19 of a computer simulated six-fold increase in resolution. At 0.2 eV linewidth all the distinct types of carbon atoms in this comparatively complex molecule can

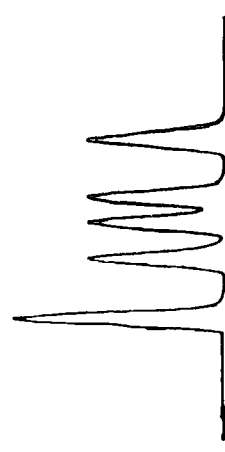
Effect of improved resolution  
 $C_{1s}$  levels (simulated)



present  
 instrumentation  
 1.2 e.v.



Dispersion  
 compensation  
 0.6 e.v.



Natural linewidth  
 $< 0.2$  e.v.

Binding  
 Energy e.v. 294.0 292.0 290.0 288.0 286.0

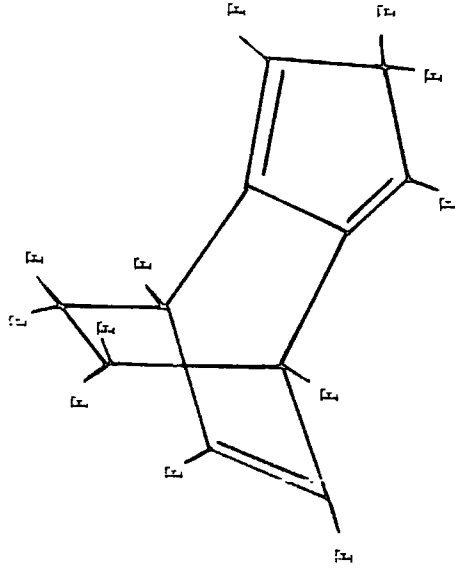


Fig. 3.18

be resolved. This type of improvement should enable wider applications of ESCA in the near future with more accurate data available from the technique.

(v) Review of ESCA Applications in Organic Chemistry

The technique of ESCA has been developed over the past 20 years (mainly by Siegbahn's group at Uppsala). It is only in the past few years that the potential of the technique for studying structure and bonding has been appreciated. However, chemists have not been slow to take up the technique; the literature relating to applications of ESCA to organic chemistry is rapidly expanding. This brief review is not intended to be comprehensive, but to illustrate those areas of organic chemistry where ESCA has been of particular value. A good indication of the rapid increase of interest in ESCA is the number of reviews that have appeared recently, covering both the technique itself<sup>154,159-161</sup> and general applications of ESCA to chemistry,<sup>162-165</sup> and the introduction of a new journal.<sup>167</sup>

The accurate measurement of molecular core binding energies has stimulated interest in the theoretical prediction of ESCA chemical shifts. A variety of methods have been used with varying degrees of success.<sup>145,146,166,167</sup> In general, non-empirical calculations are limited to small molecules mainly because of computational expense and convergence problems.<sup>168,169</sup> A theoretically valid, but computationally inexpensive model at a slightly lower level of sophistication is necessary. The most successful of these is the charge potential model.<sup>145,146</sup> This model has been widely applied to the interpretation of ESCA chemical shifts and in certain cases has



allowed structural problems in organic molecules to be resolved (see later).

The relationship (eq.3.4) developed by Siegbahn et al.<sup>146</sup> has been extensively discussed in the literature and shifts in the  $C_{1s}$  levels for substituted aliphatic,<sup>170</sup> aromatic,<sup>171,172</sup> and heterocyclic<sup>173,174</sup> molecules have been quantitatively described by the charge potential model in terms of CNDO/2 SCF MO charge distributions.

$$E_i = E_i^o + kq_i + \sum_{i \neq j} \frac{q_j}{r_{ij}} \quad (3.4)$$

where

$E_i$  = binding energy of core level on atom  $i$

$E^o$  = reference level

$q_i$  = formal charge on atom  $i$

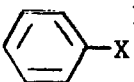
$\sum_{i \neq j} \frac{q_j}{r_{ij}}$  = an intramolecular Madelung type potential arising from charges on other atoms in the molecule.

The parameter  $k$  depends on the definition of atomic charge and, in an SCF MO treatment, on the basis set involved. It can be equated approximately to the one-centre coulomb integral between a core and valence electron and has a calculated value of 22.0 eV for carbon, using Slater type orbitals. A non rigorous derivation of Eq.3.4 is given in Appendix III starting from Koopman's Theorem.<sup>175</sup>

The charge potential model is of particular importance to organic chemists since it relates core binding energies to charge densities, and is conceptually simpler than more rigorous models.<sup>176,177</sup> Since the electron distribution in a molecule is a continuous function, defining

charge distributions in terms of electron populations on atoms is necessarily somewhat arbitrary, and this is one defect of the charge potential model. The model being related to Koopman's Theorem, which neglects electronic relaxation on ejection of a core electron, must suffer from some of the same deficiencies. This can be accommodated by treating  $k$  and  $E^0$  as variable parameters and fitting the experimental data to the equation by a least squares treatment. As electronic relaxation depends on the electronic structure of a molecule it is only for closely related series of molecules that one might expect Koopman's Theorem to provide a quantitative interpretation of shifts in core binding energies. Similarly for the charge potential model, different values of  $k$  and  $E^0$  might be expected for different series of closely related compounds. Indeed this is found to be the case. Given below are  $k$  values found for various series of organic molecules. It is evident that with charges computed from CNDO/2 calculations the value of  $k$  clusters around 25.0 eV for  $C_{1s}$  levels. Similar correlations may be made for other core levels e.g.  $F_{1s}$ ,  $Cl_{2p}$ ,  $N_{1s}$ , etc.

Charge Potential Model ( $C_{1s}$  levels)

Series	k
 <sup>179</sup>	24.6
$\underline{C}Cl_3-X$ , $\underline{C}HCl_2-X$ <sup>170</sup>	26.6 <sup>a</sup>
$\underline{C}H_3\underline{C}OX$ <sup>180</sup>	25.0
Aromatics: perhydro, perfluoro <sup>171</sup>	25.0
Six membered ring nitrogen <sup>174</sup> heterocycles: perhydro, perfluoro, perchloro	22.4

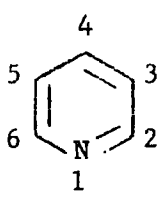
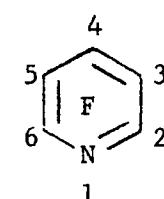
Series	k
Fluorobenzenes <sup>178</sup>	23.5
Five membered ring heterocycles <sup>173</sup>	25.4
<hr/>	
a, without d-orbitals on chlorine	

However, theoretically calculated charges are only crude guides to the electron density about the atom, and are, anyway, somewhat arbitrary, depending on how the overlap density is proportioned between atoms. Nevertheless, accepting its limitations, the idea of charge distributions in a molecule is a useful concept and one widely used by chemists. The charge distributions that an organic chemist may infer from studying the chemistry of a system may be termed 'intuitive' charge distributions and these will necessarily be different from the calculated distributions. That there are close similarities between factors determining 'intuitive' charge distributions and ESCA chemical shifts can be seen from a simple example.

The chemistry of pyridine and its perfluoro analogue shows that perfluoropyridine is a much weaker base than pyridine itself. It must be energetically less favourable to bring a proton up to the nitrogen in perfluoropyridine, and therefore one might infer that the charge density on the nitrogen is less (i.e. a more positive charge) in perfluoropyridine than in pyridine. What has been referred to here as 'charge density' is really a measure of the potential experienced by an approaching proton. This potential will depend not only on the atom concerned but also on the charges on other atoms in the molecule and this is precisely the relationship used in calculation of ESCA shifts from the charge potential model. It is interesting to note that CNDO calculations show that the charge density on the nitrogen is higher (more negative) in perfluoro-

pyridine than in pyridine. The much higher (2.1 eV)  $N_{1s}$  binding energy in perfluoropyridine arises from large contributions to the chemical shift from charges on other atoms in the molecule. It is clear from this that the ESCA shifts parallel 'intuitive' rather than calculated charge distributions making ESCA particularly valuable to the organic chemist, complementing his concept of charge distributions in molecules. (The argument can be extended in general, to refer to nucleophilic and electrophilic attack). The relevant data for pyridine and perfluoropyridine are given below.

Binding Energies, CNDO/2 charges and Madelung Potentials  
for Pyridine and Perfluoropyridine<sup>174</sup>

	Position	B.E. (eV)	$q_i$	$\sum_{i \neq j} \frac{q_i}{r_{ij}}$
	1 ( $N_{1s}$ )	400.2	-0.163	1.81
	2,6 ( $C_{1s}$ )	286.3	0.097	-1.49
	3,5 ( $C_{1s}$ )	285.5	-0.023	0.72
	4 ( $C_{1s}$ )	285.9	0.047	-0.33
	1 ( $N_{1s}$ )	402.3	0.210	4.68
	2,6 ( $C_{1s}$ )	290.1	0.290	-2.04
	3,5 ( $C_{1s}$ )	289.5	0.113	1.28
	4 ( $C_{1s}$ )	290.5	0.217	-0.21

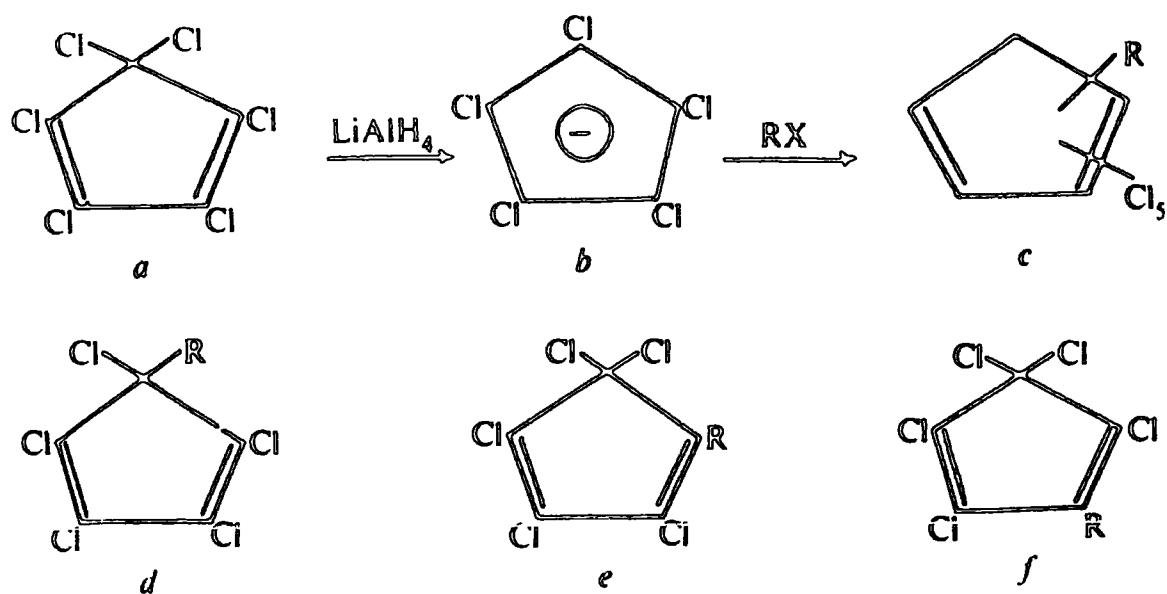
Although the charge potential model has been extensively used in assigning core levels by using CNDO/2 charge distributions to calculate theoretical chemical shifts, it is also possible to reverse the process



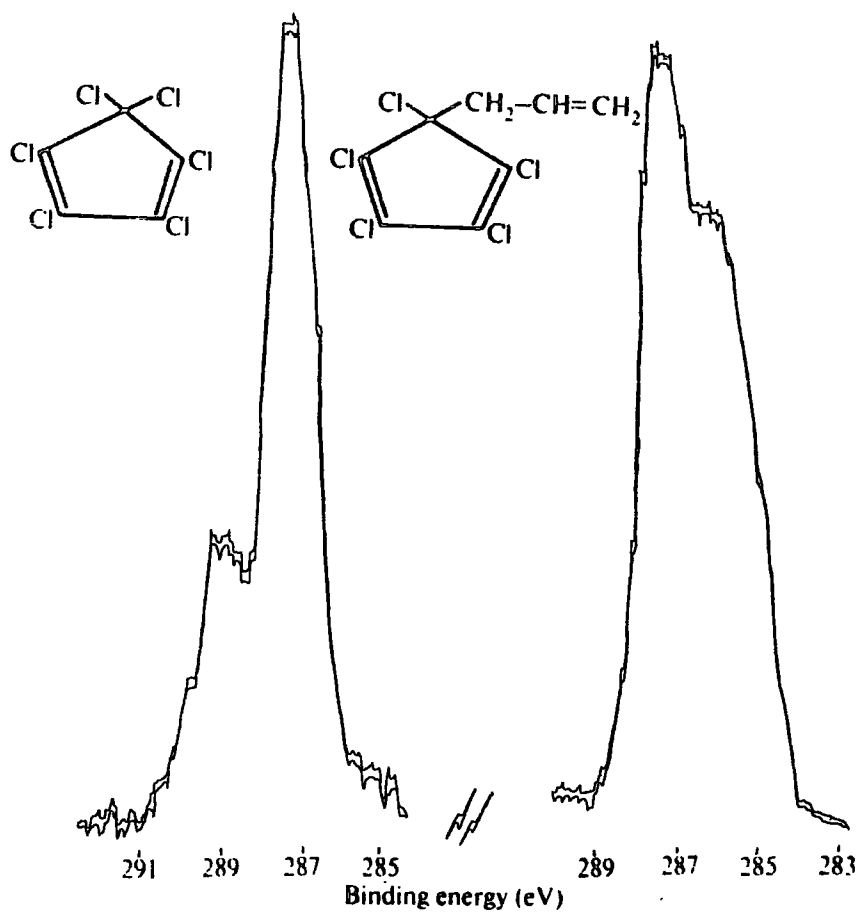
and calculate charge distributions from measured molecular core binding energies. This has now been done by several groups of workers.<sup>172,181-183</sup> Once values for  $E_i^0$  and  $k$  in eq. 3.4 have been established [by studying closely related molecules for which calculated charge distributions (usually CNDO/2) are available] for core levels of each constituent type of atom and knowing the molecular geometry and measured core binding energies ( $E_i$ ) then a series of simultaneous equations can be set up and solved for charges ( $q_i$ ). For hydrogen containing molecules a problem arises since there are no energy levels characteristic of the hydrogen  $1s$  orbital. This has been overcome by Clark et al.<sup>181</sup> who defined pseudo  $E_i - E_i^0$  and  $k$  values for hydrogen, such that they reproduced calculated charge distributions in reference molecules (methane, benzene, etc.).

Fig.3.20 shows experimental charge distribution obtained for tetradecafluorotricyclo[6,2,2,0<sup>2,7</sup>]dodeca-2,6,9-triene from measurements of the  $C_{1s}$  and  $F_{1s}$  binding energies. The close agreement with theoretically calculated (CNDO/2) charges is striking. For molecules of this size it is probably easier to obtain charge distributions by experiment rather than by direct calculation.

ESCA has been successfully applied to a number of structural problems, notably in the halocarbon field, where conventional spectroscopic techniques failed to yield unambiguous results. The treatment of hexachlorocyclopentadiene in diethyl ether at  $-20^\circ\text{C}$  with two molar proportions of  $\text{LiAlH}_4$  and allyl bromide yields an allylpentachlorocyclopentadiene<sup>184</sup> whose structure could be d, e, or f, as shown in Fig.3.21. Previous attempts at structure determination failed to distinguish between



Reaction pathway and possible chemical structures.

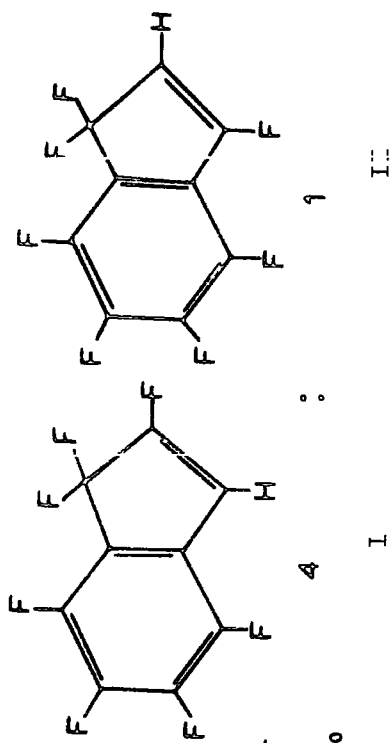
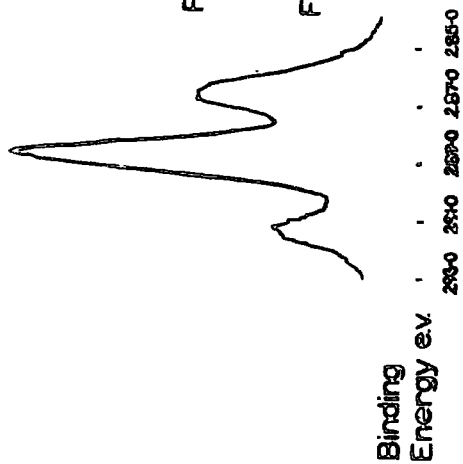


$C_{1s}$  spectra of hexachlorocyclopentadiene and allylpentachlorocyclopentadiene.

Fig. 3.21.

C<sub>1s</sub> levels

Experimental



C<sub>1s</sub> levels

Theoretical Spectrum 4:1 mixture

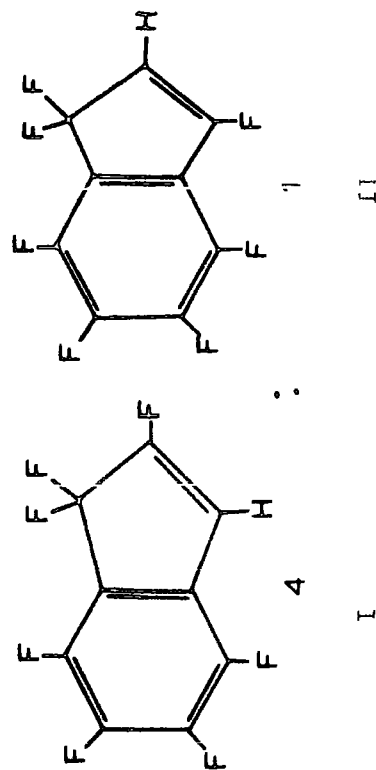
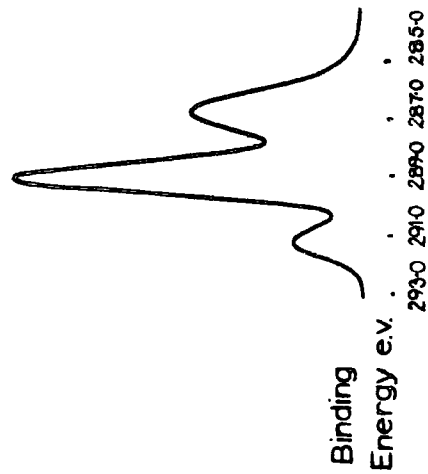


Fig. 3.22

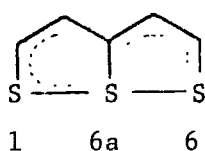
structures d and e. Comparison of the  $C_{1s}$  spectra of hexachlorocyclopentadiene and the product (Fig.3.21) allows the structure to be readily assigned to d by the absence of the peak at higher binding energy in the product, due to the  $CCl_2$  group.<sup>185</sup>

The sites of nucleophilic attack by hydride ion in perfluoroindene have been determined by ESCA.<sup>186</sup> The reaction of perfluoroindene with sodium borohydride in diglyme under controlled conditions gave a mixture of two mono substituted products in a 4:1 ratio. Conventional spectroscopy showed the mixture contained 1,1,2,4,5,6,7- and 1,1,3,4,5,6,7-heptafluoroindenes (I and II in Fig.3.22) but could not identify the major isomer. From theoretical (CNDO) SCF MO calculations of charge distributions, spectra for the  $C_{1s}$  levels of 4:1 mixtures of (I:II) and (II:I) were computed. Comparison of the simulated spectra with the experimental  $C_{1s}$  spectra of the mixture in terms of peak intensities and absolute binding energies allowed unambiguous assignment of the major isomer as I. The simulated and experimental spectra obtained are given in Fig.3.22.

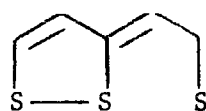
Preliminary accounts have been given of applications of ESCA to carbonium ion chemistry.<sup>187,188</sup> Measurement of the  $C_{1s}$  spectra of the t-butyl cation shows two peaks separated by 3.4 eV due to the methyls and  $C_1$  indicating a high charge localisation on the central carbon, but by contrast, both trityl and tropylium cations show a single  $C_{1s}$  line consistent with extensive charge delocalisation. Studies of 1-adamantyl and norbornyl cations indicate that the formal charge in the norbornyl cation is extensively delocalised, strongly suggesting a non-classical structure for this ion. Charge delocalisation in acyl cations, studied as the hexafluoroantimonates, has also been investigated.<sup>189</sup> The greater

shift and higher absolute binding energy for the  $\underline{\text{CO}}$  carbon  $1s$  level in  $\text{CH}_3\text{CO}^+$  compared with  $\text{C}_6\text{H}_5\text{CO}^+$  indicates much greater charge delocalisation in the latter.

The question of symmetrical and unsymmetrical structures for the thiathiophthenes has been investigated by ESCA.<sup>190-192</sup> CNDO SCF MO calculations predict that for the symmetrical structure (a), the core levels of the central sulphur will be more tightly bound than those for the outer two sulphurs, while for an unsymmetrical structure (b), the three sulphurs are predicted to have different core binding energies in the order  $S(6) < S(1) < S(6a)$ .<sup>190,191</sup>



(a)

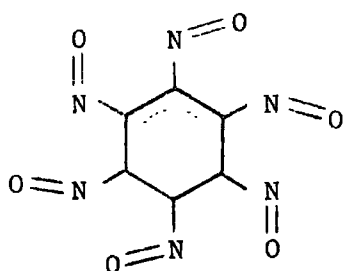


(b)

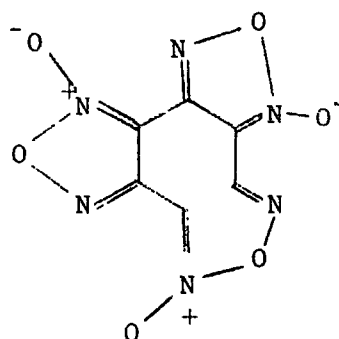
For the unsymmetrically substituted 2-methyl-, and the sterically crowded 3,4-diphenyl-thiathiophthenes the ESCA results agree with X-ray crystallographic data in assigning unsymmetrical structures.<sup>191</sup>

However, different interpretations of the ESCA data for the symmetrically substituted 2,5-dimethyl derivative have arisen<sup>190,192</sup> and further work is needed on this system.

The  $\text{C}_{1s}$ ,  $\text{N}_{1s}$  and  $\text{O}_{1s}$  spectra of hexanitrosobenzene (I) have been measured<sup>193</sup> and show that the hexanitroso structure is ruled out and support the formulation, previously suggested by X-ray diffraction and infrared studies, as benzotris[c]-2-oxyfurazan, (II).



(I)



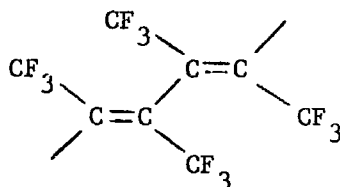
(II)

The ESCA spectra of 1,8-bis(dimethylamino)naphthalene ('proton sponge') has been recorded and the doublet nature of the  $N_{1s}$  region indicates an unsymmetrical N-H...N bridge.<sup>194</sup>

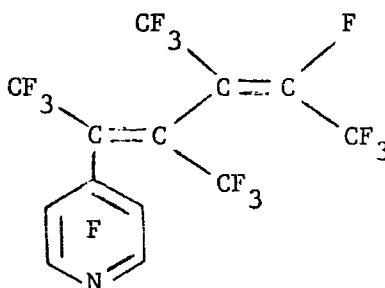
An interesting and expanding feature of ESCA is its application to polymer chemistry. Studies by Clark and co-workers suggest that there is little or no increase in linewidths on going from monomeric to a regular polymeric system.<sup>195</sup> Thus ESCA has a distinct advantage over n.m.r. spectroscopy in studying polymers, many of which are insoluble and can only be studied by broadline n.m.r. techniques. A detailed study has been made of nitroso rubbers and theoretical calculations using CNDO/2 charge distributions and the charge potential model<sup>195</sup> have shown that for saturated systems, factors determining ESCA chemical shifts are sufficiently short range for quantitative treatment of ESCA data on polymers to be feasible.

An illustrative example of the scope of the technique is the identification of an insoluble white polymer produced as a by-product in the fluoride ion initiated reaction of hexafluorobut-2-yne with

fluorinated heterocyclic molecules.<sup>196</sup> The  $C_{1s}$  spectrum of the polymer allowed identification of a  $CF_3$ -group and gave the most likely structure for the polymer (containing only C and F) as a polyene of the form:



Confirmation of the structure and an explanation of the white colour were obtained from a theoretical calculation of the relative binding energies of the two types of carbon and from the ESCA spectra of a model compound (I) of known structure



(I)

The configuration about each double bond was taken to be trans and geometry minimisation calculations showed that the ethylenic units were at right angles to each other, predicting that the polymer should have a spiral structure. The u.v. spectrum of (I) confirmed that, in that system also, the double bonds are twisted with respect to the ring. From comparison of the ESCA spectra of the polymer and (I), and from the theoretical calculations the structure of the polymer could be assigned.

The effect of fluorine substitution on molecular core binding energies in homo polymers of vinylfluoride, vinylidene fluoride and trifluoro and tetrafluoroethylenes has been investigated<sup>197</sup> and experimental and theoretical studies have been reported for the valence bond structures of PTFE<sup>198</sup> and polyethylene.<sup>199</sup>

Much interest is now being centred on information about valence electron distributions available from chemical shifts of core levels, multiplet splittings (of core levels for paramagnetic species),<sup>200</sup> and from the observation of satellite peaks associated with double ionisation (shake off) and excitation (shake up) processes, which accompany photoionisation. Hillier et al have described the calculation of satellite positions and intensities in simple molecules and rationalised the failure to observe shake up peaks in molecules like benzene, thiophen, pyrrole and furan.<sup>201</sup>

Although a theoretical connection has been shown between <sup>13</sup>C-n.m.r. and ESCA chemical shifts,<sup>202</sup> earlier linear correlations<sup>203,170</sup> should be treated with caution. It is only for closely related series of compounds that a correlation between <sup>13</sup>C-n.m.r. and ESCA might be expected and then it need not, necessarily, be linear. For example, the chloromethanes give a linear relationship between <sup>13</sup>C-n.m.r. and ESCA shifts but the corresponding bromo and iodo methanes do not.<sup>204</sup> Correlations of ESCA shifts with both <sup>35</sup>Cl n.q.r. data<sup>205</sup> and Mossbauer chemical shifts<sup>206</sup> have been demonstrated for series of similar compounds.

Jolly and Henrickson have shown that it is possible to estimate thermodynamic data from measured core binding energies and vice versa.<sup>207</sup>

Gas phase proton affinities for organic molecules have been calculated from ESCA data<sup>207</sup> and core binding energy shifts have been calculated using thermodynamic data [Equivalent Cores Method].<sup>167</sup>

CHAPTER 4

ESCA INVESTIGATIONS OF SOME HALOGENATED AROMATIC

AND HETEROCYCLIC SYSTEMS

## Introduction

The work presented here is part of a systematic investigation into the application of ESCA to studies of structure and bonding in halo carbon chemistry. Molecular core binding energies for benzene, pyridine, the diazabenzene and their perchloro and perfluoro derivatives have already been reported.<sup>171,174,178</sup> The results indicate that shifts in core binding energies are qualitatively in accord with organic chemists 'intuitive' ideas concerning charge distributions in these systems. It was also shown that a quantitative discussion of the data was possible employing the charge potential model with charge distributions computed within the CNDO/2 formalism. These, and other investigations form the basis for applications of ESCA to problems of structure and bonding in the halocarbon field. Results are presented here for indene, indole, benzo-[b]-furan, benzo-[b]-thiophen, benzo-[b]-thiophen-1,1-dioxide and some of their chloro and fluoro derivatives.

The rationale for these investigations is two fold. Firstly, previously reported work on heterocyclic and aromatic systems indicated the great utility of ESCA for providing information on ground state electron distributions and in certain cases providing solutions to previously intractable structural problems.<sup>185,186</sup> Secondly, aspects of the synthesis and reactions of the benzo-[b]-furan, indole and benzo-[b]-thiophen ring systems are of considerable interest and in the particular case of the chlorinated derivatives difficulties of

structural assignment by 'conventional' spectroscopic techniques often arise. The compounds studied in this investigation are all of known structure and therefore provide important background information - an essential prerequisite for developing ESCA as a structural tool in this field.

### Experimental

Spectra were recorded on an A.E.I. ES100 electron spectrometer using either  $\text{AlK}\alpha_{1,2}$  (1486.6eV) or  $\text{MgK}\alpha_{1,2}$  (1253.6eV) exciting radiation. Liquid samples were introduced via a heatable reservoir shaft and leaked through a Metrosil plug; solid samples were introduced in a capillary via a heatable direct inlet shaft. In all cases samples were condensed onto a cooled gold surface (at  $\sim -100^\circ$ ) and studied as thin films. A pressure of  $\sim 10^{-6}$  Torr in the source region was typical. At this pressure it was found necessary to keep the vapour pressure of the sample high enough throughout the experiment to continually renew the surface of the sample film on gold. This obviated contamination of the surface layer of the sample by the extraneous atmosphere in the sample chamber (mostly water and hydrocarbon vapour). With volatile samples control of the reservoir shaft temperature and slow leakage through the Metrosil plug ensures that only thin films on gold are obtained, minimising charging effects. Less control is available for solid samples sublimed from a capillary and in practice, thick films can occur, causing relatively large shifts in the energy scale of  $\sim 1\text{-}2\text{eV}$  due to charging effects. Previous results<sup>174,178</sup> have indicated that for compounds with a

similar degree of halogenation  $F_{1s}$  and  $Cl_{2p}$  binding energies are effectively constant. The series of compounds studied here were similar enough to allow advantage to be taken of this. By referencing spectra to either the  $F_{1s}$  level at 690.0eV or the  $Cl_{2p}$  level at 201.0eV binding energy shifts in different compounds could be compared, although absolute binding energies may not be accurate to better than  $\pm 0.3$ eV. Occasionally a peak at 285.0eV was evident in the  $C_{1s}$  spectra due to hydrocarbon contamination of the sample and this has also been used as an internal reference by other workers.<sup>196,208</sup> Measurements made using both types of reference give binding energies (both relative and absolute) in close agreement and allow confidence in comparisons made between binding energies in different molecules referenced to the halogen core levels.

Electrons expelled from the sample enter the analyser region (working pressure  $\sim 10^{-7}$  Torr) consisting of a two element retarding lens and a 10.in. mean diameter hemispherical electrostatic analyser (cf Chapter 3, p 90 ). A Mullard Channeltron electron multiplier is used as a detector, the output being fed to Nuclear Enterprises counting electronics and the spectrum being plotted on an X-Y recorder.

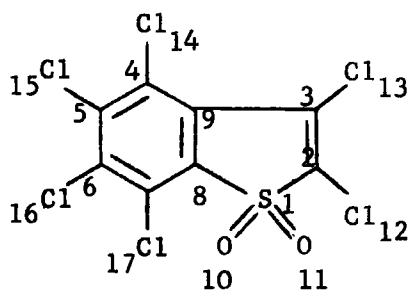
Overlapping peaks were deconvoluted using a Du Pont 310 curve resolver and assignments were made on the basis of (i) the charge potential model using charge distributions from CNDO/2 calculations (ii) correlation with previously reported data for similar systems. The internal consistency of the results support these assignments as will become clear in the detailed discussion.

The line widths used for deconvolutions were those obtained previously for similar systems<sup>174,178</sup> and from the spectrum of perchlorothiophen which showed a single peak in the  $C_{1s}$  region of half width 1.2eV. The line shapes used were Gaussian and were known to give satisfactory fits for peaks arising from atoms in a single environment (ie atoms of one 'type'). Under the conditions used in this work the gold  $4f_{7/2}$  level at 84eV (also used as a reference) had a half width of 1.15eV. Measured binding energies are estimated to be accurate to  $\pm 0.2$ eV within a particular compound and  $\pm 0.3$ eV between different samples.

Before proceeding to the discussion, mention should be made of the effect on the calculated charges due to inclusion of d-orbitals in the basis sets for second row atoms (S, Cl) in CNDO/2 calculations. In all cases charges used in conjunction with the charge potential model were calculated excluding d-orbitals on sulphur and chlorine. With the usual parameterisation of CNDO/2 the contribution of 3d orbitals on second row atoms is grossly over-estimated and more 'realistic' charge distributions are obtained if 3d-orbitals are neglected.<sup>196</sup> Table 4.1 shows the differences in charges calculated for perchloro-benzo-[b]-thiophen-1,1-dioxide with and without 3d-orbitals on chlorine and sulphur.

The most striking features of Table 4.1 are the complete reversal of charges on many atoms, the large negative charge calculated for the sulphur atom and positive charges on the oxygens when d-orbitals are included in the basis sets for second row atoms. The role of the 3d-orbitals on sulphur in heterocyclic molecules has been widely discussed in connection with both 'ab initio' and semi empirical

Table 4.1

CNDO/2 charges for Hexachlorobenzo-[b]-thiophen-1,1-dioxide

Position	Atom	3d included	3d excluded
		$q_i$	$q_i$
1	S	-0.430	0.917
2	C	-0.169	-0.030
3	C	-0.032	0.093
4	C	0.097	0.109
5	C	0.187	0.127
6	C	0.177	0.111
7	C	0.109	0.123
8	C	-0.354	-0.124
9	C	-0.151	0.001
10	O	0.264	-0.443
11	O	0.264	-0.443
12	Cl	0.118	-0.031
13	Cl	0.076	-0.063
14	Cl	0.002	-0.079
15	Cl	-0.045	-0.083
16	Cl	-0.049	-0.081
17	Cl	-0.024	-0.094

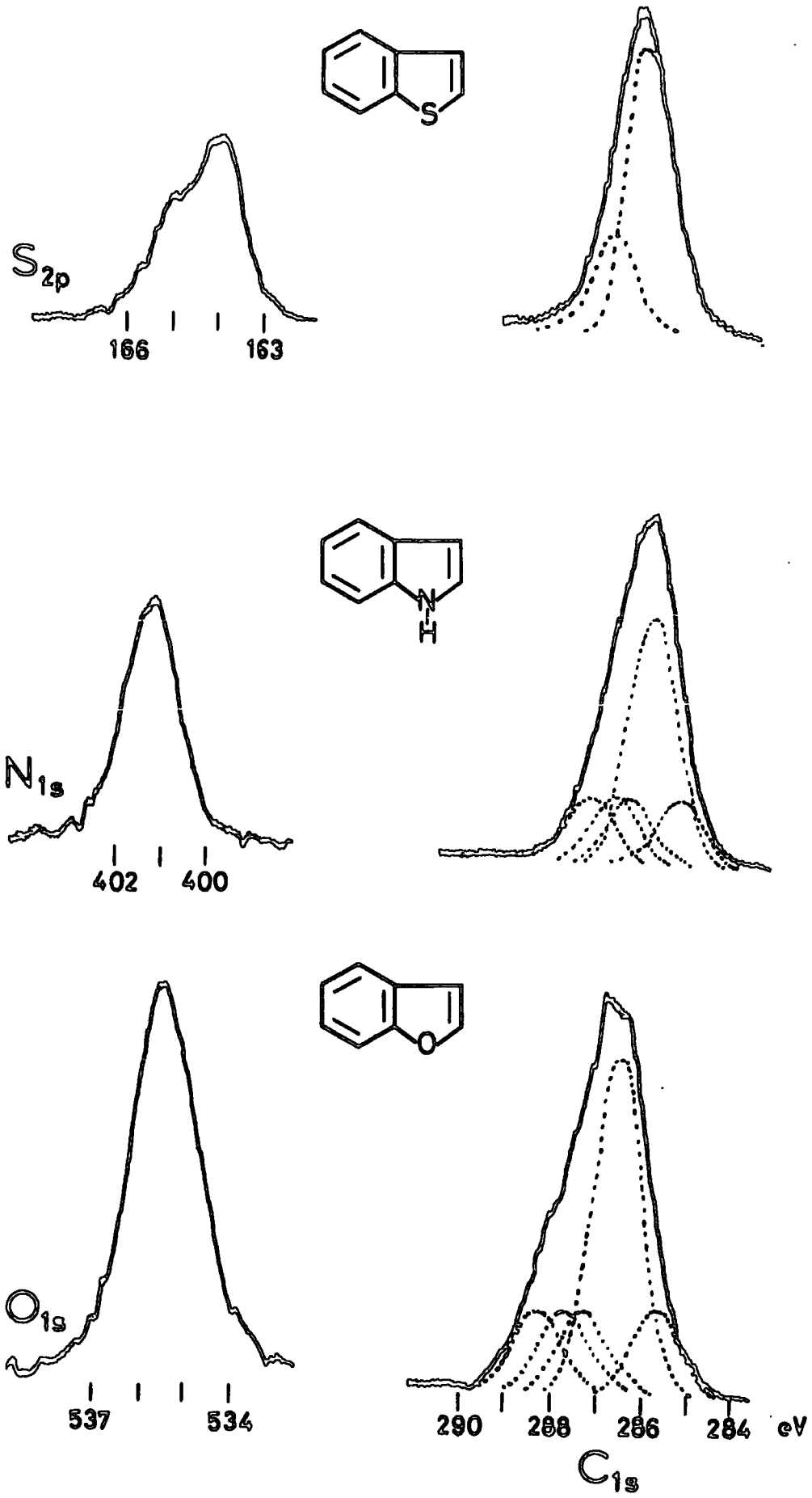


Fig. 4.1

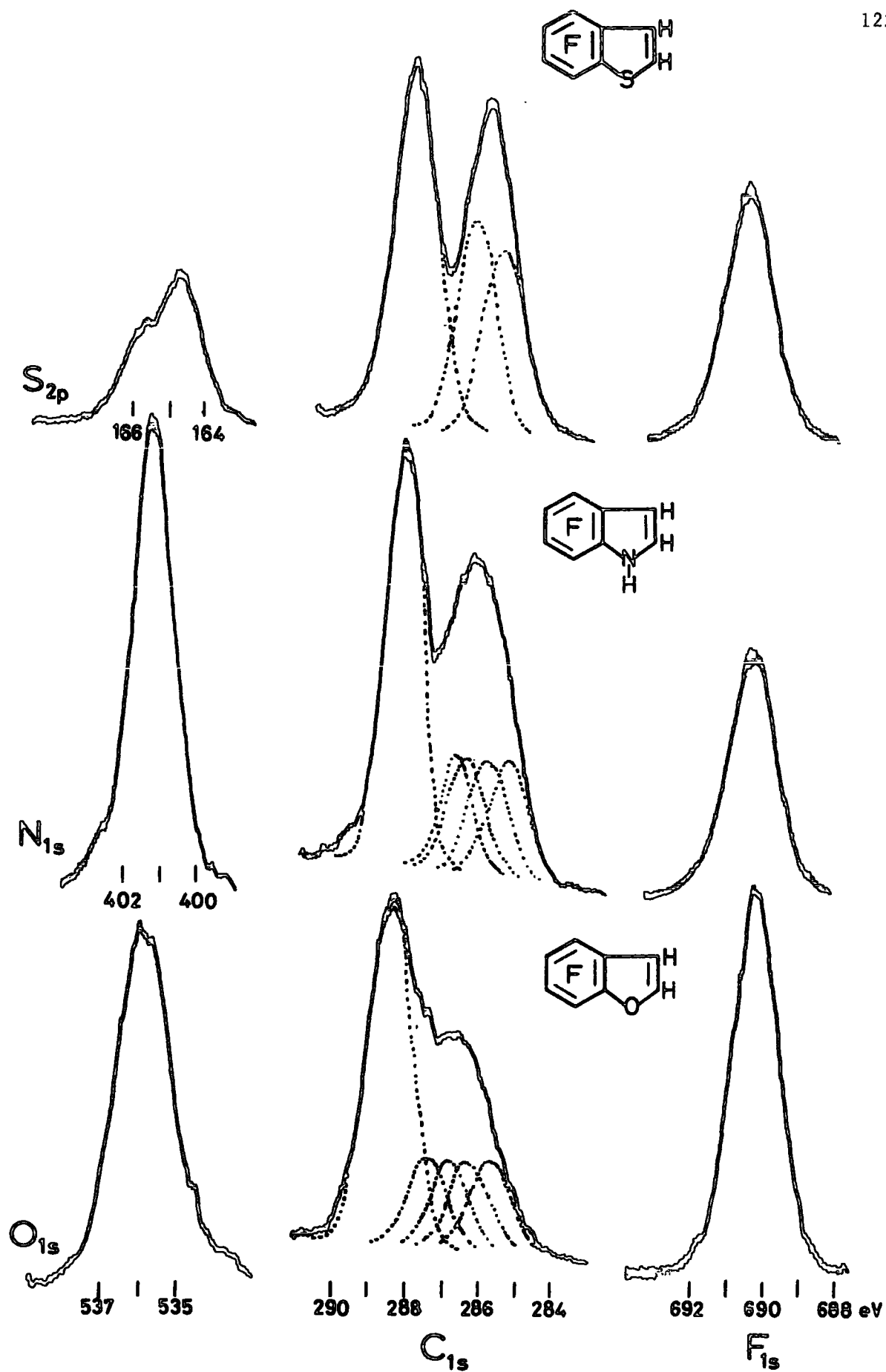


Fig. 4.1 contd.

calculations<sup>209-215</sup> and the conclusion now seems to be that, for thiophen at least, the 3d-orbitals play a minor role in bonding.<sup>215</sup>

## Results

### A. Molecular Core Binding Energies for benzo-[b]-thiophen, indole, benzo-[b]-furan and their 4,5,6,7-tetrachloro and tetrafluoro derivatives.

Molecular core binding energies for furan, pyrrole and thiophen have been reported<sup>173,211</sup> and in this section the effect of annelation and subsequent halogenation on the binding energies of the ring atoms are considered. Fig. 4.1 shows the relevant spectra and deconvolutions ( $C_{1s}$  levels) for benzo-[b]-thiophen, indole and benzo-[b]-furan and their tetrafluoro derivatives. Molecular core binding energies for the whole series are given in Table 4.2.

#### (a) Qualitative discussion

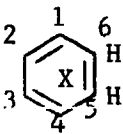
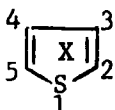
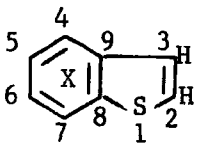
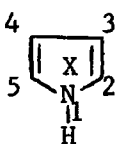
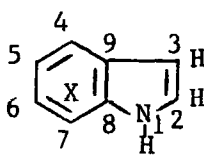
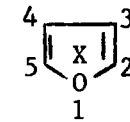
##### (i) The effect of annelation on the $C_{1s}$ levels.

The effect of annelation on the relevant core levels for the hetero atoms and  $C_{1s}$  levels of the parent five membered heterocycles is shown diagrammatically in the second two rows of Fig. 4.2. Also shown, for comparison, is similar data for benzene and naphthalene.<sup>171</sup>

The  $C_{1s}$  levels of the five membered ring carbon atoms show several distinctive features. In benzo-[b]-thiophen, indole and benzo-[b]-furan, the core levels for the two bridging carbons (8,9) are more tightly bound than in the corresponding atoms of the parent heterocycles by

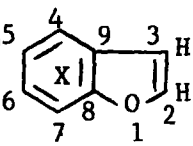
TABLE 4.2

Molecular Core Binding Energies (in eV)

		Position	X=H	X=Cl <sup>a</sup>	X=F <sup>b</sup>
	C <sub>1s</sub>	1	284.9	287.2	288.6
	C <sub>1s</sub>	1,4	284.9	287.2	288.5
		2,3	284.9	287.2	288.5
		5,6	284.9	285.7	286.2
	C <sub>1s</sub>	2,5	285.0	287.0	
		4,3	285.0	287.0	
		S <sub>2p<sub>1/2</sub></sub>	165.3	166.0	
		S <sub>2p<sub>3/2</sub></sub>	164.3	164.0	
	C <sub>1s</sub>	4,5,6,7	284.9	286.8	288.1
		8,9	285.5	285.6	286.3
		2,3	284.9	285.2	285.6
		S <sub>2p<sub>1/2</sub></sub>	165.2	165.4	165.8
		S <sub>2p<sub>3/2</sub></sub>	164.0	164.2	164.6
	C <sub>1s</sub>	2,5	285.7		
		4,3	284.8		
		N <sub>1s</sub>	401.2		
	C <sub>1s</sub>	4,5,6,7	284.9	286.8	288.3
		9	285.4	285.5	285.9
		8	286.2	286.6	286.7
		3	284.4	285.2	285.2
		2	285.7	286.3	286.4
		N <sub>1s</sub>	401.2	401.4	401.7
	C <sub>1s</sub>	2,5	286.7		
		4,3	285.6		
		O <sub>1s</sub>	535.8		

contd./

Table 4.2 contd.

	Position	X=H	X=Cl <sup>a</sup>	X=F <sup>b</sup>
 $C_{1s}$	4,5,6,7	285.4		288.5
	9	286.1		286.4
	8	287.2		287.4
	3	284.7		285.7
	2	286.7		286.9
	$O_{1s}$	535.6		535.7

In all cases: a,  $Cl_{2p_{3/2}}$  -201.0 eV

b,  $F_{1s}$  -690.0 eV

0.5-0.6eV. A similar increase in  $C_{1s}$  binding energy has been observed in other systems. The  $C_{1s}$  levels of the bridging carbon atoms in naphthalene and biphenylene show increases in binding energy, relative to benzene, of 0.4eV and 0.7eV respectively.<sup>171</sup> In marked contrast, the  $C_{1s}$  levels for C3 are displaced progressively towards lower binding energies along the series benzo-[b]-thiophen (-0.1eV) indole (-0.4eV) and benzo-[b]-furan (-0.9eV) relative to the parent heterocycles. This suggests increasing electron density at C3 in the same order and this is, in fact, supported by CNDO/2 SCF MO calculations discussed in the next section.

For all three ring systems the effect of annelation on the core binding energies for C2 is small. In the parent five membered ring heterocycles thiophen, pyrrole and furan the shift in  $C_{1s}$  binding energies between C2(C5) and C3(C4) have previously been measured as 0.0eV, 0.9eV and 1.1eV respectively.<sup>173</sup> It is of interest therefore to compare these with the corresponding shifts for the fused ring systems (ie.  $\Delta C_2-C_3$ ,  $\Delta C_8-C_9$ ).

For the C8-C9  $C_{1s}$  levels of benzo-[b]-thiophen, indole and benzo-[b]-furan the shifts are 0.0eV, 0.8eV and 1.1eV respectively, ie. identical within experimental limits to the corresponding shifts for the heterocycles, although the absolute values for individual core levels are shifted to higher binding energies by annelation. In contrast the effect of annelation on C2 and C3 for indole and benzo-[b]-furan is to considerably enhance the shift in  $C_{1s}$  binding energies between them; this being largely attributable to the much

Molecular Core Binding Energies (in eV)

HETEROCYCLIC

AROMATIC

X=O

X=NH

X=S

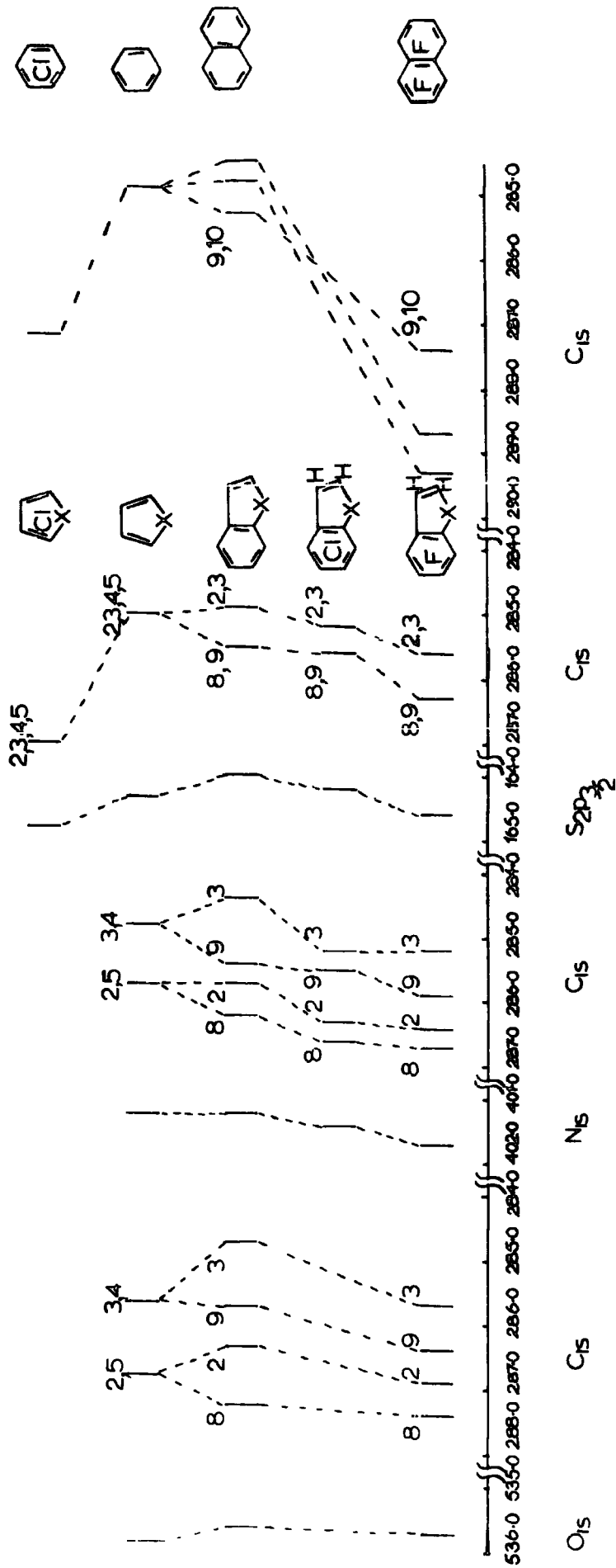


FIG. 4.2

lower absolute binding energy for the C3 C<sub>1s</sub> levels.

<u>ΔC2 C3 values (eV)</u>					
Thiophen	0.0	Pyrrole	0.9	Furan	1.1
Benzo-[b]-thiophen	0.0	Indole	1.3	Benzo-[b]-furan	2.0

These changes reflect the assymetry imposed on the five membered ring system by annelation.

(ii) Hetero atom core levels

The binding energies for the hetero atom core levels are given in Table 4.2. Fig. 4.2 shows schematically the effect of annelation on the hetero atom in the five membered ring. In all cases there seems to be a small shift to lower binding energies in going from the parent hetero cycle to the benzo derivative. This again is reflected in CNDO/2 calculations as increased negative charge on the hetero atom, indicative of overall electron transfer from the six to five membered ring (see later).

Shifts in core binding energies on annelation are given in Table 4.3.

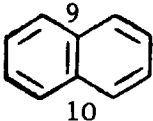
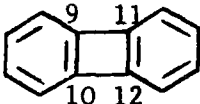
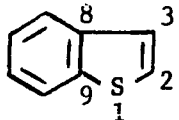
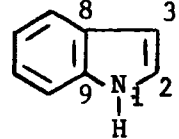
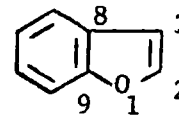
(b) Substituent effects of chlorine and fluorine in the 4,5,6,7-tetra halogen derivatives.

(i) C<sub>1s</sub> levels for atoms directly bonded to halogen.

In all cases except benzo-[b]-furan both the 4,5,6,7-tetra-chloro and tetra-fluoro derivatives were available. The effect of halogenation on the 4,5,6,7 carbons in benzo-[b]-thiophen, indole and

TABLE 4.3

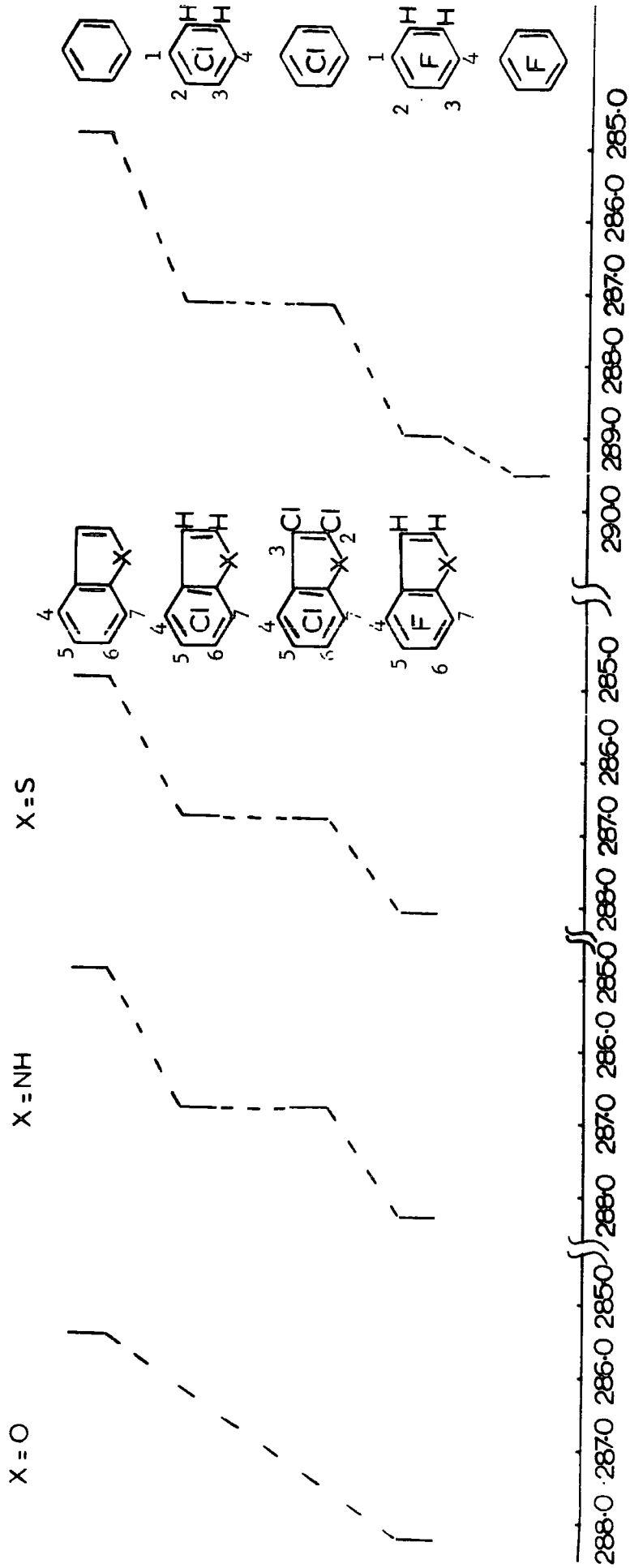
Binding Energy Shifts on Annellation

	Positions	$\Delta C_{1s}$ (eV)	$\Delta$ hetero atom (eV)
	9,10 <sup>a</sup>	0.4	
	9,10,11,12 <sup>a</sup>	0.7	
	8,9 <sup>b</sup>	0.5	
	2,3	-0.1	
	1		-0.3
	8,9 <sup>c</sup>	0.55(av)	
	2	0.0	
	3	-0.4	
	1		0.0
	8,9 <sup>d</sup>	0.5	
	2	0.0	
	3	-0.9	
	1		-0.2

Relative to: a, benzene; b, thiophen; c, pyrrole; d, furan.

HETEROCYCLES

BENZENES



C<sub>1s</sub> Binding Energies (in eV)

Fig. 4.3

benzo-[b]-furan is shown schematically in Fig. 4.3. For comparison, data is also presented for the carbon atoms attached to halogen in 1,2,3,4 tetra-halogeno benzenes, perchloro and perfluorobenzene, 2,3,4,5,6,7-hexachloroindole and perchlorobenzo-[b]-thiophen.

The effect of replacing hydrogen by chlorine or fluorine is to increase the  $C_{1s}$  binding energies for all carbon atoms directly attached to halogen, compared to the parent heterocycle. For chlorine substitution in indole and benzo-[b]-thiophen the shifts are 1.9eV which compares with a shift of 2.3eV for 1,2,3,4 tetrachlorobenzene.<sup>216</sup> [Binding energy shifts on halogenation are given in Table 4.4]. For fluorine substitution, the measured shifts in benzo-[b]-thiophen, indole and benzo-[b]-furan are 3.2eV, 3.4eV, 3.1eV respectively compared with 3.6eV for the corresponding tetrafluorobenzene.

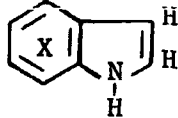
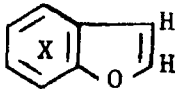
On average the shifts in  $C_{1s}$  binding energies on chlorination and fluorination in the condensed heterocycles are lower than those for the corresponding 1,2,3,4-tetrahalo benzenes.

(ii) The bridging carbon atoms (8,9)

Previous studies on perfluorinated binuclear aromatics<sup>171</sup> indicated that  $C_{1s}$  core levels for bridging carbon atoms are subject to substantial shifts to higher binding energies on replacing ring CH by CF. Such long range effects are also evident from the data in Fig. 4.2. The average  $C_{1s}$  binding energy shifts for C8 and C9 in going to the tetrafluoro derivatives are 0.85eV, 0.5eV and 0.25eV for sulphur, nitrogen and oxygen heterocycles respectively.

TABLE 4.4

Binding Energy Shifts on Chlorination and Fluorination (in eV)

	Position	X=Cl	X=F
	1,2,3,4, <sup>a</sup>	2.3	3.6
	5,6	0.8	1.3
	4,5,6,7, <sup>b</sup>	1.9	3.2
	8,9	0.1	0.8
	2,3	0.3	0.7
	1(S)	0.2	0.6
	4,5,6,7 <sup>c</sup>	1.9	3.4
	8	0.5	0.5
	9	0.1	0.5
	2	0.6	0.7
	3	0.8	0.8
1(N)	0.2	0.5	
	4,5,6,7 <sup>d</sup>		3.1
	8		0.2
	9		0.3
	2		0.2
	3		1.0
1(O)		0.1	

Relative to: a, benzene; b, benzothiophen;  
c, indole; d, benzofuran.

This may be compared with the shift of 1.3eV for C5 and C6 in 1,2,3,4 tetrafluorobenzene (w.r.t benzene). Again the shifts measured for the benzo-heterocycles are lower than those for correspondingly substituted benzenes.

(iii) Five membered ring carbons (2,3).

Both C2 and C3 show surprisingly large increases in  $C_{1s}$  binding energies on halogenation, even though they are relatively remote from the substituted positions. For benzo-[b]-furan and indole the shifts for C2 and C3 are in fact greater than for C8 and C9.

Considering C3 first; the increase in  $C_{1s}$  binding energy on replacing hydrogen by fluorine in positions 4,5,6,7- is in the order benzo-[b]-furan (1.0eV) indole (0.8eV) and benzo-[b]-thiophen (0.7eV); this is the order of increase in binding energy of C8 and C9, on fluorination. For C2 the corresponding shifts are 0.2eV, 0.7eV and 0.7eV in benzo-[b]-furan, indole and benzo-[b]-thiophen respectively. This is indicative of overall transfer of electron density from the five membered ring (positions 1,2,3), to the six membered ring on halogenation, causing large binding energy shifts for C2 and C3 but smaller increases in binding energy than expected at C8, C9 and carbons directly attached to halogen (4,5,6,7). This is again supported by CNDO/2 calculations of charge densities (see later).

(iv) The hetero atom

The increase in binding energy of the hetero atom on halogenation of the benzo ring is in the order S(0.6eV), N(0.5eV), O (0.1eV) as expected from electronegativity considerations.

c) Quantitative Discussion

In the absence of 'ab initio' calculations, assignments of the  $C_{1s}$  levels were based on CNDO/2 SCF MO calculations and the charge potential model developed by Siegbahn et. al.,<sup>146</sup> which relates shifts in binding energy of a given core level of an atom to the charge distribution, by the relationship,

$$E_i - E_i^0 = kq_i + \sum_{i \neq j} \frac{q_j}{r_{ij}}$$

where  $E_i$  is the molecular core binding energy of atom  $i$  and  $E_i^0$  is a reference level. The values of  $E_i - E_i^0$  so calculated then give a theoretical estimate of the relative binding energies. Comparison of such calculated shifts for all the carbon atoms within a molecule with those found experimentally by deconvoluting the overall peak envelopes, allows  $C_{1s}$  binding energies to be assigned.

An examination of the CNDO/2 charges and Madelung potentials in Table 4.5 shows that for the unsubstituted fused ring heterocycles, the calculated shifts are dominated by the charge term; the contribution from the Madelung potential does not affect the order of the assignments. For the chloro and fluoro derivatives however,

TABLE 4.5

CNDO/2 Charges and Madelung Potentials

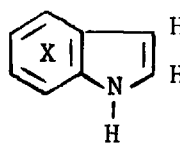
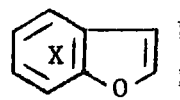
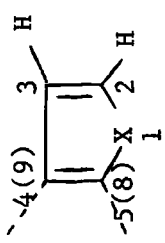
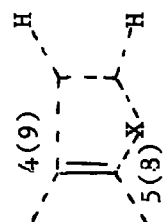
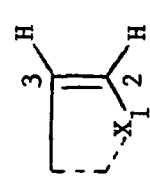
Positions							
	$q_i$	$\sum_{i \neq j} \frac{q_i}{r_{ij}}$	$q_i$	$\sum_{i \neq j} \frac{q_i}{r_{ij}}$	$q_i$	$\sum_{i \neq j} \frac{q_i}{r_{ij}}$	
X=H	4	-0.0075	0.1748	0.0072	-0.1513	-0.0099	0.1121
	5	-0.0055	0.0379	-0.0086	-0.0457	-0.0076	0.0627
	6	0.0012	0.0085	0.0087	-0.3449	0.0016	0.0533
	7	-0.0053	0.3286	-0.0405	0.5113	-0.0145	0.6522
	8	0.0610	-0.4070	0.0813	-1.0852	0.1388	-1.5878
	9	0.0271	-0.0307	0.0202	-0.1713	0.0108	0.1190
	3	-0.0336	0.5483	-0.0667	0.7949	-0.0776	1.1463
	2	0.0198	-0.2536	0.0703	-1.0514	0.1313	-1.7525
	1	-0.0551	0.5913	-0.1469	2.5004	-0.1853	2.2835
X=Cl	4	0.0960	0.0518	0.1094	-0.1818		
	5	0.0902	0.3225	0.0806	0.2337		
	6	0.0972	0.3014	0.0818	0.1150		
	7	0.1032	0.1247	0.0657	0.3336		
	8	0.0360	1.0392	0.0720	0.2809		
	9	0.0149	1.2129	0.0267	0.9932		
	3	-0.0232	1.0704	-0.0657	1.5795		
	2	0.0165	0.4791	0.0911	-0.6014		
	1	-0.0078	0.6967	-0.1472	3.2857		
X=F	4	0.1699	-0.8020	0.1778	-0.9737	0.1712	-0.8615
	5	0.1482	-0.1717	0.1365	-0.2251	0.1423	-0.0566
	6	0.1541	-0.2017	0.1434	-0.3714	0.1576	-0.1728
	7	0.1738	-0.7481	0.1439	-0.4986	0.1586	-0.2514
	8	0.0065	1.5823	0.0539	0.7902	0.1157	0.0948
	9	-0.0060	1.6682	0.0063	1.4900	-0.0300	2.0711
	3	-0.0170	1.0337	-0.0587	1.5156	-0.0543	1.6330
	2	0.0187	0.5665	0.0882	-0.4972	0.1306	-0.8841
	1	0.0067	0.5894	-0.1415	3.2558	-0.1547	2.6558

TABLE 4.6

 $\pi$ ,  $\sigma$  and Total Charges

Fragment									
	$\pi$	$\sigma$	Total	$\pi$	$\sigma$	Total	$\pi$	$\sigma$	Total
X=S									
Thiophen	0.0	-0.0113	-0.0113	-0.0858	0.0823	-0.0035	0.0859	-0.0937	-0.0078
Benzothiophen	0.0506	-0.0160	0.0346	-0.0145	0.1026	0.0881	0.0650	-0.1186	-0.0536
Tetrafluorobenzothiophen	0.9916	-0.9367	0.0549	-0.0785	0.0790	0.0050	0.0701	-0.0157	0.0544
X=NH									
Pyrrrole	0.0	0.0097	0.0097	-0.2125	0.2001	-0.0124	0.2125	-0.1904	0.0221
Indole	0.0976	-0.0275	0.0701	-0.0502	0.1284	0.0782	0.1478	-0.1792	-0.0314
Tetrafluoroindole	0.0529	0.0512	0.1041	-0.0993	0.1595	0.0602	0.1522	-0.1083	0.0439
X=O									
Furan	0.0	-0.0300	0.0300	-0.1304	0.1823	0.0519	0.1304	0.1101	0.2405
Benzofuran	0.0772	-0.0399	0.0373	-0.0132	0.1628	0.1496	0.0904	-0.2027	-0.1123
Tetrafluorobenzofuran	0.0254	0.0331	0.0585	-0.0794	0.1651	0.0857	0.1048	-0.1590	-0.0542

the shifts are determined by the large potentials due to the halogens.

Table 4.6 shows how the CNDO/2 charge densities follow qualitatively the changes in binding energies observed experimentally in the five membered ring on annelation and subsequent fluorination.  $\pi$ ,  $\sigma$  and total charges are given for the hetero ring fragment, the bridging carbons, and the 1,2,3 positions. The pattern is the same for all three heterocyclic groups. On annelation the hetero ring shows an overall increase in total positive charge caused mainly by a large loss of charge density from the carbons that form the bridge (8,9), which overrides a smaller increase in charge density at the hetero atom and C3. This reflects the higher binding energies observed for the bridging carbons and the decrease in binding energy of the hetero atom and C3. Replacing the four hydrogens in the benzo ring by fluorines causes a further increase in the total charge in the five membered ring. The two bridging carbons show only a slight increase in positive charge, the main contribution being loss of both  $\pi$  and  $\sigma$  charge density from the hetero atom and C3. Again this fits the observed small shift to higher binding energy of C8 and C9 and relatively large shifts of C3, and the hetero atom. The net effect of four halogens in the benzo ring is to cause transfer of charge density away from the far side of the five membered ring into the six membered ring and this is reflected in the measured core binding energies.

For both thiophen and benzo-[b]-thiophen CNDO/2 calculations predict a splitting of 0.3eV between C2-C3 and C8-C9. Non-empirical

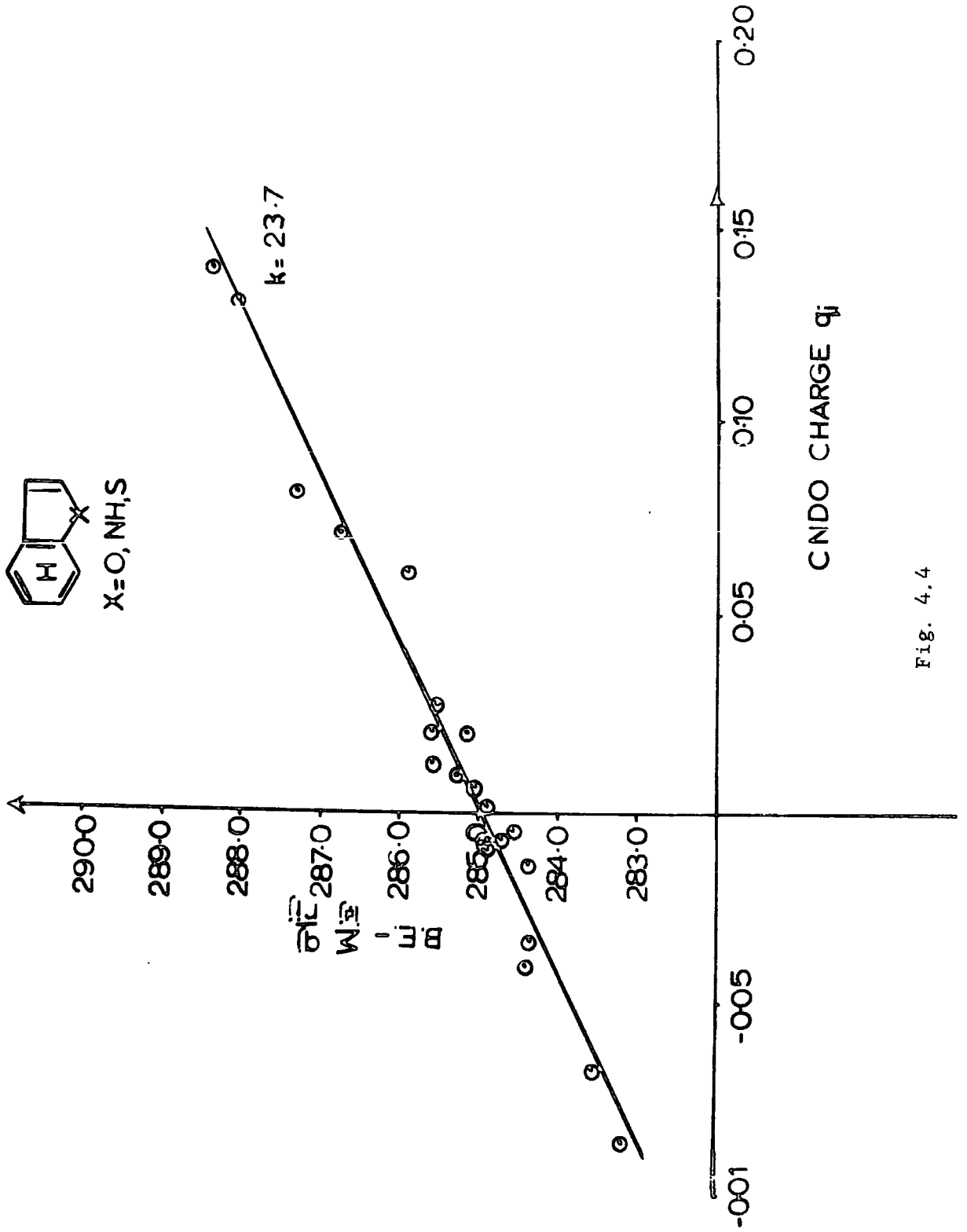


Fig. 4.4

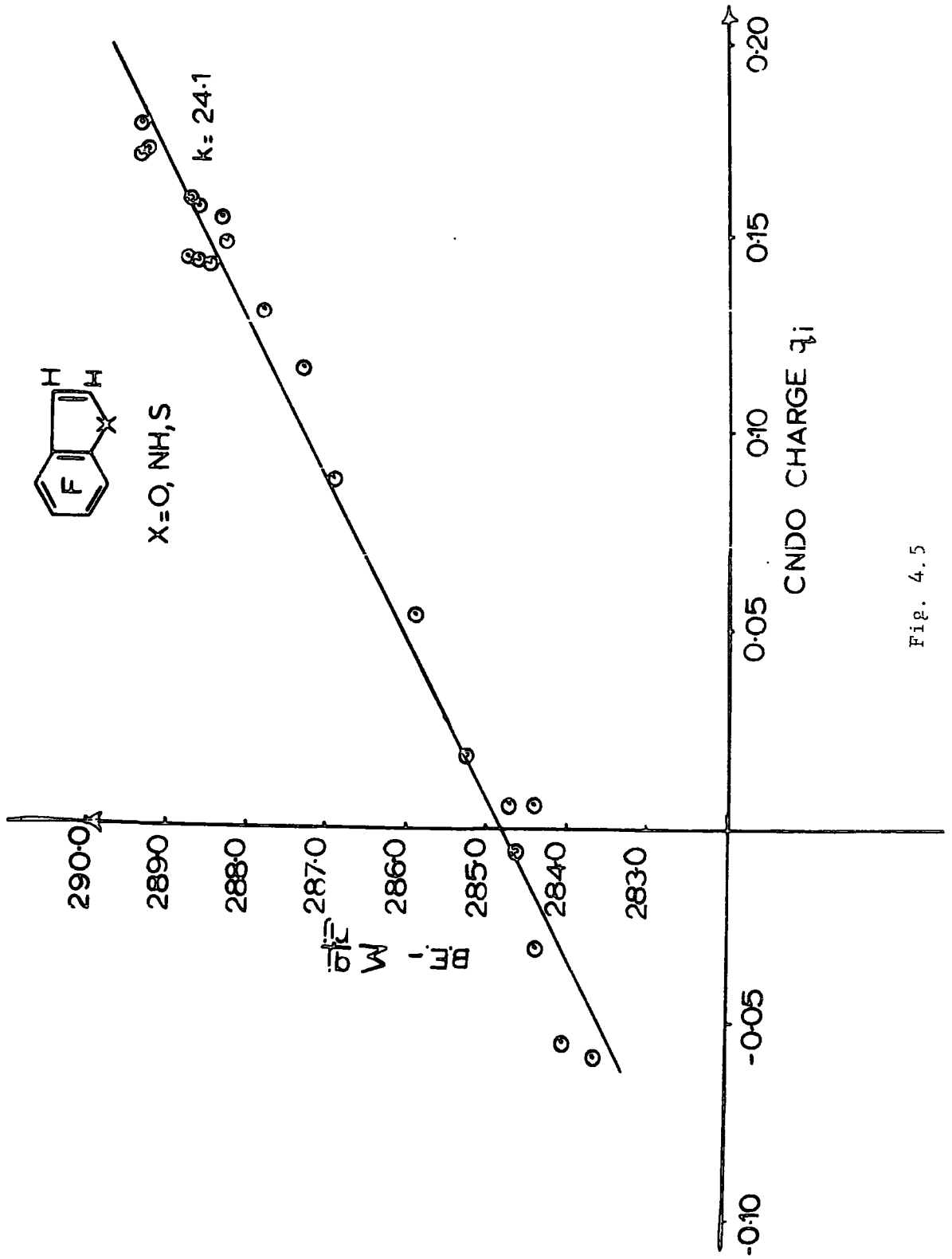


Fig. 4.5

calculations by Clark and Armstrong<sup>215</sup> for thiophen, predict essentially the same  $C_{1s}$  binding energies for C2 and C3, in better agreement with the experimental results than CNDO/2. However, 'ab initio' calculations by Siegbahn et al<sup>214</sup> predict a C2-C3 shift in the  $C_{1s}$  binding energies of 0.7eV. A comparison of the measured core binding energies for thiophen with 'ab initio' calculations has been discussed by Clark.<sup>217</sup>

A plot of binding energy corrected for Madelung potential against CNDO charge is given in Fig. 4.4 for the  $C_{1s}$  levels of benzo-[b]-thiophen, indole and benzo-[b]-furan. The slope gives  $k = 23.7$  and the intercept  $E^0 = 285.14\text{eV}$  with a correlation coefficient ( $r^2 = 0.95$ ). A similar plot, shown in Fig. 4.5, for the fluorinated derivatives gives  $k = 24.1$  and  $E^0 = 284.86\text{eV}$  with a correlation coefficient ( $r^2 = 0.98$ ). Although there is some scatter the correlations are good and the  $k$  values agree well with those previously reported (p 103 ) and are close to the theoretical value of  $k = 22.0$ .

## B. Molecular Core Binding Energies for Indene and some Highly Fluorinated Derivatives.

### Introduction

The use of ESCA in ascertaining the position of borohydride attack in perfluoro indene<sup>186</sup> has been previously discussed. In this section molecular core binding energies for indene(1), 4,5,6,7-tetrafluoro indene (2), 1,1,4,5,6,7-hexafluoro indene(3), 1,1,3,4,5,6,7-heptafluoro indene(4), 1,1,2,4,5,6,7-heptafluoro-indene(5) and perfluoro indene(6) are presented and the effect of

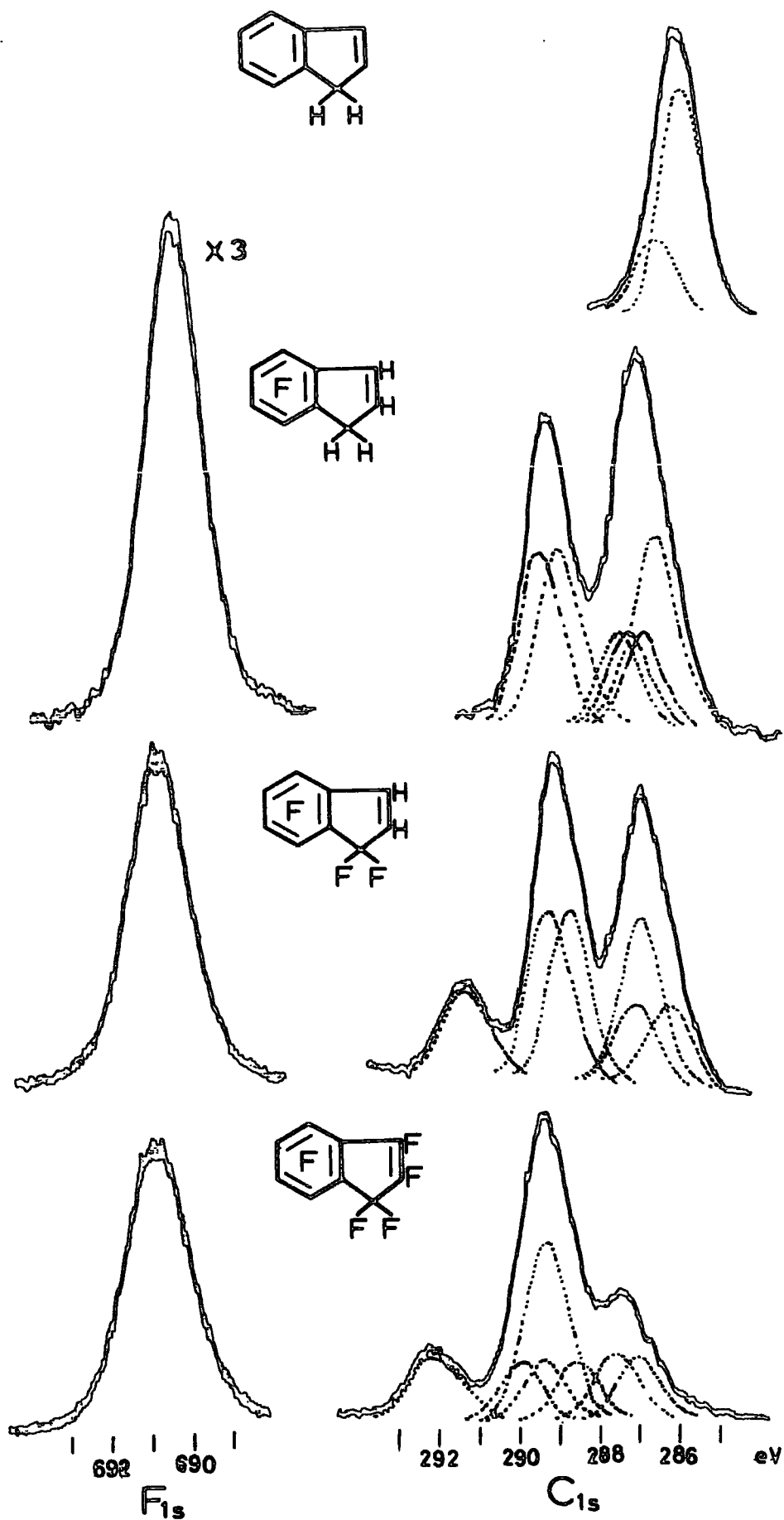


Fig. 4.6

fluorine substitution on the  $C_{1s}$  levels discussed.

The synthesis of perfluoroindene(6) has been reported previously<sup>218</sup> and the tetrafluoroindene(2) has recently been synthesised by the vacuum pyrolysis of 3,4,5,6-tetrafluorotricyclo [6.2.1.0.<sup>2,7</sup>] undeca-2,4,6-triene.<sup>219</sup> Reduction of perfluoroindene(6) with borohydride gives, depending on the conditions, the 2H, 3H hexafluoroindene(3) or a mixture of 2H- and 3H- heptafluoroindenes (4 and 5), in the ratio 1:4<sup>186</sup>.

#### a) Qualitative Discussion

##### (i) Carbon 1s levels

Fig. 4.6 shows the relevant spectra and deconvolutions ( $C_{1s}$  levels) for the pure indenenes.  $C_{1s}$  spectrum for the mixture of heptafluoroindenes is given in Fig. 3.22 (p. 109 ).

Table 4.7 summarises the  $C_{1s}$  and  $F_{1s}$  binding energies for the series.

The deconvoluted  $C_{1s}$  levels for indene (1) show the higher binding energies of the ring junction carbons (8,9) characteristic of annelated systems. The binding energy shift between carbons 8 and 9 and the four benzo carbons of 0.4eV compares well with shifts found in the condensed five membered ring heterocycles (ca. 0.5eV), naphthalene (0.4eV) and biphenylene (0.7eV). The  $CH_2$  carbon of indene(1) also appears at higher binding energy than either the aromatic or olefinic carbons. The latter two types of carbons could not be distinguished with the present resolution available.

The effect of replacing the four benzo hydrogens of (1) by fluorine is to increase the binding energies of all the positions in the

TABLE 4.7

## Molecular Core Binding Energies (eV)

Positions	(1)		(2)		(3)		(4)		(5)		(6)	
	$C_{1s}$	$F_{1s}$	$C_{1s}$	$F_{1s}$	$C_{1s}$	$F_{1s}$	$C_{1s}^*$	$F_{1s}$	$C_{1s}^*$	$F_{1s}$	$C_{1s}$	$F_{1s}$
1	285.6	-	291.4	690.6	291.0	690.8	291.3	690.8	291.3	690.8	292.0	690.8
2	285.2	-	286.4	-	284.9	-	288.8	690.8	288.8	690.8	288.5	690.8
3	285.2	-	287.0	-	288.9	690.8	285.8	-	285.8	-	288.8	690.8
4	285.2	690.0	288.9	690.6	288.9	690.8	288.8	690.8	288.8	690.8	288.9	690.8
5	285.2	690.0	289.2	690.6	288.9	690.8	288.8	690.8	288.8	690.8	289.1	690.8
6	285.2	690.0	288.9	690.6	288.9	690.8	288.8	690.8	288.8	690.8	288.9	690.8
7	285.2	690.0	289.2	690.6	288.9	690.8	288.8	690.8	288.8	690.8	289.6	690.8
8	285.6	-	287.0	-	287.0	-	286.7	-	286.7	-	287.2	-
9	285.6	-	287.2	-	287.0	-	286.7	-	286.7	-	286.8	-

\* Estimated from computed and experimental spectra.

186

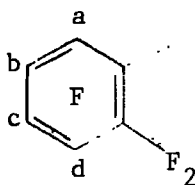
tetrafluoroindene(2). Those carbons directly attached to fluorine show the largest increase, 3.4eV on average. This increase is slightly larger than that found in the study of benzo-[b]-thiophen, indole, benzo-[b]-furan and their tetrafluoro derivatives (3.2eV average) but slightly less than the shift for 1,2,3,4-tetrafluorobenzene (3.6eV). (All values related to  $F_{1s}$  at 690.0eV). The smaller shifts found in the annelated systems with fluorines in only one ring may be due to overall transfer of charge density from the hydrocarbon ring to the fluorinated ring.

The carbons of the five membered ring in the tetrafluoroindene(2) show three main effects: (a) all the carbons show an increase in binding energy relative to indene; (b) the  $C_{1s}$  levels for C8 and C9 show an increase of 1.2eV and 1.0eV respectively [this is again slightly less than the shift found in the 1,2,3,4-tetrafluorobenzene for C5 and C6 (1.3eV), but greater than those found in the tetrafluorobenzo-[b]-thiophen, the tetrafluorobenzo-[b]-furan and the tetrafluoroindene (ca. 0.8eV, 0.3eV, 0.5eV respectively)]; and (c) C2 and C3 in (2) show a relatively large increase in  $C_{1s}$  binding energy, considering their remoteness from the fluorinated positions (1.1eV and 0.8eV respectively) and the  $CH_2$  group shows a similar increase of 0.4eV. This increase can be attributed to the transfer of electron density from the five membered ring to the six membered ring. A similar effect was observed in the condensed heterocyclic series and is born out by CNDO/2 calculations (see later).

In the case of 4,5,6,7-tetrafluoroindene(2), splittings are observed between C2 and C3 of 0.3eV, and C2 and C9 of 0.2eV. Although CNDO/2 calculations do not represent the effect of CH<sub>2</sub> or CH<sub>3</sub> groups very well, both 'ab initio' and semi-empirical calculations on toluene indicate that the CH<sub>3</sub> group is  $\pi$ -electron repelling<sup>216</sup> (see later). The C<sub>1s</sub> levels of carbon atoms directly attached ( $\alpha$ ) to CH<sub>2</sub> in (2) are at higher binding energies than those of the  $\beta$ -carbons (i.e. C2 > C3; C8 > C9), but replacing CH<sub>2</sub> by CF<sub>2</sub> in going to the hexafluoroindene(3) reverses this effect. The CF<sub>2</sub> group is  $\pi$ - and  $\sigma$ -electron attracting. The C<sub>1s</sub> level for C3 in (3) increases in binding energy by 1.0eV relative to the tetrafluoroindene(2), while the C<sub>1s</sub> level for C2 shows an increase of only 0.1eV. The C9 C<sub>1s</sub> level increases by 0.6eV and the C8 C<sub>1s</sub> level by only 0.2eV. Although C2 and C8 are directly attached to a strongly electron withdrawing CF<sub>2</sub> group in (3) and would therefore be expected at relatively higher binding energies than in (2) the increase in  $\pi$ -electron density at these positions balances this effect. The loss of  $\pi$ -electron density from C3 and C9 results in an increased binding energy for these atoms (see later). The CF<sub>2</sub> carbon (C1) increases in binding energy by 5.4eV in going from (2) to (3) (2.7eV per fluorine). The four benzo carbons in (3) attached to fluorine also show an increased binding energy relative to the tetrafluoroindene(2) of 0.4eV on average.

In going from the hexafluoroindene(3) to the 2H-heptafluoroindene(4) the replacement of the hydrogen on C3 by fluorine increases the C<sub>1s</sub> binding energy of C3 by 1.9eV relative to C3 in the hexafluoroindene(3).

TABLE 4.8

Carbon 1s binding energies (eV)

Compound	a	b	c	d
( 2 )	288.9	288.4	288.4	288.9
( 3 )	288.9	289.2	288.9	289.2
( 4 )	288.9	288.9	288.9	288.9
( 5 )	288.8	288.8	288.8	288.8
( 6 )	288.9	289.1	288.9	289.6
1,2,3,4-tetrafluorobenzene	288.8	288.8	288.8	288.8
perfluoronaphthalene	289.3	288.7	288.7	289.3
perfluorobiphenylene	288.7	289.0	289.0	288.7

However, the  $C_{1s}$  level of C2 in (4) actually decreases in binding energy by 1.5eV relative to C2 in (3) and with a binding energy of 284.9eV is 0.3eV lower than C2 in indene itself. CNDO/2 calculations indicate that this effect is due to the  $I_{\pi}$  effect of the fluorine on C3 (see later). The  $C_{1s}$  level of the  $CF_2$  group in (4) also decreases in binding energy by 0.4eV relative to C1 in the hexafluoroindene(3).

When the hydrogen attached to C2 is replaced by fluorine in going from hexafluoroindene(3) to the 3H-heptafluoroindene(5) a decrease in binding energy is also observed for C3 [-1.2eV, relative to C3 in hexafluoroindene(3)], whereas C2 shows an increase of 2.4eV. Now, with an adjacent CF group, the  $CF_2$  carbon in (5) increases in binding energy by 0.3eV (relative to (4)). Both C8 and C9 in (5) show decreases in  $C_{1s}$  binding energies of 0.3eV relative to the 2H-heptafluoroindene(4) as the  $\pi$ -repelling effect ( $I_{\pi}$ ) of the fluorine on C2 is transmitted to the six membered ring via C3.

The replacement of the final hydrogen on C3 by fluorine causes a decrease in the binding energy of C2 in perfluoroindene of 0.3eV while C3 shows an increase of 3.0eV [relative to the 3H-heptafluoroindene(5)]. The  $C_{1s}$  level of the  $CF_2$  carbon increases by 0.7eV and both C8 and C9 increase in binding energy by 0.5eV and 0.1eV respectively.

Table 4.8 shows a comparison of the binding energies of the aromatic carbons attached to fluorine in the indenenes (2) to (6) with analogous carbons in 1,2,3,4-tetrafluorobenzene perfluoro naphthalene and perfluoro biphenylene. In hexafluoroindene(3) and perfluoroindene(6)

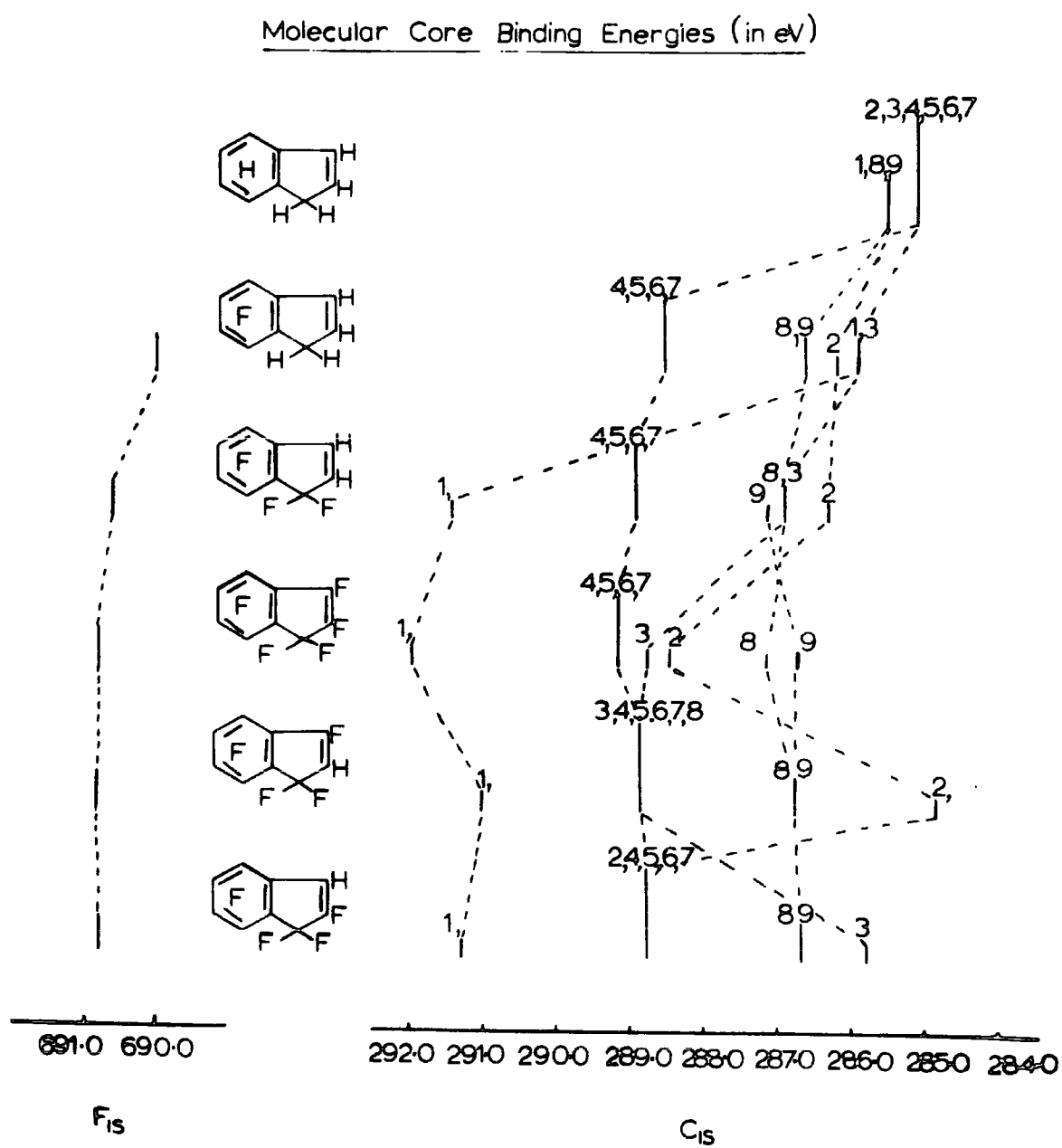


Fig. 4.7

the carbons at positions b and d have significantly higher binding energies than those at a and c. [In the computed spectra of the heptafluoroindenes (4) and (5) the  $C_{1s}$  level of all four positions were assumed identical]. In perfluoro naphthalene and tetrafluoroindene(2) b and c have lower binding energies than a and d, whereas the reverse is true for biphenylene. 1,2,3,4-Tetrafluorobenzene has all four positions identical. It should also be noted that the olefinic positions in perfluoroindene(6) have significantly lower binding energies than the aromatic carbons, a situation which also occurs in perfluoro acenaphthylene.

Fig. 4.7 shows schematically the relationship between the molecular core binding energies through the series.

(ii) Fluorine 1s levels.

No attempt was made to deconvolute  $F_{1s}$  levels within a molecule as previous results have shown that these are effectively constant.<sup>171</sup>

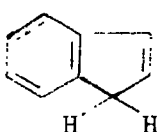
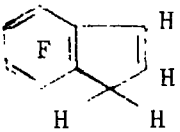
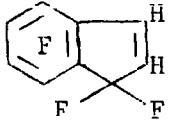
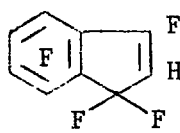
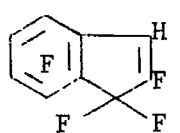
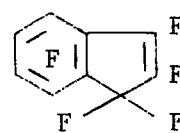
However, the degree of fluorination along the series varies from 4 to 8 fluorines. The increasing number of fluorines results in an increase in the binding energy of the  $F_{1s}$  levels. The effect of two fluorines of the  $CF_2$  group going from the tetrafluoro to hexafluoroindene increases the  $F_{1s}$  binding energies by 0.6eV. The addition of two further fluorines in going to the perfluoroindene(6) results only in a further 0.2eV increase in the  $F_{1s}$  binding energies. A similar effect has been observed in the fluorobenzenes.<sup>178</sup>

Table 4.9  
Madelung Potentials and CNDO/2 Charges

Positions	(1)		(2)		(3)		(4)		(5)		(6)	
	$q_i$	$\sum_{i \neq j} \frac{q_j}{r_{ij}}$										
1	-0.001	0.29	0.011	1.02	0.442	4.68	0.449	-4.61	0.419	-3.62	0.424	-3.47
2	-0.015	0.18	-0.014	0.93	-0.075	2.83	-0.159	4.49	0.173	-0.30	0.098	1.26
3	-0.011	0.00	0.008	0.51	0.037	0.81	0.271	-2.13	-0.048	2.57	0.196	-0.48
4	0.001	-0.01	0.172	-0.90	0.179	-0.43	0.197	-0.38	0.173	-0.20	0.190	-0.13
5	0.008	-0.10	0.152	-0.26	0.167	0.07	0.164	0.37	0.173	0.15	0.168	0.47
6	0.007	-0.11	0.152	-0.25	0.152	0.28	0.156	0.45	0.149	0.52	0.153	0.69
7	-0.006	0.06	0.170	-0.79	0.207	-0.90	0.205	-0.62	0.215	-0.77	0.213	-0.46
8	0.007	0.04	-0.012	1.78	-0.074	3.62	-0.067	3.38	-0.078	4.00	-0.067	4.27
9	0.013	0.11	-0.012	1.66	-0.002	2.83	-0.025	3.19	0.010	2.11	-0.119	3.21

TABLE 4.10

 $\pi$ ,  $\sigma$  and Total Charges for Five Membered Ring Carbons

	Position	$\pi$	$\sigma$	Total
 (1)	1	0.036	-0.037	-0.001
	2	-0.004	-0.011	-0.015
	3	-0.021	0.010	-0.011
	8	-0.003	0.010	0.007
	9	0.004	0.011	0.015
 (2)	1	0.027	-0.016	0.011
	2	-0.005	-0.009	-0.014
	3	-0.022	0.030	0.008
	8	-0.024	0.012	-0.012
	9	-0.034	0.022	-0.012
 (3)	1	0.260	0.182	0.442
	2	-0.033	-0.042	-0.075
	3	0.033	0.004	0.037
	8	-0.070	0.004	-0.074
	9	-0.013	0.011	-0.002
 (4)	1	0.253	0.196	0.449
	2	-0.127	-0.032	-0.159
	3	0.070	0.200	0.270
	8	-0.063	-0.004	-0.067
	9	-0.034	0.009	-0.025
 (5)	1	0.247	0.172	0.419
	2	0.014	0.159	0.173
	3	-0.058	0.010	-0.048
	8	-0.005	-0.073	-0.078
	9	-0.091	0.101	0.010
 (6)	1	0.240	0.184	0.424
	2	-0.076	0.174	0.098
	3	-0.013	0.209	0.196
	8	-0.026	-0.041	-0.067
	9	-0.082	-0.037	-0.119

(b). Quantitative Discussion:

Assignments for the carbon  $1s$  levels in this series of indenenes were based on CNDO SCF MO calculations and the 'point charge' model developed by Siegbahn et al. and discussed in detail elsewhere.

Table 4.9 summarises the CNDO/2 charges and Madelung potentials for the carbon  $1s$  levels in the series studied here. Table 4.10 shows how the calculated charge densities follow qualitatively the experimentally observed effects.  $\pi$ ,  $\sigma$  and total charges are given for the carbons of the five membered ring in each compound.

The higher binding energy of the ring junction carbons in indene(1) is paralleled by a relatively larger positive charge on these positions, caused mainly by loss of  $\sigma$ -electron density. The smaller than expected increase in binding energy of the 8 and 9 carbons on fluorination of benzo positions is seen as an increase in the  $\pi$ -electron density at C8 and C9, as charge density is transferred from the five membered ring to the six membered ring. This results in a decrease in charge density on C1, C2 and C3 resulting in an increase in the measured  $C_{1s}$  binding energies for these positions.

In going from the tetrafluoro(2) to the hexafluoroindene(3) the replacement of  $CH_2$  by  $CF_2$  causes a large increase in the positive charge on C1 but an increase of  $\pi$ -charge density on C2 and a decrease at C3, caused by a drift of  $\pi$ -charge density towards the  $CF_2$  group. A similar effect is also observed with C8 and C9.

In going from (3) to the 2H-heptafluoroindene(4) the introduction of fluorine at C3 reinforces this  $\pi$ -drift, increasing the total charge density on C2. This is seen experimentally as a large

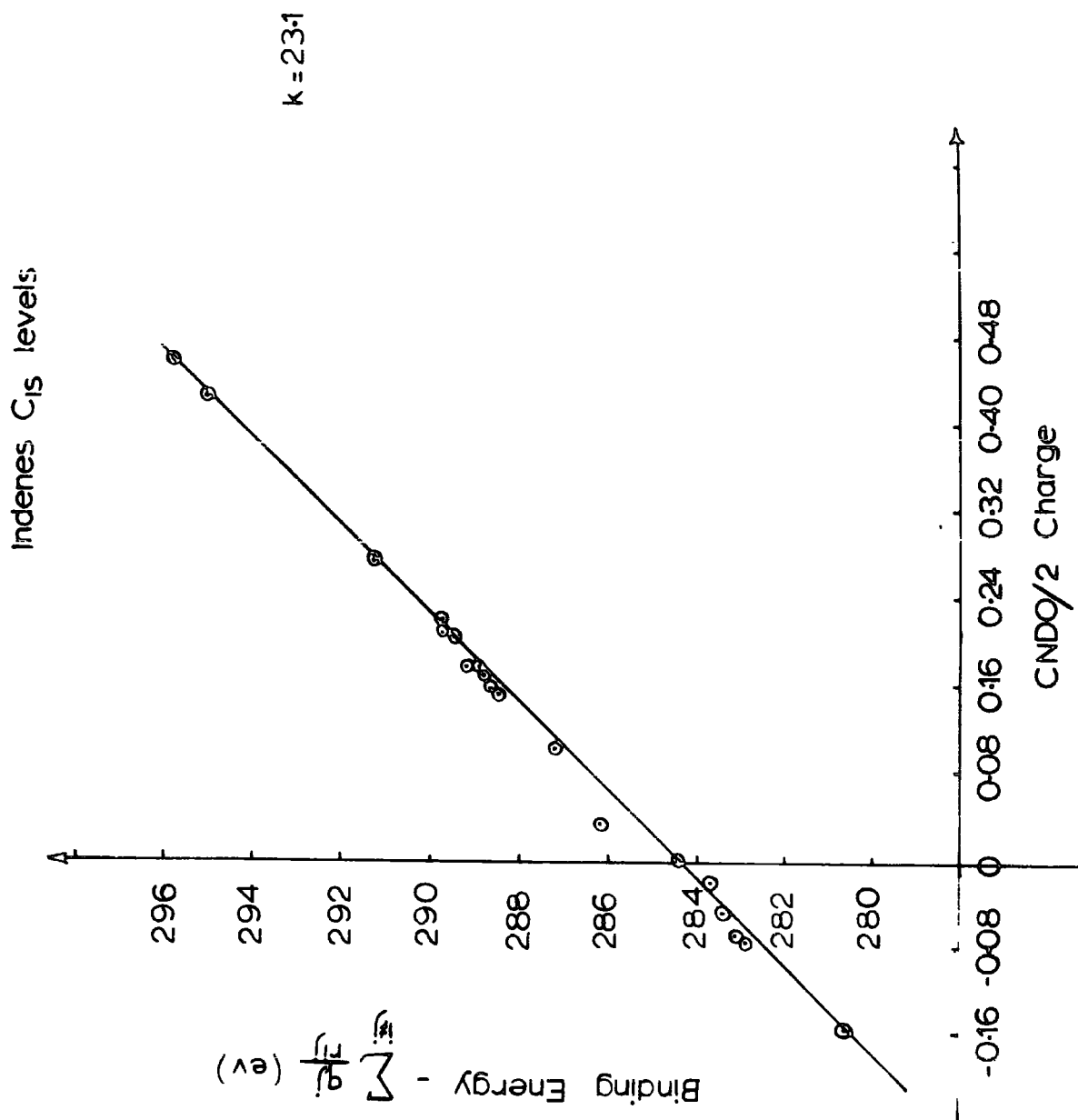


Fig. 4.3

decrease in the  $C_{1s}$  binding energy of C2. When the fluorine substituent is introduced at C2 as in (5) the  $\pi$ -drift towards the  $CF_2$  group is opposed by  $I_\pi$  effect of the fluorine on C2, causing an increase in charge density at C3 [relative to (3)]. The  $\sigma$ -attraction by the fluorine on C2 and the  $\pi$ -repulsion effect, result in a large decrease in charge density and subsequent increase in binding energy for C2.

In perfluoroindene(6)  $\sigma$ -electron density withdrawal for all carbons attached to fluorine is seen and all positions carry positive charges, except C8 and C9 where the overall charge is negative reflecting their lower binding energies.

Fig. 4.8 shows a plot of binding energy corrected for Madelung Potential against charge for the  $C_{1s}$  levels in this series of indenenes.

The points lie on a straight line with  $k = 23.1$ , and  $E^0 = 284.10$  with a correlation coefficient ( $r^2 = 0.96$ ). It should be emphasized that the average value of  $k = 25$  for  $C_{1s}$  levels has been used in assigning individual core levels. However, the assignment is internally self consistent when the derived value of  $k = 23.1$  (Fig. 4.8) is employed. This self consistency and the high correlation coefficient indicates strongly the overall correctness of the assignments.

### C. The Effect of Chlorine Substitution on the Molecular Core Binding Energies of Benzo-[b]-thiophens

#### a) Qualitative Discussion.

The relevant spectra and deconvolutions ( $C_{1s}$  levels) are shown in Fig. 4.9 for the benzo-[b]-thiophens studied. Measured core binding

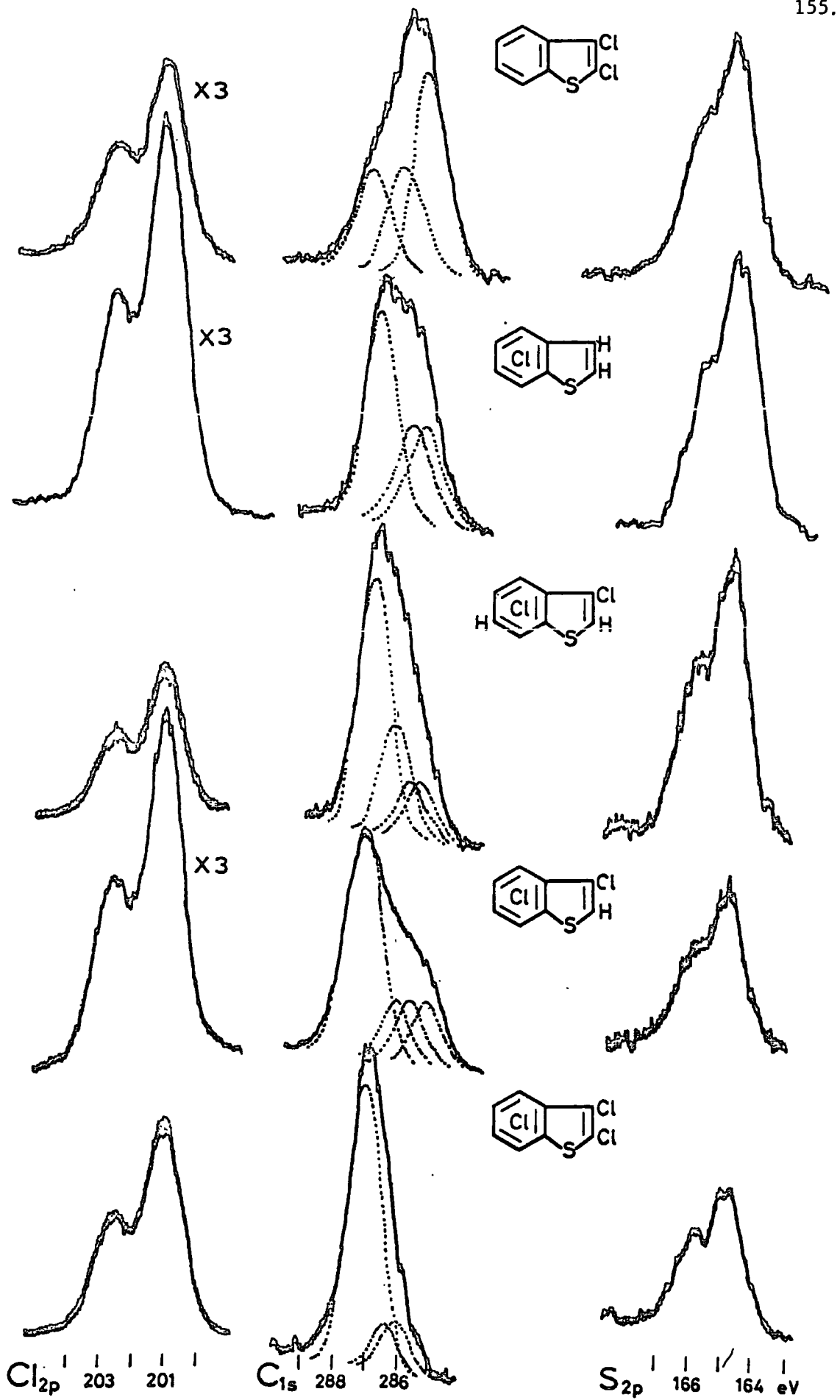
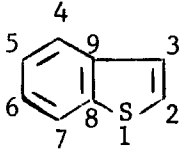
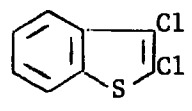
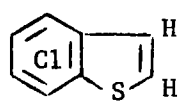


Fig. 4.9

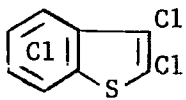
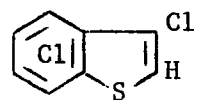
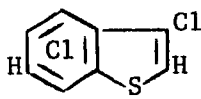
Table 4.11

Binding Energies, CNDO/2 Charges and Madelung Potentials

Compound	Position	B.E. (eV)	$q_i$	$\sum_{i \neq j} \frac{q_j}{r_{ij}}$
 (1)	$S_{2p_{1/2}}$	165.2	-0.055	0.59
	$\frac{3}{2}$	164.0		
	2	284.9	0.020	-0.25
	3	284.9	-0.034	0.55
	4	284.9	-0.008	-0.03
	5	284.9	-0.006	-0.41
	6	284.9	-0.005	0.33
	7	284.9	0.001	0.01
	8	285.5	0.061	0.04
	9	285.5	0.027	0.17
 (2)	$S_{2p_{1/2}}$	165.6	-0.031	1.00
	$\frac{3}{2}$	164.3		
	2	286.7	0.106	-0.59
	3	286.7	0.071	-0.07
	4	285.0	-0.000	0.51
	5	285.0	-0.005	0.40
	6	285.0	0.002	0.37
	7	285.0	-0.003	0.74
	8	285.8	0.064	0.21
	9	285.8	0.025	0.79
 (3)	$S_{2p_{1/2}}$	165.4	-0.008	0.70
	$\frac{3}{2}$	164.2		
	2	285.2	0.017	0.47
	3	285.2	-0.023	1.07
	4	286.8	0.096	0.52
	5	286.8	0.090	0.32
	6	286.8	0.097	0.30
	7	286.8	0.103	0.13
	8	285.6	0.036	1.04
	9	285.6	0.015	1.21

Contd.

Table 4.11 contd.

Compound	Position	B.E. (eV)	$q_i$	$\sum_{i \neq j} \frac{q_j}{r_{ij}}$
 (4)	$S_{2p_{3/2}}$	166.1	0.010	1.05
	$\frac{3}{2}$	164.8		
	2	286.9	0.093	0.07
	3	286.9	0.075	0.36
	4	286.9	0.101	0.30
	5	286.9	0.086	0.60
	6	286.9	0.097	0.57
	7	286.9	0.102	0.44
	8	285.9	0.039	1.51
9	286.2	0.015	1.88	
 (5)	$S_{2p_{3/2}}$	165.8	0.005	0.74
	$\frac{3}{2}$	164.6		
	2	285.1	-0.028	1.47
	3	286.9	0.108	-0.46
	4	286.9	0.105	0.14
	5	286.9	0.090	0.53
	6	286.9	0.097	0.43
	7	286.9	0.100	0.34
	8	285.6	0.043	1.25
9	286.1	0.008	1.84	
 (6)	$S_{2p_{3/2}}$	165.7	-0.001	0.70
	$\frac{3}{2}$	164.5		
	2	285.1	-0.025	1.36
	3	286.8	0.108	-0.50
	4	286.8	0.098	0.08
	5	286.8	0.107	-0.22
	6	286.1	-0.040	2.01
	7	286.8	0.123	-0.41
	8	285.6	0.037	1.20
9	286.1	0.024	1.54	

energies are given in Table 4.11. and shown schematically in Fig. 4.10.

The effect of annelation on the five membered thiophen ring has been discussed previously (p 123 ). The two carbon atoms forming the ring junction (8,9) are shifted to higher binding energies by 0.5eV relative to the parent thiophen, an effect observed in other annelated systems.<sup>171</sup> The effect of chlorine substitution in the benzo-[b]-thiophen, is to cause a large increase in the  $C_{1s}$  binding energies of all carbon atoms directly attached to chlorine. There appears to be a slight increase in the shift with increased degree of chlorine substitution. (1.8eV for 2,3-dichlorobenzo-[b]-thiophen to 2.0eV for perchlorobenzo-[b]-thiophen). This is somewhat less than the increase found in the fluorobenzenes<sup>178</sup> with increasing degree of fluorine substitution. The average shift on replacing hydrogen by chlorine in the benzo-[b]-thiophens is less than that observed in the benzene series. This can be attributed to the possibility, in the annelated systems, of transfer of electron density from one ring to another minimising the effect of charge withdrawal by the more electron negative chlorine atom. With the heterocyclic systems, loss of electron density at the hetero atom is also possible. This effect can be clearly seen by comparing the shifts in core binding energies in 2,3-dichlorobenzo-[b]-thiophen(2) and 4,5,6,7-tetrachlorobenzo-[b]-thiophen(3) relative to the unsubstituted heterocycle (1).

The effect of chlorine substitution in the benzo ring, as in (3), is to increase the  $C_{1s}$  binding energies of the four carbons directly

attached to chlorine by 1.9eV [relative to benzo-[b]-thiophen(1)] but the two bridging carbons (C8, C9) show very little increase (0.1eV). The more remote C2 and C3 carbons show an increase in  $C_{1s}$  level energies of 0.3eV and the  $S_{2p_{3/2}}$  level increases in binding energy by 0.2eV. CNDO/2 calculations indicate that electron density is removed from C2, C3 and the sulphur atom into the six membered ring.

In contrast, chlorine substitution in the five membered ring [as in (2)] increases the  $C_{1s}$  binding energies of both C2 and C3 by 1.8eV [relative to (1)] and has a greater effect on the other members of the heterocyclic ring. The C8 and C9  $C_{1s}$  levels and the  $S_{2p_{3/2}}$  level all increase in binding energy by 0.3eV in going from benzo-[b]-thiophen(1) to the 2,3-dichloro derivative (2). The four benzo carbons (4,5,6,7) show only a slight increase in binding energy (0.1eV).

The substitution of one chlorine atom at C3 in going from 4,5,6,7-tetrachlorobenzo-[b]-thiophen(3) to 3,4,5,6,7-pentachlorobenzo-[b]-thiophen(5) is to increase the binding energy of C9 by a further 0.5eV and the sulphur  $2p_{3/2}$  binding energy by 0.4eV, while C2 and C8 are relatively unaffected. The  $C_{1s}$  levels of all carbons attached to chlorine also increase slightly with the increased degree of substitution (0.1eV). Clearly chlorine substitution in the five membered ring has a greater effect on C8, C9 and the sulphur atom than chlorine substitution in the six membered ring, even though fewer chlorine atoms are involved. It would appear that the electron density in the five membered ring is more readily perturbed than that in the more aromatic six membered ring. N.M.R. evidence indicates that the heterocyclic ring is less aromatic than the benzo ring.<sup>220</sup> CNDO/2

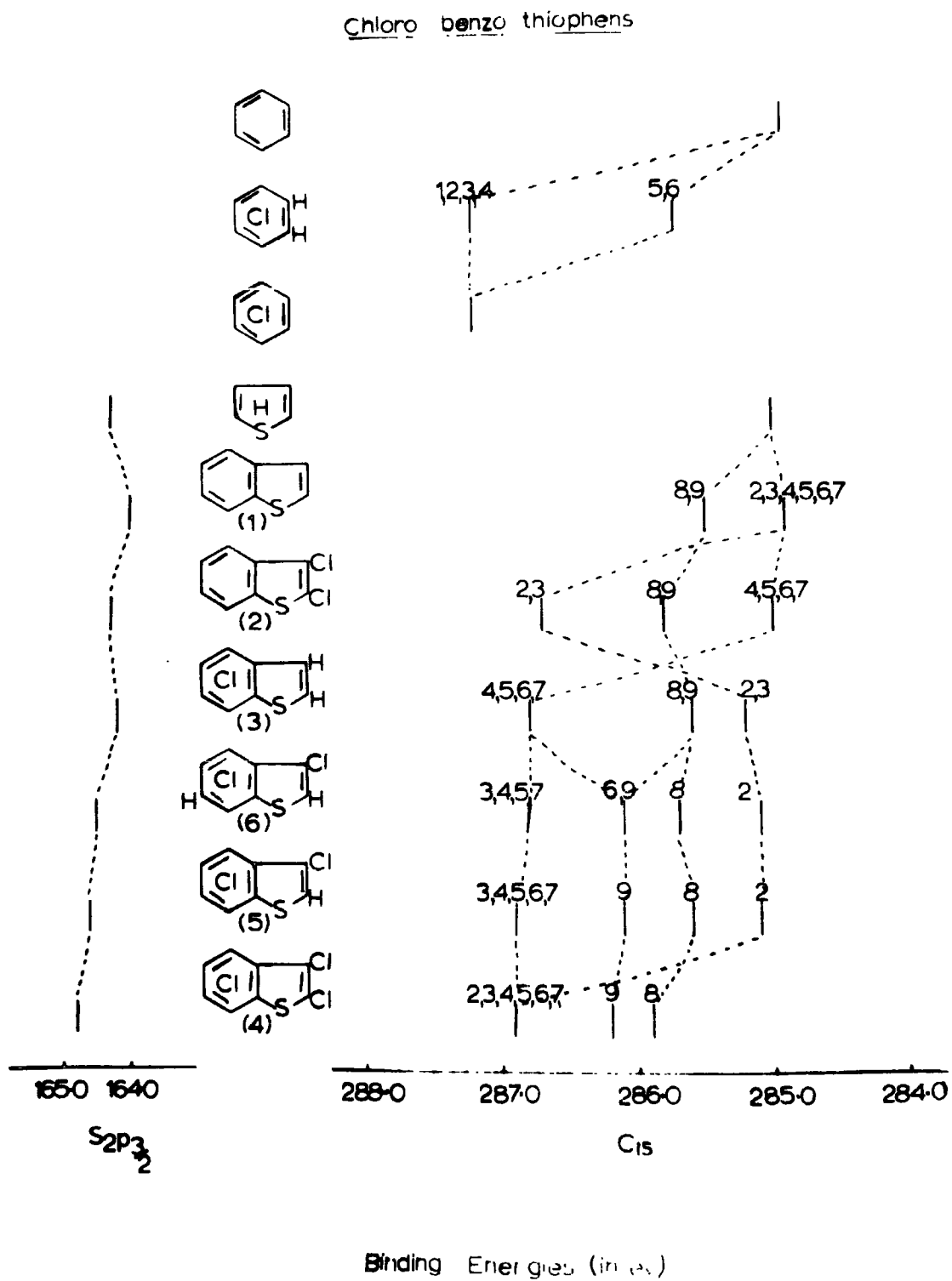


Fig. 4.10

calculations also indicate larger overall increases in positive charges at C8 and C9 on chlorine substitution in the five membered ring.

The addition of the final chlorine substituent at C2 in going from pentachloro(5) to perchlorobenzo-[b]-thiophen(4) causes both the C9 and C8  $C_{1s}$  binding energies to increase (0.1eV and 0.3eV respectively). In contrast to the unsubstituted heterocycle(1), perchlorobenzo-[b]-thiophen(4) shows a splitting between C8 and C9 of 0.3eV. This can be attributed to the fact that C9 is adjacent to two C-Cl groups whereas C8 is adjacent to only one C-Cl group and a sulphur atom. Benzo-[b]-thiophens substituted with chlorine only at C3 in the five membered ring show a much larger splitting between C8 and C9 (0.5eV). The replacement of the hydrogen at C2 in pentachlorobenzo-[b]-thiophen(5) by chlorine in going to the perchloro derivative (4) causes a further increase in the  $S_{2p_{3/2}}$  binding energy of 0.2eV. The effect of chlorine substitution on the  $S_{2p_{3/2}}$  binding energies is shown schematically in Fig. 4.10.

b). Distinction between two isomeric tetrachlorobenzo-[b]-thiophens using ESCA.

Structural problems in highly chlorinated heterocyclic systems are often not amenable to solution by conventional spectroscopic techniques.

The highly successful N.M.R. techniques used in fluorocarbon chemistry (both  $^{19}F$  and  $^1H$  resonances) are not readily applicable to the chlorine nucleus and only occasionally can  $^1H$  n.m.r. yield unambiguous

results. N.Q.R. spectroscopy, while being suited to studying chloro carbons suffers from several disadvantages, mainly difficulty in the interpretation of the results and the very large sample requirement needed to give good signal intensity (of the order of several hundred milligrams). The distinct advantages of ESCA in these respects have already been noted (independence of nuclear spin properties and modest sample requirement etc). The technique has previously been successfully applied to structural problems in polyfluoro aromatic systems.<sup>186</sup> The major obstacle in applying ESCA to chloro carbon systems is the small binding energy range obtained compared to the corresponding fluorocarbons. With the present generation photoelectron spectrometers, such as the ES100 used in this work, the resolution available does not enable individual peaks of the  $C_{1s}$  levels to be resolved and only overall peak 'envelopes' are obtained. The individual peak positions may be found by deconvolution techniques using either digital or analog computer and assignments can be made with reference to CNDO/2 type calculations.

However, in favourable circumstances detailed analysis of spectra are not necessary and the overall 'envelope' shapes may be distinctive enough to allow identification of isomers with only 'rough' deconvolutions.

The two isomers considered here, 4,5,6,7-tetrachlorobenzo-[b]-thiophen(3) and 3,4,5,7-tetrachlorobenzo-[b]-thiophen(6) can be readily distinguished by conventional  $^1H$ -nmr but a detailed analysis of their respective ESCA spectra reveals some interesting properties and shows

that in this case the two isomers could be distinguished by this technique alone.

Fig. 4.9 shows the  $C_{1s}$  spectra for the two isomers (along with their deconvolutions) and the  $Cl_{2p}$  and  $S_{2p}$  levels. It can readily be shown that the two compounds are isomeric and contain carbon, chlorine and sulphur in the ratio 8:4:1, from a knowledge of the integrated peak areas and relative photoelectron cross sections of the  $C_{1s}$ ,  $Cl_{2p}$  and  $S_{2p}$  core levels, for the exciting radiation used. ( $MgK\alpha_{1,2}$  or  $AlK\alpha_{1,2}$ ).

It has already been noted that chlorine substitution in the five membered ring causes a larger increase in the binding energies of C8 and C9 as well as the  $S_{2p_{3/2}}$  level than chlorine substituted in the six membered ring. A comparison of the  $S_{2p_{3/2}}$  levels for both compounds shows that in one case the  $S_{2p_{3/2}}$  level is at 164.2eV and in the other the  $S_{2p_{3/2}}$  level is at 164.5eV. For 3,4,5,6,7-pentachlorobenzo-[b]-thiophen(5) the  $S_{2p_{3/2}}$  level is at 164.6eV. This gives a good indication that one isomer has a chlorine substituent in the five membered ring without resorting to deconvolution of the  $C_{1s}$  levels. Deconvolution of the  $C_{1s}$  level peak envelopes of (3) and (5) using line widths of 1.2eV, can be simplified by using one peak of area 4 for the C-Cl carbons and four single peaks for the remaining carbons. This 'rough' deconvolution reveals that in both cases the  $C_{1s}$  levels of the four C-Cl carbons appear at 286.8eV but that one isomer is more complex than the other. Accepting that the isomer with the

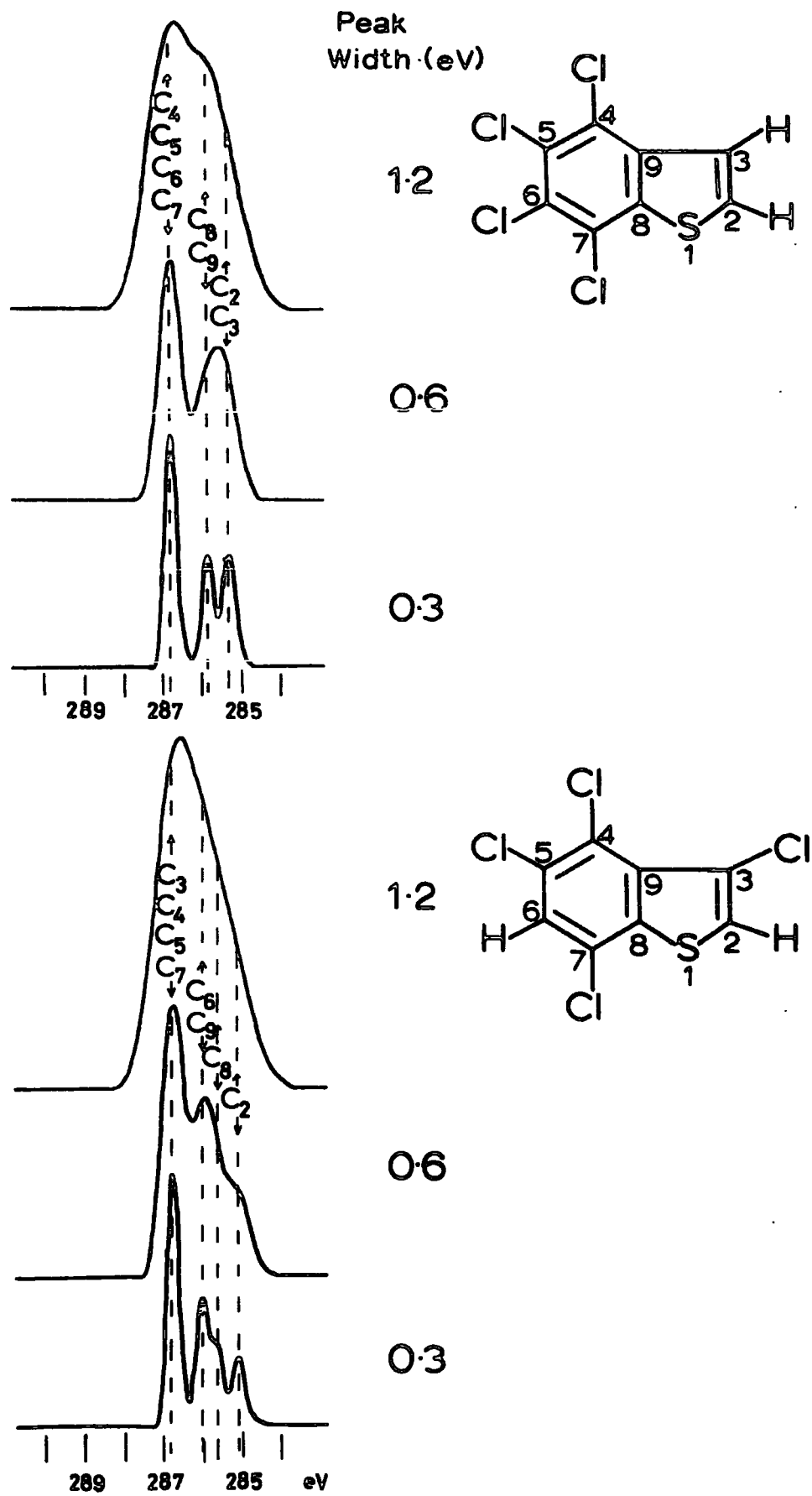
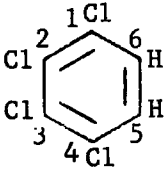
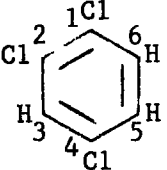
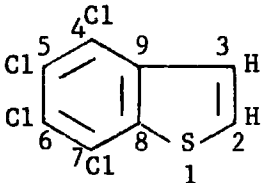
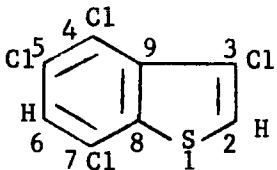
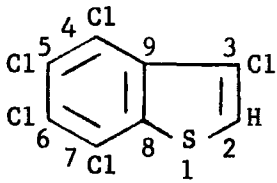
C<sub>1s</sub> Levels

Fig. 4.11

TABLE 4.12

Compound	Assignment	BE (eV)
	1	284.9
	1,2,3,4	287.2
	5,6	285.7
	1,2,4	287.2
	3	286.3
	5	286.1
	6	285.4
	4,5,6,7	286.8
	8,9	285.6
	2,3	285.2
	3,4,5,7	286.8
	6,9	286.1
	8	285.6
	2	285.1
	3,4,5,6,7	286.8
	8,	285.6
	9	286.1
	2	285.1

lowest  $S_{2p_{3/2}}$  binding energy does not have a chlorine substituent in the five membered ring, this can readily be assigned as 4,5,6,7-tetrachlorobenzo-[b]-thiophen. Unfortunately the possible remaining isomers are not as easily distinguished, so that although the two isomers are readily distinguished and the structure of one assigned, the structure of the remaining isomer could not be determined with the present obtainable resolution. Fig. 4.11 shows the computer simulated effect of increased resolution (smaller line widths) on the  $C_{1s}$  levels for the two isomers. With this type of improvement in resolution structural problems in chlorocarbon chemistry should be more amenable to solution by ESCA, in conjunction with other spectroscopic techniques. Even with the structure of 3,4,5,7-tetrachlorobenzo-[b]-thiophen(6) known, assignment of the individual  $C_{1s}$  peaks is not straight forward and CNDO/2 calculations are not helpful in this case. Comparison of the  $C_{1s}$  binding energies obtained with those for other benzo-[b]-thiophens and with the  $C_{1s}$  binding energies in the chlorobenzenes<sup>216</sup> allows the assignments shown in Table 4.12 to be made. Data is also given for benzene and the 1,2,3,4-tetrachloro and 1,2,4-trichlorobenzenes for comparison.

c. Quantitative Discussion.

Table 4.11 gives CNDO/2 charges and Madelung potentials for the series of benzo-[b]-thiophens.

An inspection of the charges in Table 4.11 shows that in many cases they follow qualitatively the experimentally observed effects.

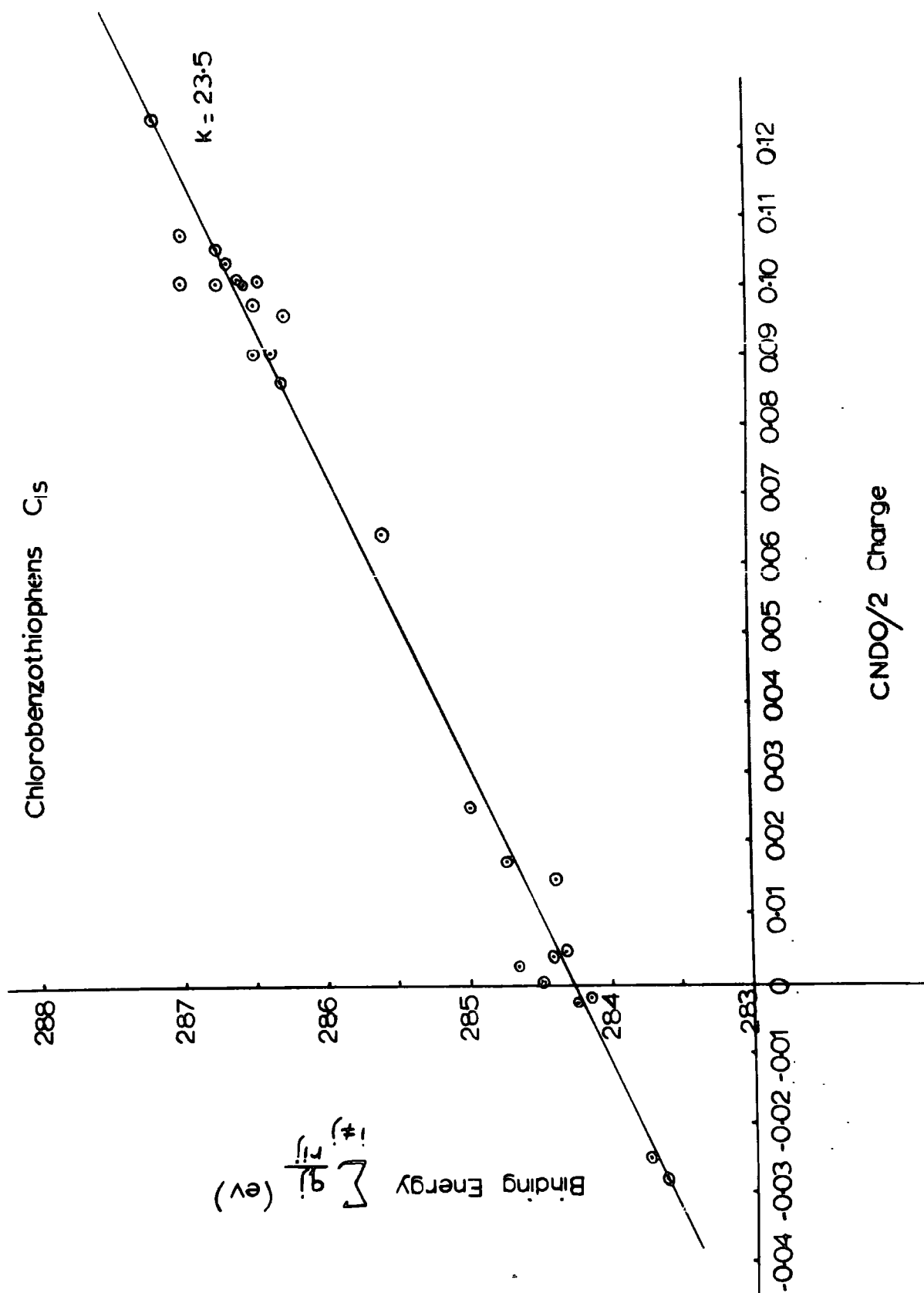


Fig. 4.12

(An exact correspondence would not be expected because of the large Madelung terms involved due to the halogen atoms). The bridging carbons (8,9) in 2,3-dichlorobenzo-[b]-thiophen(2) carry higher total positive charges than C8 and C9 in 4,5,6,7-tetrabenzo-[b]-thiophen(3). This is in accord with the observed higher binding energies for C8 and C9 in 2,3-dichlorobenzo-[b]-thiophen(2).

A plot of binding energy corrected for Madelung potential against CNDO/2 charge (Fig. 4.12) for the  $C_{1s}$  levels given a straight line with  $k = 23.5$ ,  $E^0 = 284.3$  and a correlation coefficient ( $r^2 = 0.9$ ). Although the least squares fit is good there is considerably more scatter of the points than observed with either the parent heterocycles (benzo-[b]-thiophen, benzo-[b]-furan, indole) or with the fluorinated compounds. The factors contributing to the scatter will be discussed later (see section E).

#### D. A Comparison of the Molecular Core Binding Energies in Some Benzo-[b]-thiophens and their corresponding S-dioxides.

##### Introduction

The increased oxidation state of sulphur in going from a benzo-[b]-thiophen to the corresponding S-dioxide has a dramatic effect on the properties of the heterocyclic system. Benzo-[b]-thiophens are normally stable aromatic compounds readily undergoing aromatic replacement reactions in the five membered ring rather than addition reactions to the 2,3- double bond. In the corresponding S-dioxides on the other hand, the aromaticity of the five membered ring is

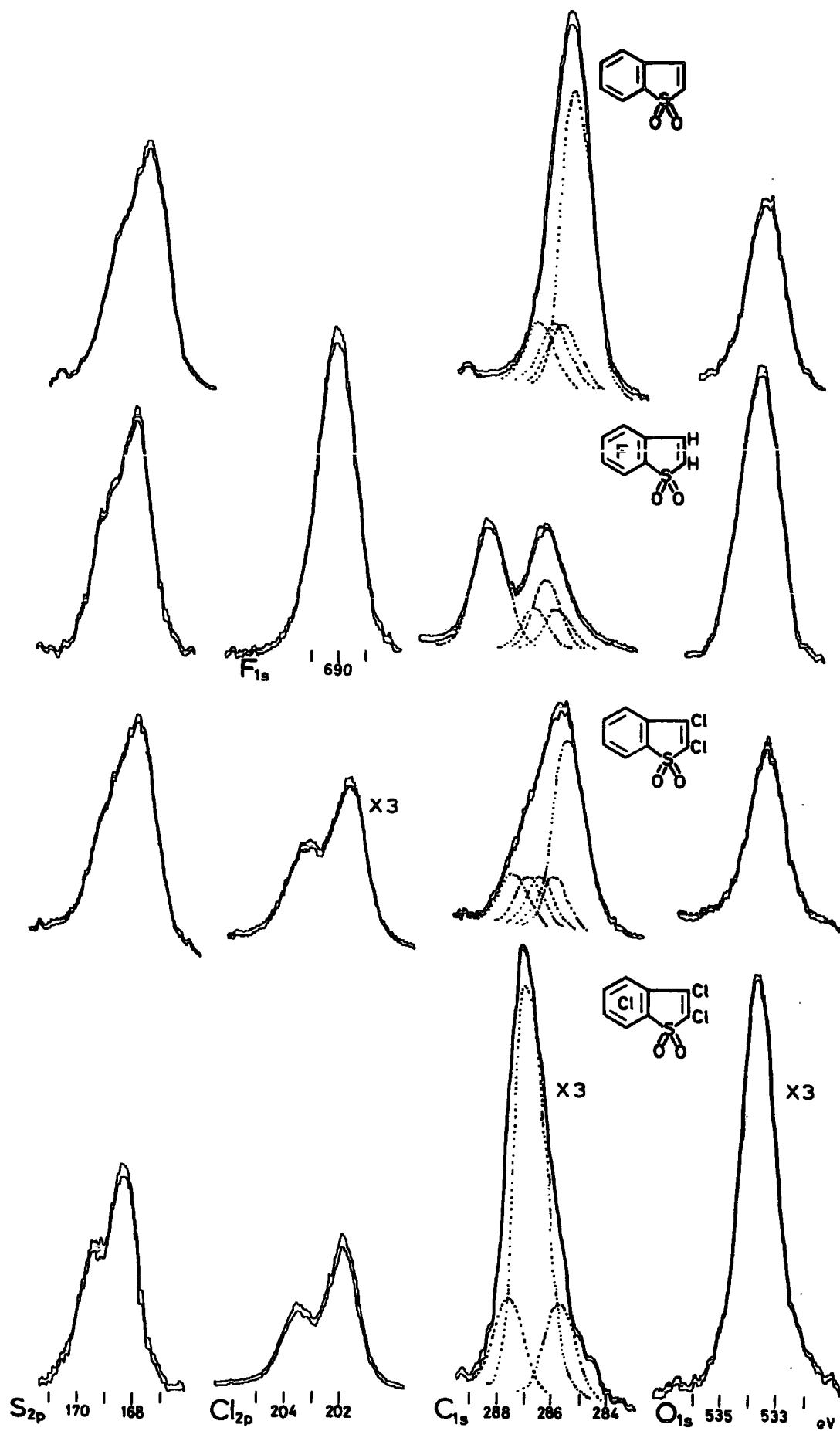
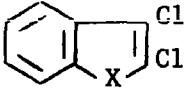
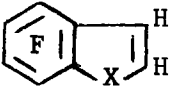
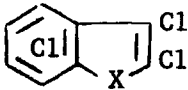


Fig. 4.13

Table 4.13  
Molecular Core Binding Energies (in eV)

Compound	Position	X = S B.E.	X = SO <sub>2</sub> B.E.
	4,5,6,7	284.9	285.0
	8	285.5	285.5
	9	285.5	286.4
	3	284.9	285.8
	2	284.9	285.0
	S <sub>2p<sub>1/2</sub></sub>	165.2	169.1
	$\frac{3}{2}$	164.0	167.8
a.	4,5,6,7	285.0	285.2
	8	285.8	285.9
	9	285.8	286.4
	3	286.7	287.5
	2	286.7	286.7
	S <sub>2p<sub>1/2</sub></sub>	165.6	169.3
	$\frac{3}{2}$	154.3	168.0
	b.	4,5,6,7	288.1
	8	286.3	286.1
	9	286.3	286.6
	3	285.6	286.1
	2	285.6	285.7
	S <sub>2p<sub>1/2</sub></sub>	165.8	169.4
	$\frac{3}{2}$	164.6	168.2
	a.	4,5,6,7	286.9
	8	285.9	285.8
	9	286.2	286.9
	3	286.9	287.4
	2	286.9	286.9
	S <sub>2p<sub>1/2</sub></sub>	166.1	169.7
	$\frac{3}{2}$	164.8	168.4

a. all Cl<sub>2p<sub>3/2</sub></sub> 201.0 eV.    b. all F<sub>1s</sub> 690.0 eV

completely disrupted as evidenced by the appearance, in the infra-red spectrum, of an absorption at around  $1590\text{cm}^{-1}$  ( $6.3\mu$ ) attributable to the 2,3-double bond. Chemically the S-dioxides behave more like vinyl sulphones than hetero aromatic compounds.

In order to assess the effect of the change from  $\text{S}^{\text{II}}$  to  $\text{S}^{\text{VI}}$  on the molecular core binding energies in the benzo-[b]-thiophen ring system a series of benzo-[b]-thiophens and their corresponding S-dioxides have been studied.

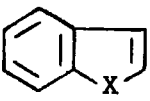
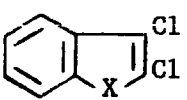
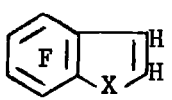
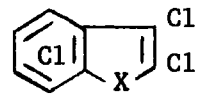
#### a. Qualitative Discussion

Spectra of the benzo-[b]-thiophen S-dioxides are shown in Fig. 4.13. The molecular core binding energies for the series are given in Table 4.13 and shown diagrammatically in Fig. 4.14.

The effect of replacing an atom of low electronegativity like sulphur by a highly polar  $\text{SO}_2$  group would be expected to be quite marked. In fact an inspection of the  $\text{C}_{1s}$  binding energies in Table 4.13 for benzo-[b]-thiophen and benzo-[b]-thiophen 1-dioxide shows that for the two carbons attached to the sulphur atom (C2, C8) the change in oxidation state has very little overall effect, while the  $\text{C}_{1s}$  levels of both C3 and C9 both increase in binding energy by 0.9eV. This effect can be understood in terms of the charge potential model (see later). The carbons in the benzo ring show only a slight increase in binding energy (0.1eV) showing that the effect of the  $\text{SO}_2$  group is limited to the five membered ring. The increase in binding energy of C3 and C9 and the small effect on C2 and C8 is a general trend throughout the series.

TABLE 4.14

Binding Energy Shifts for X = S to X = SO<sub>2</sub>

Compound	Position	Shift (in eV)
	4,5,6,7	0.1
	9	0.9
	8	0.0
	3	0.9
	2	0.0
	S <sub>2p<sub>3/2</sub></sub>	3.8
	4,5,6,7	0.2
	9	0.6
	8	0.1
	3	0.8
	2	0.0
	S <sub>2p<sub>3/2</sub></sub>	3.7
	4,5,6,7	0.1
	9	0.3
	8	-0.2
	3	0.5
	2	0.1
	S <sub>2p<sub>3/2</sub></sub>	3.6
	4,5,6,7	0.0
	9	0.7
	8	-0.1
	3	0.5
	2	0.0
	S <sub>2p<sub>3/2</sub></sub>	3.6

Replacing the two hydrogens in the five membered ring of benzo-[b]-thiophen by chlorine causes both C2 and C3 to increase in binding energy by 1.8eV. Oxidation of the sulphur atom to SO<sub>2</sub> increases the binding energy of C3 and C9 by 0.8eV and 0.6eV respectively, while C2 and C8 are relatively unchanged. Table 4.14 gives the shifts in binding energy on oxidation of the sulphur atom in the benzo-[b]-thiophens to give the corresponding sulphones.

Although the SO<sub>2</sub> group is highly polar, its main influence is not on the adjacent carbon atoms ( $\alpha$ ) but on the  $\beta$ -positions. This appears to be due to  $\pi$ -electron attraction by the SO<sub>2</sub> group ( $-I_{\pi}$  effect) away from C3 - C9 onto C2- C8 and  $\sigma$ -electron attraction from C2 and C8. The net effect being that C8 and C9 lose overall electron density (and hence increase in binding energy) while the loss of  $\sigma$ -electron density from C2 and C8 is compensated by an increase on  $\pi$ -electron density. This is substantiated by CNDO/2 calculations of charge densities (see later).

b. The hetero atom.

Binding energies for the sulphur 2p levels are given in Table 4.13 and shown diagrammatically in Fig. 4.14.

Oxidation of the sulphur in a benzo-[b]-thiophen ring system to a S-dioxide causes a marked increase in the S<sub>2p</sub> binding energies. In the case of benzo-[b]-thiophen to benzo-[b]-thiophen 1-dioxide the increase is 3.8eV. This large increase in binding energy reflects the increased positive charge on sulphur when attached to two electro-negative oxygen atoms.



The sensitivity of the sulphur 2p binding energies to changes in the thiophen ring system are clearly shown in Table 4.14. As the positive charge on the sulphur atom increases, an increased degree of halogenation, the shift in the  $S_{2p_{3/2}}$  level on oxidation of S to  $SO_2$  decreases. Hence for benzo-[b]-thiophen to benzo-[b]-thiophen 1-dioxide the  $S_{2p_{3/2}}$  shift is 3.8eV whereas for perchlorobenzo-[b]-thiophen-perchlorobenzo-[b]-thiophen-1-dioxide the  $S_{2p_{3/2}}$  shift is only 3.6eV. Obviously then the shifts due to chlorination and oxidation are not additive. The shift in  $S_{2p}$  binding energy on oxidation decreases as the existing electron demand in the parent benzo-[b]-thiophen increases. The  $O_{1s}$  binding energies also increase with increased degree of halogenation in the benzo-[b]-thiophen system, from 533.2eV in benzo-[b]-thiophen 1-dioxide to 533.6eV in the perchloro derivative.

c. Quantitative Discussion

Table 4.15 gives the CNDO/2 charges and Madelung potentials for the series. Because of the large charge separation in the S-dioxides the Madelung term becomes important for members of the heterocyclic ring.

The large increase in binding energy for the  $S_{2p}$  level is reflected in the large CNDO/2 charges on the sulphur atom in the S-dioxides.

TABLE 4.15  
CNDO/2 Charges and Madelung Potentials

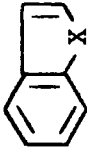
Position								
	$q_i$	$\sum_{i \neq j} \frac{q_i}{r_{ij}}$	$q_i$	$\sum_{i \neq j} \frac{q_i}{r_{ij}}$	$q_i$	$\sum_{i \neq j} \frac{q_i}{r_{ij}}$	$q_i$	$\sum_{i \neq j} \frac{q_i}{r_{ij}}$
1	-0.055	0.59	-0.031	1.00	0.010	1.05	0.007	0.59
2	0.020	-0.25	0.106	-0.59	0.093	0.07	0.019	0.57
3	-0.034	0.55	0.071	-0.07	0.075	0.36	-0.017	1.03
4	-0.008	0.17	-0.000	0.51	0.101	0.30	0.169	-0.80
5	-0.006	0.04	-0.005	0.40	0.086	0.60	0.148	-0.17
6	0.001	0.01	0.002	0.37	0.097	0.57	0.152	-0.20
7	-0.005	0.33	-0.003	0.74	0.102	0.44	0.174	-0.75
8	0.061	-0.41	0.064	0.21	0.039	1.51	0.007	1.58
9	0.027	-0.03	0.025	0.79	0.015	1.88	-0.006	1.67
1	0.890	-9.89	0.891	-9.05	0.917	-9.20	0.932	-9.61
2	-0.100	3.32	-0.020	2.91	-0.030	3.15	-0.099	4.11
3	0.012	0.98	0.112	0.46	0.093	0.59	0.030	1.46
4	0.008	0.93	0.000	1.34	0.109	0.78	0.185	-0.13
5	0.031	0.59	0.004	0.91	0.127	0.87	0.176	0.35
6	0.020	0.73	-0.007	1.13	0.111	1.04	0.165	0.46
7	0.030	0.43	0.034	0.93	0.123	0.36	0.209	-0.76
8	-0.090	3.16	-0.026	3.45	-0.124	4.71	-0.144	5.11
9	0.027	0.80	0.055	1.57	0.001	2.31	-0.001	2.43

X = S

X = SO<sub>2</sub>

Table 4.16

 $\pi$ ,  $\sigma$  and Total Charges

Position												
	$\pi$	$\sigma$	Total	$\pi$	$\sigma$	Total	$\pi$	$\sigma$	Total	$\pi$	$\sigma$	Total
4, 5, 6, 7	-0.051	0.034	-0.017	0.035	-0.096	-0.061	-0.127	0.509	0.382	-0.170	0.796	0.626
8	-0.015	0.076	0.061	-0.023	0.087	0.064	-0.039	0.078	0.039	-0.046	0.053	0.007
9	0.00	-0.027	-0.027	-0.009	0.034	0.025	-0.024	0.039	0.015	-0.032	0.026	-0.006
3	-0.041	0.007	-0.034	-0.065	0.136	0.071	-0.063	0.138	0.075	-0.039	0.022	-0.017
2	-0.018	0.038	0.020	-0.043	0.148	0.105	-0.044	0.138	0.094	-0.018	0.037	0.019
1	0.124	-0.179	-0.055	0.115	-0.146	-0.031	0.118	-0.108	0.009	0.127	-0.12	0.007
4, 5, 6, 7	0.047	0.043	0.090	0.023	0.008	0.031	-0.030	0.500	0.470	-0.083	0.817	0.734
8	-0.072	-0.018	-0.090	-0.063	0.037	-0.026	-0.100	-0.024	-0.124	-0.095	-0.048	0.143
9	0.006	0.021	0.027	0.015	0.040	0.055	-0.022	0.023	0.001	-0.026	0.025	-0.001
3	0.030	-0.019	0.011	-0.001	0.113	0.112	-0.006	0.099	0.093	0.035	-0.005	0.030
2	-0.058	-0.043	-0.100	-0.079	0.060	-0.019	-0.081	0.051	-0.030	-0.064	-0.035	-0.099
1	0.646	0.244	0.900	0.643	0.247	0.890	0.631	0.286	0.917	0.641	0.292	0.933

X

S

SO<sub>2</sub>

The increases in the  $C_{1s}$  binding energies for C3 and C9 are also reflected in the total charges at these atoms. Oxidation of the sulphur atom causes a large increase in positive charge at both C3 and C9. On the other hand C2 and C8 both show a decrease in positive charge in the S-dioxides and in fact C2 has a total negative charge in all the benzo-[b]-thiophen 1-dioxides although again the Madelung potential term is important for these positions.

Table 4.16 gives the  $\pi$ ,  $\sigma$  and Total charges for the four benzo carbons (4,5,6,7), C2, C3, C8, C9 and the sulphur atom in both the benzo-[b]-thiophens and the corresponding S-dioxides. Inspection of the data shows that the changes at C3 and C9 are due to loss of total charge density. The increased electron density at C2 and C8 is offset to a great extent by the large Madelung Potential, and the overall effect is that these two positions change very little in binding energy, in going to the S-dioxides.

The CNDO/2 calculations indicate that the 4,5,6,7 carbons lose some electron density (both  $\pi$  and  $\sigma$ ) to the five membered ring in the S-dioxides, but the effect is greatly over-estimated as indicated by the very small changes in binding energy actually observed.

The correlation of binding energy corrected for Madelung potential against charge for the  $S_{2p_{3/2}}$  levels is extremely good (correlation coefficient  $r^2 = 0.99$ ). The value of  $k = 15.3$  agrees well with the value of  $k = 15$  found by Siegbahn et al<sup>173b</sup> in a study of sulphur compounds. The intercept gives a value of  $E^0 = 163.7\text{eV}$ .

Absolute values for the  $S_{2p}$  binding energies found in this work agree well with those found from a study of sulphones by Scanlan,<sup>216</sup>

who measured the  $S_{2p_{3/2}}$  binding energy in dimethyl sulphone as 167.7eV and in 2,3-diphenyl thiirene-S-dioxide as 167.6eV. This compares with the value for the binding energy of the  $S_{2p_{3/2}}$  level in benzo-[b]-thiophen S-dioxide of 167.8eV.

#### E. The Effect of Chlorine Substitution on the Molecular Core Binding Energies of Indoles.

##### a. Qualitative Discussion.

The relevant spectra and deconvolutions ( $C_{1s}$  levels) for the indoles studied are shown in Fig. 4.15.

The effect of annelation on the pyrrole ring system has been discussed previously (p. 123) the main changes observed are an increase in the  $C_{1s}$  binding energies of the two carbons forming the ring junction, decrease in the binding energy of C3 and very little change in either C2 or the  $N_{1s}$  binding energies (relative to pyrrole). The molecular core binding energies for the series of indoles studied in this work are given in Table 4.17 and shown diagrammatically in Fig. 4.16.

Substitution of two chlorines in the five membered ring of indole(1) increase the  $C_{1s}$  binding energy of C2 and C3 by 1.5eV and 2.0eV respectively. The smaller shift in the  $C_{1s}$  binding energy of C2 can be explained by the fact that C2 is already attached to an electronegative nitrogen atom and substitution of a chlorine at C2 can not cause as large an increase in the positive charge and hence binding energy (there is already a high electron demand at this position). In contrast the shift at C3 is larger than normal

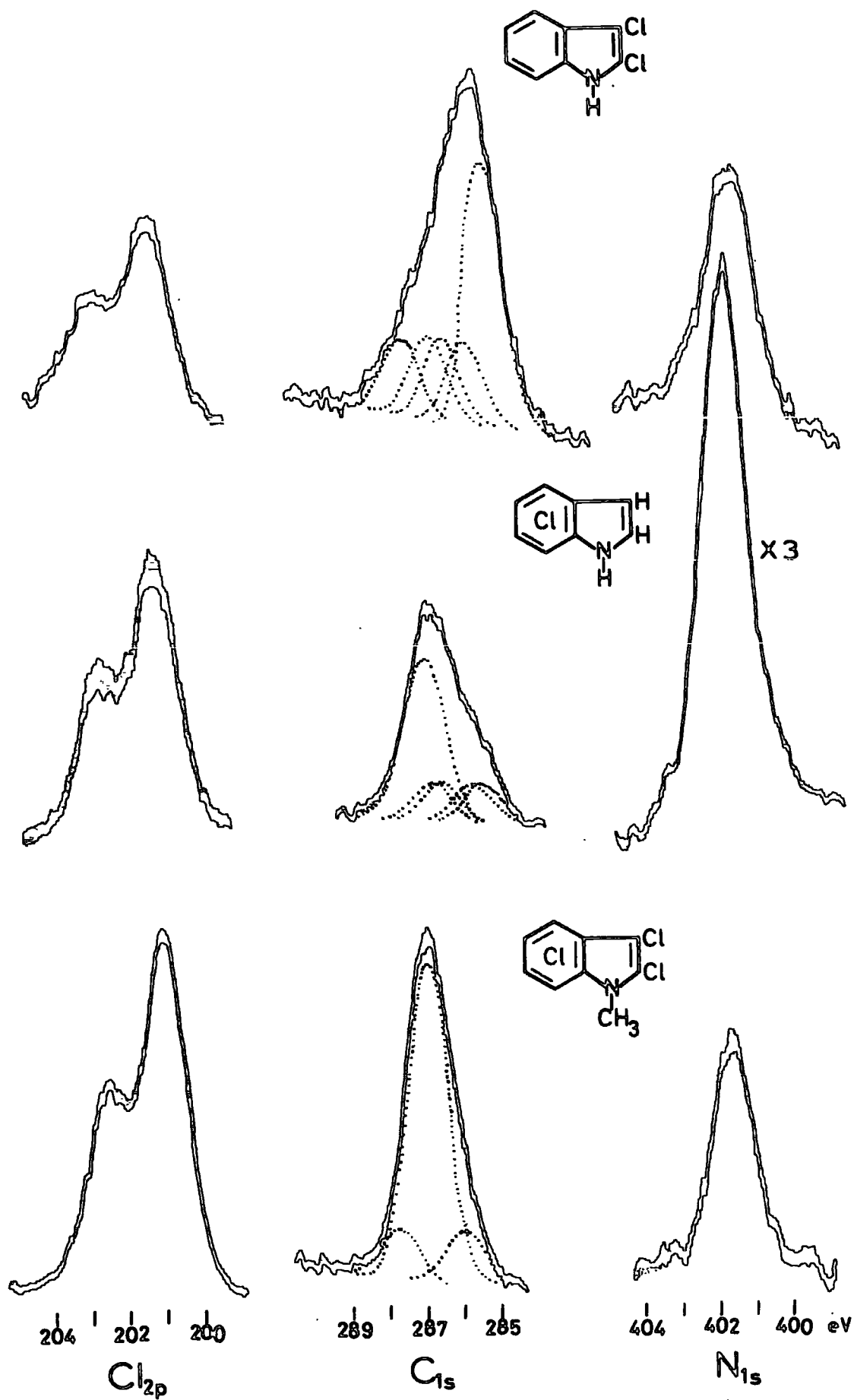


Fig. 4.15

Contd.

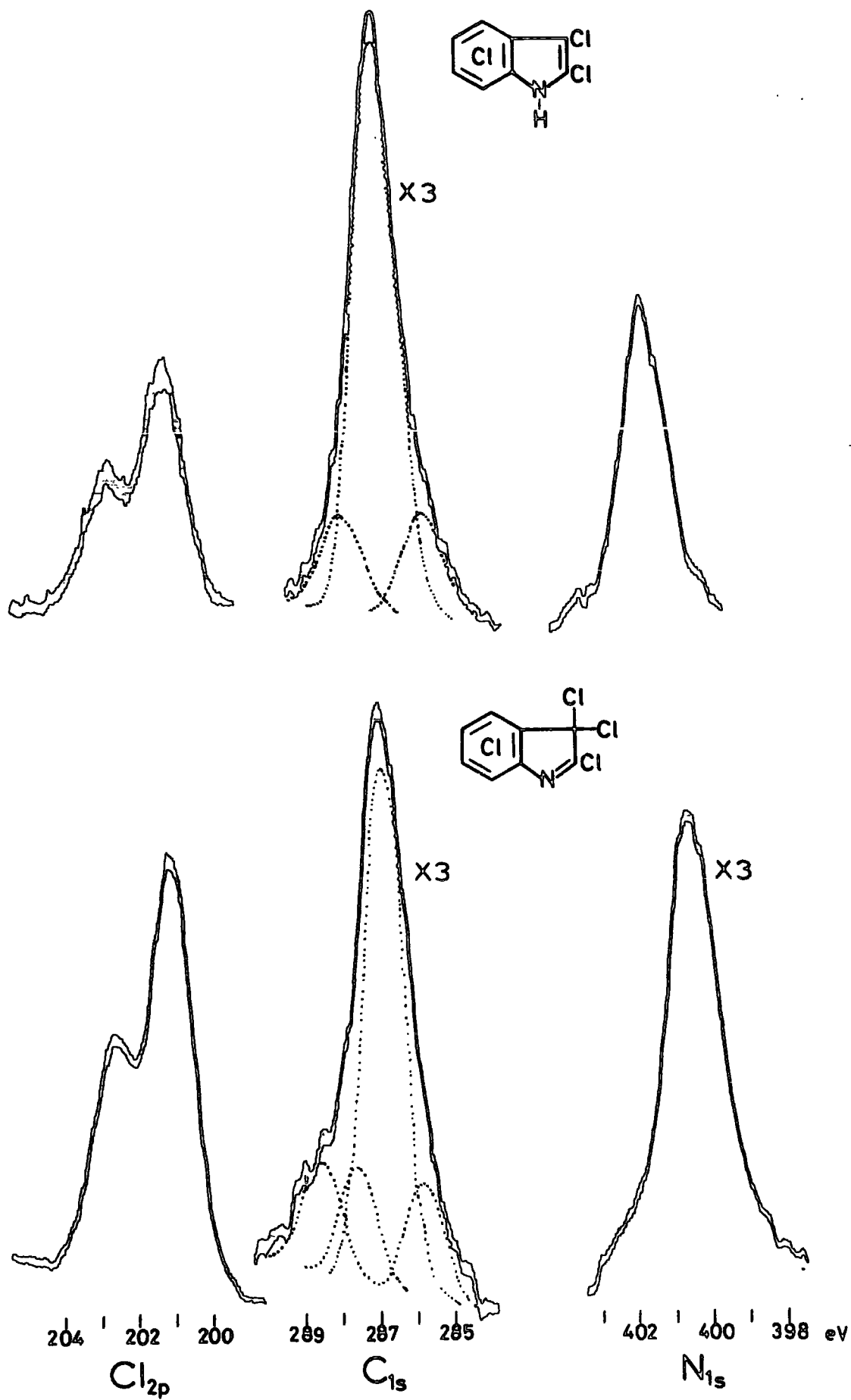


Fig. 4.15 contd.

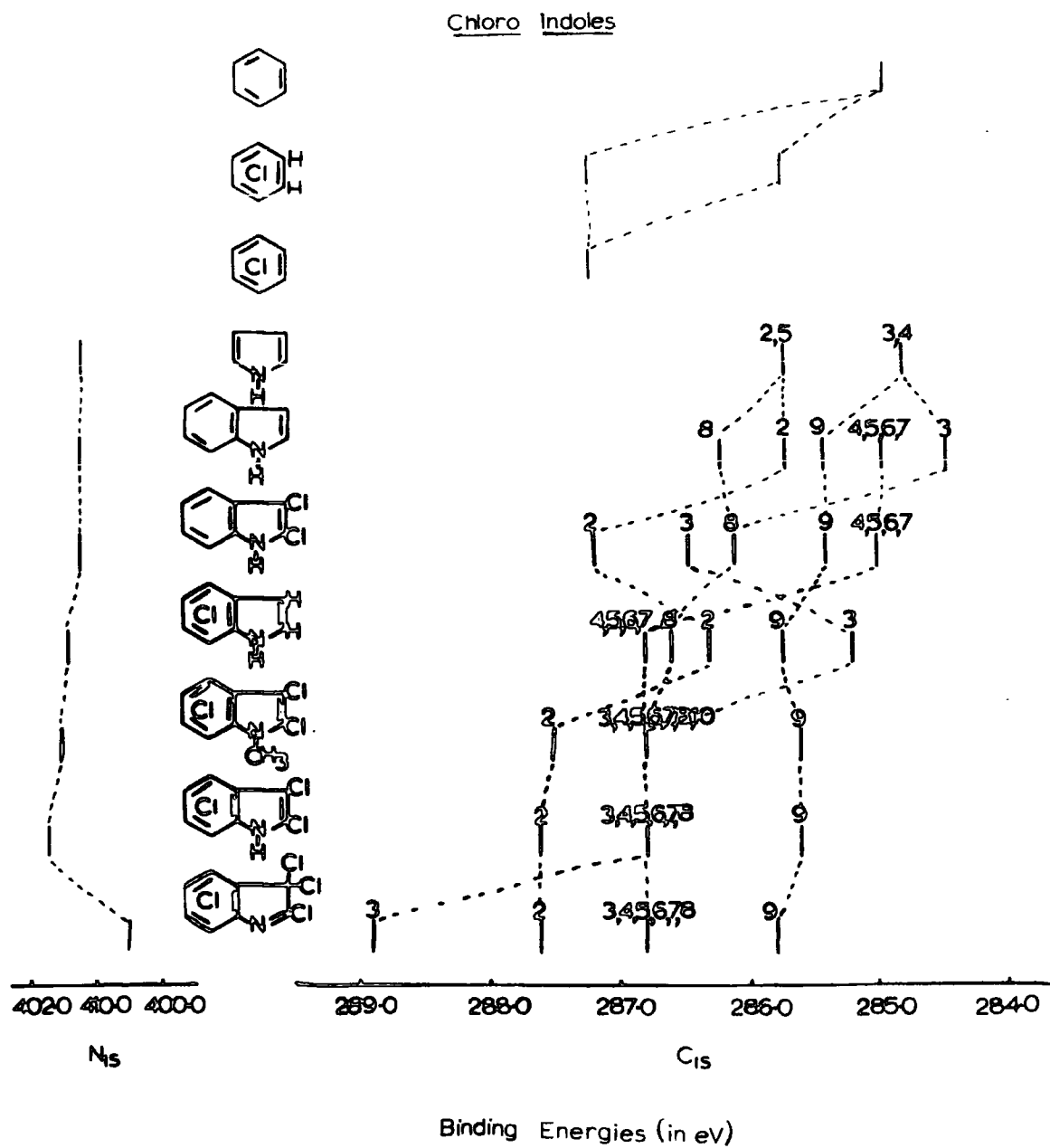
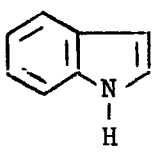
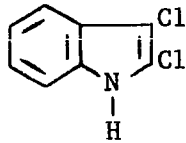
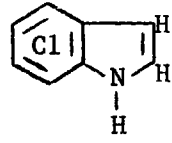
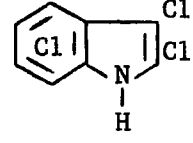


Fig. 4.16

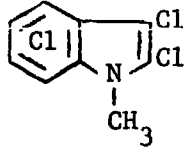
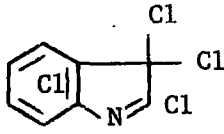
Table 4.17

Binding Energies,<sup>a</sup> CNDO/2 Charges and Madelung Potentials

Compound	Positions	B.E. (eV)	$q_i$	$\sum_{i \neq j} \frac{q_i}{r_{ij}}$
 (1)	1(N)	401.2	-0.147	2.50
	2	285.7	0.07	-1.05
	3	284.4	-0.067	0.79
	4	284.9	0.007	-0.15
	5	284.9	-0.009	-0.05
	6	284.9	0.009	-0.34
	7	284.9	-0.040	0.51
	8	286.2	0.081	-1.09
	9	285.4	0.020	-0.17
 (2)	1(N)	401.2	-0.177	3.62
	2	287.2	0.169	-1.68
	3	286.4	0.036	0.17
	4	285.0	0.012	0.27
	5	285.0	0.002	0.30
	6	285.0	0.012	0.12
	7	285.0	-0.029	0.87
	8	286.1	0.081	-0.51
	9	285.4	0.017	0.62
 (3)	1(N)	401.4	-0.147	3.29
	2	286.3	0.091	-0.60
	3	285.2	-0.066	1.58
	4	286.8	0.109	-0.18
	5	286.8	0.081	0.23
	6	286.8	0.082	0.12
	7	286.8	0.066	0.33
	8	286.6	0.072	0.28
	9	285.5	0.027	0.99
 (4)	1(N)	401.7	-0.161	4.13
	2	287.6	0.175	-1.09
	3	286.8	0.040	0.76
	4	286.8	0.114	0.09
	5	286.8	0.086	0.53
	6	286.8	0.090	0.39
	7	286.8	0.068	0.69
	8	286.8	0.075	0.68
	9	285.6	0.013	1.79

contd.

Table 4.17 contd.

Compound	Positions	B.E. (eV)	$q_i$	$\sum_{i \neq j} \frac{q_i}{r_{ij}}$
 (5)	1(N)	401.5	-0.139	2.96
	2	287.5	0.154	-1.04
	3	286.8	0.052	0.52
	4	286.8	0.123	0.07
	5	286.8	0.094	0.55
	6	286.8	0.097	0.37
	7	286.8	0.071	0.59
	8	286.8	0.056	0.75
	9	285.6	0.016	1.73
	10	286.8	0.075	-0.03
 (6)	1(N)	400.5	-0.203	3.36
	2	287.6	0.220	-1.23
	3	288.9	0.225	-0.59
	4	286.8	0.126	0.23
	5	286.8	0.085	0.78
	6	286.8	0.093	0.51
	7	286.8	0.081	0.49
	8	286.8	0.064	0.64
	9	285.8	-0.010	2.71

a. All Cl  $2p_{3/2}$  -201.0 eV

but C3 carries a negative charge in indole which is more readily removed by an electronegative substituent. In the benzo-[b]-thiophen series chlorine substitution in the five membered ring causes an increase in the  $S_{2p}$  binding energy whereas in the indoles there is very little change in the  $N_{1s}$  binding energy. The electronegative substituents withdraw charge from the most readily polarisable position ie. the sulphur atom in benzo-[b]-thiophens and C3 in the indoles.

Once the charge density at C3 has been removed by the substituents, further chlorination in going from (2) to the hexachloroindole(4) causes an increase in the  $N_{1s}$  binding energy of 0.5eV. This is the same as the shift in  $S_{2p_{3/2}}$  binding energy between 2,3-dichloro and perchlorobenzo-[b]-thiophen. In the case of both indole and benzo-[b]-thiophen complete chlorine substitution in the benzo ring alone has relatively little effect on the hetero atom core levels. The  $N_{1s}$  binding energy shift for 4,5,6,7-tetrachlorindole, relative to indole, is only 0.2eV.

The replacement of N-H by N-CH<sub>3</sub> in going from the hexachloroindole(4) to the N-methylhexachloroindole(5) has very little effect on the  $C_{1s}$  binding energies of the ring carbons. However, the  $N_{1s}$  level shows the decrease in binding energy expected when a more electron releasing group is attached to nitrogen.

In marked contrast to the other indoles in this series is the hepta-chloroindolenine(6). This system has similarities with both the benzo-[b]-thiophen S-dioxides and the indenenes (in fact it could

be classed as a 3-aza indene). The five membered ring is no longer aromatic but the major changes occur at C3 and C9. The introduction of a second chlorine atom at C3 causes an increase in the  $C_{1s}$  binding energy of 2.1eV [relative to C3 in the hexa-chloroindole(4)], whereas the introduction of the first chlorine at C3 in going from the tetrachloroindole(3) to the hexachloroindole(4) gave a shift of 1.6eV in the  $C_{1s}$  binding energy. The  $C_{1s}$  binding energy shift of C9 (0.2eV) is due to the large potential at C3 rather than an increased positive charge (see later). Neither C2 nor C8 are greatly affected by the change from the hexachloroindole(4) to the heptachloroindolenine. The electronegativity of the nitrogen atom is more important than the type of bonding as far as adjacent carbon atoms are concerned.

For the nitrogen atom of (6) the change is more drastic, causing a decrease in the  $N_{1s}$  binding energy of 1.2eV (relative to hexachloroindole). This can be simply explained by considering the change in bonding at the nitrogen atom. In the indole, the nitrogen atom can be considered approximately  $sp^2$  hybridised, with the nitrogen lone pair electrons located in a p-orbital at right angles to the plane of the molecule. This lone pair is an integral part of the aromatic  $\pi$ -system of the indole and is not essentially localised on the nitrogen atom. In the indolenine(6), the nitrogen can again be considered  $sp^2$  hybridised but now the lone pair is located in an  $sp^2$  hybrid orbital in the plane of the molecule. In this configuration it can not interact to any great extent with the  $\pi$ -system and is effectively localised

on the nitrogen atom. Therefore, the nitrogen atom in the indolenine has a greater electron density and correspondingly a lower binding energy.

The low binding energy of tertiary, compared to secondary, ring nitrogen atoms has also been observed in the five membered ring nitrogen heterocycles.<sup>173</sup> In pyrazole the  $N_{1s}$  level of the secondary nitrogen occurs at 402.4eV and the tertiary  $N_{1s}$  at 401.1eV, (a shift of 1.3eV). In imidazole the  $N_{1s}$  binding energy shift between the secondary and tertiary nitrogens is 1.6eV. This compares with the binding energy of the  $N_{1s}$  level in heptachloroindolenine(6) of 400.5eV.

The large binding energy difference between the  $N_{1s}$  levels of indoles and indolenines provides a basis for differentiation between these isomeric forms, especially when combined with the presence or absence of an  $sp^3$  type carbon atom at C3. That this can be distinguished from aromatic or olefinic carbons has been shown in the study of indene where the  $C_{1s}$  level of the  $CH_2$  carbon appears at higher binding energy along with the ring junction carbons.

b. Quantitative Discussion.

CNDO/2 charges and Madelung potentials are given in Table 4.17.

An inspection of the charges in the table shows that in N-methyl perchloroindole(5) the calculated charge on the nitrogen is actually less negative than the charge on the nitrogen of the hexachloroindole(4), while the measured  $N_{1s}$  binding energy of the N-methyl

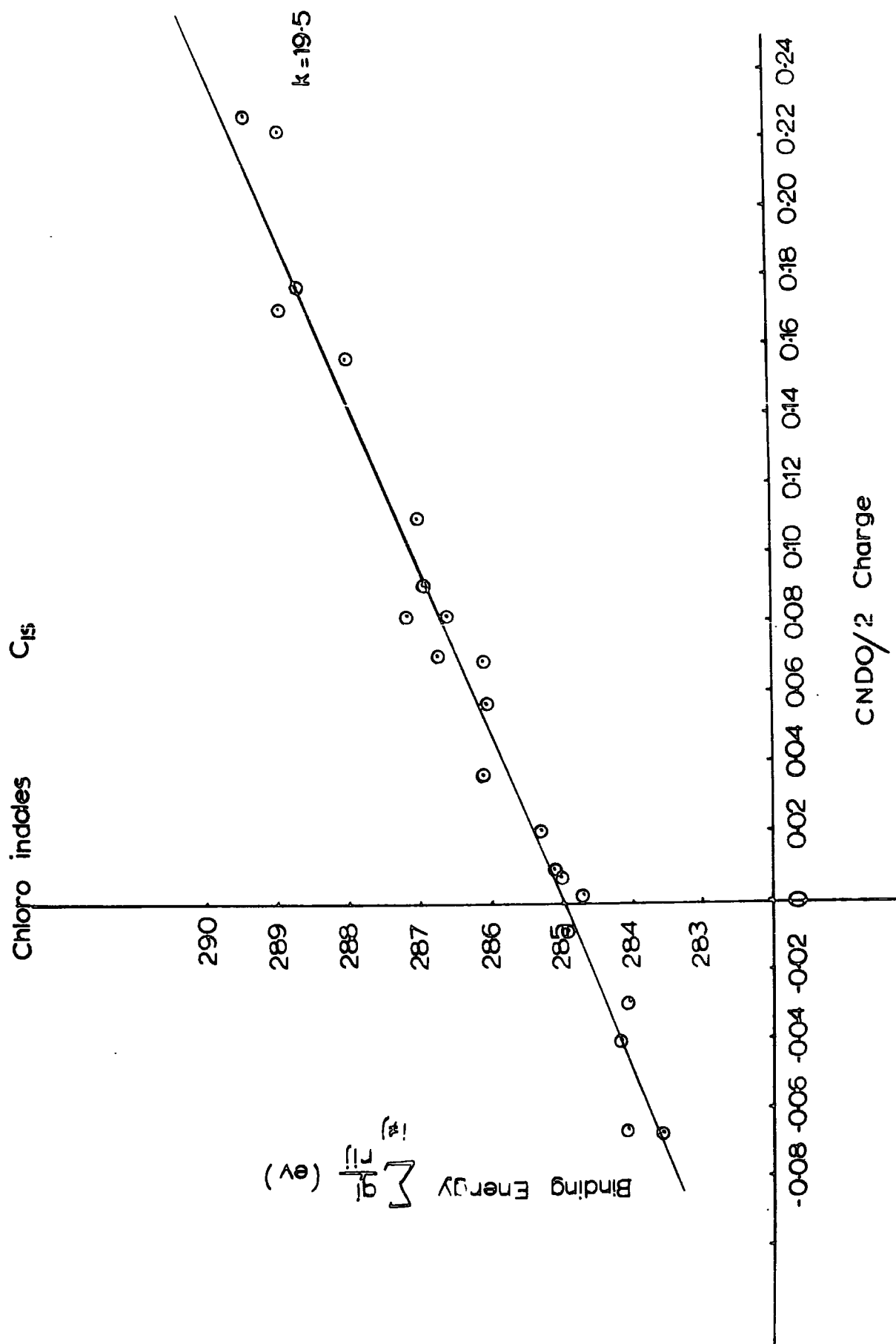


Fig. 4.17

derivative is lower than the hexachloroindole by 0.2eV. This is because the binding energy of a given core level is determined by both the charge and the potential at an atom. A similar effect is observed for the  $C_{1s}$  level of C9 in heptachloroindolenine and N-methylhexachloroindole where the Madelung term is again dominant.

For the nitrogen atoms in the hexachloroindole(4) and heptachloroindolenine(6) the CNDO calculations indicate a greater negative charge on the nitrogen in (6) in accord with its lower measured  $N_{1s}$  binding energy but the potential effect is still important in determining the magnitude of the calculated shift.

Fig. 4.17 shows a plot of binding energy corrected for Madelung potential against charge for the  $C_{1s}$  levels. A least squares treatment gives:

$$\text{for } C_{1s} \quad k = 19.5 \quad E^{\circ} = 284.5\text{eV}$$

with a correlation coefficient  $r^2 = 0.88$

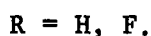
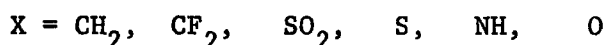
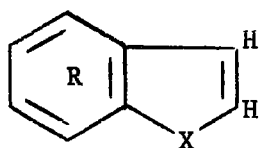
$$\text{for } N_{1s} \quad k = 22.7 \quad E^{\circ} = 401.63$$

with a correlation coefficient  $r^2 = 0.80$ .

The plots show considerable scatter, but as the  $N_{1s}$  correlation is only over six values a good least squares fit might not be expected. For the  $C_{1s}$  levels of both the chlorinated indoles and benzo-[b]-thiophens (see section C) the correlations are not as good as those obtained for either the parent heterocycles or the fluoro derivatives. This can be attributed to several factors. The binding energy range in both cases is small (2.0eV for chlorobenzo-[b]-thiophens and 4.0eV

for chloroindoles) and so is the charge range (0.16 and 0.29 respectively). This should be compared with an estimated experimental error of  $\pm 0.3\text{eV}$  between different samples. Sample charging, which has been eliminated as far as possible, and the use of unoptimised geometries for the CNDO/2 charge calculations may be factors contributing to the scatter. It is known that the CNDO SCF MO treatment of second row atoms is less adequate than for first row atoms and this will effect the calculated charge distributions in chlorine-containing molecules. This can be overcome by better parameterisation for the CNDO calculations involving second row atoms but the computational effort involved has not allowed a detailed examination of these factors in this work.

F. A Comparison of Hetero atom Effects on Molecular Core Binding Energies in the Series:

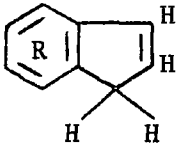
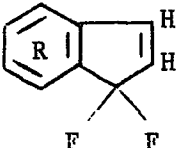
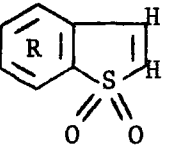
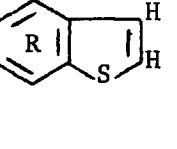


Introduction

Molecular core binding energies for members of this series have been discussed in previous sections. Here the effects of the group X are considered in relation to a fixed ring system. For this purpose the groups  $\text{CH}_2$ ,  $\text{CF}_2$  and  $\text{SO}_2$  may be considered as 'hetero atoms'.

TABLE 4.18

## Molecular Core Binding Energies (in eV)

	Position	R = H	R = F
	4,5,6,7	285.2	288.6
	8	285.6	286.8
	9	285.6	286.6
	3	285.2	286.0
	2	285.2	286.3
	1 (CH <sub>2</sub> )	285.6	286.0
		4,5,6,7	
8			287.0
9			287.2
3			287.0
2			286.4
1 (CF <sub>2</sub> )			291.4
		4,5,6,7	285.0
	8	285.5	286.1
	9	286.4	286.6
	3	285.8	286.1
	2	285.0	285.7
	1 (S <sub>2p<sub>1/2</sub></sub> )	169.1	169.4
	1 (S <sub>2p<sub>3/2</sub></sub> )	167.8	168.2
C <sub>1s</sub>	533.2	533.4	
	4,5,6,7	284.9	288.1
	8	285.5	286.3
	9	285.5	286.3
	3	284.9	285.6
	2	284.9	285.6
	1 (S <sub>2p<sub>1/2</sub></sub> )	165.2	165.8
	1 (S <sub>2p<sub>3/2</sub></sub> )	164.0	164.6

contd./

Table 4.18 contd.

	Position	R = H	R = F
	4,5,6,7	284.9	288.3
	8	286.2	286.7
	9	285.4	285.9
	3	284.4	285.2
	2	285.7	286.4
	1 (N <sub>1s</sub> )	401.2	401.7
	4,5,6,7	285.4	288.5
	8	287.2	287.4
	9	286.1	286.4
	3	284.7	285.7
	2	286.7	286.9
	1 (O <sub>1s</sub> )	535.6	535.7

### Discussion

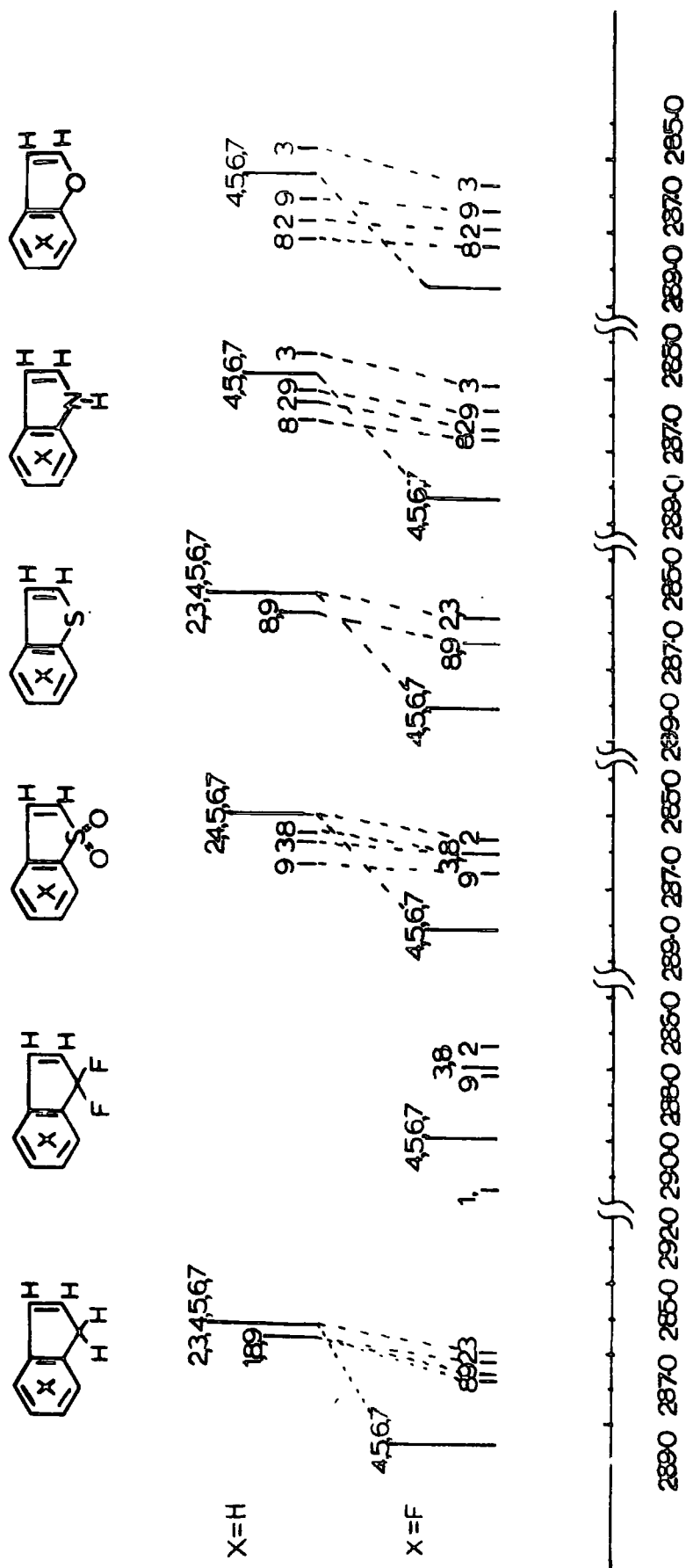
The measured molecular core binding energies for the series are given in Table 4.18 and shown schematically in Fig. 4.19.

CNDO charges and Madelung potentials are given in Table 4.19.

The effects of the group X can be partly understood in terms of a simple model considering only the electronegativity and  $I_{\pi}$  effects of the group. The groups appear to fall into a series in which the  $I_{\pi}$  effect varies from  $CF_2$  (strongly  $-I_{\pi}$ ) to O (strongly  $+I_{\pi}$ ).

Both  $CF_2$  and  $SO_2$  are highly polar groups carrying large positive charges on the carbon and sulphur atoms respectively. Yet compared to  $CH_2$  and S these groups have relatively little effect on the  $C_{1s}$  binding energies of adjacent carbon atoms (C2, C8). While both  $CF_2$  and  $SO_2$  attract  $\sigma$ -electron density away from adjacent carbon atoms this is to a great extent compensated for by the increased  $\pi$ -electron density at these positions (C2, C8) due to the  $-I_{\pi}$  effect of the groups. In these cases it is the  $\beta$ -carbon atoms (C3, C9) that experience a loss of electron density and consequent increase in  $C_{1s}$  binding energy. So that for  $CF_2$  and  $SO_2$  the  $I_{\pi}$  effect and electronegativity act in the same directions.

The groups S and  $CH_2$  would be expected to have little perturbing effect on the core binding energies of the ring carbon atoms, both having low electronegativities and both showing little or no  $I_{\pi}$  effects. This is certainly true for sulphur. In neither thiophens nor benzo-[b]-thiophens has a measurable shift been observed between



$C_{1s}$  Binding Energies (in eV)

Fig. 4.18

the  $C_{1s}$  binding energies of C2 and C3. The  $CH_2$  group may have a small  $I_\pi$  effect, as in the 4,5,6,7-tetrafluoroindene the  $C_{1s}$  level of C3 appears at 0.3eV lower than that of C2.

Considering the hetero atoms, sulphur, nitrogen and oxygen the electronegativities increase in the order  $S < N < O$  while the  $I_\pi$  effects are believed to be in the order  $S < O < N$ .<sup>110</sup> In these cases the two effects now act in opposite directions and this can readily be seen from the  $C_{1s}$  binding energies of the carbon atoms in the heterocyclic ring.

The core binding energies of carbons directly attached to the heteroatom (C2, C8) increase along the series  $S < N < O$  in the same order as the increase in electronegativity of the hetero atom. On the other hand, the  $C_{1s}$  binding energies of C3 decrease in the order  $S > O > N$ . This is the same as the order of increasing  $I_\pi$  effect. In benzo-[b]-furan the electronegativity of the hetero atom is greatest and this heterocycle shows the highest  $C_{1s}$  binding energy for C2 in the series (286.7eV). In indole the  $I_\pi$  effect of the hetero atom is greatest and indole shows the lowest measured  $C_{1s}$  binding for C3 in the series (284.4eV).

An inspection of the CNDO/2 charges and Madelung potentials in Table 4.19 shows that in most cases the potential terms are of major importance and, for the most highly polar or electronegative groups, are often dominant factors in determining the magnitude of binding energies for adjacent atoms. This means that shifts in core binding energies can not be predicted on the basis of simple considerations



of group polarities. The situation is more complex than might at first appear and assignments of molecular core binding energies made without reference to either calculations of the charge potential type or data from related systems should be treated with caution.

APPENDIX I

## Apparatus and Instrumentation

### Vacuum System

A conventional vacuum system incorporating a rotary oil pump and a mercury diffusion pump was used for handling volatile compounds, vacuum sublimation and vacuum pyrolysis.

Infrared Spectra were recorded on either a Grubb Parson Spectromaster or a Perkin Elmer 157 (sodium chloride) spectrometer.

Mass Spectra were measured with an A.E.I. MS9 spectrometer at an ionising beam energy of 70eV.

$^1\text{H}$  nmr Spectra were measured with a Varian A56/60 spectrometer, operating at 60.0MHz.  $^1\text{H}$  chemical shifts are measured on the  $\tau$  scale relative to tetramethyl silane used as an internal reference in either carbontetrachloride or acetone solutions.

Carbon and Hydrogen Analyses were carried out with a Perkin-Elmer 240 CHN Analyser.

Melting Points are uncorrected.

### Experimental.

#### 2,3,4,5,6,7-Hexachlorobenzo-[b]-thiophen(I)

This material was prepared by the method of Barger and Ewins.<sup>52</sup>  
In a typical experiment, dibromostyrene (1.5g), thionyl chloride (5.0ml)

and sulphuryl chloride (2.0ml) in a sealed Carius tube, were heated to 270° for 18hr. On cooling and opening the tube contained the product (0.7g), as needle crystals in a red liquid, which were filtered off. M.p. 156-157° [from light petroleum (b.p. 60-80°)] [lit. 158°]. [Found C, 28.36; Cl, 62.7; C<sub>8</sub>Cl<sub>6</sub>S requires C, 28.2; Cl, 62.5%] [M = 338 (base peak); 303 (P-Cl, 17.5%); 268 (P-2Cl, 30.5%); 233 (P-3Cl, 34.8%); 198 (P-4Cl, 65.0%)].

Attempted preparation of 6-methoxy, 2,3,4,5,7-Pentachlorobenzo-[b]-thiophen.

4-methoxy  $\alpha,\beta$ -dibromoethylbenzene (1.0g), thionyl chloride (5.0ml) and sulphuryl chloride (2.0ml), in a sealed Carius tube, were heated to 200°C for 18 hrs., poured into water, extracted with chloroform and the extracts washed with sodium bicarbonate solution and water. The dried (MgSO<sub>4</sub>) extracts from three such reactions were evaporated to give the crude product containing two components, which were separated by chromatography on silica [light petroleum (b.p. 40-60°) as eluant]. The first component (1.046g) was Hexachlorobenzo-[b]-thiophen m.p. 156-157°, identified by I.R. spectroscopy. The second component was pentachlorostyrene (1.226g) mp. 109-109.5° (from methanol) (lit m.p. 108°). [Found Cl, 63.7; C<sub>8</sub>H<sub>3</sub>Cl<sub>5</sub> requires Cl, 64.1%]  
 $\tau$  (CDCl<sub>3</sub>) 2.50 (doublet), 2.05 (doublet of doublets) [ $J_{\text{Trans}} = 8.6\text{Hz}$  vicinal vinyl protons] 1.85 (doublet,  $J_{\text{cis}} = 2.4\text{Hz}$  vicinal vinyl protons).  
 [M = 274].

3,4,5,6,7-Pentachlorobenzo[b]thiophen

(a) From the 2-lithio derivatives Hexachlorobenzo-[b]-thiophen(I) (1.04g.) in dry tetrahydrofuran (100ml.) was treated at -70° with

n-butyl-lithium in hexane (1.6 ml., 2.0N) and the mixture stirred for 1 hr. The temperature was allowed to rise to 0° and aqueous tetrahydrofuran (20ml., 50% v/v) added. The mixture was acidified with hydrochloric acid (100ml., 2N), extracted with ether and the dried (MgSO<sub>4</sub>) extracts evaporated. Two components were present which were separated by chromatography on silica [light petroleum (b.p. 60-80°) as eluant]. The first component (0.404g.) was unreacted starting material (I), identified by I.R. spectroscopy. The second component (0.52g.) was 3,4,5,6,7-pentachloro-benzo[b]thiophen m.p. 212-213° (from methanol) (Found: C, 31.2; H, 0.5; C<sub>8</sub>HCl<sub>5</sub>S requires C, 31.4; H, 0.3%). The <sup>1</sup>H n.m.r. spectrum showed a sharp singlet at τ 2.60 (in CCl<sub>4</sub>) and at τ 2.02 (in acetone). [M = 304 (base peak); 269 (P-Cl, 29%); 234 (P-2Cl, 35%)].

(b) From compound (I) and lithium aluminium hydride - compound (I) (0.5g.) and lithium aluminium hydride in tetrahydrofuran (20ml., 0.076M) were stirred under nitrogen at room temperature for 48hr. The mixture was treated with water (50ml.), extracted with ether and the dried (MgSO<sub>4</sub>) extracts evaporated. Two components were present which were separated by chromatography on silica [light petroleum (b.p. 60-80°) as eluant]. The first component (0.212g.) was unreacted starting material (I), identified by I.R. spectroscopy. The second component (0.189g.) was 3,4,5,6,7-pentachlorobenzo-[b]-thiophen m.p. 212-213° identified by I.R. spectroscopy.

3,4,5,7-Tetrachlorobenzo[b]thiophen

(a) From a dilithio derivative - (i) Hexachlorobenzo-[b]-thiophen (1.0g.) in dry tetrahydrofuran (150ml.) was treated at  $-70^{\circ}$  with n-buty-lithium in hexane (10ml., 2.0N). The mixture was stirred at  $-15$  to  $-20^{\circ}$  for 1 hr., water (50 ml.) was added and the mixture extracted with ether and worked up as before. Two components were present which were separated by chromatography on silica (light petroleum [b.p.  $60-80^{\circ}$ ] as eluant). The first component was 3,4,5,7-tetrachlorobenzo[b]thiophen (0.713g.), m.p.  $146-147^{\circ}$  [from light petroleum (b.p.  $60-80^{\circ}$ )]. (Found: C, 35.2; H, 1.0;  $C_8H_2Cl_4S$  requires C, 35.3; H, 0.7%). The  $^1H$  n.m.r. showed two doublets  $J_{2,6}$  (0.6 Hz) at  $\tau$  2.60 (due to H-2) and at  $\tau$  2.54 (due to H-6) (in  $CCl_4$ ); and at  $\tau$  2.04 (due to H-2) and at  $\tau$  2.29 (due to H-6) (in acetone) [M = 270 (base peak); 235 (P-Cl, 23%)]. The second component, a yellow oil, was not identified.

(ii) The dilithio derivative was prepared as above in dry tetrahydrofuran. Dry carbon dioxide was passed through the solution for 1hr. during which time the reaction reached room temperature. The mixture was acidified (25ml. 2NHC1), extracted with ether and the dried ( $MgSO_4$ ) extracts evaporated to give the crude product which was leached with chloroform to remove unreacted starting material. The 3,4,5,7-tetrachlorobenzo-[b]-thiophen-2,6-dicarboxylic acid [M = 358] was not characterised but was heated under reflux with copper powder (0.6g) and quinoline (25ml) for 1 hr. The mixture was poured into sulphuric acid (100ml, 50% u/v), extracted with ether and the dried

(MgSO<sub>4</sub>) extracts evaporated to give the crude product. Chromatography on silica [light petroleum (b.p. 60-80°) as eluant] gave 3,4,5,7-tetrachlorobenzo-[b]-thiophen, identified by I.R. spectroscopy.

(b) From a Grignard reagent - Compound (I) (0.55g.) and magnesium (0.6g.) in dry tetrahydrofuran (20ml.) were treated with ethylene dibromide (0.25ml.). After the initial reaction had subsided, the mixture was stirred at room temperature for 3hr. and then heated under reflux for a further 1hr. during which time ethylene dibromide (10 ml.) was added. The mixture was treated with water (50ml.), extracted with ether, and the dried (MgSO<sub>4</sub>) extracts evaporated to give a brown oil which crystallised on standing.

Recrystallisation of the crude product from light petroleum (b.p. 40-60°) gave 3,4,5,7-tetrachlorobenzo-[b]-thiophen (0.04g.) identified by I.R. Spectroscopy.

Reaction of compound (I) (0.98g.) with magnesium (0.45g.) in dry tetrahydrofuran (40ml.) at room temperature for 0.5 hr. with activation of the metal by ethylene dibromide (0.2ml.), followed by hydrolysis gave a product containing three components which were partially separated by chromatography on silica [light petroleum (b.p. 60-80°) as eluant]. The first component was unreacted starting material (I) (0.283g.), identified by I.R. spectroscopy, while the second and third components could not be separated on the preparative scale. This material (0.48g.) was shown by <sup>1</sup>H n.m.r. spectroscopy to be an

equimolar mixture of 3,4,5,6,7-pentachlorobenzo[b]thiophen and 3,4,5,7-tetrachlorobenzo-[b]-thiophen [In  $\text{CCl}_4$ , the absorptions at  $\tau$  2.6 and  $\tau$  2.54 were in the ratio 2:1; in acetone, the absorptions at  $\tau$  2.29 and  $\tau$  2.04 were in the ratio 1:2], from which 3,4,5,6,7-pentachlorobenzo-[b]-thiophen could be separated by fractional recrystallisation.

A mono-isopropoxy-pentachlorobenzo[b]thiophen.

A mixture of hexachlorobenzo-[b]-thiophen(I) (0.51g.), sodium isopropoxide (0.6g.) and dry pyridine (100ml.) was heated under reflux under nitrogen for 3hr. The mixture was diluted with water, extracted with ether and the extracts washed with excess hydrochloric acid (5N). The extracts were dried ( $\text{MgSO}_4$ ) and evaporated, and the two components present were separated by chromatography on silica [light petroleum (b.p. 60-80°) as eluant]. The first component (0.115g.) was identified as unreacted starting material (I) by I.R. spectroscopy. The second component (0.35g.) was mono-isopropoxypentachlorobenzo[b]-thiophen, m.p. 100-100.5° [from light petroleum (b.p. 40-60°)] (Found: C, 36.1; H, 2.3;  $\text{C}_{11}\text{H}_7\text{Cl}_5\text{OS}$  requires C, 36.3; H, 1.9%). [M = 362 (15%), 320 (P- $\text{CH}_3\text{CH}=\text{CH}_2$ , base peak)].

A monochloro-monothiophenoxy-4,5,6,7-tetrachlorobenzo-[b]-thiophen

Thiophenol (0.39g.) in dry pyridine (20ml.) was treated with sodium hydride (0.1g.) and the filtered solution was added dropwise to a solution of hexachlorobenzo-[b]-thiophen(I) (1.01g.) in dry pyridine (50ml.). The mixture was heated under reflux for 48hr., and

worked up as in the previous experiment. Two components were present which were separated by chromatography on silica. The first component was unreacted starting material (I) (0.05g.) identified by I.R. spectroscopy and the second component (0.50g.) was a monochloromonothiophenoxy-4,5,6,7-tetrachlorobenzo[b]thiophen m.p. 146-147° [from light petroleum (b.p. 60-80°)] (Found: C, 40.3; H, 1.2; Cl, 43.3;  $C_{14}H_5Cl_5S_2$  requires C, 40.6; H, 1.2; Cl, 42.8%). [M = 412 (base peak); 377 (P-Cl, 37%)].

A dichloro-tetrathiomethoxybenzo-[b]-thiophen

Hexachlorobenzo-[b]-thiophen(I) (0.499g), sodium thiomethoxide in methanol (6.5ml, 1.0M) and dry pyridine (40ml) were heated under reflux for 6hrs. and worked up as above. Chromatography on silica [carbon tetrachloride/10% chloroform as eluant] gave the crude product (0.3g) which was sublimed (120°/0.01mmHg) to give a dichloro-tetrathiomethoxy benzo-[b]-thiophen m.p 121-122° [from light petroleum (b.p.60-80°)] [Found C, 37.49; H, 3.06;  $C_{12}H_{12}Cl_2S_5$  requires C, 37.2; H, 3.21%]. The  $^1H$  n.m.r. spectrum showed four absorptions at  $\tau$  0.755,  $\tau$  0.749,  $\tau$  0.742, and  $\tau$  0.733. [M = 386 (base peak); 371 (P-CH<sub>3</sub>, 20%); 356 (P-2CH<sub>3</sub>, 8%); 341 (P-3CH<sub>3</sub>, 6%)].

2,3,4,5,6,7-Hexachlorobenzo[b]thiophen-1,1-dioxide

Hexachlorobenzo-[b]-thiophen(I) (0.86g.) in carbon tetrachloride (50ml.) was added to a stirred solution of trifluoroacetic anhydride (10 ml.) and hydrogen peroxide (5 ml., 90%) in carbon tetrachloride

(50 ml.) at room temperature. The mixture was heated under reflux for 5 hr., diluted with water and the organic layer separated, dried ( $\text{MgSO}_4$ ) and evaporated to give 2,3,4,5,6,7-hexachlorobenzo[b]-thiophen-1,1-dioxide (0.8g.) m.p. 166-167° [from light petroleum (b.p. 60-80°)]. (Found: C, 25.7; Cl, 56.7; S, 8.6.  $\text{C}_8\text{Cl}_6\text{SO}_2$  requires C, 25.8; Cl, 57.0; S, 8.6%). [M = 370 (73%); 306 (P-SO<sub>2</sub>, base peak)].

#### Pyrolysis of Hexachlorobenzo-[b]-thiophen-1,1-dioxide

The dioxide (0.035g.) was slowly sublimed at  $10^{-2}$  mm. into a quartz pyrolysis tube packed with silica wool and heated to 840°. Volatile material from the tube was collected in a liquid nitrogen trap and chromatographed on silica [light petroleum (b.p. 60-80°) as eluant] to give hexachlorophenylacetylene (0.033g.) m.p. 137-138°, identified by I.R. spectroscopy.

#### Diethyl 4,5,6,7-tetrachlorobenzo[b]thiophen-2,3-dicarboxylate

Pentachlorothiophenol (6.3g.) in dry tetrahydrofuran (200 ml.) was treated with sodium hydride (0.55g.) and after the initial reaction had ceased, diethyl acetylenedicarboxylate (4.5g.) in dry tetrahydrofuran (20 ml.) was added and the mixture was heated under reflux for 18 hr. The solution was treated with hydrochloric acid (100ml., 4N), extracted with ether and the dried ( $\text{MgSO}_4$ ) extracts evaporated. The major component in the product separated by chromatography on silica (carbon tetrachloride followed by chloroform as eluants) was diethyl-4,5,6,7-tetrachlorobenzo[b]thiophen-2,3-dicarboxylate (7.1g.) m.p. 119-120°

[from light petroleum (b.p. 60-80°)] (Found: C, 40.6; H, 2.4;

Cl, 34.6;  $C_{14}H_{10}Cl_4O_4S$  requires C, 40.3; H, 2.5; Cl, 34.9%).

[M = 414 (61%); 399 (P-CH<sub>3</sub>, 6.4%); 386 (P-C<sub>2</sub>H<sub>4</sub>, 9.5%); 369 (P-C<sub>2</sub>H<sub>5</sub>O, 32%); 341 (P-C<sub>2</sub>H<sub>5</sub>OCO, base peak)].

Treatment of pentachlorothiophenol (10.0g.) in dry tetrahydrofuran (300 ml.) with sodium hydride (0.8g.) followed by reaction with diethyl acetylenedicarboxylate (6.4g.) in tetrahydrofuran (20ml.) at reflux temperature for 3hr. gave, after working the mixture up as before, a crude product (9.3g.) which was separated by chromatography on silica (benzene as eluant) into two components. The first component was the above diester (1.2g.), identified by I.R. spectroscopy, and the second component was trans-diethyl-1-pentachlorothiophenoxybutenedioic acid (6.7g.), m.p. 125-127°

[from light petroleum (b.p. 60-80°)] (Found: C, 36.9; H, 2.4; Cl, 38.8;

S, 7.4;  $C_{14}H_{11}Cl_5O_4S$  requires C, 37.1; H, 2.5; Cl, 39.2; S, 7.1%).

[M = 450 (base peak); 415 (P-Cl, 86%); 405 (P-C<sub>2</sub>H<sub>5</sub>O, 28%); 387 (P-C<sub>2</sub>H<sub>4</sub>Cl, 71%); 377 (P-C<sub>2</sub>H<sub>5</sub>OCO, 35%)].

Cis-ethyl β-pentachlorophenylthioacrylate.

Pentachlorothiophenol (3.0g) in dry tetrahydrofuran (80ml) was treated with sodium hydride (0.5g) followed by ethyl propiolate (1.0g) in dry tetrahydrofuran (20ml.) and the mixture heated under reflux for 0.5hr. and worked up as above to give the crude product (3.4g). A portion of this (1.1g) was chromatographed on silica

[carbon tetrachloride followed by benzene as eluants] to give cis-ethyl  $\beta$ -pentachlorophenylthioacrylate (0.6g) m.p. 167-168° [from light petroleum (b.p. 80-100°)] [Found C, 34.48; H, 1.59;  $C_{11}H_7Cl_5O_2S$  requires C, 34.72; H, 1.86%]. [M = 378 (75%); 333 (P-C<sub>2</sub>H<sub>5</sub>O, 70%); 245 (P-SCH=CH-CO<sub>2</sub>C<sub>2</sub>H<sub>5</sub>, base peak)].

Ethyl 4,5,6,7-tetrachlorobenzo-[b]-thiophen-2-carboxylate

Diethyl 4,5,6,7-tetrachlorobenzo-[b]-thiophen-2,3-dicarboxylate (0.5g), sodium ethoxide (0.1g) and dry pyridine (50ml) were heated under reflux for 24hr., poured into sulphuric acid (100ml., 50% u/v) and extracted with ether. The extracts were washed with further sulphuric acid and finally washed with water. Evaporation of the dried (MgSO<sub>4</sub>) extracts gave the crude solid (0.49g). Two components were present which were separated by chromatography on silica [benzene as eluant]. The first component was unchanged starting material (0.11g) identified by I.R. spectroscopy. The second component was ethyl 4,5,6,7-tetrachlorobenzo-[b]-thiophen-2-carboxylate (0.26g) m.p. 109-110° [from light petroleum (b.p. 60-80°)] [Found C, 38.49; H, 1.88; Cl, 41.8; S, 9.7;  $C_{11}H_6Cl_4O_2S$  requires C, 38.40; H, 1.76; Cl, 41.23; S, 9.23%]. The <sup>1</sup>H n.m.r. spectrum in CCl<sub>4</sub> showed a triplet  $\tau$  9.6 (methyl protons), quartet  $\tau$  5.6 (methylene) [J = 7Hz] and a singlet  $\tau$  2.04 [ $\tau$  1.77 (acetone)]. [M = 341 (45%); 312 (P-C<sub>2</sub>H<sub>5</sub>, 26%); 296 (P-C<sub>2</sub>H<sub>5</sub>O, base peak); 268 (P-C<sub>2</sub>H<sub>5</sub>OCO, 20%)].

4,5,6,7-Tetrachlorobenzo[b]thiophen-2,3-dicarboxylic acid dihydrate.

Diethyl 4,5,6,7-tetrachlorobenzo-[b]-thiophen-2,3-dicarboxylate (0.5g.) was heated under reflux with sulphuric acid (40ml., 50% v/v) for 7.5hr. The mixture was diluted with water, extracted with ether, and the dried ( $\text{MgSO}_4$ ) extracts evaporated. The crude residue (0.41g) was leached with boiling benzene, and the impure product which did not dissolve was recrystallised from water to give 4,5,6,7-tetrachlorobenzo[b]thiophen-2,3-dicarboxylic acid dihydrate m.p.  $280^\circ$  (decomp.) (Found: C, 30.2; H, 1.2;  $\text{C}_{10}\text{H}_6\text{Cl}_4\text{O}_6\text{S}$  requires C, 30.3; H, 1.5%).

4,5,6,7-Tetrachlorobenzo[b]thiophen.

(a) From 4,5,6,7-tetrachlorobenzo[b]thiophen-2,3-dicarboxylic acid dihydrate. The above diacid (0.9g.), copper powder (1.0g.) and quinoline (60ml.) were heated under reflux for 1hr. The mixture was acidified with sulphuric acid (200ml., 50% v/v) extracted with ether and the extracts washed with further sulphuric acid (50% v/v), dried ( $\text{MgSO}_4$ ) and evaporated. The crude red oil which remained (0.79g.) was chromatographed on silica [light petroleum (b.p.  $60-80^\circ$ ) as eluant] to give 4,5,6,7-tetrachlorobenzo[b]thiophen (0.32g.) m.p.  $209-211^\circ$  [from light petroleum, (b.p.  $60-80^\circ$ )] (Found: C, 35.1; H, 0.7;  $\text{C}_8\text{H}_2\text{Cl}_4\text{S}$  requires C, 35.3; H, 0.7%). The  $^1\text{H}$  n.m.r. spectrum in  $\text{CCl}_4$  was a distorted AB spectrum with H-2 at  $2.46\tau$  and H-3 at  $2.56\tau$  ( $J_{2,3}$  5.6Hz). In acetone, the chemical shifts were: H-2,  $1.96\tau$ ; H-3,  $2.38\tau$  ( $J_{2,3}$  5.6Hz). [M = 270 (90%); 235 (P-Cl, base peak); 200 (P-2Cl, 20%); 165 (P-3Cl, 20%)].

(b) From 2,3,4,5,6,7-hexachlorobenzo[b]thiophen(I) - A mixture of compound (I) (0.2g.), the catalyst (0.15g., 10% Pd on Charcoal) potassium hydroxide (0.2g.) and methanol (40 ml.) was shaken in an atmosphere of hydrogen at room temperature and atmospheric pressure until 30ml. of hydrogen had been absorbed. The solution was filtered, diluted with water, extracted with ether and the dried ( $\text{MgSO}_4$ ) extracts evaporated to give 4,5,6,7-tetrachlorobenzo-[b]-thiophen (0.157g.) m.p. 210-211<sup>o</sup>, identified by I.R. spectroscopy.

(c) From 3,4,5,6,7-pentachlorobenzo[b]thiophen - a mixture of this compound (0.12g.), the catalyst (0.1g., 10% Pd on C), potassium hydroxide (0.2g.) and methanol (20 ml.) was shaken with hydrogen at room temperature and atmospheric pressure until 8 ml. of hydrogen had been absorbed. The mixture was worked up as before to give 4,5,6,7-tetrachlorobenzo-[b]-thiophen (0.105g.) m.p. 210-211<sup>o</sup>, identified by I.R. spectroscopy.

(d) From the monochloro monothiophenoxy-4,5,6,7-tetrachlorobenzo[b]-thiophen - a mixture of this compound (0.46g.), the catalyst (0.9g., 10% Pd-C), potassium hydroxide (0.3g.) and methanol (40ml.) was shaken with hydrogen at room temperature and atmospheric pressure for 8hr. and the solution was worked up as before. Two components were present which were separated by chromatography on silica [light petroleum (b.p. 40-60<sup>o</sup>) as eluant]. The first component was unreacted starting material (0.146g.), identified by I.R. spectroscopy and the second

component was 4,5,6,7-tetrachlorobenzo-[b]-thiophen (0.236g.)  
m.p. 210-211° identified by I.R. spectroscopy.

Reactions of 4,5,6,7-Tetrachlorobenzo-[b]-thiophen.

a. Sodium thiophenoxide

Sodium thiophenoxide in dry pyridine (10ml., 0.01M) was added to 4,5,6,7-tetrachlorobenzo[b]thiophen (0.25g.) in dry pyridine (40ml.) and the mixture heated under reflux for 4hr., poured into water, extracted with ether and the extracts washed with hydrochloric acid (50% v/v) and water. Evaporation of the dried ( $\text{MgSO}_4$ ) extracts gave a crude yellow solid (0.442g) shown to contain three components which were separated by chromatography on silica.

The first two components [light petroleum (b.p. 60-80°)/carbon tetrachloride (75/25 v/v) as eluant] were unreacted starting material (0.14g.) identified by I.R. spectroscopy and the major product (0.115g) a dichloro-di(thiophenoxy)benzo-[b]-thiophen m.p. 159.5-160° [from light petroleum (b.p. 80-100°)] [Found C, 56.98; H, 2.6;  $\text{C}_{20}\text{H}_{12}\text{Cl}_2\text{S}_3$  requires C, 57.28; H, 2.9%] [M = 418 (27%); 310 (36%); 277 (P-PhS, base peak)].

The third component (carbon tetrachloride as eluant) was a monothiophenoxy trichlorobenzo-[b]-thiophen (0.025g.) identified by Mass Spectroscopy [M = 343.900,  $\text{C}_{14}\text{H}_7\text{Cl}_3\text{S}_2$  requires 343.905].

b. Sodium thiomethoxide.

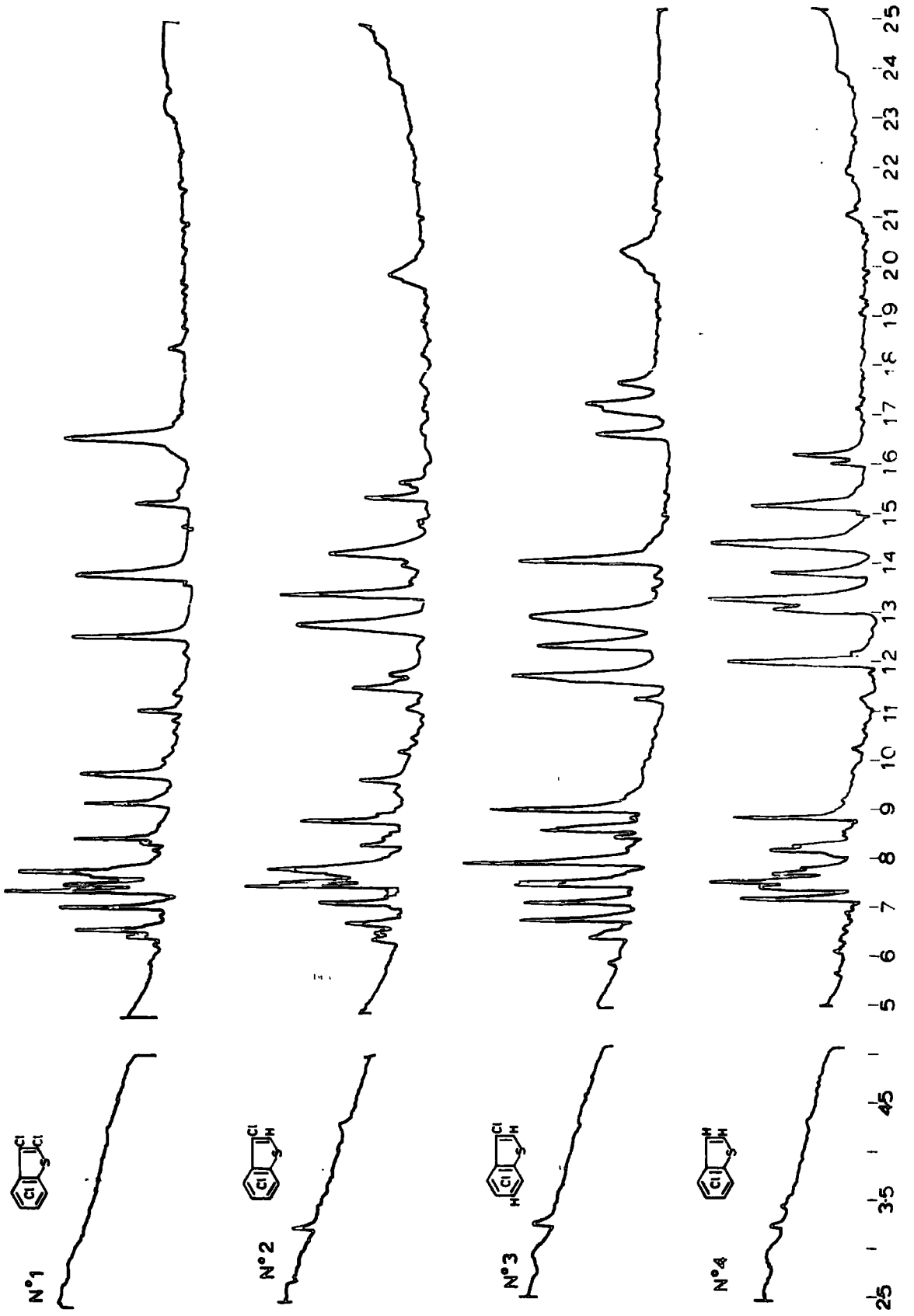
i. Room Temperature - Sodium thiomethoxide in methanol

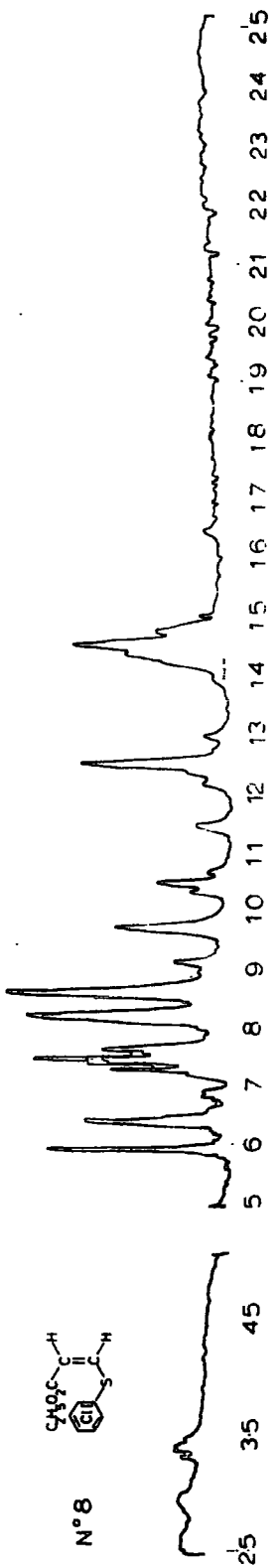
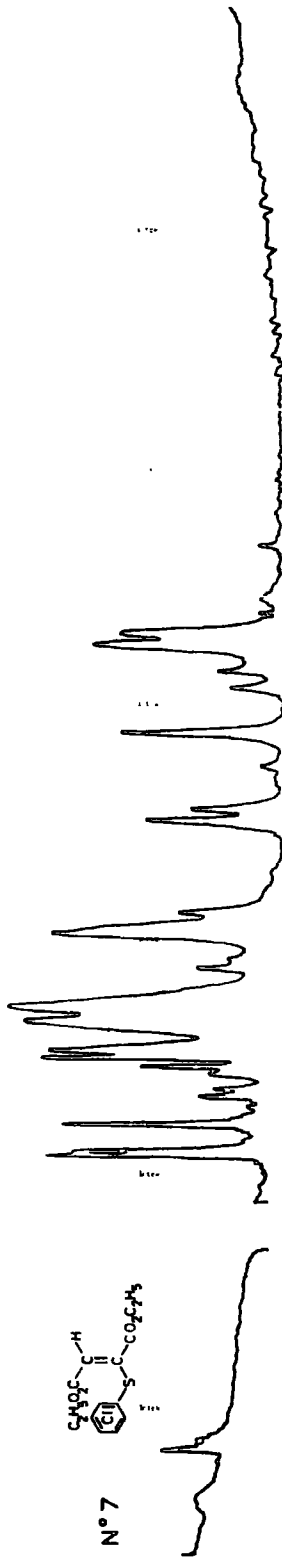
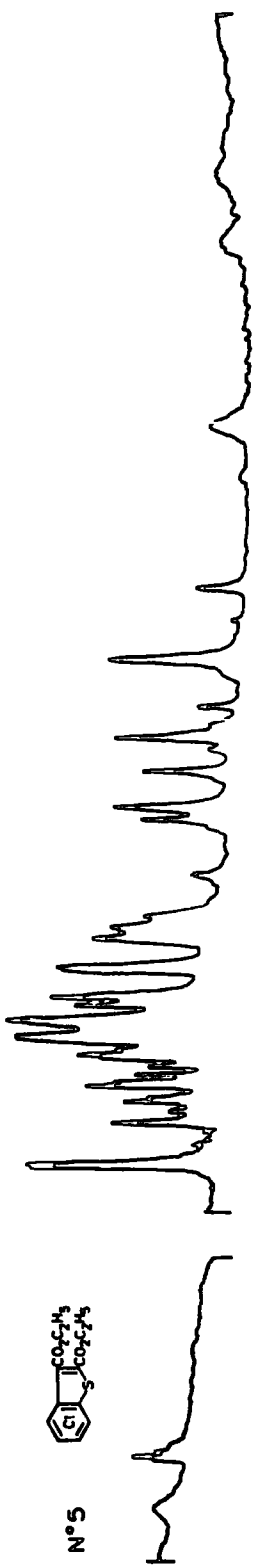
(9.9ml., 0.23M), 4,5,6,7-tetrachlorobenzo-[b]-thiophen (0.605g) and dry pyridine (40ml.) were stirred at room temperature for 18hr., and worked up as above. Evaporation of the dried ( $\text{MgSO}_4$ ) extracts gave the crude product shown to contain three components which were separated by chromatography on silica [light petroleum (b.p. 60-80°) as eluant]. The first component (0.22g) was unreacted starting material identified by I.R. spectroscopy, the second component (0.06g) was an impure oil shown to contain as the major component a mono(thiomethoxy)trichlorobenzo-[b]-thiophen by Mass Spectroscopy [M = 281.887;  $\text{C}_9\text{H}_5\text{Cl}_3\text{S}_2$  requires M = 281.889]. The third component (0.31g) was a dichloro-di(thiomethoxy)benzo-[b]-thiophen m.p. 127-128° (from methanol) [Found C, 40.86; H, 3.06;  $\text{C}_{10}\text{H}_8\text{Cl}_2\text{S}_3$  requires C, 40.68; H, 2.73%] [M = 294 (base peak); 279 (P- $\text{CH}_3$ , 60%); 264 (P- $2\text{CH}_3$ , 10%)].

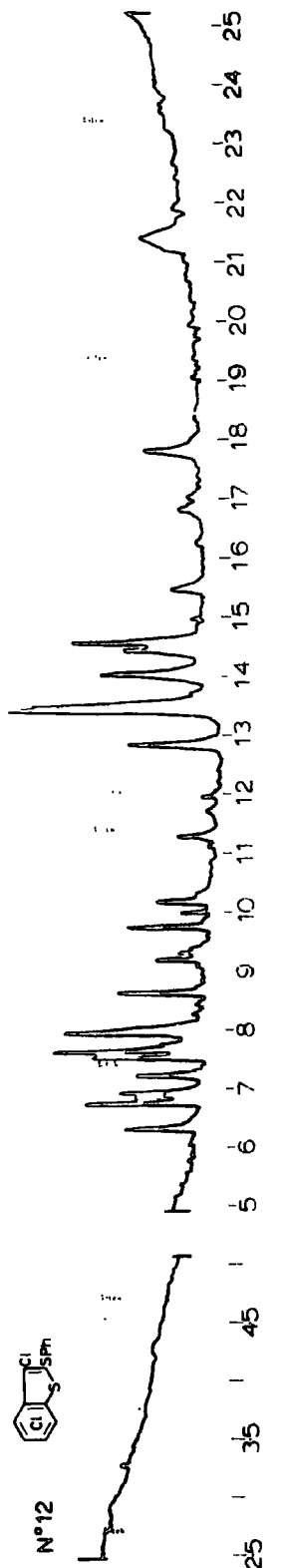
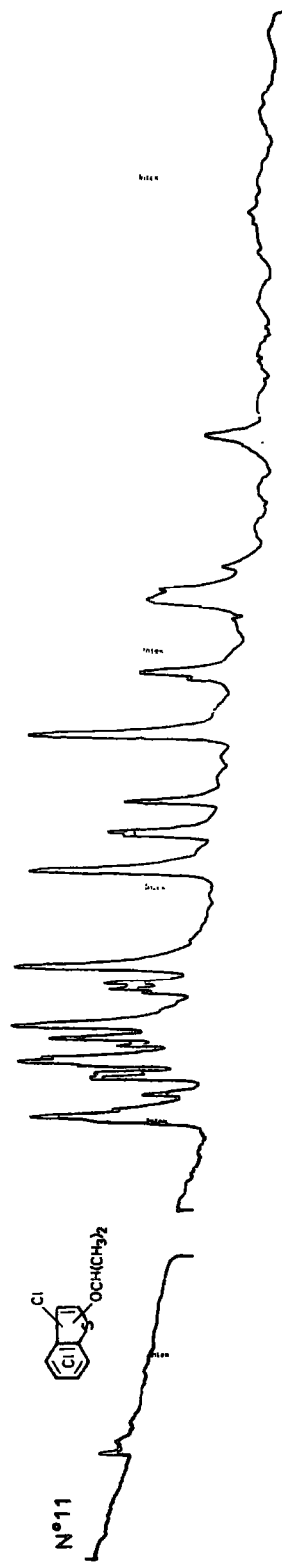
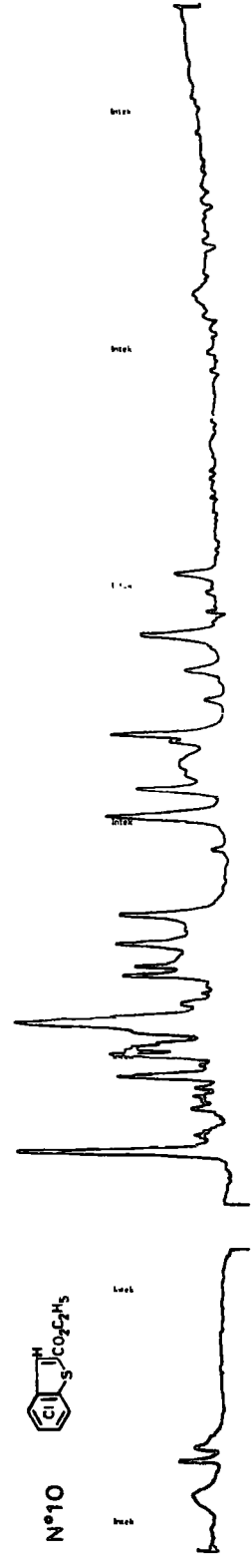
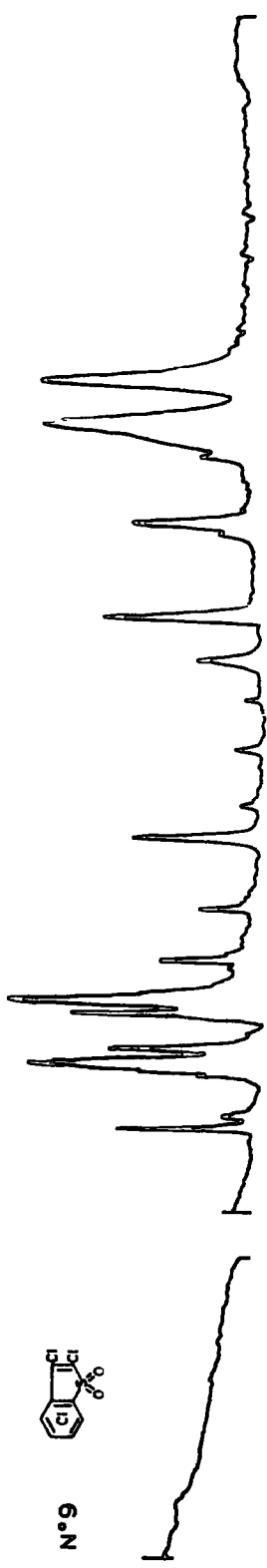
ii. Reflux Temperature - Sodium thiomethoxide (4ml. 2.0M) 4,5,6,7-tetrachlorobenzo-[b]-thiophen (0.51g) and dry pyridine (40ml.) were heated under reflux for 5hr. and worked up as before. Evaporation of the dried ( $\text{MgSO}_4$ ) extracts gave the crude product shown to contain two components which were separated by chromatography on silica [carbon tetrachloride as eluant]. The first component (0.17g) was the dichloro-di(thiomethoxy)benzo-[b]-thiophen m.p. 127-128° prepared previously, identified by I.R. spectroscopy. The second component (0.19g) was a tri-(thiomethoxy)monochlorobenzo-[b]-thiophen m.p. 99-100°

(from methanol) [Found C, 43.1; H, 3.25;  $C_{11}H_{11}ClS_4$  requires C, 43.05; H, 3.6%] [M = 306 (base peak); 291 (P-CH<sub>3</sub>, 16%); 276 (P-2CH<sub>3</sub>, 10%)].

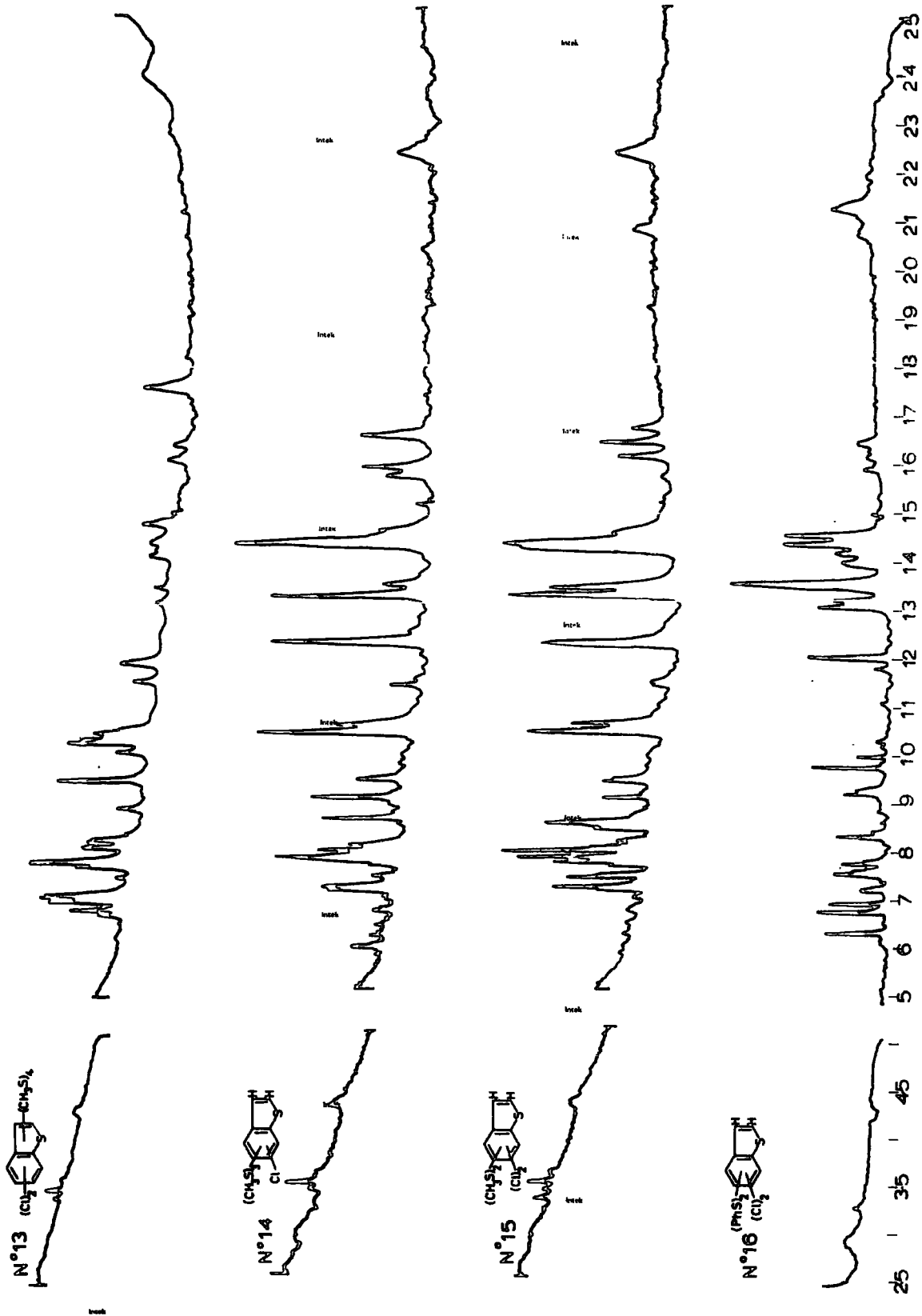
INFRARED SPECTRA







25 | 35 | 45 | 5 | 6 | 7 | 8 | 9 | 10 | 11 | 12 | 13 | 14 | 15 | 16 | 17 | 18 | 19 | 20 | 21 | 22 | 23 | 24 | 25



APPENDIX II

## Theoretical Calculations

### Introduction

The discussion here provides background theory for the semi-empirical molecular orbital treatment used in this work to obtain charge distributions for molecules investigated by ESCA, that could be used in conjunction with the charge potential model (discussed in CH<sub>3</sub> and CH<sub>4</sub>). The calculation of ground state energies and electron distributions involves solving the Shrodinger wave equation for each of the molecules considered. The complexities of these were such that a major non-empirical LCAO MO treatment was not possible. The calculations have therefore been carried out employing an approximate treatment in the all valence complete neglect of differential overlap (CNDO) SCF MO formalism as developed by J.A. Pople and co-workers.<sup>222</sup> The program to perform the calculations has been implemented on the Northumbrian Universities Multiple Access Computer (NUMAC) IBM 360/67. Modifications by D.B. Adams, to allow increased basis sets, and I.W. Scanlan, to allow exclusion of d-orbitals on second row atoms have been included.

### A. Elementary Quantum Mechanics<sup>223</sup>

The Schrodinger equation for a conservative system (one whose total energy does not vary with time) is given by:

$$H \psi = E \psi \qquad \text{II.1}$$

where  $H$  is the Hamiltonian or total energy operator,  $E$  is the eigenvalue corresponding to the total energy of the system and  $\Psi$  is a mathematical function of all the co-ordinates of the system (excluding time) called the eigen or wavefunction.

For molecules, the Born-Oppenheimer<sup>224</sup> approximation assumes that the nuclear and electronic wavefunctions are separable.

$$\Psi = \Psi_e \Psi_n \quad \text{II.2}$$

Using the Born-Oppenheimer approximation the electronic Schrodinger equation

$$H_e \Psi_e = E_e \Psi_e \quad \text{II.3}$$

is first solved for fixed positions of the  $N$  atoms within the molecule. The resulting electronic energies  $E_e$  form a potential energy surface  $V(\vec{R}_1, \vec{R}_2, \dots, \vec{R}_N)$  where  $\vec{R}_N$  specifies the co-ordinates of the  $N$ th atom within the molecule. This leads to the Schrodinger equation describing the motion of the nuclei.

$$H_n \Psi_n = E_n \Psi_n \quad \text{II.4}$$

The nuclear Hamiltonian is given by:

$$H_n = \sum_N -\frac{\hbar^2}{2M_N} \nabla_N^2 + V(\vec{R}_1, \vec{R}_2, \dots, \vec{R}_N) \quad \text{II.5}$$

where  $\frac{-\hbar^2}{2M_N} \nabla_N^2$  is the kinetic energy operator for the Nth nucleus. Equation II.4 may then be solved to yield (with II.3) the approximate total wave function  $\Psi$  and total energy  $E$ .

A further approximation made in the solution of (II.3) is the neglect of relativistic effects. The non-relativistic, spin free, electronic Hamiltonian is given, in atomic units, by the expression:

$$H_e = \sum_i \left( -\frac{1}{2} \nabla_i^2 - \sum_N \frac{Z_N}{r_{Ni}} \right) + \sum_{i>j} \frac{1}{r_{ij}} \quad (\text{II.6})$$

where  $-\frac{1}{2} \nabla_i^2$  represents the kinetic energy operators of the individual electrons  $i$ ,  $-\sum_N \frac{Z_N}{r_{Ni}}$  are the nuclear-electron attraction potential energy operators,  $Z_N$  being the charge on nucleus  $N$  and  $r_{Ni}$  the distance between this nucleus and electron  $i$ ,  $\frac{1}{r_{ij}}$  are the mutual repulsion operators for electron repulsion between electron pairs  $ij$ .

Solution of equation II.6 gives the electronic energy,  $E_e$ , of the molecule and this with the nuclear repulsion energy,  $E_{Nr}$ , gives the total energy of the molecule for fixed co-ordinates of the  $N$  atoms of the molecule. The nuclear repulsion energy is given by:

$$E_{Nr} = \sum_A \sum_B \frac{Z_A Z_B}{R_{AB}}$$

where  $Z_A$  is the core charge of atom  $A$  and  $R_{AB}$  is the inter-nuclear distance.

For many electron systems terms in  $\frac{1}{r_{ij}}$ , representing inter-electronic repulsions have to be included as part of the potential

energy of the Schrodinger equation. If interelectronic interactions could be neglected the total wave function could be expressed in terms of a summation of products of one electron functions,

$$\Psi = \psi_a(1) \psi_b(2) \dots \psi_k(n) \quad \text{II.7}$$

and

$$H = H_1 + H_2 \dots H_k \quad \text{II.8}$$

In this form the wave function would be separable into a set of equations each involving only the co-ordinates of one electron and solution of these equations would give the  $\psi$ 's. Although interelectronic repulsion cannot be completely neglected it cannot be taken properly into account since the many body problem is not exactly soluble in either quantum or classical mechanics. The idea of a one-electron function (the orbital approximation) is conceptually simple and it is therefore useful to consider products of one electron functions and to determine how close they may be made to approach to the exact functions. Within the orbital approximation the average repulsion experienced by one electron due to the other electrons in the system can be adequately described, but instantaneous correlations of electronic motions are relatively difficult to incorporate.

Associated with each electron is a spin ( $m_s = \pm \frac{1}{2}$ ) and the two possible spin functions are written as  $\alpha(m_s = +\frac{1}{2})$  and  $\beta(m_s = -\frac{1}{2})$ .

The product of a spacial orbital and a spin function is known as a spin orbital  $\phi$ .

$$\phi_i(1) = \psi_i(1)\alpha \quad \text{or} \quad \psi_i(1)\beta \quad \text{II.9}$$

where  $\psi_i$  is a function depending only on the space coordinates of the electron. Also,  $\alpha$  and  $\beta$  are orthogonal

$$\int \alpha\beta \, d\tau = 0 \quad \text{II.10}$$

This separation into spin and space coordinates is only possible because the non-relativistic (spin free) Hamiltonian was used.

The total wave function must be in accord with the Pauli anti-symmetric principle that interchange of any two electrons changes the sign of the wave function. The single product wave function

$$\Psi(1,2, \dots, 2n) = \psi_1(1)\alpha \psi_1(2)\beta \psi_2(3)\alpha \dots \psi_n(2n)\beta \quad \text{II.11}$$

( $n$  spin orbitals,  $2n$  electrons).

is not antisymmetric but can be made so by writing it in determinantal form.

$$\Psi(1,2, \dots, 2n) = \frac{1}{\sqrt{2n!}} \begin{vmatrix} \psi_1(1)\alpha & \psi_1(1)\beta & \psi_2(1)\alpha & \dots & \psi_n(1)\beta \\ \psi_1(2)\alpha & \psi_1(2)\beta & \psi_2(2)\alpha & \dots & \psi_n(2)\beta \\ \dots & \dots & \dots & \dots & \dots \\ \psi_1(2n)\alpha & \psi_1(2n)\beta & \psi_2(2n)\alpha & \dots & \psi_n(2n)\beta \end{vmatrix}$$

where  $\sqrt{\frac{1}{2n!}}$  is a normalising constant. This is known as a Slater determinant and is often written in abbreviated form.

$$\Psi(1, 2 \dots 2n) = \begin{vmatrix} \psi_{1\alpha} & \psi_{1\beta} & \psi_{2\alpha} & \psi_{2\beta} & \dots & \psi_{n\alpha} & \psi_{n\beta} \end{vmatrix} \quad \text{II.13}$$

where only the diagonal elements are shown on the normalisation constant is understood. Exchange of any two electrons interchanges two rows of the determinant therefore reverses the sign ensuring antisymmetry.

The wavefunctions must be continuous, single valued, and have an integrable square capable of being normalised.

$$\int \psi_i^2 d\tau = 1 \quad \text{II.14}$$

Also different eigenfunctions of the same Hamiltonian corresponding to different eigenvalues are mutually orthogonal. Therefore

$$\int \psi_i \psi_j d\tau = \delta_{ij} \quad \begin{array}{l} \delta = 1 \text{ for } i = j \\ \delta = 0 \text{ for } i \neq j \end{array} \quad \text{II.15}$$

As the determinantal wave functions are approximations a measure of how close the approximate wave functions approach the true wave function description of a given system is required. The variation theorem provides such a criterion.

The variation principle states that, given any approximate

wave function satisfying the boundary conditions of the problem, the expectation value of the energy calculated from this function will always be higher than the true ground state energy.

Therefore if  $\psi$  is an approximation to the exact wave function

$$\int \psi^* H \psi d\tau = E \geq E^0$$

where  $E^0$  is the true energy. The variation method is used by starting with a trial wave function containing one or more variational parameters and then minimising the energy with respect to the parameters. The simplest approach to obtaining suitable trial functions for molecular orbitals is to take a linear combination of atomic orbitals (LCAO method) based on the reasonable assumption that the electronic distribution in a molecule can be represented as a sum of atomic distributions. This linear combination of basis functions is known as the 'basis set' and, as the number of functions tends to infinity the perfect wave function is approached.

Now if the molecular orbital  $\psi$  is a linear combination of appropriate atomic orbitals  $\chi_i$

$$\psi = \sum_i^n C_i \chi_i \quad \text{II.16}$$

The coefficients  $C_i$  are used as variational parameters, although the parameters could equally well be incorporated into the basis functions  $\chi_i$

themselves.

$$\begin{aligned}
 E &= \frac{\int \psi^* H \psi \, d\tau}{\int \psi^* \psi \, d\tau} \\
 &= \frac{\sum_{ij} C_i^* C_j \int \chi_i H \chi_j \, d\tau}{\sum_{ij} C_i^* C_j \int \chi_i \chi_j \, d\tau} \\
 &= \frac{\sum_{ij} C_i^* C_j H_{ij}}{\sum_{ij} C_i^* C_j S_{ij}}
 \end{aligned}$$

where

$$\begin{aligned}
 H_{ij} &= \int \chi_i^* H \chi_j \, d\tau \\
 S_{ij} &= \int \chi_i^* \chi_j \, d\tau
 \end{aligned}$$

$$\therefore \sum_{ij} C_i^* C_j (H_{ij} - E S_{ij}) = 0$$

differentiating with respect to  $C_k$

$$\sum_{i=1}^n C_i^* (H_{ik} - E S_{ik}) - \sum_{i,j} C_i^* C_j S_{ij} \frac{\partial E}{\partial C_k} = 0$$

For a minimum value of  $E$ ,  $\frac{\partial E}{\partial C_k} = 0$  for all  $k$ .

$$\therefore \sum_i^n C_i^* (H_{ik} - E S_{ik}) = 0. \quad k = 1 \text{ to } n. \quad \text{II.17}$$

The sets of  $n$  simultaneous equations are known as secular equations as for a non-trivial solution the  $n \times n$  secular determinant must equal zero

$$|H_{ik} - E S_{ik}| = 0$$

The roots of the equations  $E_1, E_2 \dots E_n$  can be found and by substitution back into II.17 the coefficients  $C_i$  may be determined and hence (from II.16) the molecular orbitals.

a. The Hartree-Fock Self Consistent Field Method<sup>225,226</sup>

The method consists of minimising the energy resulting from the single determinantal wave function to derive a set of integrodifferential equations (the Hartree-Fock equations). The Hartree-Fock wave function is the best wave function which can be constructed by assigning each electron to a separate function (or orbital) depending only on the coordinates of that electron. In molecular orbital calculations it is not possible to use a mathematically complete set of functions (an infinite set) and only approximate solutions can be obtained. The best single determinantal function constructed within a finite basis set is the self consistent field function.

Suppose the wave function for a system of  $n$  electrons is written as a single product of  $n$  spin orbitals.

$$\Psi = \psi_a(1) \psi_b(2) \dots \psi_k(n) \quad \text{II.18}$$

The energy of this wave function is given by:

$$E = \int \Psi H \Psi d\tau \quad \text{II.19}$$

where  $H$  is the complete electronic Hamiltonian written in the form

$$H = \sum_i H^C(i) + \sum_{ij} \left(\frac{1}{r_{ij}}\right) + V_{nn} \quad \text{II.20}$$

where  $H^C(i)$  is the so-called core Hamiltonian which consists of the kinetic energy operator and the electron-nuclear attraction terms for electron  $i$  and  $V_{nn}$  is the nuclear repulsion energy.

Substitution of II.18 and .20 into .19 gives

$$E = \sum_{r=a}^k H^C_{rr} + \sum_{\substack{\text{pairs} \\ rs}} J_{rs} + V_{nn} \quad \text{II.21}$$

where  $H^C_{rr} = \int \psi_r H^C \psi_r d\tau$

and

$$J_{rs} = \iint \psi_r(i) \psi_s(j) \left(\frac{1}{r_{ij}}\right) \psi_r(i) \psi_s(j) d\tau_i d\tau_j$$

Terms involving  $H^C$  are the energies that each electron would have if all other electrons were absent. The final parts of II.21 give the total repulsion energy. The wave function II.18 does not satisfy the antisymmetric requirement but this can be corrected by

converting it to a Slater determinant of spin orbitals

$$\Psi = |\psi_a \psi_b \dots \psi_k| \quad \text{II.22}$$

Providing the spin orbitals are mutually orthogonal, substituting II.22 into II.19 gives

$$\bar{E} = \sum_{r=a}^k \bar{H}_{rr}^C + \sum_{\substack{\text{pairs} \\ rs}} (J_{rs} - K_{rs}) + \bar{V}_{nn} \quad \text{II.23}$$

This differs from II.21 by terms in  $K_{rs}$

$$K_{rs} = \iint \psi_r(i) \psi_s(j) \left( \frac{1}{r_{ij}} \right) \psi_s(i) \psi_r(j) d\tau_i d\tau_j \quad \text{II.24}$$

$J_{rs}$  is termed a coulomb integral and  $K_{rs}$  an exchange integral. If  $\psi_r$  and  $\psi_s$  have different associated spin orbitals (one  $\alpha$ , the other  $\beta$ ) then it follows from integration over the spin co-ordinates that  $K_{rs}$  is zero.

Applying the variation principle to the wave functions in II.18 and II.22 and requiring that the respective energies be minimised is sufficient to define the orbitals  $\psi$ . Orbitals defined this way are known as SCF orbitals. Orbitals defined with respect to the anti-symmetrised product (II.22) are the Hartree-Fock orbitals. The conditions defining these orbitals are now examined.

Suppose the function II.22 does not give the lowest energy of the state. Then there is some other function say

$$\Psi' = |\psi'_a \psi_b \dots \psi_k| \quad \text{II.25}$$

which has a lower energy. Assuming that  $\psi'_a$  differs only slightly from  $\psi_a$  and can be written

$$\psi'_a = \psi_a + C_t \psi_t \quad \text{II.26}$$

where  $\psi_t$  is a spin orbital orthogonal to the set  $\psi_a \dots \psi_k$ .

Providing  $C_t$  is small  $\psi'_a$  will still be normalised, as re-normalisation only involves a term in  $C_t^2$ . Using II.26, II.25 can be written

$$\begin{aligned} \Psi' &= |\psi_a \psi_b \dots \psi_k| + C_t |\psi_t \psi_b \dots \psi_k| \\ &= \Psi + C_t \Psi_a^t \end{aligned} \quad \text{II.27}$$

ie  $\Psi'$  is formed by adding to  $\Psi$  a small amount of the state  $\Psi_a^t$  which arises from excitation of an electron from  $\psi_a$  to  $\psi_t$ . For  $\Psi$  to be the best wave function of its type  $C_t$  must be zero and the Hamiltonian integral between  $\Psi$  and  $\Psi_a^t$  (termed  $F_{at}$ ) must also be zero.

$$F_{at} = \int \Psi H \Psi_a^t d\tau = 0 \quad \text{II.28}$$

Expressing II.28 in terms of spin orbitals

$$\begin{aligned} F_{at} = H_{at}^C + \sum_{s=a}^k \left\{ \iint \psi_a(i) \psi_s(j) \left( \frac{1}{r_{ij}} \right) \psi_t(i) \psi_s(j) d\tau_i d\tau_j \right. \\ \left. - \iint \psi_a(i) \psi_s(j) \left( \frac{1}{r_{ij}} \right) \psi_s(i) \psi_t(j) d\tau_i d\tau_j \right\} \end{aligned} \quad \text{II.29}$$

For this to be zero for any spin orbital (not just  $\psi_a$ ) it is necessary that the  $\psi$  be eigenfunctions of the operator  $F$ . This operator must

then depend on its own eigenfunctions, II.29 can be written

$$F = H^C + \sum_{s=a}^k (J_s - K_s) \quad \text{II.30}$$

where  $J_s$  and  $K_s$  are coulomb and exchange operators defined by their integrals

$$\begin{aligned} (J_s)_{at} &= \iint \psi_a(i) \psi_s(j) \left( \frac{1}{r_{ij}} \right) \psi_t(i) \psi_s(j) d\tau_i d\tau_j \\ (K_s)_{at} &= \iint \psi_a(i) \psi_s(j) \left( \frac{1}{r_{ij}} \right) \psi_s(i) \psi_t(j) d\tau_i d\tau_j \end{aligned} \quad \text{II.31}$$

The potential governing the SCF orbitals consists of the core potential, the coulomb potential of all the electrons and an exchange potential for each electron. Since the coulomb and exchange potential depend on the orbitals themselves, an iterative method has to be used to calculate the SCF orbitals.

The eigenvalues of  $F$  (the Fock operator) may be called the orbital energies. Thus from II.29

$$\epsilon_r = F_{rr} = H_{rr}^C + \sum_{s=a}^k (J_{rs} - K_{rs}) \quad \text{II.32}$$

Summing the energies over all occupied orbitals

$$\sum_{r=a}^k \epsilon_r = \sum_{r=a}^k H_{rr}^C + \sum_{r=a}^k \sum_{s=a}^k (J_{rs} + K_{rs}) \quad \text{II.33}$$

Comparing this with II.23 and noting since  $J_{rr} = K_{rr}$  that

$$\sum_{r=a}^k \sum_{s=a}^k (J_{rs} + K_{rs}) = 2 \sum_{\substack{\text{pair} \\ rs}} (J_{rs} - K_{rs}) \quad \text{II.34}$$

then

$$E = \sum_{r=a}^k \epsilon_r - \sum_{\substack{\text{pairs} \\ rs}} (J_{rs} - K_{rs}) + V_{nn} \quad \text{II.35}$$

Thus even for SCF orbitals the total electronic energy is not just the sum of the orbital energies plus nuclear repulsion energy.

For a closed-shell configuration with each orbital being occupied by two electron with  $\alpha + \beta$  spins, expressions II.23, II.29 and II.32 are:

$$\text{(II.23)} \quad E = 2 \sum_r H_{rr}^C + 2 \sum_{\substack{\text{pairs} \\ rs}} (2J_{rs} - K_{rs}) + \sum_r J_{rr} + V_{nn} \quad \text{II.36}$$

$$\text{(II.29)} \quad F_{at} = H_{at}^C + \sum_{s=a}^k \left\{ 2 \iint \psi_a(i) \psi_s(j) \left( \frac{1}{r_{ij}} \right) \psi_t(i) \psi_s(j) d\tau_i d\tau_j \right. \\ \left. - \iint \psi_a(i) \psi_s(j) \left( \frac{1}{r_{ij}} \right) \psi_s(i) \psi_t(j) d\tau_i d\tau_j \right\} \quad \text{II.37}$$

$$\text{(II.32)} \quad \epsilon_r = H_{rr}^C + \sum_{s=a}^k (2J_{rs} - K_{rs}) = F_{rr} \quad \text{II.38}$$

where the summation is carried out over all occupied orbitals, not spin-orbitals.

If the SCF orbitals are represented by the LCAO approximation

$$\psi = \sum_{\nu} C_{\nu} \phi_{\nu} \quad \text{II.39}$$

then substituting II.39 into II.37 and picking out terms in

$$C_{a\mu} C_{tv}$$

$$F_{\mu\nu} = H_{\mu\nu}^C + \sum_{s=a}^k \sum_{\rho} \sum_{\sigma} C_{\rho s} C_{\sigma s} \left\{ 2 \iint \phi_{\mu}(i) \phi_{\rho}(j) \left( \frac{1}{r_{ij}} \right) \phi_{\nu}(i) \phi_{\sigma}(j) d\tau_i d\tau_j \right. \\ \left. - \iint \phi_{\mu}(i) \phi_{\rho}(j) \left( \frac{1}{r_{ij}} \right) \phi_{\sigma}(i) \phi_{\nu}(j) d\tau_i d\tau_j \right\} \quad \text{II.40}$$

The SCF orbitals for a closed-shell system in this form are then determined by solving the secular equations

$$\sum_{\nu} C_{\nu} (F_{\mu\nu} - E S_{\mu\nu}) = 0 \quad \text{II.41}$$

through the determinant

$$|F_{\mu\nu} - E S_{\mu\nu}| = 0 \quad \text{II.42}$$

These are known as Roothaan's equations.<sup>227</sup> An iterative process is necessary for the solutions of II.41 since  $F_{\mu\nu}$  depends the co-efficients  $C_{\nu}$ .

### The Basis Functions

The molecular orbitals used to describe a system of electrons and nuclei are generally expanded in terms of a linear combination

of atomic orbitals (cf equation II.39) and the atomic orbitals can be further described as a linear combination of functions  $\chi_i$  known as the basis functions (cf equation II.16)

$$\text{ie.} \quad \psi_{\text{MO}} = \sum_i c_i \psi_i$$

$$\text{and} \quad \psi_i = \sum_{\mu} c_{\mu i} \chi_{\mu}$$

A complete solution of the Hartree-Fock problem requires an infinite basis set but a good approximation can be achieved with a limited number of functions. Molecular orbital theory is simplest to apply and interpret if the basis set is minimal, that is, when it consists of the least number of atomic orbitals of the appropriate symmetry for the ground state. A typical basis set for organic molecules consists of a 1s orbital for hydrogen, 1s, 2s, 2p<sub>x</sub>, 2p<sub>y</sub>, 2p<sub>z</sub> for carbon, nitrogen etc. and 1s, 2s, 2p<sub>x</sub>, 2p<sub>y</sub>, 2p<sub>z</sub>, 3s, 3p<sub>x</sub>, 3p<sub>y</sub>, 3p<sub>z</sub> for chlorine, sulphur etc.

Two types of basis function are used in Hartree-Fock calculations, Slater type functions and gaussian type functions. The simplest type of atomic orbital to use in a minimal basis set (and the one used in CNDO/2) involves the Slater type orbitals and the functions are of the type

$$\psi(r, \theta, \phi) = N_r^{n-1} e^{-\xi, r} \cdot Y_{lm}(\theta, \phi) \quad \text{II.43}$$

where N is a normalisation factor, n is the principle quantum number

and  $\xi_y$  is the orbital exponent. Angular dependence is given by the spherical harmonic terms  $Y_{lm}(\theta \phi)$ . These are, for hydrogen,

$$\chi_{1s} = (\xi^3/\pi)^{\frac{1}{2}} e^{-\xi r}$$

for atoms lithium to fluorine,

$$\chi_{2p} = (\xi^5/32\pi)^{\frac{1}{2}} r \cos \theta e^{-\xi r/2}$$

$$\chi_{2s} = (\xi^5/96\pi)^{\frac{1}{2}} r e^{-\xi r/2}$$

For gaussian type functions the radial part is of the form  $[\exp(-\alpha r^2)]$ . The disadvantage of the G.T.O's (gaussian type orbitals) is that in the vicinity of the nucleus a linear combination of several G.T.O's must be used to give correct radial dependence where only a single STO is needed

b. Semi-empirical All Valence Electron, Neglect of Diatomic Overlap Method. (NDDO).

For molecules of even moderate size, minimal basis set calculations of the non-empirical type can be come computationally very expensive.

One of the main obstacles is the evaluation of all the multicentre integrals involved. The NDDO method reduces the number of integrals to be evaluated either by approximating them to zero or estimating them from empirical data.

The approximations involved are:

- (i) Only valence electrons are specifically accounted for, the inner shells being regarded as an unpolarisable core.
- (ii) Only atomic orbitals of the same principle quantum number as that of the highest occupied orbitals in the isolated atoms are included in the basis set.
- (iii) Diatomic differential overlap is neglected. That is, if the orbitals  $\chi_i$  and  $\chi_j$  are not on the same atom.

$$S_{ij} = \int \chi_i(\mu) \chi_j(\mu) d\tau = 0$$

and

$$\iint \chi_i(\mu) \chi_k(\nu) \left( \frac{1}{r_{\mu\nu}} \right) \chi_j(\mu) \chi_e(\nu) d\tau_\mu d\tau_\nu = \langle ij | k1 \rangle = 0$$

unless  $\chi_i$  and  $\chi_j$  are atomic orbitals of atom A and  $\chi_k$  and  $\chi_e$  are atomic orbitals belonging to the same atom A or B.

The first approximation permits the inner electrons to be neglected, taking them as part of a core where charge will be approximately equal to the nuclear charge minus the number of core electrons. The second approximation considerably reduces the initial number of integrals to be calculated. Thirdly, all three and four centre integrals and some two centre integrals are reduced to zero.

c. All Valence Electron Complete Neglect of Differential Overlap Method (CNDO).

Even with the above approximations the number of integrals to be evaluated is still large and further simplifications are desirable.

In the CNDO method all one and two centre integrals involving differential overlap are set to zero. Writing the electronic interaction integrals

$$\int \chi_A^2(\mu) \left( \frac{1}{r_{\mu\nu}} \right) \chi_B^2(\nu) d\tau_\mu d\tau_\nu \quad \text{II.44}$$

as  $\Gamma_{AB}$ . The Fock matrix elements  $F_{ij}$  become

$$F_{ii} = H_{ii} + (P_{AA} - \frac{1}{2} P_{ii}) \Gamma_{AA} + P_{BB} \Gamma_{AB} \quad \text{II.45}$$

and

$$F_{ij} = H_{ij} - \frac{1}{2} P_{ij} \Gamma_{AB} \quad (i \neq j) \quad \text{II.46}$$

where the atomic orbital  $\chi_i$  is centre on atom A and  $\chi_j$  on atom B.  $P_{ij}$  are the components of the charge density and bond order matrix,

$$P_{ij} = 2 \sum_m^{\text{occ}} a_{mi} a_{mj} \quad \text{II.47}$$

and  $P_{AA}$  is the charge on atom A

$$P_{AA} = \sum_i^A P_{ii} \quad \text{II.48}$$

The core matrix elements  $H_{ii}$  may be separated into two components, the diagonal matrix elements of  $\chi_i$  with respect to the one-electron Hamiltonian containing only the core of its own

atom ( $U_{ii}$ ), and the interactions of an electron in  $\chi_i$  on atom A with the cores of other atoms B.

$$H_{ii} = U_{ii} - \sum_{B \neq A} V_{AB} \quad \text{II.49}$$

Therefore II.45 may be written as

$$F_{ii} = U_{ii} + (P_{AA} - \frac{1}{2} P_{ii}) \Gamma_{AB} + \sum_{B \neq A} (P_{BB} \Gamma_{AB} - V_{AB}) \quad \text{II.50}$$

and the total energy may be written as the sum of one and two atom terms.

$$E = \sum_A E_A + \sum_{A < B} E_{AB} \quad \text{II.51}$$

where

$$E_A = \sum_i P_{ii} U_{ii} + \frac{1}{2} \sum_i \sum_i^{A B} (P_{ii} P_{jj} - \frac{1}{2} P_{ij}^2) r_{AB} \quad \text{II.52}$$

and

$$E_{AB} = \sum_i \sum_i^{A B} (2P_{ij} H_{ij} - \frac{1}{2} P_{ij}^2 \Gamma_{AB}) + (Z_A Z_B \frac{1}{R_{AB}} - P_{AA} V_{AB} - P_{BB} V_{AA} + P_{AA} \Gamma_{AB}) \quad \text{II.53}$$

where  $R_{AB}$  is the distance between nuclei A and B.

Due to neglect of the one-centre electron interactions involving differential overlap between two orbitals some one centre exchange integrals such as  $\langle 2s 2p_x | 2s 2p_x \rangle$  are omitted and the CNDO method does not show quantitatively the effects of Hund's rules. For calculations on closed shell ground states this defect is not serious.

### Evaluation of Integrals in CNDO/2.

#### (i) One electron integrals $U_{ii}$

An estimate of this integral can be obtained from spectroscopic data. It can be shown that

$$U_{ii} = -I_i - (Z_A - 1)\Gamma_{AA} \quad \text{II.54}$$

where  $I_i$  is the ionisation potential of an electron from an orbital  $\chi_i$  on atom A (referred to the appropriate average atomic states). Alternatively, atomic electron affinities ( $A_i$ ) may be used

$$-A_i = U_{ii} + Z_A \Gamma_{AA} \quad \text{II.55}$$

but in order to account for the tendency of an atomic orbital to acquire and loose electrons, the relationship used in CNDO/2 calculations is:

$$-\frac{1}{2}(I_i + A_i) = U_{ii} + (Z_A - \frac{1}{2})\Gamma_{AA} \quad \text{II.56}$$

$$\therefore U_{ii} = -\frac{1}{2}(I_i + A_i) - (Z_A - \frac{1}{2})\Gamma_{AA} \quad \text{II.57}$$

(ii) One-centre, two electron integrals  $\Gamma_{AA}$ 

These are calculated from the electrostatic repulsion energy of two electrons in a Slater s-orbital irrespective of the fact that the orbitals concerned may be p or d-orbitals. Thus,

$$\Gamma_{AA} = \iint \chi_{SA}^2(\mu) \left( \frac{1}{r_{\mu\nu}} \right) \chi_{SA}^2(\nu) d\tau_{\mu} d\tau_{\nu} \quad \text{II.58}$$

(iii) Two-centre, two electron integrals  $\Gamma_{AB}$ 

The most difficult problem in semi-empirical methods of solving the Hartree-Fock problem is satisfactory evaluation of two-centre, two electron integrals. In CNDO/2 these are calculated as

$$\Gamma_{AB} = \iint \chi_{SA}^2(\mu) \left( \frac{1}{r_{\mu\nu}} \right) \chi_{SB}^2(\nu) d\tau_{\mu} d\tau_{\nu} \quad \text{II.59}$$

where  $\chi_{SA}$  and  $\chi_{SB}$  are the Slater s-type orbitals for atoms A and B. These integrals represent the interaction between electrons in valence orbitals on atoms A and B. Formulae for these integrals have been listed by Roothaan,<sup>228</sup>

(iv) Two-centre, one electron integrals  $H_{i,j}$  (Resonance integrals).

This integral is taken as being directly proportional to the overlap integral  $S_{ij}$  between orbitals  $\chi_i$  and  $\chi_j$  centred on A and B respectively.

$$H_{ij} = \beta_{AB}^0 S_{ij} \quad \text{II.60}$$

where Slater atomic orbitals are used to calculate  $S_{ij}$ . To preserve rotational invariance,  $\beta_{AB}^0$  should be characteristic of  $\chi_i$  and  $\chi_j$  but independent of their coordinates. The parameter  $\beta_{AB}^0$  is therefore taken as the average of a  $\beta^0$  parameter for each atom.

$$\beta_{AB}^0 = \frac{1}{2} (\beta_A^0 + \beta_B^0) \quad \text{II.61}$$

where the parameters  $\beta_A^0$  are chosen to reproduce results obtained from experiment or 'ab initio' calculations.<sup>229</sup>

(v) Coulomb Penetration Integrals  $V_{AB}$

In the CNDO/2 method the effect of the interaction of an electron in orbital  $\chi_i$  on atom A with the cores of other atoms B (equation II.49) are neglected and coulomb penetration integrals estimated as:

$$V_{AB} = Z_B \Gamma_{AB} \quad \text{II.62}$$

Electron Distribution in Molecules.

Charge Density

When the molecular orbitals  $\psi_m$  have been determined the charge density may be analysed in terms of the basis functions  $\chi_i$ . For two electrons in each occupied molecular orbital the total charge density  $P$  is given by:

$$P = 2 \sum_m^{\text{occ}} \psi_m = \sum_k \sum_l P_{kl} \chi_k \chi_l \quad \text{II.63}$$

where  $P_{kl}$  is the density matrix defined in equation II.47. The

diagonal element  $P_{kk}$  is the coefficient of the distribution  $\chi_k^2$  and measures the electron population of that orbital. The off diagonal elements  $P_{kl}$  are overlap populations related to the overlap region of atomic orbitals  $\chi_k$  and  $\chi_l$ . In order to assign a specific charge to each atom a Mulliken population analysis is used. The total electron population of an orbital  $\chi_k$  is given by

$$q_k = P_{kk} + \sum_{k \neq l} P_{kl} S_{kl} \quad \text{II.64}$$

where  $S_{kl}$  is the overlap integral. Since in the CNDO approximation overlap is ignored, then

$$q_k = P_{kk} \quad \text{II.65}$$

and the total charge density on atom A is given by the sum over all atomic orbitals centred on A.

$$P_{AA} = \sum_k^A P_{kk} \quad \text{II.66}$$

and the net charge on atoms A is given by:

$$\text{charge} = P_{AA} - Z_A \quad \text{II.67}$$

where  $Z_A$  is the effective atomic number (i.e. the atomic number minus the number of core electrons).

### $\pi$ Charge

The  $\pi$  electron charge of an atom is taken as the value of the diagonal element  $P_{kk}$  of the electron density matrix, out of the plane of the molecule. The difference between this value of  $P_{kk}$  and the number of  $\pi$  electrons the atom contributes is then taken as the  $\pi$  charge on the atom.

### $\sigma$ Charge

The difference between the net (or total) charge on an atom (equation II.67) and the  $\pi$  charge as defined above is taken as the  $\sigma$ -charge.

As observed previously, ascribing an electron population to a given atom is a simplification since the electron distribution is a continuous function. The analysis gives only a crude idea of the electron distribution within a molecule but the idea is conceptually close to qualitative ideas of charge distributions in organic molecules. The CNDO/2 charge distributions, used in conjunction with the charge potential model, have been shown to give a good quantitative description of observed ESCA chemical shifts. The treatment is, however, less accurate for second row atoms but this should be overcome by better parameterisation of the basis functions in the CNDO treatment.

APPENDIX III

A Nonrigorous Derivation of the Charge Potential Model.

For a closed shell molecule described by the Slater determinantal wave function (cf II.13)

$$\Psi_M = |\psi_a \dots \dots \psi_k| \quad \text{III.1}$$

the total energy may be written as (cf II.35)

$$E_M = \sum_{r=a}^k \epsilon_r - \sum_{\substack{\text{pairs} \\ rs}} (2J_{rs} - K_{rs}) + V_{nn} \quad \text{III.2}$$

The orbital energies  $\epsilon_r$  may be expressed as:

$$\begin{aligned} \epsilon_r &= \langle \psi_r | -\frac{1}{2} \nabla^2 - \sum_{nl} \frac{Z_n}{r_{nl}} | \psi_r \rangle + \sum_{s=a}^k (2J_{rs} - K_{rs}) \\ &= H_{rr}^{\text{core}} + \sum_{s=a}^k (2J_{rs} - K_{rs}) \end{aligned}$$

$$\therefore \sum_{r=a}^k \epsilon_r = \sum_{r=a}^k H_{rr}^{\text{core}} + \sum_{r=a}^k \sum_{s=a}^k (2J_{rs} - K_{rs})$$

$$\text{now } \sum_{r=a}^k \sum_{s=a}^k (2J_{rs} - K_{rs}) = 2 \sum_{\substack{\text{pairs} \\ rs}} (2J_{rs} - K_{rs})$$

$$\therefore \sum_{r=a}^k \epsilon_r = \sum_{r=a}^k H_{rr}^{\text{core}} + 2 \sum_{\substack{\text{pairs} \\ rs}} (2J_{rs} - K_{rs})$$

$$\therefore E_M = \sum_{r=a}^k H_{rr}^{\text{core}} + \sum_{\substack{\text{pairs} \\ rs}} (2J_{rs} - K_{rs}) + V_{nn} \quad \text{III.3}$$

If one electron is now removed from spin orbital  $\psi_a$ , then the energy of the ionised state (provided the wavefunctions of the other electrons remain unchanged) is given by:

$$\psi_{M^+} = |\psi_b \dots \dots \psi_k| \quad \text{III.4}$$

$$E_{M^+} = \sum_{r=b}^k H_{rr}^{\text{core}} + \sum_{\substack{\text{pairs } rs \\ r \neq a, s \neq a}} (2J_{rs} - K_{rs}) + V_{nn} \quad \text{III.5}$$

$$\therefore E_M - E_{M^+} = H_{aa}^{\text{core}} + \sum_{s=a}^k (2J_{as} - K_{as}) = \epsilon_a \quad \text{III.6}$$

It follows that  $-\epsilon_a$  can be equated to the ionisation potential ( $E_{M^+} - E_M$ ) which is the energy required to ionise the molecule, providing that the ionisation process can be adequately represented by the removal of an electron from an orbital without a change in the wavefunctions of the other electrons. This is known as Koopmans' Theorem.

In practice the wavefunctions of the other electrons do change in going to the ionised state and this electronic reorganisation lowers the energy, so that ionisation potentials computed assuming Koopmans' theorem are too large. The degree of 'localisation' about the nucleus of core electrons depends very little on the chemical environment

of the atom so that  $\Delta E_{\text{reorg}}$ . (the reorganisation energy) is roughly constant for a given core level. The shift in a given core level is given by;

$$\Delta_{\text{shift}} = \Delta\epsilon + \Delta E_{\text{reorg}} + \Delta E_{\text{corr}} + \Delta E_{\text{rel}},$$

and other terms being either small or effectively constant

$$\Delta_{\text{shift}} \approx \Delta\epsilon \quad \text{III.7}$$

The change in electronic environment about a given atom in going from one molecule to another is due to the difference in valence electron distribution, the core electrons being localised on their respective atoms. It is natural therefore to develop a model in which shifts in core binding energies may be related to changes in valence electron distribution. The potential model attempts to do this.

Consider the expression for the orbital energy,

$$\epsilon_r = \langle \psi_r | -\frac{1}{2} \nabla^2 - \sum_n \frac{Z_n}{r_{nl}} | \psi_r \rangle + \sum_{s=a}^k (2J_{rs} - K_{rs}) \quad \text{III.8}$$

where the  $\psi_{r,s}$  are MO's,  $Z_n$  is the nuclear charge of atom  $n$  and the summation of the second term extends over all occupied MO's.

Expanding,

$$\begin{aligned} \epsilon_r = & \langle \psi_r | -\frac{1}{2}\nabla_1^2 - \frac{Z_m}{r_{m1}} | \psi_r \rangle + J_{rr} \\ & + \langle \psi_r | - \sum_{n \neq m} \frac{Z_n}{r_{n1}} | \psi_r \rangle + \sum_{s \neq r}^k (2J_{rs} - K_{rs}) \end{aligned} \quad \text{III.9}$$

Consider the first term of expression III.9. If  $\epsilon_r$  corresponds to a core level centered on atom  $m$ , then this one centre kinetic and nuclear attraction integral is constant for a given atom and is independent of the valence electron distribution. The one centre coulomb repulsion integral  $J_{rr}$  is also independent of the valence electron distribution. In considering 'shifts' in core levels the first two terms in III.9 may be ignored. Similarly in the expansion,

$$\sum_{s \neq r}^k (2J_{rs} - K_{rs})$$

the one centre coulomb and exchange integrals involving other core orbitals on atom  $m$  will be invariant to changes in valence electron distribution, whilst exchange integrals involving the localised core orbital on atom  $m$  and core and valence orbitals on other atoms are small and may be neglected, III.9 may be re-written as;

$$\epsilon_r = E^0 + \langle \psi_r | - \sum_{n \neq m} \frac{Z_n}{r_{n1}} | \psi_r \rangle + \sum_{s \neq r}^k 2J_{rs} \quad \text{III.10}$$

where  $E^0$  is a constant and the summation of coulomb repulsion integrals extends over valence orbitals and core orbitals on atoms other than  $m$ . The second term in III.10 represents the attraction between a core electron in orbital  $\psi_r$  which is localised on atom  $m$  and the nuclei of the other atoms in the molecule. This term may be re-written as

$$\sum_{n \neq m}^k - \frac{Z_n}{r_{nm}}$$

The third term involves coulomb integrals. Consider firstly the terms involving the core orbital  $\psi_r$  on atom  $m$  and a core orbital  $\psi_j$  on atom  $n$ ;

$$J_{rj} = \langle \psi_r(1)\psi_j(2) | \frac{1}{r_{12}} | \psi_r(1)\psi_j(2) \rangle$$

This represents the interaction between the charge cloud  $\psi_r^2$  localised on atom  $m$  and  $\psi_j^2$  localised on atom  $n$  and hence, can be written as  $\frac{1}{r_{nm}}$ . The term  $J_{ri}$  where  $\psi_i$  is a valence molecular orbital can be written as;

$$\langle \psi_r(1) \psi_i(2) | \frac{1}{r_{12}} | \psi_r(1)\psi_i(2) \rangle \quad \text{III.11}$$

expanding  $\psi_i$  in terms of the basis set of atomic orbitals;

$$J_{ri} = \sum_p c_{ip}^2 \langle \psi_r(1) \phi_p(2) | \frac{1}{r_{12}} | \psi_r(1) \phi_p(2) \rangle \quad \text{III.12}$$

The terms involved in III.12 are of two types:

- (1)  $\phi_p$  is a valence atomic orbital on atom m
- (2)  $\phi_p$  is a valence atomic orbital on atoms n other than m.

The second type, (2), again represents the electrostatic repulsion between charge clouds on different atoms and III.12 can be written as:

$$J_{ri} = \sum C_{ip}^2 \langle \psi_r(1) \phi_p(2) | \frac{1}{r_{12}} | \psi_r(1) \phi_p(2) \rangle + \sum C_{ip}^2 \frac{1}{r_{nm}} \quad \text{III.13}$$

The first summation extends over valence atomic orbitals  $\phi_p$  on atoms n other than m and the second summation extends over valence atomic orbitals  $\phi_p$  on atom m.

III.10 can now be written as:

$$\epsilon_r = E^0 + \sum -\frac{Z_n}{r_{nm}} + \sum \frac{2}{r_{nm}} + \sum \sum \frac{2C_{ip}^2}{r_{nm}}$$

over all atoms n other than m	over all core orbitals on atoms other than m	over all valence MO's and all constituent atomic orbitals in the linear combination on atoms other than m
----------------------------------	---	---

$$+ \sum C_{ip}^2 \langle \psi_r(1) \phi_p(2) | \frac{1}{r_{12}} | \psi_r(1) \phi_p(2) \rangle$$

over all valence atomic orbitals on atom m.

Collecting terms common to each atom

$$\epsilon_r = E^0 + \sum_n \left( -\frac{Z_n}{r_{nm}} + \frac{2}{r_{nm}} \right) + \sum \frac{2C_{ip}^2}{r_{nm}} \\ + \sum C_{ip}^2 \langle \psi_r(1)\phi_p(2) | \frac{1}{r_{12}} | \psi_r(1)\phi_p(2) \rangle$$

but  $\sum 2 + \sum 2C_{ip}^2$  is the total electron population on a given atom n

$\therefore -Z_n + \sum 2 + \sum 2C_{ip}^2$  represents the charge  $q_n$  on atom n.

$$\therefore \epsilon_r = E^0 + \sum_{n \neq m} \frac{q_n}{r_{mn}} + \sum 2C_{ip}^2 \langle \psi_r(1)\phi_p(2) | \frac{1}{r_{12}} | \psi_r(1)\phi_p(2) \rangle \quad \text{III.14}$$

Now,  $\sum 2C_{ip}^2$  in III.14 represents the total valence electron population on atom m and this is directly proportional to the charge  $q_m$ .

III.14 may be re-written in the form

$$\epsilon_r = E^0 + k_{qm} + \sum_{n \neq m} \frac{q_n}{r_{nm}} \quad \text{III.15}$$

Theoretically, k should be the average repulsion between a core and valence electron on atom m, however, to allow for the approximations involved in deriving III.15, it is better to treat k as a parameter which depends on the definition of atomic charge and in an SCF MO treatment, on the basis set employed.

III.15 relates the binding energy of a core level of an atom to the charge distribution in the molecule and allows ready extension to a discussion of ionic lattices. For molecular solids the third term

in III.15 may be regarded as an intramolecular Madelung potential. In the extension to ionic solids, this becomes an intermolecular potential and in principle extends over the whole lattice.

REFERENCES

1. H.D. Hartough and S.L. Meisel, 'Compounds with Condensed Thiophene Rings', (A. Wiessberger. Ed.), Wiley (Interscience) N.Y., 1954.
2. D.K. Fukushima in 'Heterocyclic Compounds Vol. 2' (Elderfield Ed.) p.145 J. Wiley and Sons, N.Y., 1951.
3. B.D. Tilak, Tetrahedron, 1960, 9, 76.
4. B. Iddon and R.M. Scrowston, Adv. Het. Chem., 1970, 11, 177.
5. R.P. Napier, H.A. Kaufman, P.R. Driscoll, L.A. Glick, C. Chu and H.M. Foster, J. Het. Chem., 1970, 7, 393.
6. S. Hauptmann, M. Weissinfels, M. Schloz, E.M. Werner, H.J. Kohler and J. Weisflog, Tetrahedron Letters, 1968, 1317.
7. F. Bohlmann and E. Bresinsky, Chem. Ber., 1964, 97, 2109.
8. Rodd (Ed.), 'Chemistry of Carbon Compounds Vol. 4', Elsevier Publishing Co., 1957, p.225.
9. N.B. Chapman, K. Clark, R.M. Pinder and S.N. Sawhney, J. Chem. Soc. (C), 1967, 293.
10. O. Dann and M. Kokorudz, Chem. Ber., 1953, 86, 1449.
11. M.A. Quasem, Ph.D. Thesis (Durham), 1967, p.45.
12. G. Mellani and G. Modena, J. Chem. Soc. (Perkin I), 1972, 218 and papers therein.
13. G. Capozzi, G. Mellani and G. Modena, J. Chem. Soc. (C), 1970, 2617.
14. G.M. Brooke and M.A. Quasem, J. Chem. Soc. (C), 1967, 865.
15. G.M. Brooke and M.A. Quasem, J. Chem. Soc. (Perkin I), 1973, 429.
16. D.E.L. Carrington, K. Clarke, S.M. Scrowston, Tetrahedron Letters, 1971, 1075.

17. E.W. McClelland, M.J. Rose and D.W. Stammers, J. Chem. Soc., 1948, 81.
18. C. Hansch, B. Schmidhalter, F. Reiter and W. Saltonstall, J. Org. Chem., 1955, 20, 1056.
19. Ref. 1, p.71.
20. C.E. Castro, E.J. Gaughan and D.C. Owsley, J. Org. Chem., 1966, 31, 4071.
21. A.M. Malte and C.E. Castro, J. Amer. Chem. Soc., 1967, 89, 6770.
22. P. Bravo, G. Gaudiano and M.G. Zubiani, J. Het. Chem., 1970, 7, 967.
23. A. Schonberg and L.V. Vargha, Chem. Ber., 1931, 1390.
24. E. Campaigne, T. Bosin and E.S. Neiss, J. Med. Chem., 1967, 10, 270.
25. E. Campaigne and R.E. Cline, J. Org. Chem., 1956, 21, 39.
26. P.M. Chakrabarti, N.B. Chapman and K. Clarke, Tetrahedron, 1969, 25, 2781.
27. T.J. Barton and R.G. Zika, J. Org. Chem., 1870, 35, 1729.
28. S. Nakagawa, J. Okumura, F. Sakai, H. Hoshi and T. Naio, Tetrahedron Letters, 1970, 3719.
29. W.B. Wright Jr., and H.J. Brabandier, J. Het. Chem., 1971, 8, 711.
30. A.J. Krubsack and T. Higa, Tetrahedron Letters, 1968, 5149.
31. A.J. Krubsack and T. Higa, Tetrahedron Letters, 1972, 4826.
32. A.J. Krubsack and T. Higa, Tetrahedron Letters, 1973, 125.
33. L. Thi J. Strating and B. Zwanenberg, Recl. Trav. Chim. Pays-Bas., 1972, 91, 1345.
34. G. Borger and A.J. Ewins, J. Chem. Soc., 1908, 2086.

35. Ref 1, p.155.
36. M.D. Castle, R.G. Plevy and J.C. Tatlow, J. Chem. Soc., (C),  
1968, 1225.
37. G.M. Brooke, Tetrahedron Letters, 1968, 4049.
38. V.P. Petrov, V.A. Barkhasch, G.S. Schegoleva, T.D. Petrova,  
T.I. Savchenko and G.G. Yagkobsen, Doklady. Akad. Nauk. S.S.S.R.,  
1968, 178, 864.
39. E.K. Fields and S. Meyerson in 'Organosulphur Chemistry'  
(M.J. Janssen Ed.), J. Wiley and Sons (Interscience), N.Y.,  
1967, p.143.
40. D.D. Callender, P.L. Coe, J.C. Tatlow and A.J. Uff, Tetrahedron,  
1969, 25, 25.
- 41a. R.D. Chambers, J. Hutchinson and W.K.R. Musgrave, J. Chem. Soc.,  
1964, 3573.
- 41b. R.E. Banks, R.N. Haszeldine J.V. Latham and I.M. Young, J. Chem.  
Soc., 1965, 549.
42. R.D. Chambers, J.A.H. MacBride and W.K.R. Musgrave, J. Chem.Soc.  
(C), 1968, 2116.
43. R.E. Banks, O.S. Field, and R.N. Haszeldine, J. Chem. Soc. (C),  
1970, 1280.
44. R.D. Chambers, J.A.H. MacBride and W.K.R. Musgrave, Chem. and Ind.,  
1966, 1721.
45. R.D. Chambers, M. Hole, B. Iddon, W.K.R. Musgrave and R.A. Storey,  
J. Chem. Soc. (C), 1966, 2328.

46. R.D. Chambers, J.A.H. MacBride and W.K.R. Musgrave, Chem. Comms., 1970, 739.
47. R.D. Chambers, J.A.H. MacBride, W.K.R. Musgrave and I.S. Reilley, Tetrahedron Letters, 1970, 1, 57.
48. C.G. Allison, R.D. Chambers, J.A.H. MacBride and W.K.R. Musgrave, Tetrahedron Letters, 1970, 23, 1979.
49. C.G. Allison, R.D. Chambers, J.A.H. MacBride and W.K.R. Musgrave, J. Fluorine Chem. 1971/72 1. 59.
50. D.J. Berry, J.D. Cook and B.J. Wakefield, J. Chem. Soc. (C), 1972, 2190.
51. J. Burdon, I.W. Parsons and J.C. Tatlow, J. Chem. Soc. (C), 1971, 346.
52. G. Barger and A.J. Ewins, J. Chem. Soc., 1908, 2086.
53. G. Huett and S.I. Miller, J. Amer. Chem. Soc., 1961, 83, 408.
54. S.I. Miller and R. Tanaka in 'Selective Organic Transformations' Vol. 1, (B.S. Thyagarajan Ed.), Wiley (Interscience), N.Y., 1970, p.143.
55. W.E. Truce, H.G. Klein and R.B. Kruse, J. Amer. Chem. Soc., 1961 83, 4636.
56. W.E. Truce, D.L. Goldhammer and R.B. Kruse, J. Amer. Chem. Soc., 1959, 81, 4931.
57. J.E. Delfini, J. Org. Chem., 1965, 30, 1298.
58. E. Winterfeldt and H. Preuss, Chem. Ber., 1966, 99, 450.
59. J.B. Hendrikson, J. Amer. Chem. Soc., 1961, 83, 1250.
60. J.B. Hendrikson, R. Rees, and J.F. Templeton, J. Amer. Chem. Soc., 1961, 83, 1250.

61. A.L. Rocklin, J. Org. Chem., 1956, 21, 1478.
62. G.M. Brooke and R.J.D. Rutherford, J. Chem. Soc. (C), 1967, 1189.
63. L.M. Jackman 'Applications of Nuclear Magnetic Resonance Spectroscopy to Organic Chemistry', Pergamon Press Inc., N.Y. 1959, p.17.
64. Ref. 4, p.187.
- 65a. K.D. Bartle, D.W. Jones and R.S. Matthews, Tetrahedron, 1971, 21, 5177.
- 65b. F. Yuste and F. Walls, Aust. J. Chem., 1973, 26, 201.
66. D.A. Shirley and M.D. Cameron, J. Amer. Chem. Soc., 1950, 72, 2788.
67. E. Ziegler and E. Noelken, Monatsh. Chem., 1961, 92, 1184.
68. W. Reid and H. Bender, Chem. Ber., 1955, 88, 34.
69. W. Reid and H. Bender, Chem. Ber., 1956, 89, 1574.
70. R.P. Dickinson and B. Iddon, J. Chem. Soc. (C), 1968, 2733.
71. V.V. Ghaisas, B.J. Kane and F.F. Nord, J. Org. Chem., 1958, 23, 560.
72. F. Balkan and M.L. Hefferman, Aust. J. Chem., 1972, 25, 327.
73. H.F. Ramsden, A.E. Balint, W.R. Whitford, J.J. Walburn and R. Cserr, J. Org. Chem., 1957, 22, 1202.
74. D.E. Peatson, D. Cowan and J.D. Beckler, J. Org. Chem., 1959, 24, 504.
75. J.D. Cook and B.J. Wakefield, J. Organomet. Chem., 1968, 13, 15.
- 76a. F. Binns and H. Suschitzky, J. Chem. Soc. (C), 1971, 1913.
- 76b. F. Binns, S.M. Roberts and H. Suschitzky, J. Chem. Soc. (C), 1970, 1375.
77. R.S. Dickson and G.D. Sutcliffe, Aust. J. Chem., 1971, 24, 295.

78. P.L. Coe, G.M. Peach and J.C. Tatlow, J. Chem. Soc. (C),  
1971, 604.
79. Ref. 4, p.375.
80. G.M. Brooke and M.A. Quasem, Tetrahedron Letters, 1967, 26, 2507.
81. R. Huisgen, H. König, G. Binsch, and H.J. Sturm, Angew. Chem.,  
1961, 73, 368.
82. R.L. Augustine, 'Catalytic Hydrogenation', Edward Arnold Ltd.,  
London 1965.
83. M. Martin-Smith and M. Gates, J. Amer. Chem. Soc., 1956, 78,  
5351.
84. Ref. 4, p.271.
85. G.M. Brooke and J. Yeadon, Unpublished results.
86. A.H. Schlesinger and D.T. Mowry, J. Amer. Chem. Soc., 1951  
73, 2614.
87. Ref. 4, p.356.
88. R.D. Chambers, J.A. Cunningham and D.J. Spring, J. Chem. Soc. (C),  
1968, 1560.
89. Ref. 11, p.98.
- 90a. N.P. Neureiter, J. Amer. Chem. Soc., 1966, 88, 558.
- 90b. N. Tokura, T. Nagai and S. Matsumura, J. Org. Chem., 1966, 31,  
349.
- 90c. E.M. LaCombe and B. Stewart, J. Amer. Chem. Soc., 1961, 83,  
3457.
91. E.K. Fields and S. Meyerson, J. Amer. Chem. Soc., 1966, 88, 2836.
92. G.E. Hartzell and J.N. Paige, J. Amer. Chem. Soc., 1966, 88, 2616.

93. G.E. Hartzell and J.N. Paige, J. Amer. Chem. Soc., 1967, 32, 459.
94. J.H. Bowie, D.H. Williams, S.O. Lawesson, J.Ø.Madsen, C. Nolde and J. Schroll, Tetrahedron, 1966, 22, 3515.
95. R.D. Chambers and J.A.H. MacBride, unpublished results.
96. J.A.H. MacBride, Chem. Comms., 1972, 1219.
97. I. Collins and H. Suschitzky, J. Chem. Soc. (C), 1967, 2337.
98. E.J. Forbes, R.D. Richardson, M. Stacey and J.C. Tatlow, J. Chem. Soc., 1959, 2019.
99. J.M. Birchall and R.N. Haszeldine, J. Chem. Soc., 1959, 13.
100. G.M. Brooke, J. Burdon, M. Stacey and J.C. Tatlow, J. Chem. Soc., 1960, 1768.
101. P. Robson, M. Stacey, R. Stephens and J.C. Tatlow, J. Chem. Soc., 1960, 4754.
102. J.M. Birchall and R.N. Haszeldine, J. Chem. Soc., 1961, 3719.
103. M.T. Chaudhry and R. Stephens, J. Chem. Soc., 1963, 4281.
104. J. Burdon, W.B. Hollyhead and J.C. Tatlow, J. Chem. Soc., 1965, 5152.
105. J.G. Allen, J. Burdon and J.C. Tatlow, J. Chem. Soc., 1965, 6329.
106. J.G. Allen, J. Burdon and J.C. Tatlow, J. Chem. Soc., 1965, 1045.
107. J. Burdon and D.F. Thomas, Tetrahedron, 1965, 21, 2389.
108. J. Burdon, D. Fisher, D. King and J.C. Tatlow, Chem. Comms., 1965, 65.
109. G.M. Brooke, J. Burdon and J.C. Tatlow, J. Chem. Soc., 1961, 802.

110. J. Burdon, Tetrahedron, 1965, 21, 3375.
111. D.T. Clark, J.N. Murrell and J.M. Tedder, J. Chem. Soc., 1963, 1250.
112. J. Burdon, D.R. King and J.C. Tatlow, Tetrahedron, 1966, 22, 2541.
113. G.G. Yakobson, L.S. Kobrina and C.K. Serin, Zh. Org. Khim., 1966, 2 (3), 495.
114. N.N. Vorozhtsov, J. Gen. Chem. U.S.S.R., 1965, 35, 136.
115. R.D. Chambers and J.S. Waterhouse, unpublished results.
116. W.T. Flowers, R.N. Haszeldine and S.A. Majid, Tetrahedron Letters, 1967, 26, 2503.
117. R. Schönbeck and E. Kleinstein, Monatshafte fur Chemie., 1968, 99, 15.
118. H. Ackermann and P. Dussey, Helv. Chim. Acta., 1962, 45, 1683.
119. R.D. Chambers, M. Hole, W.K.R. Musgrave, R.A. Storey, and B. Iddon, J. Chem. Soc. (C), 1966, 2331.
120. G.M. Brooke, B.S. Furniss and W.K.R. Musgrave, J. Chem. Soc. (C), 1968, 580.
121. G.M. Brooke and M.A. Quasem, Tetrahedron Letters, 1967, 26, 2507.
122. R.D. Chambers and D.J. Spring, Tetrahedron, 1971, 27, 669.
123. J. Burdon, B.C. Kane and J.C. Tatlow, J. Fluorine Chem., 1971/72, 1, 185.
124. J. Burdon, J.G. Campbell, I.W. Parsons and J.C. Tatlow, J. Chem. Soc. (C), 1971, 352.
125. S.M. Shein and V.A. Ignatov, Zh. Obs. Khim., 1962, 32, 3165  
(English Trans).
126. A.J. Parker, Chem. Revs., 1969, 69, 1.

- 127a. J. Burdon, V.A. Damodaran and J.C. Tatlow, J. Chem. Soc., 1964, 763.
- 127b. E.V. Aroshar, P.J.W. Brown, R.G. Plevey and R. Stevens, J. Chem. Soc. (C), 1968, 1569.
128. K.R. Langille and M.E. Peach, J. Fluorine Chem., 1971/72, 1, 407.
129. D.E. Eastman in 'Techniques in Metal Research VI', (E. Passaglia Ed.), Wiley (Interscience), 1972.
130. D.W. Turner, C. Baker, A.D. Baker and C.R. Brundie, 'Molecular Photoelectron Spectroscopy', Wiley (Interscience), 1970.
131. T.W. Haas, G.J. Dooley, A.G. Jackson and M.P. Hooker, 'Progress in surface Science', Vol. 1 (2), Pergamon, 1971.
- 132a. H. Robinson and W.F. Rawlinson, Phil. Mag., 1914, 28, 277.
- 132b. H. Robinson, Proc. Roy. Soc., 1923, A104, 455.
- 132c. H. Robinson, Phil. Mag., 1925, 50, 241.
133. M. de Broglie, Compt. Rend., 1921, 172, 274.
134. J.A. Van Akker and E.C. Watson, Phys. Rev., 1931, 37, 1631.
135. M. Farence Jr., Phys. Rev., 1937, 51, 720.
136. A. Bazin, Zh. Eks. noi. i. Teoret. Fiziki, 1944, 14, 23.
137. R.G. Steinhardt Jr., F.A.D. Granados and G.I. Post, Anal. Chem., 1955, 27, 1046.
138. B.L. Henke, Tech.Report No. 6, Contract No AF.49 (638)-394, Air Force Office of Scientific Research, 1962.
139. K. Siegbahn and K. Edvarrson, Nucl. Phys., 1956, 1, 137.
140. A.M. Lindh, 'Handbuch der Experimental Physik', 24. Teil 4, (W. Wien and F. Harnes Ed.), Leipzig, 1930.

141. H.W.B. Skinner and J.E. Johnstone, Proc. Roy. Soc., 1937, A161,  
420.
142. C. Nordling, E. Sokolowski and K. Siegbahn, Arkiv. Fys., 1958, 13,  
483.
143. S. Hagstrom, C. Nordling and K. Siegbahn, Phys. Lett., 1964, 9,  
235.
144. C. Nordling, S. Hagstrom and K. Siegbahn, Z. Physik, 1964,  
176, 433.
145. K. Siegbahn, C. Nordling, A. Fahlam, R. Nordbert, K. Hamrin,  
J. Hedman, G. Johansson, T. Bergman, S.E. Karlsson, J. Lidgren  
and B. Lindberg, 'ESCA - atomic, molecular and solid state  
structure studied by means of electron spectroscopy',  
Uppsala, 1967.
146. K. Siegbahn, C. Nordling, G. Johansson, J. Hedman, P.F. Heden,  
K. Hamrin, U. Gelius, T. Bergmark, L.O. Werme, R. Manne and  
Y. Baer, 'ESCA applied to free molecules', North Holland,  
Amsterdam, 1969.
147. D.T. Clark and D.R. Armstrong, Theoret. Chim. Acta. (Berl), 1968, 13,  
1968.
- 148a. M.I. Al-Jobourny and D.W. Turner, J. Chem. Soc., 1963, 5154.
- 148b. *ibid.*, 1965, 4434.
149. C.R. Brundle, Applied Spectroscopy, 1971, 25, 8.
150. A.L. Hughes and H. McMillan, Phys. Rev., 1929, 34, 293.
151. H. Hafner, J.A. Simpson and C.E. Kuyatt, Rev. Sci. Instrum.,  
1968, 39, 33.
152. F.W. Aston, Phil. Mag., 1919, 38, 710.

153. C. Nordling, E. Sokolowski and K. Siegbahn, Phys. Rev., 1957, 105, 1676.
154. D.M. Hercules, Anal. Chem., 1970, 42, 20.
155. J.A. Simpson, Rev. Sci. Instrum., 1964, 35, 1968.
156. J.C. Helmer and N.H. Weichert, Appl. Phys. Lett., 1968, 13, 266.
157. K. Siegbahn, D. Hammond, H. Feller-Feldegg and E.F. Barnett, Science, 1972, 176, 245.
158. K. Siegbahn, Endavour, 1973, XXXII (16), 51.
159. L.G. Parratt, Rev. Mod. Phys., 1959, 31, 616.
160. C. Nordling, Angew. Chemie (Int. Ed.), 1972, 11, 83.
161. B. Wolfgang, Fortschr. Chem. Forsch, 1972, 36, 1. (Eng.).
162. C.R. Brundle, A.D. Baker and M. Thompson, Chem. Soc. Reviews, 1972, 1, 355.
163. B. Lindberg, Colloq. Spectrosc. Int. Plenery Lect Rep. 1971 (Pub. 1972), 95, Adam Hilger Ltd. London.
164. A. Hammett and A.F. Orchard, Electron. Struct. Magn. Inorg. Compounds., 1972, 1, 1.
165. C.R. Brundle, Surface Defect. Prop. Solids, 1972, 1, 172.
166. D.T. Clark, Chem. Comms., 1971, 230.
167. D.T. Clark and D.B. Adams, J. Electron Spec. and Rel. Phenom., 1972/73, 1, 302.
168. P. Siegbahn, Chem. Phys. Lett., 1971, 8, 245.
169. F.A. Gianturco and G. Gindotti, Chem. Phys. Lett., 1971, 9, 539.
170. D.T. Clark and D. Kilcast, J. Chem. Soc. (A), 1971, 3286.

171. D.T. Clark and D. Kilcast, J. Chem. Soc. (B), 1971, 2243.
172. D.W. Davis, D.A. Shirley and T.D. Thomas, J. Amer. Chem. Soc.,  
1972, 94, 6565.
- 173a. D.T. Clark and D.M.J. Lilley, Chem. Phys Lett., 1971, 9, 234.
- 173b. K. Siegbahn, B.J. Lindberg, C. Nordling, U. Gelius, K. Hamrin  
and A. Fahlman, Physica Scripta, 1971, 3, 237.
174. D.T. Clark, R.D. Chambers, D. Kilcast and W.K.R. Musgrave, J. Chem.  
Soc. (Faraday II), 1972, 68, 309.
175. T. Koopmans, Physica, 1933, 1, 104.
176. M.E. Schwartz, Chem. Phys. Lett., 1970, 6, 631.
177. M.E. Schwartz, Chem. Phys. Lett., 1970, 7, 78.
178. D.T. Clark, D. Kilcast and W.K.R. Musgrave, Chem. Comm., 1971, 576.
179. D.T. Clark, D. Kilcast and W.K.R. Musgrave, J. Chem. Soc. (D),  
1971, 516.
180. D.T. Clark, D.M.J. Lilley, D. Kilcast and M. Barber, unpublished  
results.
181. D.T. Clark, D.B. Adams and D. Kilcast, Chem. Phys. Letters,  
1972, 13, 439.
182. D.T. Clark, D.B. Adams, D. Kilcast, W.J. Feast and W.E. Preston,  
J. Flourine Chem., 1972, 2, 199.
183. G.D. Stucky, D.A. Matthews, J. Hedman and C. Nordling, J. Amer.  
Chem. Soc., 1972, 94, 8009.
184. E.T. McBee, U.S. Patent, 3,317,497, May 2 1967.
185. D.T. Clark, W.J. Feast, M. Foster and D. Kilcast, Nature,  
1972, 236, 107.

186. D.T. Clark, D.B. Adams, W.J. Feast, D. Kilcast, W.K.R. Musgrave and W.E. Preston, Nature, 1972, 239, 47.
187. G.A. Olah, G.D. Mateescu, L.A. Wilson and M.H. Gross, J. Amer. Chem. Soc., 1970, 92, 7231.
188. G.A. Olah, G.D. Mateescu, L.A. Wilson and M.H. Gross, J. Amer. Chem. Soc., 1972, 94, 808.
189. G.D. Mateescu, J.L. Rumenschneider, J.J. Svoboda and G.A. Olah, J. Amer. Chem. Soc., 1972, 94, 7191.
190. D.T. Clark, D. Kilcast and D.H. Reid, Chem. Comm, 1971, 638.
191. D.T. Clark and D. Kilcast, Tetrahedron, 1972, 27, 4367.
192. R. Gleiter, V. Hamrig, B. Lindberg, S. Hogberg, and N. Lozach, Chem. Phys Lett., 1971, 41, 401.
193. J. Bus, Recueil., 1972, 91, 552.
194. E. Haselback, A. Hendricksson, F. Jackimowicz and J. Wirz, Helv. Chim. Acta., 1972, 55, 1757.
195. D.T. Clark, D. Kilcast, W.J. Feast and W.K.R. Musgrave, J. Polymer Sci. (A), 1972, 10, 1637.
196. D.T. Clark, D. Kilcast and D.B. Adams, Faraday Disc. Chem. Soc., 1972, 54, 182.
197. C.R. Ginnard and W.M. Riggs, Anal. Chem., 1972, 44, 1310.
198. D.T. Clark and D. Kilcast, Nature Phys. Sci., 1971, 233, 77.
199. M.H. Wood, M. Barber, I.H. Hillier and J.M. Thomas, J. Chem. Phys., 1972, 56, 1788.
200. D.W. Davis and D.A. Shirley, J. Chem. Phys., 1972, 56, 669.

201. L.J. Aarons, M.F. Guest and I.H. Hillier, J. Chem. Soc. (Faraday Trans. II), 1972, 68, 1866.
202. U. Gelius, G. Johansson, H. Siegbahn, C.J. Allan, D.A. Allison and J. Allison, J. Electron Spec. and Rel. Phenom., 1972, 1, 285.
203. R.E. Block, J. Magn. Resonance, 1971, 5, 155.
204. U. Gelius and K. Siegbahn, Faraday Disc. Chem. Soc., 1972, 54, 257.
205. D.T. Clark, D. Briggs and D.B. Adams, J. Chem. Soc. (Dalton Trans), 1973, 169.
206. I. Adams, J.M. Thomas, G.M. Bancroft, K.D. Butler and M. Barber, Chem. Comm., 1972, 751.
207. W.L. Jolly and D.N. Hendrickson, J. Amer. Chem. Soc., 1970, 92, 1865.
208. D.T. Clark and D. Briggs, Nature Phys. Sci., 1972, 15, 237.
209. L.Klasinc, E. Pop, N. Trinajstic and J.V. Knop, Tetrahedron, 1972, 28, 3465.
210. R.A.W. Johnstone and S.D. Ward, Tetrahedron, 1969, 25, 5485.
211. M.H. Palmer and R.H. Findlay, Tetrahedron Letters, 1972, 4165.
212. U. Gelius, B. Roos and P. Siegbahn, Theoret. Chim. Acta (Berl.), 1972, 27, 171.
213. J.W. van Reijendam and M.J. Janssen, Tetrahedron, 1970, 26, 1303.
214. U. Gelius, B. Ross and P. Siegbahn, Chem. Phys. Lett., 1970, 4, 471.
215. D.T. Clark and D.R. Armstrong, J. Chem. Soc. (D), 1970, 319.

216. D.T. Clark, D.B. Adams, I.W. Scanlan, D. Kilcast, unpublished results.
217. D.T. Clark, Chem. Comm., 1971, 230.
218. W.J. Feast and W.E. Preston, Tetrahedron, 1972, 28, 2805.
219. A.C. Young and G.M. Brooke unpublished results.
220. N.B. Chapman; D.F. Ewing, R.M. Scrowston and R. Westwood, J. Chem. Soc. (C), 1968, 764.
221. B.J. Lindberg, K. Hamrin, G. Johansson, U. Gelius, A. Fahlman, C. Nordling and K. Siegbahn, Physica Scripta, 1970, 1, 286.
222. J.A. Pople and D.L. Beveridge, 'Approximate Molecular Orbital Theory', McGraw-Hill, 1970.
223. J.N. Murrell, S.F.A. Kettle and J.M. Tedder, 'Valence Theory', J. Wiley and Sons Ltd., London 1965.
224. M. Born and J.R. Oppenheimer, Annalen der Physik, 1927, 84, 456.
225. D.R. Hartree, Proc. Cam. Phil. Soc., 1928, 24, 89.
226. V. Fock, Z. Physik, 1930, 61, 126.
227. C.C.J. Roothaan, Rev. Mod. Phys., 1951, 23, 69.
228. C.C.J. Roothaan, J. Chem. Phys., 1951, 19, 1445.
229. D.P. Santry and G.A. Segal, J. Chem. Phys., 1967, 47, 158.